Natural Killer Cell Activity Assessment in a Whole Blood-Based Culture System Using Multiplex Cytokine and Flow Cytometry Measurements

Dissertation

der Mathematisch-Naturwissenschaftlichen Fakultät

der Eberhard Karls Universität Tübingen

zur Erlangung des Grades eines

Doktors der Naturwissenschaften

(Dr. rer. nat.)

vorgelegt von

Meike Jakobi

aus Heidenheim

Tübingen

2022

Gedruckt mit Genehmigung der Mathematisch-Naturwissenschaftlichen Fakultät der Eberhard Karls Universität Tübingen.

Tag der mündlichen Qualifikation:	08.11.2022
Dekan:	Prof. Dr. Thilo Stehle
1. Berichterstatter/-in:	Prof. Dr. Ulrich Rothbauer
2. Berichterstatter/-in:	Prof. Dr. Katja Schenke-Layland

Betreuer an der Eberhard Karls Universität Tübingen

Prof. Dr. Ulrich Rothbauer

und

Prof. Dr. Katja Schenke-Layland

Betreuer am Naturwissenschaftlichen und Medizinischen Institut

an der Universität Tübingen

Dr. Nicole Schneiderhan-Marra, Dr. Jens Goepfert

und

Dr. Thomas Joos

Betreuer der Firma HOT Screen GmbH

Dr. Sascha Klimosch und Dr. Manfred Schmolz

EIDESSTATTLICHE ERKLÄRUNG

ICH ERKLÄRE HIERMIT, DASS ICH DIE ZUR PROMOTION EINGEREICHTE ARBEIT MIT DEM TITEL: „NATURAL KILLER CELL ACTIVITY ASSESSMENT IN A WHOLE BLOOD-BASED CULTURE SYSTEM USING MULTIPLEX CYTOKINE AND FLOW CYTOMETRY MEASUREMENTS“ SELBSTÄNDIG VERFASST, NUR DIE ANGEGEBENEN QUELLEN UND HILFSMITTEL BENUTZT UND WÖRTLICH ODER INHALTLICH ÜBERNOMMENE STELLEN ALS SOLCHE GEKENNZEICHNET HABE.

ICH ERKLÄRE, DASS DIE RICHTLINIEN ZUR SICHERUNG GUTER WISSENSCHAFTLICHER PRAXIS DER UNIVERSITÄT TÜBINGEN (BESCHLUSS DES SENATS VOM 25.5.2000) BEACHTET WURDEN. ICH VERSICHERE AN EIDES STATT, DASS DIESE ANGABEN WAHR SIND UND DASS ICH NICHTS VERSCHWIEGEN HABE. MIR IST BEKANNT, DASS DIE FALSCHE ABGABE EINER VERSICHERUNG AN EIDES STATT MIT FREIHEITSSTRAFE BIS ZU DREI JAHREN ODER MIT GELDSTRAFE BESTRAFT WIRD.

TÜBINGEN, DEN _____

MEIKE JAKOBI

DANKSAGUNG

DIESE ARBEIT WURDE AM NMI NATURWISSENSCHAFTLICHES UND MEDIZINISCHES INSTITUT AN DER UNIVERSITÄT TÜBINGEN IN REUTLINGEN IN DER ABTEILUNG MULTIPLEXE IMMUNOASSAYS ANGEFERTIGT.

ICH MÖCHTE MICH HERZLICH BEI **PROF. DR. ULRICH ROTHBAUER** FÜR DIE BETREUUNG DIESER ARBEIT BEDANKEN ALS AUCH BEI FRAU **PROF. DR. KATJA SCHENKE-LAYLAND**, DIE MEINE ARBEIT ALS ZWEITGUTACHTERIN BETREUT HAT.

WEITER BEDANKE ICH MICH BEI **DR. NICOLE SCHNEIDERHAN-MARRA**, **DR. JENS GÖPFERT** UND **DR. THOMAS JOOS** FÜR DIE MÖGLICHKEIT, DIESE ARBEIT AM NMI DURCHFÜHREN ZU KÖNNEN UND DAFÜR, DASS SIE MICH IN ALLEN ARBEITSSCHRITTEN SEHR UNTERSTÜTZT HABEN.

MEIN BESONDERER DANK GILT DER HOT SCREEN GMBH FÜR DIE AUßERORDENTLICH GUTE ZUSAMMENARBEIT UND DIE TATKRÄFTIGE UNTERSTÜTZUNG, ALLEN VORAN **DR. SASCHA KLIMOSCH** UND **DR. MANFRED SCHMOLZ**. VIELEN DANK FÜR DIE GENERIERUNG DER ZELLKULTURPROBEN UND DEREN BEREITSTELLUNG, DIE BEGLEITUNG DER EINARBEITUNG IN DIE DURCHFLUSSZYTOMETRIE UND VOR ALLEM FÜR DIE DISKUSSIONEN, WELCHE MAßGEBLICH ZUR BEREICHERUNG DIESER ARBEIT BEIGETRAGEN HABEN.

EIN HERZLICHER DANK GEHT AN MEINE KOLLEGINNEN UND KOLLEGEN AM NMI FÜR IHRE UNTERSTÜTZUNG, HILFE UND FÜR DAS GUTE ARBEITSKLIMA. BESONDERS DANKEN MÖCHTE ICH MEINEN KOLLEGINNEN **DR. VIVIANA CARCAMO YAÑEZ, ANNA GÜNTHER** UND **MADELEINE FANDRICH** FÜR DIE TATKRÄFTIGE HILFE UND UNTERSTÜTZUNG IM ARBEITSALLTAG UND DARÜBER HINAUS.
EBENFALLS BEDANKE ICH MICH BEI **MATTHIAS BECKER** FÜR SEINE UNTERSTÜTZUNG BEI DER ENTWICKLUNG DES MULTIPLEXEN ANALYTIK-PANEL 2, ALS AUCH **DANIEL JUNKER** FÜR DEREN UNTERSTÜTZUNG BEI DER HERSTELLUNG VON REAGENZIEN DER DRITTEN KIT-CHARGE.

VON GANZEM HERZEN MÖCHTE ICH MICH BEI **MEINEM EHEMANN UND MEINER FAMILIE** BEDANKEN, DIE MIR STETS ZUR SEITE STANDEN UND DEN NOTWENDIGEN RÜCKHALT BOTEN, ALS AUCH BEI MEINEN **FREUNDEN**, DIE, WENN IMMER NOTWENDIG, FÜR MOTIVATION ODER AUCH ABLENKUNG GESORGT HABEN.

VIELEN DANK!

LIST OF CONTENT

LIST OF FIGURES

LIST OF TABLES

LIST OF ABBREVIATIONS

AEB	average enzymes per bead
AS	analyte stability sample
AU	arbitrary units
B cells	B lymphocytes
beads	paramagnetic microspheres
BRE	Blocking Reagent for ELISA
CAL	calibrator
CBII	Chemiblock II
CCD	charge coupled device
CI	confidence interval
conc.	concentration
CSIF	cytokine synthesis inhibitory factor
CV	coefficient of variation
DC	dendritic cells
ddH_2O	double-distilled water
DL	dilution
EDC	1-Ethyl-3-(3-dimethylaminopropyl)carbodiimid
ELISA	enzyme-linked immunosorbent assay
EMA	European Medicines Agency
EPS	Encapsulated PostScript
FBS	fetal bovine serum
FCS	fetal calf serum
FDA	U.S. Food and Drug Administration
G-CSF	granulocyte colony-stimulating factor
GM-CSF	granulocyte/macrophage colony-stimulating factor
HAMA	human anti-mouse antibody
HEPES	4-(2-hydroxyethyl)-1-piperazineethanesulfonic acid
HLA	human leucocyte antigens
ID	identification
IFN	interferon
IL	interleukin
IL-1R1	interleucin 1 receptor 1
IL-1Ra	interleucin 1 receptor antagonist
IMAP	inflammatory multiplex analyte panel
ITAM	immunoreceptor tyrosine-based activation motif
ITIM	immunoreceptor tyrosine-based inhibition motif
KIR	killer cell immunoglobulin-like receptor
KLR	killer cell lectin-like receptor
LAMP-1	lysosomal-associated membrane protein 1
LC	long-chain
LLOQ	lower limit of quantification

LOD	limit of detection
LPS	lipopolysaccharide
MCP	monocyte chemoattractant protein
M-CSF	macrophage colony-stimulating factor
MES	2-(N-morpholino)ethanesulfonic acid
MFI	median of fluorescent intensity
MHC	major histocompatibility complex
MIP	macrophage inflammatory protein
MTOC	microtubule organization center
n.q.	not quantifiable
N/A	not analyzed
NCR	natural cytotoxicity receptor
PBMC	peripheral blood mononuclear cells
PE	Phycoerythrin
NK cells	natural killer cells
NP	native protein sample
PMNs	polymorphonuclear neutrophils
PMT	photomultiplier
PPR	pattern-recognition receptor
QC sample	quality control sample
R848	Resiquimod
Ref.	reference
RGP	resorufin-β-D-galactopyranoside
RT	room temperature
S/N	signal-to-noise
SBG	streptavidin-β-galactosidase
SEB	staphylococcal enterotoxin b
Simoa	single molecule-array
sNHS	sulfo-N-hydroxysuccinimid
Strep-PE	streptavidin-phycoerythrin
T cells	T lymphocytes
TACE	tumor necrosis factor-alpha converting enzyme
TC-GM	TruCulture medium
Th1 cells	T helper type 1 cells
Th2 cells	T helper type 2 cells
TLR	toll-like receptor
TNF	tumor necrosis factor
TNFR	tumor necrosis factor receptor
TRAIL-R	TNF-related apoptosis-inducing ligand receptor
Tregs	regulatroy T lymphocytes
Tris	tris(hydroxymethyl)aminomethane
ULOQ	upper limit of quantification
VEGF	vascular endothelial growth factor
VS	validation samples
γc	common gamma

ABSTRACT

Natural killer (NK) cells represent crucial players of the innate immune system and fulfil their main function in first line of defense by recognizing and eliminating tumor degenerated and virus infected cells. To analyze and influence NK cell behavior it is necessary to be able to specifically activate NK cells. In this work, known NK cell-specific stimulants were used in whole blood cultures (TruCulture) to investigate the specificity of the NK cell-activating stimuli in the high complexity of this culture system and to determine whether and to what extent co-activation of further immune cells of the peripheral blood occurs. For this purpose, it was necessary to generate appropriate test systems. Thus, two bead-based multiplex Luminex immunoassays, IMAP 1 and IMAP 2, were developed for the detection of nine (IL-4, -6, -8, -10, GM-CSF, IFN-γ, MCP-1, MIP-1β, TNF-α) and six (IL-1β, -1Ra, -12p70, -13, VEGF, M-CSF) analytes respectively. Additionally, highly sensitive single-molecule arrays (Simoa) were established for IL-4 and IL-12p70 as single-plex assays and for IL-6 and TNF-α as 2-plex assays as these four analytes required higher sensitivities than those provided by the Luminex technology. During assay development, parameters such as the basic buffer system and detector antibody concentration were optimized for optimal performance and sensitivity, with cross-reactivity between multiplexed analytes evaluated and reduced. Developed assays were then validated to confirm their potential as an analytical method for the TruCulture system and to confirm their reproducibility and validity. Method suitability was confirmed for the majority of analytes. Only for VEGF the pre-defined acceptance criteria for precision were not met, while for IL-4, IL-12p70, GM-CSF, VEGF and M-CSF, as part of the IMAPs, parallelism could not be demonstrated. A method comparison (Luminex vs. Simoa) using Passing-Bablok regression and Blant-Altman plots was performed for IL-6 and TNF-α assays to be able to use data from both assays for analysis. This showed comparability for both technologies.

The developed and validated assays were then used to assess NK cell activation in whole blood cultures, supplemented by flow cytometric analyses. Synergistic effects of the stimulant combinations IL-12 + IL-18, R848 + IL-2 and K562 cells + IL-2 were shown to induce the strongest activation states of NK cells. It was observed that R848 + IL-2 stimulated not only cytokine production but also the degranulation process as NK cell effector functions and led to a broad activation of all immune cell populations of the peripheral blood. In contrast, the combination IL-12 + IL-18 showed NK cell stimulation only in the direction of cytokine production and moderately activated other immune cells. Although it is not yet possible to

store these cells at -20 °C, which is a prerequisite for their use as default stimulant in the TruCulture application, the most specific NK cell activation was observed by stimulation with K562 cells in combination with IL-2.

ZUSAMMENFASSUNG

Natürliche Killerzellen (NK-Zellen) sind wichtige Akteure des angeborenen Immunsystems und erfüllen ihre Hauptfunktion in der ersten Ebene der Abwehr, indem sie tumorentartete und virusinfizierte Zellen erkennen und eliminieren. Um das Verhalten von NK-Zellen zu analysieren und zu beeinflussen, ist es notwendig, NK-Zellen spezifisch aktivieren zu können. In dieser Arbeit wurden bekannte NK-Zell-spezifische Stimulanzien in Vollblutkulturen (TruCulture) eingesetzt, um die Spezifität der NK-Zell-aktivierenden Stimuli in der hohen Komplexität dieses Kultursystems zu untersuchen und festzustellen, ob und inwieweit eine Koaktivierung weiterer Immunzellen des peripheren Blutes stattfindet. Zu diesem Zweck war es notwendig, geeignete Testsysteme zu generieren. So wurden zwei Mikrosphären-basierte multiplexe Luminex-Immunoassays, IMAP 1 und IMAP 2, für den Nachweis von neun (IL-4, -6, -8, -10, GM-CSF, IFN-γ, MCP-1, MIP-1β, TNF-α) bzw. sechs (IL-1β, -1Ra, -12p70, -13, VEGF, M-CSF) Analyten entwickelt. Darüber hinaus wurden hochempfindliche Single-Molecule-Arrays (Simoa) für IL-4 und IL-12p70 als Singleplex-Assays und für IL-6 und TNF-α als 2-Plex-Assays entwickelt, da für diese vier Analyten höhere Sensitivitäten erforderlich waren, als sie die Luminex-Technologie bieten konnte. Während der Assayentwicklung wurden Parameter wie das grundlegende Puffersystem und die Konzentration der Detektorantikörper für eine optimale Performance und Sensitivität optimiert, wobei die Kreuzreaktivitäten zwischen den Analyten eines multiplexen Assays bewertet und reduziert wurden. Die entwickelten Assays wurden anschließend validiert, um ihr Potenzial als Analysemethode für das TruCulture-System zu bestätigen und ihre Reproduzierbarkeit und Validität zu belegen. Die Eignung der Methode wurde für die Mehrzahl der Analyten bestätigt. Lediglich für VEGF wurden die definierten Akzeptanzkriterien der Präzision nicht erfüllt, während für IL 4, IL-12p70, GM-CSF, VEGF und M-CSF, als Teil der IMAPs, die Parallelität nicht nachgewiesen werden konnte. Ein Methodenvergleich (Luminex vs. Simoa) mittels Passing-Bablok-Regression und Blant-Altman-Diagrammen wurde für IL-6- und TNF-α-Assays durchgeführt, um die Daten beider Methoden für die Analyse verwenden zu können. Dieser zeigte die Vergleichbarkeit der beiden Technologien.

Die entwickelten und validierten Assays wurden dann zur Bewertung der NK-Zellaktivierung in Vollblutkulturen verwendet, ergänzt durch durchflusszytometrische Analysen. Es zeigte sich, dass die Synergieeffekte der Stimulanzkombinationen IL-12 + IL-18, R848 + IL-2 und K562-Zellen + IL-2 die stärksten Aktivierungszustände von NK-Zellen hervorriefen. Es wurde

beobachtet, dass R848 + IL-2 nicht nur die Zytokinproduktion, sondern auch den Degranulationsprozess als NK-Zell-Effektorfunktion stimulierte und zu einer breiten Aktivierung aller Immunzellpopulationen des peripheren Blutes führte. Im Gegensatz dazu zeigte die Kombination IL-12 + IL-18 eine Stimulation der NK-Zellen lediglich in Richtung der Zytokinproduktion und aktivierte andere Immunzellen nur mäßig. Obwohl es noch nicht möglich ist, diese Zellen bei -20 °C zu lagern, was eine Voraussetzung für ihre Verwendung als Standardstimulanz in der TruCulture-Anwendung ist, wurde die spezifischste NK-Zellaktivierung durch die Stimulation mit K562-Zellen in Kombination mit IL-2 beobachtet.

1. Introduction

1.1 Immunoassays

The immunoassay success story began with the work of Solomon Berson and Rosalyn S. Yalow in 1959 [1], who invented the first immunoassay for the detection of insulin. They demonstrated that diabetes patients treated with exogenous insulin of animal origin developed antibodies against it [2]. Upon further insulin administration, these antibodies specifically scavenged the hormone, leading to a retardation of the rate at which insulin disappeared from the blood compared to subjects who were not previously treated with insulin. These specific insulin antibodies were then isolated from insulin-treated patients and were purified to be used in the first radioimmunoassay to detect insulin. Because Berson and Yalow decided not to patent their method, the development of numerous other immunoassays for a variety of analytes was accelerated. For their discovery, Yalow was honored with the Nobel Prize in Medicine in 1977, five years after Berson's premature death [3]. Immunoassays are still used today and it is impossible to imagine the field of research, diagnostics and clinical practice without them. Nowadays, they are also widely available directly to end consumers, for example to detect pregnancy or as a point of care test to detect a corona-virus infection.

Immunoassays are sensitive bioanalytical methods based on the recognition and binding of target molecules in a complex liquid sample, such as urine, whole blood, serum or plasma. Analytes can be quantified either indirectly by using a calibration curve or the detection can occur in a qualitative manner. Immunoassays take advantage of three unique properties of antibodies for the specific detection of analytes:

- Firstly, their ability to bind a wide range of natural and artificially generated chemical and biological molecules, as well as cells and viruses.
- Secondly, their high specificity to the targeted substances.
- Thirdly, their high affinity to their target molecules to which they bind via a very strong non-covalent bond [4, 5].

Since the principle of the first immunoassay was published in 1959, there has been continuing progress in assay generation and development resulting in a variety of different assay designs. Assay sensitivity, for example, is a parameter continually being optimized to maximize assay performance and to make previously unmeasurable effects detectable. A historic breakthrough was the implementation of monoclonal antibody production by Kohler and

Milstein [6]. Their use in immunoassays not only increased the relevance of immunoassays [3] but also led to an increase in assay sensitivity and reproducibility of results [7] making their application in immunoassays still attractive today. The solid phase based assay principle was another important development that led to a significant improvement in feasibility [8, 9]. Increased throughput was mainly achieved by using microspheres as the solid phase. This laid the foundation for the simultaneous detection and quantification of several analytes in one reaction chamber, also known as multiplexing. Therefore, labor, time and cost reduction could be achieved in comparison to single-reaction based methods like e.g. classical enzyme-linked immunosorbent assay (ELISA) [10, 11].

Additional progress has been made in further improving sensitivity and enlarging the assay ranges, for example by detecting single molecules and amplifying assay signals [12].

1.2 Luminex-xMAP technology

xMAP technology is a bead-based assay platform developed by the company Luminex (Austin, TX, USA, www.luminexcorp.com). The Luminex Corporation was founded in 1995 and rapidly became the leading force in bead-based multiplexed detection procedures for proteins and nucleic acids. Today it remains the most frequently employed platform, due to its ability to enable the simultaneous analysis of a variety of different analytes in a single test. This multiplexing option not only increases information output, but also reduces time, labor and costs in comparison to single-reaction based methods [10]. In addition, multiplexing has the added advantage of requiring far less sample volume for the detection of a large number of analytes compared to single detection-based methods. xMAP technology can be used in a diversity of applications – like different types of immunoassays and nucleic acid assays [10, 11].

The main element of the xMAP technology is polystyrene microspheres also called beads. These beads are physically identical, except for their ratio of two to three fluorescent dyes, enabling them to be distinguished from each other. Microspheres of one bead-ID (identification) share the same unique color composition, meaning that each individual ID has a unique emission profile and spectral characteristics, enabling differentiation. Overall, up to 500 different bead IDs are currently available. The surface of these beads is functionalized with carboxyl groups that allow the covalent immobilization of capture components. Thus, the surface of each bead ID can be coated with a specific capture compound. If different bead IDs

are subsequently combined, the different analytes can be detected simultaneously. Furthermore, the 6.5 µm sized beads are superparamagnetic what leads to easy automation and simplifies the process of coating the surface of microspheres and the performance of washing processes [10].

To quantify binding events, R-Phycoerythrin (PE) is normally used as fluorescent reporter [10]. PE is a water-soluble protein with fluorescent properties, isolated from red algae *Gracilaria lemaneiformis*, and is commonly used as a fluorescent tag in many biochemical techniques [13, 14].

The FLEXMAP 3D instrument launched in 2009, is a high throughput analyzer that allows a rapid analysis of 96- and 384-well plates due to a dual syringe system. The measurement technique is based on the principle of flow cytometry, whereby, beads are arranged like a string of pearls and passed individually through a flow chamber, where they are detected and analyzed by a laser and detection system. The FLEXMAP 3D device is equipped with two lasers. The red diode laser uses a wavelength of 638 nm to excite the internal fluorescent dyes of the beads. The resulting emission is detected by two avalanche photodiodes. This process is essential to be able to differentiate between the different bead regions and therefore also to distinguish different analytes in a multiplex application. Bead aggregates and air bubbles are gated out and side scattering is employed for the gating of single beads. The reporter fluorophore R-Phycoerythrin is excited by a second, green laser using a wavelength of 532 nm. The emission is detected by a photomultiplier (PMT) and the reporter signal is quantitated by digital signal processing. Usually, between 50-100 beads are analyzed per bead-ID and well. The results are presented as the median fluorescent intensity (MFI) [10].

Different immunoassay formats can be performed using xMAP technology, with competitive assays, serological assays and immunometric assays, also referred to as sandwich immunoassay, the most common types [10]. This name, sandwich immunoassay, perfectly describes the assay format, as the analyte to be detected is located between a capture antibody and a detection antibody, thus forming a sandwich. The capture antibody is, for this purpose, irreversibly immobilized onto a solid phase, which corresponds to the microspheres' surface. During incubation of coated beads and sample, the capture antibody binds specifically the analyte of interest. Afterwards, a second analyte-specific antibody is added which is linked to a detection system for signal generation, also called tracer. In case of xMAP technology the detection antibody is linked to biotin. After further incubation, the excess of unbound labeled

antibody is washed away. Streptavidin-labelled PE (Strep-PE) that specifically binds the biotin tag on the detection antibody, is added and after further incubation, the signal is measured in a FLEXMAP 3D instrument. **Figure 1** illustrates the general set-up of a sandwich immunoassay and the basic detection procedure based on xMAP technology.

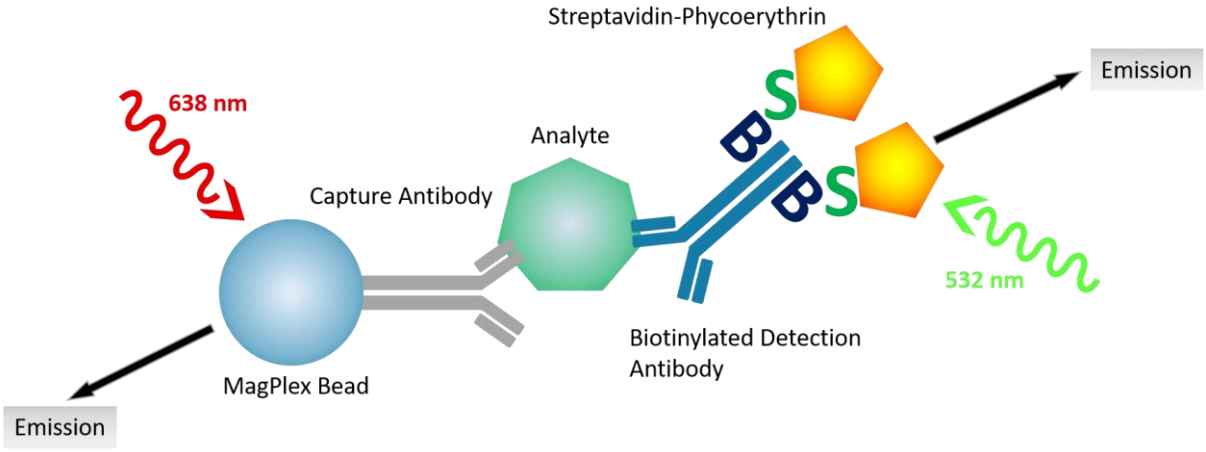

Figure 1: Setup of a bead-based sandwich immunoassay and illustration of laser-based detection. *Paramagnetic polystyrene microspheres, so called MagPlex Beads, are coated with analyte-specific capture antibodies. These specifically bind their epitope of the analyte. After addition of the detection antibody, a second antibody linked to biotin, the detection system is finalized by adding streptavidin-phycoerythrin that specifically binds to biotin on the detector. In a flow cell of the FLEXMAP 3D instrument, the beads are separated and bypass two lasers. While the red laser (638 nm) excites the fluorophores of the beads, the green laser (532 nm) excites phycoerythrin. The respective resulting emissions are recorded by a detection system.*
(Adapted from figure 1A in [15])

1.3 Single molecule-array technology (Simoa, Quanterix)

Some biomarkers are only present in very low amounts in different sample matrices exceeding the sensitivity of the described xMAP technology, meaning that a more sensitive immunoassay is required. When this occurs, the single molecule array (Simoa) technology of the company Quanterix Corporation (Billerica, MA, USA, www.quanterix.com) can be applied. Simoa technology is a bead-based, highly sensitive immunoassay platform employing an enzymatic reporter, analogue to the conventional ELISA. However, in contrast to the conventional ELISA, Simoa uses femtoliter-sized reaction chambers. While conventional ELISAs demand for the detection of a multitude of protein molecules in assay volumes in the µL-to-mL-range [16], Simoa enables the isolation of single enzyme molecules in an extremely small reaction volume (50 fL) permitting the detection of very low sample concentrations (low $pg \cdot mL^{-1}$ range or below) [16-19].

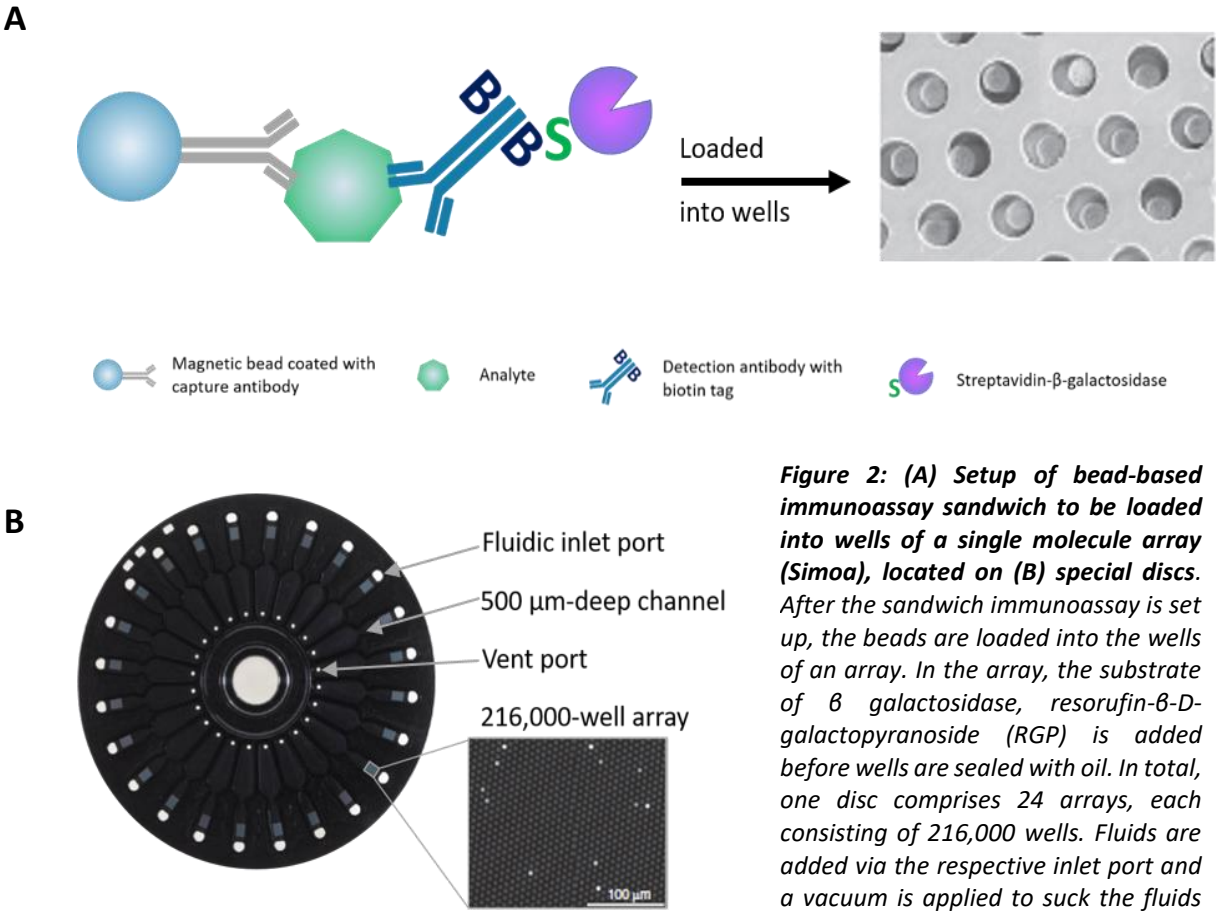

(Adapted from figure 1A and C in [18] and figure 2B in [20])

***Figure 2: (A) Setup of bead-based immunoassay sandwich to be loaded into wells of a single molecule array (Simoa), located on (B) special discs**. After the sandwich immunoassay is set up, the beads are loaded into the wells of an array. In the array, the substrate of β galactosidase, resorufin-β-D-galactopyranoside (RGP) is added before wells are sealed with oil. In total, one disc comprises 24 arrays, each consisting of 216,000 wells. Fluids are added via the respective inlet port and a vacuum is applied to suck the fluids into the array.*

For Simoa, the analytes of interest are captured by binding to paramagnetic beads of 2.7 µm in diameter, which are coated with antibodies specific for the target protein. A sandwich antigen-antibody-complex, as already described for the xMAP technology, is formed after a biotinylated detection antibody is applied. These sandwich complexes are enzymatically labeled with the enzyme conjugate streptavidin-β-galactosidase (SBG) that specifically binds to biotin or the biotinylated detector antibodies. After the application of the detection system, beads are loaded into the wells of an array. The setup of the sandwich immunoassay as well as a schematic section of the wells of an array is presented in **Figure 2A**. The arrays are located on a disc, which contains 24 arrays, each consisting of 216,000 individual femtoliter-sized micro wells bonded to a microfluidic manifold [19, 21]. The disc and its structure is shown in **Figure 2B**. For analysis, the microspheres are supplied with resorufin-β-D-galactopyranoside (RGP) which is cleaved by β-galactosidase-catalyzed hydrolysis into a fluorogenic substrate (resorufin) and D-galactose. The arrays are sealed with a fluorocarbon oil in order to remove aqueous solution and excess beads outside the arrays. Further, a liquid-tight seal is generated

covering the wells containing the beads and enzyme substrate enabling the accumulation of the fluorescent signal from single enzymes. Standard detection technologies, such as plate readers are unable to detect these low concentrations in conventional immunoassays as ELISAs, as the fluorophores generated diffuse into a large reaction volume (Simoa approx. 50 fL vs. µL-mL-range conventional ELISA). This means, hundreds of thousands of enzymatic tracers are necessary to generate a signal that contrasts with the background. With the Simoa technology, generated fluorophores are restricted to a very small reaction volume rapidly leading to high enrichment. The resulting signal is detected by using a CCD (= charge coupled device) camera and a white light illumination source [18, 19].

Simoa technology is also suitable for multiplexing approaches. Similar to the xMAP technology, beads can be distinguished from each other by combining three different fluorescent dyes - Alexa Fluor 488, Cy5 and HiLyte Fluor 750 – in different ratios. In contrast to MagPlex beads, these beads do not possess an internal dye but are dye-coded by reaction of different amounts of a single hydrazide dye with paramagnetic beads functionalized with carboxyl-groups [19, 22].

The detection of the signal generated in the single molecule array follows sequential steps. After focusing, image acquisition is carried out in seven steps. Initially (step 1), an image is acquired to determine in which wells of the arrays beads are located. Following this (step 2), an "Image at time point 0" is generated. Between this image and an image, generated 30 seconds later (step 6), an increase in fluorescence must be detectable in order to be evaluated as a signal. As steps 3 to 5 and 7, additional images are generated which serve to identify the fluorescence-labelled beads [19]. Since the readout in the Simoa instruments is automated, a strict time sequence of the assay process steps ensures reproducibility of the signal strengths.

The success of Simoa is not only due to the high sensitivity resulting from signal amplification in an extremely small reaction volume, but also to the wide dynamic range it offers. For the detection of low analyte concentrations, with very low ratios of enzyme labelled sandwich complexes to beads, a digital approach which is independent of the absolute fluorescence intensity measured for an individual bead is used. At low analyte concentrations, many beads are present without a bound enzyme (considered "off"). Beads with one (or more) bound enzymes (considered "on") are counted (digital approach) and used in relation to the total bead count using the Poisson distribution to determine the average of enzymes per bead

(AEB). However, at high analyte concentrations, when the majority of beads have bound one or more analytes and thus may carry multiple enzymes, the AEB value is determined by the averaged fluorescence intensity. This is the analogue approach. By combining both detection approaches with Simoa technology, both very low and high analyte concentrations can be detected, as this extends the dynamic range [16].

Currently, several instruments from Quanterix are on the market for performing Simoa assays. In addition to the fully automated HD-X device, there is the SR-X device (used in this work), a bench-top cost-effective alternative. SR-X Simoa assays are performed manually, whereby the addition of the enzyme complex (SBG), followed by several washing steps, represents the final manual step. All further processing steps (RGP addition and sealing) as well as the readout are carried out fully automated by the SR-X instrument. A corresponding Simoa microplate washer is provided for the device, which takes over the respective washing steps with corresponding wash buffers. The device is suitable for processing 96-well plates.

1.4 Immunoassay validation

Assay validation is performed to demonstrate that reliable results are generated and to confirm that the particular method is suitable for its specific intended use. The aim of the process of validating methods is to provide objective proof that certain requirements, such as assay quality and accuracy, are met [23-26].

Regulations are provided by national and international legal authorities for method validation processes (e.g. European Medicines Agency (EMA) [23], U.S. Food and Drug Administration (FDA) [24]). Both, the EMA and FDA regulations are suitable for the validation of bioanalytical methods, with the 2018 FDA regulation increasingly addressing ligand binding assays. Both regulations and the validation parameters and methods of determination described therein can be used as guidance for defining the scope of a validation. In addition, individual requirements and demands of an assay must be taken into account. Often it is not useful, necessary or possible to follow all points of these guidelines, but to use specific aspects of them.

The scope of a method validation depends largely on the intended field of application of the bioanalytical method. For example, if a method is to be applied in an early phase of research and development, with focus on fast turnaround of results, a full validation considering all proposed parameters is not necessarily required or useful. By contrast, the use of a method

in the GLP area of clinical studies absolutely requires full validation [27]. Therefore, a iterative and practical “fit-for-purpose” approach is suggested for method validation taking into account the intended area of use of the measurement data, at the same time considering the regulatory terms and conditions necessary for this use [28]. In course of a basic validation for a “fit-for-purpose - research and development (R&D)” immunoassay, it is considered necessary to experimentally investigate or determine at least the following validation parameters: the calibration curve model, limits of quantification, limit of detection, precision (intra and inter assay precision), dilution linearity, parallelism and analyte stability (short-term and stability to freezing and thawing processes).

1.4.1 Model of the calibration curve

To determine the concentration of an analyte of interest in a biological sample matrix, calibration curves are employed. Calibration curves, also known as standard curves, represent the relationship between a signal generated in an immunoassay and the reference concentration of the standard that is assumed to represent the analyte of interest in a sample matrix [29].

As the accuracy of the quantification of the analyte of interest is dependent on the reproducibility and the robustness of the calibration curve, it is important to choose a suitable calibration model. Calibration curves of immunoassays are usually described in a non-linear relationship and most often fitted by a four- or five-parametric logistic fitting model. Other models can also be considered, but the simplest one that adequately describes the relationship between the concentration and the corresponding signal should always be chosen [24, 27-29]. For each analyte analyzed, an individual standard curve is needed. It is recommended to prepare the standard curve in the same matrix as the biological sample matrix to be analyzed in in the following intended study. Therefore, the blank matrix is spiked with a defined concentration of the target analyte. However, if the matrix already contains the analyte of interest, the generation of standard points below this endogenous concentration would negatively impact assay sensitivity, and removal of the analyte would be associated with enormous efforts (e.g. depletion) [23, 24], meaning, the matrix is only of limited suitability for the generation of the calibrator. Therefore, surrogate matrices can be applied but need to be verified and calibration curves need to be properly validated [24, 28]. A calibration curve should consist of at least six known calibrator concentrations and an

additional blank value, meaning a plain sample matrix without the analyte [23]. Besides this, an additional criterion for generating a continuous and reproducible calibration curve is a proper weighting scheme. As for most immunoassays, the standard deviation of the assay signal generated is not constant. Instead, it increases between replicate signals proportional to the mean of the signal. To decrease these errors, weighting functions such as $1/X$, $1/X^2$, $1/Y$ or $1/Y^2$ are applied to correct for the diverging standard deviations [24, 28, 29].

1.4.2 Quantification limits and dynamic range

The dynamic range of an assay, also defined as reportable range, is the area of the standard curve between the lower and upper limits of quantification. In between these limits, the analyte of interest can be assessed with acceptable accuracy and precision [25]. The definition of the lower limit of quantification (LLOQ) is the lowest concentration of the analyte of interest for which quantification can be reliably performed. By analogy, the upper limit of quantification (ULOQ) corresponds to the highest concentration of the analyte of interest that can be quantified with the necessary reliability. In this context, reliability refers to the accuracy achieved, which is expressed by the recovery or the relative error with respect to the nominal concentration, as well as to the achieved precision assessed by the coefficient of variation (CV) [23-25, 28]. It is recommended that the respective upper and lower limit of quantification correspond to the highest and lowest calibration concentrations. Further, so-called anchor points can be applied. These are points outside the dynamic range that may be beneficial when performing curve-fitting leading to a better precision and accuracy. They are not suitable to be defined as part of the acceptance criteria used during a measurement [23, 24, 27-29].

1.4.3 Limit of detection

The limit of detection (LOD) is defined as the lowest qualitatively detectable concentration of the target analyte. This means, it is the lowest concentration possible to be distinguished significantly from the background signal. The LOD is determined by calculating the average of the background signal and adding its two- or three-fold standard deviation [27, 28].

1.4.4 Precision

According to official directives, the definition of precision is the degree of agreement of replicate independent measurements of the target analyte [23, 24]. Precision, indicated as CV,

is expressed as the ratio of standard deviation of measured values to their mean in percent. For the determination of intra assay precision, validation samples (VS) with a defined concentration in the upper, lower and middle part of the calibration curve are measured in replicates within a single run. Same samples are analyzed between different runs for each analyte generating inter assay precision values [23-25, 28].

1.4.5 Dilution linearity

Dilution linearity allows the accurate measurement of the target analyte in a biological sample matrix present at concentrations above the ULOQ. Such a sample must be diluted to obtain signals within the given dynamic range of the assay. Thereby, the analyte of interest can be accurately quantified. This means the dilution linearity demonstrates whether the relation of signal to the concentration of the analyte in the sample matrix is linear within the range of the calibrator. Further, the event of a possible prozone or "hook effect" could be detected (excess antigen binds both the capture and detection antibodies before a sandwich-complex can be formed). In this case, signal suppression occurs due to high analyte concentrations. Dilution linearity is determined by spiking biological matrix with calibrator protein in a concentration 100-1000-fold above the ULOQ. Afterwards, this mix is linearly diluted in assay buffer into the range of the standard curve [23-25, 28].

1.4.6 Parallelism

In order to detect potential matrix effects or possible interaction between critical reagents or metabolites in an assay, parallelism experiments are performed. It is investigated whether the parallelism between the calibration curve and the concentration-signal relationship of a target analyte in a serially diluted sample is given. If so, it can be assumed that the binding characteristics of the native protein in the biological sample to the antibodies used in the immunoassay are comparable to those of the calibrator protein. Parallelism experiments are performed by using biological samples with high endogenous analyte concentrations. These are serially diluted in assay buffer to be assessed within the dynamic range of the calibrator. If possible, the endogenous concentration should be beyond the ULOQ. Although dilution linearity and parallelism are quite comparable in regard of implementation, the main difference is that no spike of recombinant protein is allowed for investigating parallelism, because the behavior of endogenous protein being diluted is tested. A significant deviation of

parallelism is considered invalid [23-25, 27, 28, 30] as it means that the protein in a sample behaves differently through dilution than the standard protein in the matrix used to produce the standard curve and results from differently diluted samples cannot be compared.

1.4.7 Analyte stability

The stability of the analyte in the biological sample matrix is a further validation parameter to be evaluated. Analyte stability is determined under specific conditions of storage and use that could influence the measurement results. For example, handling and storage procedures and conditions could affect the physicochemical stability and therefore influence the measured concentration of the analyte in the matrix. Investigation of stability is performed by using VS containing endogenous analyte and should cover short-term and freeze-thaw stability. Short-term (bench top) stability investigates the analyte stability at room temperature (RT) and at 4 °C, corresponding to the storage on ice and on the lab bench, during sample preparation. Duration of the incubation at the different conditions needs to be adjusted to minimally reflect the actual length of sample preparation. Determination of freeze-thaw stability is necessary, as for example some measurements require to be repeated more than once to get analytes into the dynamic range of the standard curve, especially in regard of multiplex analysis. Therefore, several freeze-thaw cycles may be required in addition to extended evaluation of short-term stability. Stability is assessed by determining the recovery rate of stability test samples exposed to respective mentioned conditions in relation to an untreated reference sample [23-25].

1.5 Cytokines and chemokines

Cytokines are small proteins with a molecular weight around 25 kDa. Various cell populations all over the body release cytokines as a response to an activating stimulus. Cytokines trigger further reactions via binding to their specific receptors and contribute to cellular signaling. Based upon their half-life and their ability to be released into the blood stream, cytokines can act in different ways. For example, cytokines can act on responsive cells in the direct neighborhood of the secreting cell (paracrine), or, they can influence cells at greater distance (endocrine). Further, cytokines may affect the cell that secreted them (autocrine) [31]. Released cytokines serve communication between cells and have specific effects on cell-cell interaction. Thereby, different cell types can release the same cytokine to affect different cell

populations. Additionally, different cytokines may have comparable functions and can act synergistically or antagonistically. They are most often released in cascades, meaning that the secretion and action of one cytokine stimulates a responsive cell, which further produces cytokines. The predominant producers of cytokines within the immune system are macrophages and helper T cells [32]. Cytokines can also be classified as either pro-inflammatory as they are capable of favoring the inflammatory process by leading to events like the recruitment of circulating leukocytes and boosting their specific activities, proteolysis or increasing vascular permeability. Or they are defined as anti-inflammatory, as they can repress pro-inflammatory events and therefore limit inflammatory events in order to regulate immune response [33].

Chemokines represent a group of cytokines ranging from 7 to 15 kDa in size and are secreted mainly in the first phase of an infection in the affected tissue. They induce a directed chemotaxis of responsive cells nearby that migrate to the area of the local event, meaning they act as recruiters of effector cells [31, 34]. This family, together with their receptors control not only the chemotaxis of immune cells, but also their residence. Chemokines can be grouped in pro-inflammatory and homeostatic chemokines. While pro-inflammatory chemokines are released at the site of infection as part of an immune response, the latter is able to control cell migration in terms of tissue development and maintenance [34, 35].

Taken together, cytokines and chemokine span a network of immense complexity through which the different cell populations communicate with each other, coordinate and perform their tasks. A highly simplified example of the network between immune cells present in whole blood is shown in **Figure 3**.

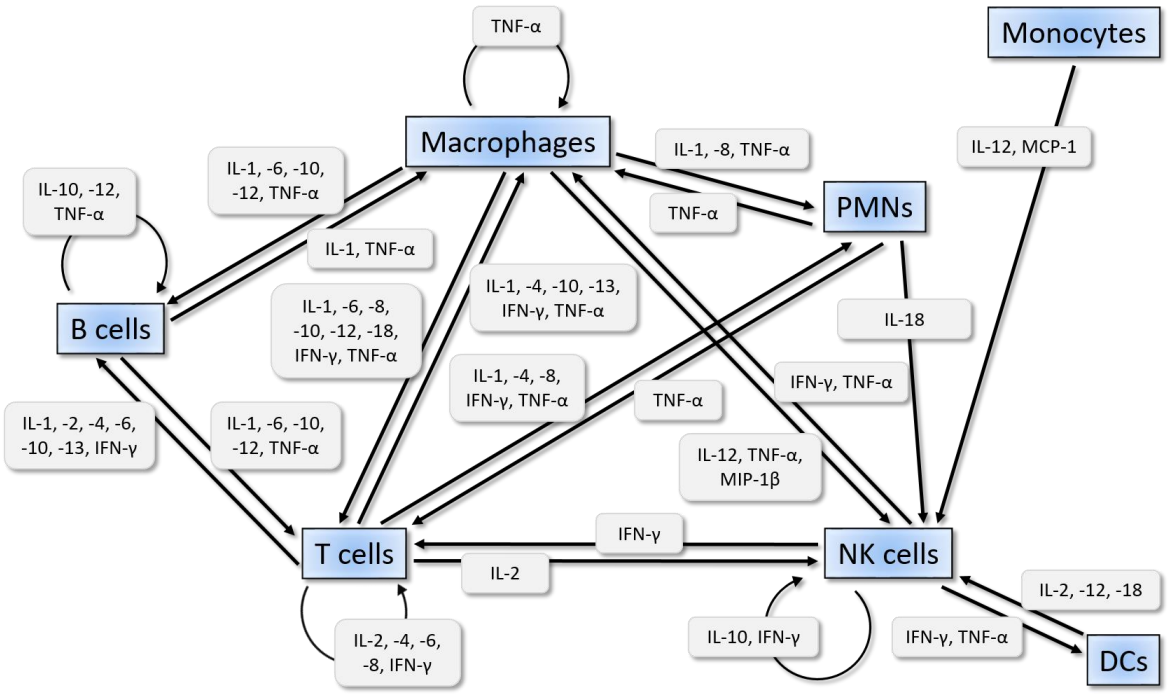

Figure 3: Cytokine and chemokine network between immune cells. *The figure contains only selected cytokines and chemokines that are relevant in the further course of this thesis, which is why only a small section of the highly complex interrelationships is presented. (DCs = dendritic cells; NK = natural killer cells; PMNs = Polymorphonuclear neutrophils). (Adapted from figure 1 in [32] and supplemented by [36, 37])*

In the following section, some pro- and anti-inflammatory cytokines and chemokines, which are relevant to this thesis, are briefly described with their most important activities mentioned.

IL-1β is a representative of the group of pro-inflammatory cytokines. It is an essential player in the host-defense response towards infection and tissue damage. Within the IL-1 cytokine family, which consists of eleven members, IL-1β is the best characterized and studied. As a pleiotropic cytokine, IL-1β affects a multitude of cell types and is secreted by a variety of cells. Even though macrophages and monocytes represent the predominant producers of the cytokine IL-1β, dendritic cells (DC), B lymphocytes (B cells), neutrophils and natural killer (NK) cells are also capable to produce IL-1β [38]. IL-1β is available at low concentrations under usual conditions and requires induction to be produced and secreted [39-41]. In order to control homeostasis, IL-1β production and secretion are tightly regulated. If this regulation is disturbed or lost, syndromes characterized by fever, skin rash and arthritis occur [41, 42].

While **IL-6** was first reported as a factor to stimulate B cells [43], its pleiotropic character, which fulfills a variety of functions during the immune response as the regulation of acute phase response, T lymphocyte (T cell) activation and the expansion of T cell populations [44,

45] has since then been discovered. Besides its multiple roles in coordination and regulation of the immune system, IL-6 is also involved in metabolism [46] and the nervous system [44, 47, 48]. IL-6 cannot be classified as either pro- or anti-inflammatory cytokine as it has both – pro- and anti-inflammatory properties [44]. Many cell types are able to produce IL-6 including monocytes, macrophages, T cells, B cells, granulocytes, endothelial cells, fibroblasts and many others [48, 49].

IL-8 or CXCL8, as it is part of the CXC chemokine family (CXC chemokines as their amino terminus possess two cysteines which are separated by one further amino acid, displayed as "X"), represents a potent chemotactic factor for neutrophils, but also for the attraction of basophils and T cells in context of immune response, but not for monocytes. During inflammation, it is secreted predominantly by monocytes, macrophages, and neutrophilic granulocytes. Beyond inflammation, IL-8 is comprising many functions related with mitogenesis, neutrophil degranulation, leucocyte activation and calcium homeostasis [34, 50, 51].

Two further chemokines that belong to the so-called CC chemokine family (CC chemokines as their amino terminus possess two adjoining cysteines) are **MIP-1β** (macrophage inflammatory protein-1 beta) and **MCP-1** (monocyte chemoattractant protein-1), which are named CCL4 and CCL2, respectively. MCP-1 is a powerful attractant for monocytes and a weak inducer of monocytic cytokine expression. It further is engaged in regulating T cell and NK cell migration [52]. Stromal cells that are activated by binding of molecules to pattern-recognition receptors (PRR) or by cytokines are able to quickly produce MCP-1 to rapidly recruit monocytes to the place of infection [34, 53]. Although a multitude of cells constitutively produce MCP-1, or upon induction [52], the main source of MCP-1 are macrophages and monocytes [52, 54, 55].

Specific regulators can induce the production of MIP-1β in several hematopoietic cells. Production can be induced in monocytes [56], T cells [57], B cells [58], NK cells [59], DCs [60] and neutrophils [61], but also in non-hematopoietic cells [62]. Several pro-inflammatory agents and cytokines can act as potent inducers of MIP-1 induction, such as lipopolysaccharide (LPS), TNF-α (tumor necrosis factor-alpha), IFN-γ (Interferon-gamma) and IL-1α/β, but also viral infection [63]. MIP-1β is, together with its family member MIP-1α (CCL3), produced and released by activated macrophages in order to recruit further pro-inflammatory cells and also macrophages themselves to the point of inflammation [63].

TNF-α was first reported in 1975 as a serum factor which was induced by the endotoxin LPS leading to hemorrhagic necrosis of sarcomas in mice [64]. Since then, the important role of TNF-α in several inflammatory, infectious and malignant processes has been shown [65]. As a highly pleiotropic cytokine, TNF-α has mainly pro- but also anti-inflammatory effects [66]. It is an early mediator of immune response and is released by macrophages in the course of first-line defense against infectious pathogens [67]. Its pro-inflammatory properties are also associated with diseases comprising for example rheumatoid arthritis [68], psoriatic arthritis [66], Crohn's disease [69], multiple sclerosis [70] and others. However, an immunosuppressive property of TNF-α has been shown in connection with autoimmune diseases, as well [71-74]. Furthermore, in studies with TNF-α-deficient mice, it was found that TNF-α has a regulatory effect on the inflammatory response and can reduce its duration and extent by acting on the macrophage-based production of IL-12 [75]. Primarily TNF-α is produced and expressed on the plasma membrane of activated macrophages and T cells. The protease TNF-α converting enzyme (TACE), a matrix metalloprotease, sheds the extracellular domain, leading to a soluble form being released. Both forms, the soluble and the membrane-bound form are active [31, 65, 76]. TNF-α interacts with the two receptors TNFR1 and TNFR2 on the surface of cells [77]. Further, TNF-α is also produced by NK cells [65] and has an effect on NK cell activation and the corresponding IFN-γ production [78].

IFN-γ was first described in 1965 [79]. It is a pleiotropic cytokine regulating and controlling effects of innate and adaptive immunity [80]. It is released predominantly by activated T lymphocytes [80-83] and NK cells [80, 84, 85]. IFN-γ coordinates the recruitment of leukocytes, growth as well as the maturation and differentiation processes of a variety of cell populations [86-89]. It is also involved in the regulation of B cell-based immunoglobulin production and in the switch of the immunoglobulin classes [86, 87, 90]. Additionally, IFN-γ is known to be an enhancer of NK cell activity [86, 91].

IL-12 is a pro-inflammatory cytokine comprising two different subunits (heterodimeric), alpha (p35) and beta (p40) which are linked via disulphide bonds to form the biological active component IL-12p70 [80, 92]. B cells, DCs and macrophages upon microbial infections release this cytokine [93-95]. Besides its function in stimulating cytolytic activities of NK cells, and cytotoxic T cells, it enhances antigen presentation [80, 96] and triggers IFN-γ production in NK cells and T cells [93].

IL-4 and **IL-13** are involved in the regulation of not only the responses towards parasites or allergens of lymphocytes but also of myeloid cells and non-hematopoietic cells after an inflammatory response. Primarily, both cytokines are produced by CD4 positive T cells but are also secreted by basophils, eosinophils, mast cells and other immune cells [97]. IL-4 and IL-13 affect B cells by either increasing their proliferation (IL-13) [98] or switch B cells to an IgE-producing cell (IL-4) [98, 99]. Further, they induce alternative macrophage activation that differs from the classical pro-inflammatory pathway [99, 100]. IL-4 is also known to be an inducer of the differentiation process of naïve CD4 T cells into Th2 cells [97].

IL-10, also named "cytokine synthesis inhibitory factor" (CSIF), represents a further anti-inflammatory cytokine. As a pleiotropic cytokine, it influences the activity of many immune cell populations. Many cells such as activated T cells, monocytes, macrophages, DCs, NK cells and B cells primarily produce IL-10 [101-104]. As an anti-inflammatory cytokine, IL-10 is capable of suppressing expression levels of inflammatory cytokines including for instance IL-1, TNF-α and IL-6 that are mainly produced by activated monocytes. Further, IL-10 is able to down-regulate pro-inflammatory receptors and to up-regulate further anti-inflammatory cytokines [32]. In addition, IL-10 can affect DCs and CD4 T cells. Depending on the kind, site and stadium of infection, different cell populations release IL-10. This decisively determines the effect of IL-10 in terms of regulation [105].

IL-1Ra (IL-1 receptor antagonist) is a further member of the IL-1 cytokine family. As its name suggests, it acts as an inhibitor to IL-1α and IL-1β by binding IL-1 receptor 1 (IL-1R1) and blocking the binding sites for the two agonists but without inducing any intracellular response. In many cell types, the production of IL-1α and IL-1β induces the expression of IL-1Ra but also LPS or IgG complexes are capable of acting as stimuli for IL-1Ra induction. Other anti-inflammatory cytokines (e.g. IL-4 and IL-10), can reinforce the process of induction caused by different signals. Two types of IL-1Ra exist. The first one, sIL-1Ra, is 17 kDa in size and is secreted from various immune cells like macrophages, monocytes, neutrophils. The other form, icIL-Ra, is 16 kDa in size and remains within cytoplasm of keratinocytes and other epithelial cells, monocytes, and fibroblasts [41, 106]. After cell death, the second, icIL-1Ra, is set free, extracellularly acting on IL-1R1 [41, 107].

GM-CSF (granulocyte/macrophage colony-stimulating factor) and **M-CSF** (macrophage colony-stimulating factor), as their names suggest, were shown to be capable of forming colonies of matured myeloid cells *in vitro* derived from bone-marrow progenitors after these

cells have proliferated and differentiated. The resulting colonies were composed of macrophages and granulocytes after stimulation with GM-CSF and macrophages after treatment with M-CSF [108-110]. It is suggested that CSFs (GM-CSF, M-CSF together with G-CSF = granulocyte colony-stimulating factor) are part of a network during inflammatory events defining the inflammatory response [109, 111]. Under normal conditions, M-CSF is available in measurable concentrations and is produced by several cells as fibroblasts, endothelial cells, macrophages, and smooth muscle cells. The expression of GM-CSF, on the other hand, requires stimulants such as LPS, TNF-α or IL-1 in order to be captured in detectable concentrations. While GM-CSF is able to support survival and activation of macrophages, neutrophilic and eosinophilic granulocytes and DCs, M-CSF can only foster the macrophage lineage effecting their survival, proliferation, differentiation and activation [109].

1.6 TruCulture whole blood culture system

Peripheral blood mononuclear cell (PBMC) preparations and subsequent cultures are frequently used to investigate cytokine release to answer various immunological questions. This primary cell culture model consists of lymphocytes, monocytes, and macrophages, which are purified from peripheral blood prior to their use in culture. This step is time-consuming and requires special equipment and training and it introduces physical cell stress within the sample. As the results of natural cell-to-cell communication between the mononuclear cells and those elements of the human immune system are eliminated during PBMC preparation (granulocytes, platelets, soluble factors), artificially skewed results may be observed from PBMC culture experiments. A comparatively more suitable culture model is a whole blood culture systems, like the TruCulture system [112]. This involves blood collection tubes, pre-filled with a particular cell culture medium, into which blood is drawn followed by a subsequent culture of all blood cells. At the end of the culture period, cellular components are separated from the supernatant and cells and supernatant can be subsequently analyzed. TruCulture whole blood assay thus not only represents a time and labor-saving method, but also provides a more complete picture of cytokine release and associated cell interactions and immunological effects through the presence of all immune cells in the peripheral blood. Consequently, it is more likely to reflect what is happening *in vivo* compared to PBMC cultures. To perform specific target cell activations of, for example, monocytes and T cell subtypes, TruCulture tubes are available with or without appropriate stimulants [113].

1.7 Natural killer cells

In the 1960s, NK cells were accidentally discovered during an attempt to characterize T cell-mediated cytotoxicity [114-117]. Within the following decade, this cell population was identified to be a lymphatic cell population that is cytotoxic by nature without the requirement of prior contact to an antigen [114, 118, 119]. NK cells are large granular innate lymphocytes [31] residing in lymphoid and non-lymphoid tissues as bone marrow, lymph nodes, tonsils, liver, gut, skin, and lungs [114, 120]. NK cells make up between 5 and 20 % of circulating lymphocytes and are defined based on the presence and absence of specific surface markers as $CD16^+$ $CD56^+$ $CD3^-$ [121]. Upon activation, NK cells respond with cell killing and cytokine secretion to target cells, which are physiologically stressed corresponding to cells undergoing malignant transformation or that have been infected by viruses or other intracellular pathogens.

1.7.1 NK cell receptors

The stimulation of NK cells and the resulting effector functions are dependent on signals, which are derived from two different receptor types – inhibitory and activating receptors.

Inhibitory receptors bind predominantly major histocompatibility complex (MHC) class I molecules as their ligand, which are abundantly expressed on the surface of normal healthy cells. MHC class I molecules function as markers for “self” and therefore their binding to inhibitory receptors leads to self-tolerance of NK cells. Contrary, cellular stress caused by viral infection or neoplastic transformation as response to damaged DNA, senescence programming or tumor suppressor genes leads to the loss of MHC class I molecules on the cell surface. At the same time, ligands for a second type of receptors, known as activating receptors, can be upregulated and the signal generated by activating receptors shifts the NK cells into the state of activation [122, 123]. An activated state can also result from a constant signal from activating receptors alone or when the signal from activating receptors overwhelms that from inhibiting receptors. In the latter case, there is a shift in the equilibrium, which leads to NK cell activation as well [124-127].

Activating receptors are necessary as lack of MHC I molecules on NK-target cells is insufficient to induce effector functions in NK cells and as already mentioned these ligands of activating receptors are induced by cellular stress [122]. Most receptors involved in the regulation of NK cell activation belong to two major structural families - the killer cell immunoglobulin-like

receptor (KIR) family and the killer cell lectin-like receptor (KLR) family. Both receptor types - activating and inhibitory receptors - come from the same structural families. The decisive factor for whether a receptor has an activating or inhibitory effect is the presence of specific signaling motifs. While inhibitory receptors carry a long cytoplasmic tail containing an immunoreceptor tyrosine-based inhibition motif (ITIM), activating receptors carry short cytoplasmic tails without an ITIM sequence. Instead of these, activating receptors possess a charged residue within their transmembrane region, which binds to accessory signal pore proteins, like DAP12, CD3ζ and FcRγ [31, 114]. These transmembrane proteins have an immunoreceptor tyrosine-based activation motif (ITAM) sequence in its cytoplasmic domain. Through the continuation of the corresponding signaling pathways, signals are either inhibited or corresponding effector functions are triggered, which places the NK cell in an inhibited or activated state [31].

1.7.2 NK cell effector functions

Upon activation, different effector functions by NK cells are triggered to deal with target cells. Either these target cells are eliminated by cytotoxicity mediated by NK cells or they are indirectly targeted through pro-inflammatory cytokines secreted in high amounts by NK cells. Two mechanisms contribute to the cell destruction process, direct cytotoxic NK cell response and death receptor ligation mediated apoptosis.

Direct cytotoxic NK cell response occurs through the release of lytic molecules. This process consists of four major steps. At first, an immunological synapse (alternatively described as immune synapse), is formed between a NK cell and the cell to be targeted. Almost simultaneously, the actin cytoskeleton is reorganized within the NK cell for lysosome transportation. Then, as a second step, polarization of the microtubule organization center (MTOC) and the secretory lysosome towards the immune synapse follows. Thirdly, the secretory lysosomes docks with the NK cell cytoplasmic membrane before it fuses in step four with the target cell membrane and the lytic and therefore cytotoxic molecules, like perforin and granzymes, are released. This process is also named degranulation [122]. Perforin is a glycoprotein that polymerizes and forms pores after its release into the target cell, therefore facilitating the access of granzymes [114, 122]. Granzymes display, together with perforin and granulysin, the main cytotoxic components of the secretory granules of NK cells, but also cytotoxic T cells. The granyzme family contains five members – granzyme A, B, H, K and M –

and are serine proteases that are capable of activating caspase molecules and therefore leading to apoptosis of the target cell [122, 128-130].

Death receptor ligation mediated apoptosis acts via death receptors expressed on the surface of the plasma membrane of target cells. Among these receptors are TNF-related apoptosis-inducing ligand receptor (TRAIL-R) and Fas (CD95) which are activated upon binding of their appropriate ligand, Fas ligand (FasL, CD95L) and TRAIL. These ligands are expressed on the surface of NK cells [114, 131]. The activation of death receptors initiates the extrinsic apoptotic pathway by employing a cytoplasmic death domain that enables the activation of apoptosis using initiator caspases-8 and 10 [114, 132, 133].

The **production of pro-inflammatory and immunosuppressive cytokines** upon activation represents the third effector function of NK cells. Although a variety of cytokines are secreted, NK cells predominantly produce IFN-γ, TNF-α and GM-CSF as these cytokines enable T cell activation and activation of other immune cells of the innate immune system, including macrophages, DCs and neutrophils. Further, NK cells produce and release chemokines including MIP-1β, RANTES, and IL-8 [114, 134, 135]. Having antiviral, antibacterial, and antitumor activity, IFN-γ is, together with TNF-α, one of the key players among cytokines secreted by NK cells. IFN-γ was also reported to modulate not only the expression of caspase but also of ligands corresponding to death receptors on the NK cell surface therefore contributing to the process of death receptor ligation mediated apoptosis [122, 136].

1.7.3 NK cell stimulation

The regulation of NK cell activity is not only based on the balance between activating and inhibiting receptor signals, but also on stimulation by certain cytokines.

It has been known since about 1980 that NK cells isolated from bone marrow can be activated by the addition of IL-2, which then act cytotoxically [137-139]. Although the high affinity receptor IL-2Rα (CD25) of IL-2 is only expressed on activated NK cells, IL-2 can interact through complexes of the common gamma (γ_c) chain and IL2Rβ subunit [140] supporting NK cell proliferation, differentiation, survival and acquisition of cytotoxic potential [137] by pushing the production of lytic molecules [141]. Further, IL-2 contributes in synergy with IL-21 to the expression of receptors that occur on the NK cell surface upon activation like NKG2A, CD25, CD69, CD86 as well as of lytic molecules what in turn supports cytotoxic effector function [142]. It is supposed that IL-2 released by T cells, that are found in the close neighborhood of

NK cells, provides the interaction between innate and adaptive lymphocytes during infection [143]. This, in combination with the fact that IL-2 is mainly produced as a result of immune system stimulation, underlines the role of IL-2 acting as primer for NK cell activity [137]. As an example, R848 also named Resiquimod, which is a human Toll-like receptor 7 and 8 (TLR7/8) agonist, needs NK cell priming by either IL-2 or IFN-α to be able to activate resting NK cells which are non-responsive to R848 itself [144].

R848 is a further stimulus for NK cell activation. Toll-like receptors (TLR) are important structures of the innate immune system and are able to identify conserved structures of pathogens [145]. Human TLR7 and TLR8 respond to single-stranded RNA as their ligands [146]. It was shown that NK cells also respond through TLRs but effector functions as response to TLR7/8 agonist were mediated mainly by accessory cells like monocytes. Already very low numbers of accessory cells enabled potent NK cell stimulation by R848. The activation of NK cells was triggered directly by R848 binding to TLR7 and TLR8 resulting in high production levels of IFN-γ in purified NK cells. But also indirect activation of NK cells by IL-12 secreted by R848 stimulated monocytes led to NK cell activation accompanied by increased cytotoxicity and high IFN-γ production [144].

This reveals IL-12 as an additional potent stimulus for NK cell activation. IL-12 can be provided to NK cells either by DCs or, as already mentioned, by activated monocytes and macrophages [93]. IL-12 can, in synergy with other cytokines as IL-2, IL-15 and IL-18, lead to highly increased IFN-γ production in NK cells [147]. While IL-18, which belongs to the IL-1 cytokine family, alone is not able to increase the IFN-γ production it provides a kind of “third signal” to NK cells leading to NK cell effector function in combination with IL-12 signaling [114].

These stimuli are commonly used for the investigation of NK cell activity and related effector functions in cell culture.

A further trigger for the assessment of NK cell cytotoxicity is K562 cells. These lymphoblasts were initially isolated from bone marrow of a patient suffering on chronic myelogenous leukemia in the age of 53 [148]. The cell line is commonly used as NK cell-sensitive target for *in vitro* investigations of NK cells. On the plasma membrane of K562 cells, MHC-class I molecules respectively human leucocyte antigens (HLA) molecules HLA-A, -B, and -C are not available [124, 149]. Therefore, K562 cells are also referred to as HLA-null cell line. Additionally, K562 express a variety of ligands for the two major classes of activating NK cell receptors C-type lectin NKG2D receptor (NKG2D) and natural cytotoxicity receptor (NCR) as

well as ligands for several further receptors contributing to NK cell activation [124] rendering them a perfect target for NK cell killing.

2. Aim

Inflammation is an immune response triggered, for example, by infections, physical injuries or poisoning. It results in cellular changes and pro- as well as anti-inflammatory processes which ultimately lead to the elimination of infectious agents or the repair of tissue damage. However, in some cases, inflammation may persist because either the cause could not be repaired or control mechanisms related to stopping the inflammatory response failed. Consequently, the inflammatory event may become chronic [150]. Chronic inflammation is linked to many diseases, such as cancer, autoimmune diseases, neurological disorders such as Parkinson's or Alzheimer's disease, arthritis, and many others [151, 152].

Cytokines and chemokines are mediators and regulators of these inflammatory events. Their quantification provides valuable information and contributes to the investigation and elucidation of still unclear relationships and processes related to diseases associated with chronic inflammation.

The body's response towards implants and other medical devices is also associated with pro- and anti-inflammatory events. The nature of the prevailing inflammatory processes is highly dependent on the material and its surface properties. The interactions of various immune cells with the material surface, but also among one another determine whether the implant is smoothly integrated, rejected or encapsulated in connective tissue. Such immune cell interactions are based on the release of mediators and regulators, named cytokines and chemokines, as well as on the presence of corresponding receptors on the different cell surfaces. To improve the understanding of these processes, the interdisciplinary project "Systems Immunology at Biological-Technical Interfaces" was initiated. Through the cooperation of industry, material and life sciences, physicochemical and immunological characterizations were correlated to be able to predict immunological reactivity towards a variety of implant materials, material surfaces and structures. With these findings, a causal understanding of the rejection processes could lead to improved functionality and biocompatibility of medical devices. Additionally, biomaterial surfaces could be developed for controlled implant integration.

The aim of this work was the development of a bead-based multiplex immunoassay to quantify cytokine and chemokine levels which can be used to investigate diverse immunological questions. The main scope of application was the investigation of immune responses induced by specific implant respectively biomaterials in context of the project

"Systems Immunology at Biological-Technical Interfaces". For this purpose, implant materials were cultured in three different cellular test systems with increasing complexity, reflecting the behavior of the immune system. Since the relevant inflammatory processes associated with implant materials are mainly induced by macrophages, a human macrophage monoculture of THP-1 cells served as the system of lowest complexity, followed by PBMC and whole blood cultures (TruCulture).

In the course of this work, two multiplex panels focusing on macrophage-associated pro- and anti-inflammatory processes (hereinafter referred to as inflammatory multiplex analyte panel 1 and 2 (IMAP 1 & 2)) were developed and subsequently validated for a fit-for-purpose approach considering FDA and EMA guidelines. IMAP 1 consists of nine analytes (IL-4, IL-6, IL-8, IL-10, GM-CSF, IFN-γ, MCP-1, MIP-1β and TNF-α) and IMAP 2 comprises six analytes (IL-1β, IL-1Ra, IL-12p70, VEGF, IL-13 and M-CSF).

Cytokines are often present in very low concentrations in body fluids. Thus, the sensitivity of the standard immunoassay technology is not sufficient to detect very low levels of target molecules. For this reason, three additional immunoassays were developed and validated on the ultrasensitive Simoa (Quanterix) SR-X platform. Two single-plexes were developed and validated for the analytes IL-4 and IL-12p70, supplemented by a 2-plex containing IL-6 and TNF-α.

These assays were used in combination with the expression analysis of certain surface markers via flow cytometric measurements to shed light on the question, which NK cell effector functions are triggered by certain stimulants. For this purpose, whole blood assays were stimulated with IL-12 and IL-18, as well as with IL-2 and R848 and their respective combinations. The extent to which other immune cell populations were activated in the complex culture system and whether they contributed to the immune response was assessed. In addition, the question was investigated whether K562 cells, as a natural cellular specific target for NK cells, can induce effector functions in whole blood cultures that are comparable to the default stimulant combinations used or if K562 represent possibly a more specific and therefore more suitable stimulus for NK cells. Since the whole blood assay system contains all the other leukocytes of the peripheral blood in addition to platelets and erythrocytes, it is particularly suitable for addressing these questions.

3. Material and Methods

3.1 Material

3.1.1 Antibodies

Table 1: Antibodies. *(mc = monoclonal; pc = polyclonal)*

Analyte	Species	Clonality	Vendor
Anti-Human IL-4	Mouse	mc	BD Pharmingen
Anti-human IL-4	Mouse	mc	Biolegend
Anti-Human/Primate IL-6	Mouse	mc	R&D Systems
Anti-human IL-6	Rat	mc	Biolegend
Anti-Human/Primate IL-6	Mouse	mc	R&D Systems
Anti-Human IL-6	Goat	pc	R&D Systems
Anti-Human IL-8	Mouse	mc	BD Pharmingen
Anti-Human IL-10	Rat	mc	BD Pharmingen
Anti-Human GM-CSF	Rat	mc	BD Pharmingen
Anti-Human IFN-γ	Mouse	mc	R&D Systems
Anti-Human MCP-1	Mouse	mc	BD Pharmingen
Anti-Human CCL4/MIP-1β	Mouse	mc	R&D Systems
Anti-Human CCL4/MIP-1β	Goat	pc	R&D Systems
Anti-Human TNF-α	Mouse	mc	R&D Systems
Anti-Human TNF-α	Goat	pc	R&D Systems
Anti-Human IL-1β /IL-1F2	Mouse	mc	R&D Systems
Anti-Human IL-1β /IL-1F2	Goat	pc	R&D Systems
Anti-Human IL-1Ra	Mouse	mc	Invitrogen
Anti-human IL-12/-23 (p40)	Mouse	mc	Mabtech
Anti-Human IL-12 (p70)	Rat	mc	BD Pharmingen
Anti- Human IL-12 p70	Mouse	mc	R&D Systems
Anti-Human VEGF165	Goat	pc	R&D Systems
Anti-Human IL-13	Rat	mc	BD Pharmingen
Anti-Human M-CSF	Mouse	mc	R&D Systems

Table 2: Biotinylated antibodies. *(mc = monoclonal; pc = polyclonal)*

Analyte	Species	Clonality	Vendor
Anti-Human IL-4	Rat	mc	BD Pharmingen
Anti-human IL-4	Rat	mc	Biolegend
Anti-Human IL-8	Mouse	mc	BD Pharmingen
Anti-Human and Viral IL-10	Rat	mc	BD Pharmingen
Anti-Human GM-CSF	Rat	mc	BD Pharmingen
Anti-Human IFN-γ	Mouse	mc	R&D Systems
Anti-Human IFN-γ	Mouse	mc	Mabtech
Anti-Human MCP-1	Mouse	mc	BD Pharmingen
Anti-Human TNF-alpha	Goat	pc	R&D Systems
Anti-Human IL-1Ra/IL-1F3	Goat	pc	R&D Systems
Anti-Human IL-12 (p40/p70)	Mouse	mc	BD Pharmingen
Anti-Human/Primate VEGF165	Goat	pc	R&D Systems
Anti-Human IL-13	Mouse	mc	BD Pharmingen
Anti-Human M-CSF	Goat	pc	R&D Systems

Table 3: Antibodies for flow cytometry.

Surface marker	Color	Supplier
CD4	VioBlue	Miltenyi Biotech
CD8	Viogreen	Miltenyi Biotech
CD14	BV650	Biolegend
CD19	BV711	Biolegend
CD69	BV785	Biolegend
CD25	VioBright 515	Miltenyi Biotech
CD107a	PerCP-Vio700	Miltenyi Biotech
CD62L	PE	Miltenyi Biotech
CD86	PE-Vio615	Miltenyi Biotech
CD3	PE-Vio770	Miltenyi Biotech
CD127	APC	Miltenyi Biotech
CD66b	Alexa700	Biolegend
CD56	APC-Vio770	Miltenyi Biotech

3.1.2 Recombinant proteins

Table 4: Calibrator proteins.

Recombinant protein	Vendor
Human IL-4	BD Pharmingen
Human IL-6	R&D Systems
Human IL-8	BD Pharmingen
Human IL-10	BD Pharmingen
Human GM-CSF	BD Pharmingen
Human IFN-γ	BD Pharmingen
Human MCP-1	BD Pharmingen
Human TNF-alpha Protein	R&D Systems
Human CCL4/MIP-1 beta	R&D Systems
Human IL-1 beta/IL-1F2	R&D Systems
Human IL-1Ra/IL-1F3	R&D Systems
Human IL-12 (p70)	BD Pharmingen
Human VEGF 165	R&D Systems
Human IL-13	R&D Systems
Human M-CSF	R&D Systems

Table 5: Stimuli for NK cell activation.

Recombinant Protein	Vendor
Human IL-2	Peprotec
R848	Biogen
Human IL-18	R&D Systems
Human IL-12	MBL
Lipopolysaccharide (LPS)	Hycultec
Staphylococcal enterotoxin B (SEB)	Bernhard-Nocht-Institut, Hamburg

3.1.3 Animal serum

Table 6: Animal sera.

Serum	Vendor
Fetal Bovine Serum, heat inactivated (Hi FBS)	Gibco (Life Technologies)
Fetal Calf Serum (FCS)	Sigma-Aldrich
Horse serum	Sigma-Aldrich

3.1.4 Chemicals and reagents

Table 7: Chemicals and reagents.

Chemical / Reagent	Vendor
EDC, No-Weigh Format	Pierce
Sulfo-NHS (N-Hydroxysulfosuccinimide), No-Weigh Format	Pierce
EZ-Link Sulfo-NHS-LC-LC-Biotin	Pierce
EDC, No-Weigh Format	Thermo Fisher Scientific
EZ-Link NHS-PEG4-Biotin, No-Weigh Format	Thermo Fisher Scientific
Streptavidin-Phycoerythrin conjugate	Moss
Streptavidin-β-galactosidase (SBG)	Quanterix
TRU Block	Meridian
Chemiblock Reagent	Merck
TWEEN 20	Sigma-Aldrich
ProClin 300	Sigma-Aldrich
Ethylenediaminetetraacetic acid (EDTA)	Sigma-Aldrich
Natrium Acid	Roth
Bovine Serum Albumin, Reagent Grade	Proliant
Albiomin *(= human serum albumin, HSA)*	Biotest
Sodium Chloride (NaCl)	Roth
MES	Roth
Di-sodium hydrogen phosphate (Na_2HPO_4)	Roth
ZombieYellow	Biolegend

3.1.5 Buffers and solutions

Table 8: Buffers and solutions.

Buffer / Solution	Vendor/Composition
Phosphate buffered saline	Fisher Scientific
LowCross Buffer	Candor
Blocking Reagent for ELISA	Roche
Activation Buffer	100 mM Na_2HPO_4, pH 6.2
Immobilization Buffer	50 mM MES, pH 5.0
Bead Storage Buffer	CBS + 0.05 % TWEEN 20 + 0.05 % ProClin 300
Detection Antibody Storage Buffer	CBS + 0.05 % ProClin 300
CBS buffer	1x PBS + 1 % BSA
Wash Buffer	1x PBS + 0.05 % TWEEN 20
Assay Buffer 1	NMI - proprietary
Assay Buffer 2	NMI - proprietary
Homebrew Sample/Detector Diluent	Quanterix
SBG Diluent	Quanterix
Simoa Washing Buffer A	Quanterix
Simoa Washing Buffer B	Quanterix
Bead Diluent	Quanterix
SBG Concentrate	Quanterix
RGP	Quanterix
TC-GM + HSA	HOT Screen GmbH - proprietary
Red Blood Cell Lysis Buffer	Biolegend
FACS Buffer	1x PBS, 2mM EDTA, 2% FCS, 0.01% Natrium Acid

3.1.6 Commercial kits

Table 9: Commercially available kits.

Kit	Vendor
ArC Amine Reactive Compensation Beads	Thermo Fisher Scientific
MACS Comp Bead Kit, anti-mouse Igκ	Miltenyi Biotec
MACS Comp Bead Kit, anti-REA	Miltenyi Biotec
BD FACSuit CS&T Research Beads	BD Bioscience
Granzym B ELISA	Mabtech

3.1.7 Consumables

Table 10: Consumables.

Name	Vendor
Half well plates	Corning
Tubes 1.5 mL LoBind	Eppendorf
Tubes 5 mL LoBind	Eppendorf
Simoa-reading discs	Quanterix
Simoa pipetting tips	Quanterix
Simoa sealing oil	Quanterix
Centrifugal concentrators	Merck
S-Monovette 2,7 ml	Sarstedt
FACS tubes, 2 mL	Corning

3.1.8 Devices

Table 11: Devices.

Device	Vendor
FlexMAP 3D	Luminex
SR-X	Quanterix
Simoa microplate washer	Quanterix
Dynamap magnet	ThermoFisher
HuLa mixer	Thermo fisher
Micro centrifuge	VWR
pH-Meter 766 Calimatic	Knick
Sonicator	Bandelin
Vortex-Genie 2	Scientific Industries
Centrifuge 5417R	Eppendorf
BD LSRFortessa Cell Analyzer	BD Biosciences
Heraeus Multifuge 8R	ThermoFisher Scientific

3.1.9 Software

Table 12: Software.

Software	Supplier
Xponent	Luminex corp.
SR-X Reader Software	Quanterix
Prism	GraphPad Software
MasterPlex	MiraiBio Group of Hitachi Software Engineering America, Ltd
FlowJo	BD Biosciences
FACSDiva	BD Biosciences
Endnote	Clarivate Analytics
Microsoft Office	Microsoft
ClustVis	BIIT Research Group
GIMP 2.10.30	GNU Image Manipulation Program

3.2 Methods

3.2.1 Suspension bead arrays - IMAPs

3.2.1.1 Antibody immobilization

Capture antibodies were immobilized onto paramagnetic microspheres, hereafter referred to as “beads”. The beads’ surface is functionalized with carboxyl groups that can be activated using 1-Ethyl-3-(3-dimethylaminopropyl)carbodiimid (EDC) resulting in a o-acylisourea intermediate which is susceptible to hydrolysis. For stabilizing the acylisourea, the carboxyl groups on the bead surface are activated using EDC in combination with amine reactive sulfo-N-hydroxysuccinimid (sNHS). The resulting stabilized active ester binds to a primary amino group on the protein that is aimed to be immobilized to the bead surface by forming an amide bond. At the same time, sNHS is set free [153].

At the beginning of the immobilization process, the bead stock was vortexed thoroughly for 15 sec and was then sonicated for 30 sec. In total 7.5 x 10^6 beads per bead-ID were washed three times with ddH_2O (double-distilled water). All washing steps were performed using a magnetic separator (e.g. DynaMag – 2 Magnet, Invitrogen). Through magnetic forces, the microspheres can be separated at the tube wall enabling the removal of supernatant without the loss of beads. Following removal of the supernatant, an activation mix of 5 mg·mL^{-1} EDC and sNHS in activation buffer was prepared and 100 µL of this mix was added onto washed beads. The beads were then incubated for 20 min at RT rotating on a HuLa mixer. After activation, beads were washed three times with 500 µL immobilization buffer before antibodies were applied in a defined coupling concentration onto the beads in a total volume of 500 µL immobilization buffer. After mixing the beads by vortexing, incubation under rotation on a HuLa mixer followed for 2 h at RT. Afterwards, beads with immobilized antibodies were washed using 1 mL of PBST (PBS + 0.05 % Tween20). For storage, 600 µL of bead storage buffer was applied and beads were stored at 2 – 8 °C.

To confirm a successful immobilization process a coupling control was performed. PE-labeled species-specific antibodies were titrated and applied to coated microspheres and read on a FLEXMAP 3D instrument.

For IMAP 1 and 2 bead mixtures were generated, each mix was calculated sufficiently for the measurement of 200 plates. Single bead-ID stock solutions were diluted 1:10 from their initial concentrations with the remaining volume difference supplemented with bead storage buffer.

3.2.1.2 Biotinylation of detection antibody

The quantification of analytes is based on Strep-PE binding specifically to biotin, which is linked to detection antibodies. As some detection antibodies were only available unbiotinylated, biotin was covalently bound using sulfo-NHS-LC-LC-Biotin. Sulfo-NHS reacts with primary amines on the antibody`s surface forming a covalent bond with the LC-LC-linker functions as spacer making biotin more accessible to streptavidin.

For biotinylation, antibodies were reconstituted to a concentration of 500 µg·mL^{-1}. 100 µL of antibody stock was transferred into a 1.5 mL reaction tube and 2 µL biotin dissolved in ddH_2O were added to reach a 200-fold molar excess of biotin. Incubation followed overnight at 4 °C for 16 h. Afterwards, unbound biotin was removed using centrifugal concentrators (Amicon Ultra 0.5 mL centrifugal Filters, Merck) according to the manufacturers protocol, except that centrifugation was performed at 4 °C. Antibody concentration after elution was determined by NanoDrop (UV/VIS at 280 nm) and the final concentration was adjusted to 200 µg·mL^{-1} in 1X PBS + 0.05 % ProClin300. Biotinylated antibodies were stored at 2 – 8 °C.

To confirm the success of biotinylation of detection antibodies, beads functionalized with anti-species antibodies were applied. Detection antibodies were titrated and incubated with respective beads. Biotin coupling to detection antibodies was verified by the application of Strep-PE and readout on a FLEXMAP 3D instrument.

A detection antibody mix was generated for IMAP 1 and 2 for a better assay reproducibility. Single detectors were prepared at 20X higher concentration than applied in the assay. The mix was stored in detection antibody storage buffer and was stored at 2 – 8 °C.

3.2.1.3 Generation of the calibrator mix

A mix of the calibrators was generated for each IMAP. Single recombinant proteins were stored at 20X the concentration of the highest calibrator and only diluted prior use. The calibrator mixes for IMAP 1 and IMAP 2 were prepared in CBS, aliquoted for single use and stored at -80 °C.

3.2.1.4 IMAP assay procedure

For cytokine assessment in supernatants of whole blood assays, samples were thawed and vortexed before they were centrifuged at 18,000 g and 4 °C for 1 min. All assay components of IMAP 1 (IL-4, IL-6, IL-8, IL-10, GM-CSF, IFN-γ, MCP-1, MIP-1β and TNF-α) and IMAP 2 (IL-1β,

IL-1Ra, IL-12p70, VEGF, IL-13 and M-CSF) were brought to RT. 100 µL of wash buffer were added to each well of a 96-half-well plate to block the surface of the wells. The plate was incubated for at least 15 min at 21 °C and 750 rpm in a thermal mixer. Afterwards, the content was discarded and the wells emptied completely by tapping the plate up-side-down onto a paper towel.

Beads of the generated bead mix were centrifuged for 15 sec using a tabletop centrifuge, vortexed thoroughly, sonicated for further 15 sec and diluted 1:25 in the IMAP specific assay buffer (assay buffer 1 and assay buffer 2). The bead suspension was then stored in the dark until use.

To generate the calibration curve, each calibrator mix produced for IMAP 1 and 2 was diluted 1:20 in the respective assay buffer to create the highest concentrated calibrator. For the remaining standard points (two to seven), a dilution series using dilution factor 3 was made over six steps in the respective assay buffer.

Samples were diluted 1:4 and 1:256 in the specific assay buffer of IMAP 1 or IMAP 2, respectively. Quality control (QC) samples for each IMAP were diluted 1:2, also in the IMAP-specific assay buffer. Afterwards, 25 µL of diluted samples, QC samples and standard dilutions were added to the blocked 96-half-well plate, with standard and QC samples being applied in duplicates. Samples were analyzed individually but at two dilution factors. 25 µL of the already prepared bead solution was then added to each well and the plate was incubated at 21 °C and 750 rpm for 2 h. This resulted in final dilution factors of 8 and 512 for samples and a dilution factor of 4 for QC samples, respectively. Following incubation, the plate was washed three times with 100 µL wash buffer per well using a magnetic separator to fixate the magnetic beads on the bottom of the plate, with the supernatant discarded.

The detection antibody mix was diluted 1:20 in assay buffer 1 and 2, respectively, and 30 µL of the detection antibody solution was pipetted per well. Afterwards the plate was again incubated at 21 °C and 750 rpm for 1 h in a thermal mixer and then washed three times as already described, after which 30 µL of Strep-PE, diluted 1:500 in CBS including 0.05 % Tween20 was added per well. Incubation followed for 30 min at 750 rpm and 21 °C, after which the plate was washed again three times. 100 µL of wash buffer was pipetted into each well and beads were re-suspended for 3 min at 750 rpm and 21 °C.

Readout was performed on a FLEXMAP 3D instrument using the following settings: sample volume of 80 µL, a timeout of 60 sec, gating between 7,500 and 15,000, Standard PMT

detector and bead count was set to 100. MFI per bead-ID in each well was assessed using Xponent software. The fitting of the standard curve and the back-calculation of signals of sample dilutions was performed using MasterPlex QT software. The final calculation of results and the assessment of QC samples was carried out using Microsoft Excel.

3.2.2 Suspension bead arrays – Simoa SR-X

3.2.2.1 Antibody immobilization

Before capture antibodies could be immobilized to beads suitable for SR-X (Simoa) technology, a buffer exchange was performed to remove any agents present in the provided antibody solutions that could potentially interfere with the coating process. Centrifugal separators were used according to the manufacturer's protocol, replacing the buffer in which the antibodies were supplied with Bead Coupling Buffer. Antibody concentration was determined employing UV/VIS (NanoDrop) and the final concentration was adjusted to 500 $\mu g \cdot mL^{-1}$ in Bead Coupling Buffer.

Following this, beads were vortexed for 10 sec and sonicated for 30 sec before 8.4 x 10^8 beads were transferred to a 1.5 mL tube. Beads were then washed three times with 500 µL Bead Wash Buffer and twice with Bead Coupling Buffer supplemented with 0.01 % Triton before resuspension in the latter. All washing steps were performed using a magnet to pellet the beads and fix them before removal of the supernatant. To activate the bead surface, EDC was added at a final concentration of 0.5 $mg \cdot mL^{-1}$ and incubated for 30 min at RT on a HuLa mixer. Contrary to the coupling method of Luminex beads, no sNHS was used to activate Quanterix beads. After activation, beads were washed three times with 600 µL Bead Coupling Buffer supplemented with 0.01 % Triton. After the final wash step, 600 µL of antibody solution, adjusted to the required coupling concentration in Bead Coupling Buffer as previously described, was added to the activated beads. The immobilization reaction was carried out for 2 h under rotation on a HuLa mixer in the dark at RT. Beads were then washed twice with bead wash buffer by applying a magnetic separator, before 1 mL of Bead Blocking Buffer was added. Coated beads were blocked for 30 min at RT rotating on a HuLa mixer. In a final washing step, beads were treated with 1 mL Bead Diluent and were re-suspended in 600 µL of the same diluent. Beads were stored at 2 – 8 °C.

3.2.2.2 Biotinylation of detection antibody

To biotinylate the detection antibodies for SR-X (Simoa) technology, a NHS-PEG4-Biotin reagent was employed. 100 µg of the antibody was transferred into a 1.5 mL tube. To reach a 60-fold molar excess of biotin, 5 µL of a 1 mg·mL^{-1} NHS-PEG4-Biotin solution was added. The antibody-biotin mix was vortexed and incubated for 30 min at RT. Unbound biotin was removed afterwards using centrifugal concentrators following the manufacturer's protocol. Subsequently, the concentration of biotinylated antibody was determined by UV/VIS measurement (NanoDrop) and the final concentration was adjusted with Biotinylation Reaction Buffer to 200 µg·mL^{-1}. The biotinylated antibodies were stored at 2 – 8 °C.

3.2.2.3 SR-X assay procedure

The assays developed for the SR-X (Simoa) technology were developed as two single-plexes (IL-4 and IL-12p70) and as a 2-plex (TNF-α and IL-6). In contrast to the Luminex assay, the developed SR-X procedures were carried out as a two-step method, meaning, that detection antibodies are incubated in one step together with samples and beads, instead of performing a separate incubation step (three-step assay). First, all assay components were brought to RT. Whole blood assay supernatants were thawed, vortexed and centrifuged for 1 min at 18,000 g and 4 °C.

For all Simoa assays, bead stocks were thoroughly vortexed and sonicated, before being diluted 120-fold in bead diluent. The bead solutions were then stored in the dark until use.

For the calibration curve, the highest standard for each analyte was prepared by diluting the respective stock solution of recombinant protein in the assay-specific buffer to reach the needed standard concentration. Then, by generating a dilution series, the remaining six standard points were prepared in the respective assay buffer. For IL-4 and IL-12p70 dilution factor 4, and for the 2-plex dilution factor 3.5 was applied for the creation of the standard curve.

Samples and QC samples were diluted in the specific assay buffer of each analyte. The QC samples of all analytes were diluted with dilution factor 2.5, as well as the samples to measure IL-4. Samples for the analysis of IL-12p70, IL-6 and TNF-α were diluted 1:5. The application of beads resulted in a further dilution of 1:2, leading to the final dilution factors of 5 and 10, respectively. Further, detection antibodies were diluted in assay buffer to create concentrations four-times higher than their assay concentration (assay concentration see

Table 17). After all assay compounds were prepared, 50 µL of each sample, QC sample and standard were pipetted into a 96-well plate. Then, 25 µL of each, diluted beads and diluted detection antibody, were added. After an incubation of 1 h at 800 rpm and 21 °C in a thermal mixer, the plate was applied into the Simoa microplate washer and was washed three times using wash buffer A (volumes: first washing step: 150 µL – second step: 400 µL – third step: 150 µL). During automated washing steps, SBG was diluted to a final concentration of 150 pM in SBG Diluent and 100 µL were applied to the washed beads at the end of the washing procedure. A further incubation followed for 15 min at 800 rpm and 21 °C. A second washing procedure was carried out employing wash buffer A three times. Beads were then washed twice in 150 µL wash buffer B, incubated for 1 min by shaking at 800 rpm before wash buffer B was completely removed by the washer. Beads were dried for 10 min at RT and the plate was inserted into the SR-X instrument together with RGP Reagent, which was pre-incubated at 30 °C in a thermal shaker for at least 30 min.

The SR-X reader software carried out the fitting of the standard curve and the final calculation of the concentration of the analyte in the sample. For this, all necessary parameters, like standard concentrations and sample dilution factors were applied to the instrument prior measurement.

3.2.3 Immunoassay development

Many factors are decisive for the quality of an immunoassay, such as the antibodies used, the buffer composition or the concentration of the individual assay reagents. The aim of proper assay development is therefore to adapt these parameters in the best possible way for the determination of the desired analytes.

For the assay development of the Luminex and SR-X assays, commercially available recombinant proteins and antibodies were used. For the analytes of interest, the existing know-how on the performance of commercially available antibodies in combination with the corresponding recombinant standards was used.

3.2.3.1 Selection of a suitable assay buffer

The choice of the appropriate assay buffer is a crucial point in assay development. Three basic assay buffers were tested for IMAP 1 and 2 – Blocking reagent for ELISA (BRE), CBS including 150 mM NaCl and LowCross Buffer (LCB). All three buffers were supplemented with 0.05 %

Tween20. For SR-X assays, Homebrew Sample/Detector Diluent was used as basic buffer and no further buffers were tested. Evaluation was done by the assessment of the standard curve and background signals. The testing was carried out as explained in 3.2.1.4 (Luminex) and 3.2.2.3 (SR-X), respectively.

3.2.3.2 Cross-reactivity

Multiplexed assays need to be tested for several types of cross-reactivity, meaning non-specific bindings between the individual assay components. This is necessary to determine if reagents are of sufficiently high specificity to yield true positive results. To test whether unspecific binding occurs between detection and capture antibodies the assay procedure was carried out by using multiplexed beads and single detection antibodies without recombinant proteins. Cross-reactivity between antigen and capture antibody was tested by using multiplexed beads and detection antibodies in combination with single standard protein. The third kind of cross-reactivity can occur between detection antibody and recombinant protein. Using multiplexed beads and a mix of recombinant proteins and single detection antibodies tested this kind of cross-reactivity. Cross-reactivity of IMAP 1 and 2 were assessed in CBS buffer including 0.05 % Tween20 and 150 mM NaCl (referred to as CBST). The assay was performed as described under 3.2.1.4. For the SR-X 2-plex assay, Homebrew Sample/Detector Diluent was used and the assay procedure was performed as explained under 3.2.2.3. For both methods, the highest calibrator concentration was used if recombinant proteins were applied and evaluation was based on signal strength as MFI [AU] generated by the analyzed assay components. The assessment of the calibration curve and background signal were used for evaluation.

3.2.3.3 Assay buffer optimization

To further reduce unspecific binding, cross-reactivity or matrix effects, the assay buffers were additionally optimized. To adapt the assay buffer to the sample matrix they were supplemented with animal sera and blocker. For IMAP 1, CBST was supplemented with different concentrations of horse serum and fetal bovine serum (FBS) - 2.5, 5 and 10 %, and additionally Chemiblock II (CBII) blocker was added at a concentration of 5 $\mu g \cdot mL^{-1}$. Buffer for IMAP 2 was supplemented with different concentrations of CBII, in detail 5, 10 and 50 $\mu g \cdot mL^{-1}$. The assays was performed as described under 3.2.1.4.

No optimization of the SR-X assays was carried out, as the sensitivity achieved was sufficiently high and the obtained background signals were acceptably low. An exception was the assay buffer for the detection of IL-12p70. For this assay, supplementation of the assay buffer with horse serum was tested at concentrations of 2, 5 and 10 % in Homebrew Sample/Detector Diluent. The test assays were performed following the procedure described under 3.2.2.3. The calibration curve results and the background signal were used to evaluate the assay buffers tested.

3.2.3.4 Optimization of detection antibody concentration

The optimization of assay reagents is a further important factor during assay development. The detection antibody concentration can also affect assay sensitivity and performance. For IMAP 1 and 2, the detection antibody concentrations of 0.1, 0.25, 0.5 and 1 $\mu g \cdot mL^{-1}$ were tested. For SR-X assays, different concentrations were tested over several experiments with various assay components. Assays were processed as described in section 3.2.1.4 (Luminex) or 3.2.2.3 (SR-X), respectively. Evaluation was based on calibration curve performance and the highest achievable sensitivity.

3.2.4 Validation of developed immunoassays

3.2.4.1 Validation guidelines and parameters

Validation of the Luminex and SR-X assays was carried out in a fit-for-purpose approach considering EMA [23] and FDA [24] guidelines. The following parameters were evaluated during the validation of the immunoassays: performance of standard curve, quantification and detection limits, intra and inter assay precision, parallelism, dilution linearity and analyte stability in form of short-term and freeze-thaw stability.

3.2.4.2 Generation of validation samples

For VS generation, the endogenous analyte concentrations in unstimulated and LPS/SEB (staphylococcal enterotoxin b) stimulated samples of three donors U, V and W were determined using the developed immunoassays. The same was applied to pooled samples of donors X, Y and Z. The samples were mixed in different ratios or diluted in TruCulture medium (TC-GM) to bring most of the analytes in the upper (VS H = VS high), middle (VS M = VS mid) and lower (VS L = VS low) region of the respective calibration curves. Since it is almost

impossible to cover a calibration curve region with one VS for all analytes with endogenous proteins only, recombinant protein was spiked into the generated matrix when an analyte was not present in native samples in needed concentrations. This was applied for VS H, VS M and VS L of both IMAPs and also for VS H for the Simoa assay for the detection of IL-12p70. The other VS levels for SR-X assays could be reached by only combining native samples. After VS were generated, they were aliquoted for single use and frozen at ≤ -60 °C.

The analyte levels of the VS produced also met the requirements for QC samples, which were used to test the reproducibility and validity in each analytical run. Therefore, they were produced in sufficient quantities and used for this purpose. For analysis, VS respectively QC samples were diluted in the respective assay buffer using a dilution factor of 4 for the performance of IMAP 1 and 2 or, concerning Simoa SR-X assays, a dilution factor of 5 was applied.

For some validation parameters, such as sample stability assessment, only samples containing native protein in a known concentration should be used. As mentioned above, some VS of IMAP 1 and 2 were needed to be spiked with recombinant protein to get the samples in the respective dynamic calibration curve range. For this reason, further samples were selected for the evaluation of the mentioned parameters. These samples were produced by combining stimulated and unstimulated samples of which the endogenous levels had already been determined for VS generation. These samples are referred to as NP samples in this thesis.

3.2.4.3 Validation of the calibration curve model

Validation of the calibration model was assessed by performing six (SR-X assays) and eight (IMAP 1 & 2) independent experiments, respectively. Standard curves were analyzed in triplicates in each run and the recovery in percentage calculated on the basis of the nominal standard concentration and the precision over all back-calculated concentrations were determined. Precision is given as CV in percentages.

3.2.4.4 Limits of quantification

For the determination of the LLOQ, a dilution series of calibrator 4 was generated using dilution factor 2 over eight steps. Analysis was repeated in three independent experiments on different days in triplicates. The recovery in relation to the nominal concentration of calibrator 4 and precision (CV) of back-calculated concentrations were evaluated for the

determination of the analyte-specific LLOQ.

The ULOQ was assessed based on results obtained in the validation of the calibration model over six (SR-X assays) and eight (IMAP 1 & 2) independent experiments respectively. Standard curves were analyzed in triplicates. The recovery rate and precision in terms of the CV of all acquired back-calculated concentrations of all runs (n = 24 for IMAPs, n = 18 for SR-X) of the highest standard point were evaluated.

3.2.4.5 Limit of detection

The LOD was determined as three times the standard deviation above the average signal of 20 replicates of calibrator 8 which represents the blank value (e.g. assay buffer respectively sample diluent) (average blank + 3 × SD value). To calculate the concentration of the LOD, nominal concentrations of the calibrators 6 and 7 were used. These concentrations and the nominal concentration of the average blank, assumed to be zero, were plotted against the corresponding MFI and AEB, respectively. The concentration of the LOD is then calculated using a linear regression. By employing the equation of regression, the concentration of background signal was determined and defined as LOD.

3.2.4.6 Precision

For determination of inter and intra assay precision VS in low, mid and high range were used and in case of IMAP 1 and 2 also the samples including only native protein (NP samples) were employed. Samples were diluted using a final dilution factor of 4 for Luminex assays and factor 5 for SR-X. For the inter assay precision, the samples were run in triplicates over eight independent runs (Luminex) and six independent runs (SR-X), respectively. Precision was calculated by assessing the CV of back-calculated concentrations of the 24 (Luminex) and 18 values (SR-X), respectively.

For intra assay precision, twelve replicates of each VS and NP sample were assayed on one plate. Their precision (CV) was calculated on basis of the variation of the back-calculated concentrations.

3.2.4.7 Dilution linearity

For the determination of dilution linearity, recombinant protein was spiked in sample matrix in a concentration 350-500 fold above the concentration of the highest calibrator. Then, the

spiked samples were initially diluted 1:40 for IMAP 1 and 2, and 1:25 for SR-X assays, and subsequently serially diluted over the whole range of the calibrator applying dilution factor 2. Analysis of the dilution was carried out in triplicates in a single run. Means of the back-calculated concentrations were created and multiplied with the respective dilution factor. Recovery of these values was determined based on the reference level of spiked in concentrations.

3.2.4.8 Parallelism

Parallelism was determined by serially diluting supernatants from the whole blood culture system with high endogenous levels of native protein in assay buffer. This validation parameter could not be determined for analytes having only low levels of native protein in the samples. The samples were initially diluted with factor 2.5 (SR-X) respectively 4 (Luminex) and were subsequently diluted 1:2 in assay buffer over the calibration range. Analysis was performed in triplicates and the mean of back-calculated concentration was multiplied with their respective dilution factor. Then, the reference concentration was calculated as mean of all concentrations measured within the calibration range while the CV of the triplicates should not exceed 20 % at the same time. Further, these final concentrations should be diverging less than 25 % from each other. Based on this reference concentration the recovery of back-calculated concentrations including the dilution factor was determined.

3.2.4.9 Analyte stability

Two different aspects of sample stability were investigated in the course of validation – short-term and freeze-thaw stability. Samples containing the analytes as native proteins were used and analyzed in triplicates (NP samples). For the examination of short-term stability, samples were stored for 2, 4 and 24 h at RT and 4 °C, respectively. Regarding freeze-thaw stability, samples were thawed, stored for one hour at RT and frozen again at ≤ -60 °C – once, twice and three times. Then, samples were diluted 1:4 in assay buffer and analyzed in triplicates. As reference, an unstressed sample was used, also diluted 1:4 in assay buffer. The mean of the triplicates of analyzed concentrations was multiplied with the dilution factor and the recovery in relation to the reference sample was determined.

3.3 Sample generation

3.3.1 Whole blood donors

Peripheral blood samples were acquired from healthy donors, based on their informed consent. This was carried out at HOT Screen GmbH and the wording was adopted for this thesis. Exclusion criteria of individuals for blood donation were:

- Symptoms of systemic/ local inflammatory reactions with the exception of single small and superficial skin lesions
- Last symptoms of systemic/ local inflammatory reactions of an inflammatory disease or first symptoms of a new episode within the last 14 days before blood donation
- Vaccination within the last six weeks
- Surgery within the last three months
- Chronic diseases with inflammatory components, even during symptom-free intervals
- Intake of drugs within the last 14 days, except contraceptives
- Alcohol consumption (e.g. >0.5 L of wine or 1 L of beer within 24 hours prior blood donation)
- Exhausting exercise within three hours prior to blood donation

The experiments with blood samples were carried out in accordance with the rules for investigations on humans as defined in the Declaration of Helsinki.

3.3.2 TruCulture whole blood culture system

Culturing of whole blood was performed using TruCulture (HOT Screen GmbH), a platform established for *in vitro* monitoring of immune reactions triggered from pharmaceuticals in whole blood [113]. Blood was drawn by venipuncture, employing butterfly needles and heparinized syringes. To prevent non-specific leucocyte activation and/or any loss of cell activity, the whole blood cultures were initiated within 60 min after blood collection. 1 mL of whole blood was added to whole blood culture tubes containing 2 mL TruCulture medium (TC-GM) with the respective stimulating agents (e.g. IL-2, R848, IL-18 and IL-12 – alone or in combination). To assess the overall activation of immune cells, present in whole blood LPS in combination with SEB were applied and incubated for 24 h at 37 °C. Unstimulated samples at time points t = 0 h and t = 24 h served as negative controls.

To generate samples for cytokine analysis, culture tubes were centrifuged (500 g for 5 min) to sediment cellular components and 2 mL supernatant were isolated and stored at -20 °C until

assaying. The cellular fraction was resuspended and used for flow cytometry.

Base levels of cell surface markers were measured right after blood donation (t = 0). For assessing immune activation at a later time point, the tubes were incubated at 37 °C for 24 h. Several stimuli and respective combinations for NK cell activation were tested and in total four independent whole blood culture-based experiments were performed. **Table 13** presents the extent of the experiments - in detail the used donors, stimuli and respective combinations and cell numbers. The concentrations of the stimulants used are proprietary knowledge of the HOT Screen GmbH and are not stated.

Table 13: Experimental details of the four performed partial experiments. *Performed whole blood assays to generate samples for cytokine readouts and analyses by flow cytometry.*

Partial experiment no.	Description	Donors	Tested K562 cell numbers
1	IL-12, IL-18 and combination of IL-12 + IL-18	A, B and C	---
2	IL-2, R848 and combination of IL-2 + R848	D, E and F	---
3	Titration of K562 cells without and combined with IL-2	a, b and c	1.0, 0.5, 0.25, 0.125, 0.0625 and 0.03125 x 10^6 cells
4	LPS/SEB, K562 and K562 + IL-2	G, H and I	0.125 x 10^6 cells

3.3.3 K562 cell culture

K562 cells (DSMZ, ACC 10) were thawed and seeded at 5 x 10^5 cells·mL^{-1}. Cells were maintained at cell numbers between 0.1-1.0 x 10^6 cells in RPMI containing 10 % FCS and were split every three days. The cells were cultured in medium free of Penicillin and Streptomycin for four days. Afterwards, cells were centrifuged (500 g for 3 min) and resuspended in TC-GM at a cell concentration of 4 x 10^6 cells·mL^{-1}. According to the experimental setup, cells were serially diluted in TC-GM and used at the respective concentrations for the co-culture with whole blood.

All TruCulture and K562 cell cultures were performed at HOT Screen GmbH by Dr. Sascha Klimosch.

3.4 Flow Cytometry

3.4.1 Compensation controls

All flow cytometric measurements were carried out on the BD LSRFortessaTM instrument. To ensure proper functionality and valid, reproducible analysis, a quality control employing BD FACSuite CS&T Research Beads was performed each day prior analyzing experiments. Therefore, beads were thoroughly mixed and one drop of the bead solution was added to 300 µL of ddH_2O. After thoroughly vortexing the diluted beads the CS&T measurement was performed.

To be able to correct by calculation, the overlapping fluorescence signals inevitable occurring at multi-color flow cytometric measurements compensation controls were performed. For this purpose, antibody-specific beads were used to capture antibodies against surface markers. For the recombinant REAfinity Antibodies (Miltenyi Biotec), specific anti-REA compensation beads (MACS Comp Bead Kit, anti-REA) were used, while anti-mouse Igκ compensation beads were required for conjugated antibodies obtained from Biolegend.

Antibodies were diluted by adding the volume of antibody recommended by the manufacturer per test to 100 µL PBS. Specifically coated compensation beads were mixed 1:1 with corresponding blank beads and 50 µL of the bead mix were pipetted into the diluted antibody. The bead-antibody mixture was thoroughly vortexed and incubated for 10 min at RT protected from light, after which compensation control measurement was performed.

Amine Reactive Compensation (ArC) Beads were required for compensating ZombieYellow, a live/dead marker. To one drop of these beads, 2 µL of in DMSO reconstituted (50 µL/100 tests) ZombieYellow dye were added and incubated at RT for 30 min, protected from light. After applying 3 mL of PBS, beads were centrifuged at 300 g for 5 min at RT and the supernatant was discarded. The compensation control was applied to the flow cytometry instrument for measuring after 500 µL FACS buffer and one drop of negative ArC Beads were added.

3.4.2 Cell staining for flow cytometric analysis

For live/dead discrimination of cells during flow cytometric analysis, 2 µL of ZombieYellow were applied into a FACS tube and 100 µL of the resuspended cellular components (see section 3.3.2) were added and mixed gently. The tubes were incubated for 10 min at RT, protected from light. Fluorescent-labeled antibodies against specific surface markers were mixed according to instructions of the manufacturer and added to the whole blood culture stained

with ZombieYellow. Tubes were mixed gently and incubated for 10 min at 4 °C in the dark. 1.8 mL 1X Red Blood Cell Lysis Buffer (1:10 dilution of 10X stock in ddH_2O) were applied. Tubes were vortexed and incubated at RT for 30 min. Cells were centrifuged (500 g for 3 min at 4°C), supernatant was discarded and FACS buffer (500 µL) was applied to resuspend the cell pellet. This was repeated two times before the pellet of cells was resuspended in 75 µL FACS buffer for subsequent flow cytometric analysis. Until measurement, samples were stored on ice protected from light.

Analysis of flow cytometry data was performed using FlowJo software. The applied gating strategy is applied in **Annex - Figure 1** and **Annex - Figure 2**. Values of gated populations were exported to Excel and further evaluated using GraphPad Prism.

3.5 Granzyme B ELISA

The level of granzyme B from whole blood assay supernatants was determined by ELISA (Mabtech, Nacka Strand, Sweden) to analyze the degranulation process after NK cell stimulation. The data were recorded as individual values. The measurements were performed by HOT Screen GmbH according to the manufacturer's protocol and the data were kindly provided.

3.6 Data analysis

3.6.1 Analysis of Luminex data

For analysis, all Luminex assays were analyzed using FLEXMAP 3D instruments (Luminex) equipped with Xponent software version 4.3. By measuring the fluorescent intensity of phycoerythrin bound to the beads, the software generated a signal, the “median of fluorescent intensity” (MFI) of the analyzed beads. The minimum count was adjusted to 100 beads for each individual bead ID. The validity of the signal was given when at least 35 beads were assessed. Data were exported after measurement as CSV-files and transferred to MasterPlex QT software for data analysis. Standard curve fitting and the resulting quantification of the analyte concentrations in the samples were performed based on MFI values. The fitting function of the calibration curve was a five-parametric logistic fit. Further, weighting $1/Y^2$ was applied in order to gain a better fit in the lower calibration curve area.

3.6.2 Analysis of SR-X data

For the analysis of SR-X data, the SR-X instrument (Quanterix) was used for all measurements. The instrument was equipped with Simoa operating software version 2.13.0.1250. The measured signals in form of "Average Enzymes per Bead" (AEB) were generated by the software based on image analysis of the arrays. This means that the average enzymes per bead were recorded. For an AEB signal to be considered as valid, at least 1000 beads had to be detected. The signals were processed by the software integrated in the instrument and a calibration curve was generated based on the AEBs. The calibration curve was based on a four-parametric logistic fit with a weighting of $1/Y^2$. Using the standard curve, the AEB values of the respective analytes were calculated back to the original concentration in the samples.

3.6.3 Test of normal distribution following Shapiro-Wilk

The Shapiro-Wilk test is a strong test for examining the normal distribution of metric data when the sample size is small. The test statistic calculates the quotient of two ways of estimating the sample variance. In the numerator, the square of the regression of the quantile-quantile plot, which corresponds to the variance of the sample expected under normal distribution, is calculated (b^2) and in the denominator, the square of the uncorrected sample variance (s^2) is assessed. The calculation of the test size W, after sorting the samples in ascending order of size, is calculated using the formula below, with n representing the sample number:

$$W = \frac{b^2}{(n-1)s^2}$$

The null hypothesis H_0 "The data are normally distributed" is rejected if $W < W_{cr}$ (critical limit). W_{cr} is taken from tables (table 5 and 6 in [154]) and depends on the sample size n and the level of significance α [154]. The test for normal distribution was performed as a pre-test for the Blant-Altman plot using GraphPad Prism software.

3.6.4 Spearman rank correlation coefficient

Spearman rank correlation coefficient was calculated using the software GraphPad Prism in order to determine whether the two methods Luminex and Simoa are related to each other in regard of the analysis of IL-6 and TNF-α.

The Spearman rank coefficient is a tool for the analysis of correlation that measures the

degree of association of two variables [155]. It is independent on data distribution and requires neither a normal distribution of the data nor a linear correlation between the two variables (non-parametric) [156]. Moreover, this type of correlation analysis is relatively robust to outliers. For the determination of the Spearman rank coefficient (r_s) the data are replaced by ranks. For this purpose, the data of the variables are first sorted in ascending order of magnitude and then a ranking is created with likewise ascending rank numbers. The Spearman rank coefficient ranges from -1 to 1, while $r_s = 0$ describes no association of the two variables, r = 1 or r = -1 describe a monotonic relation [155]. The +/- sign indicates a positive or negative relationship, respectively. The closer r_s approaches zero, the weaker the relation between the variables, and the more r_s approximates plus or minus one, the stronger the correlation.

3.6.5 Passing-Bablok regression

A non-parametric model for method comparison is the Passing-Bablok regression [157, 158]. It is robust to outliers and implies that both methods have a uniform distribution of measurement errors, a constant ratio of variances, and that the distribution of samples and their imprecision are random. Passing-Bablok regression requires a linear relationship between the two methods and data that are continuously distributed covering a large concentration range [157].

The model determines a linear regression line ($y = ax + b$) with slope (a) and intercept (b). For the comparison of the two methods Luminex and Simoa for the analytes IL-6 and TNF-α, samples were measured employing both methods and Passing-Bablok regression was performed using back-calculated concentrations.

For calculation of the Passing-Bablok regression, the slope of each pair of data is determined using the defined straight line. The slope of the regression line results from the median of all determined slopes. The intercept is computed from the slope of the regression line and the single x- and y-values of each data pair ($b = y_i – ax_i$). The intercept of the regression line is determined by the median of all calculated intercepts. Passing-Bablok regression was executed by applying an Excel-tool from Acromed Statistik [159].

3.6.6 Blant-Altman method comparison

To describe the agreement of the two methods Luminex and Simoa for analytes IL-6 and TNF-α, the Blant-Altman method was applied. This method generates statistical boundaries of consistency using the average and the standard deviation of the differences between the results of the two quantitative methods [160], which are to be compared. Therefore, a sample set was analyzed employing both methods. For comparison, the back-calculated concentration of both methods are paired and data are sorted increasing from the smallest to the highest value of method A. Then, the mean ((method A + method B)/2) of the results of the two paired values is calculated. Following this, the difference between the paired values of method A and B are computed (A-B) as well as the relative difference between the values in relation to the mean ((A-B)/Mean*100). Next, the bias, which is the mean of the average of the differences $\overline{d}$, is computed. Lastly, based on the standard deviation of the differences, the agreement area, in which 95 % of the differences would lie between, is calculated. The limits are expected to range between $\overline{d}$ *-1.96s* and $\overline{d}$ *+1.96s* (with s = standard deviation). The requirement for this calculation is, however, that the differences are normally distributed [161].

The result is displayed in the form of a scatter plot, where the differences between the two paired methods are plotted on the Y-axis and the X-axis represents the mean value of the measurements. Another way of displaying this is to show the relative differences instead of the absolute ones and to indicate them as percentages on the Y-axis [161]. The evaluation of the comparability of the methods is based on the scatterplots and the distribution or the availability or absence of a trend.

3.6.7 Heatmaps

Heatmaps were used to visualize the complexity of analysis results of NK cell stimulation in whole blood assays. Heatmaps are a tool for visualizing data in a matrix by employing a color gradient, so that an overview of high and low values can easily be given and interpretations can be done of rows and columns rather than examining individual parameters. Correlations of different parameters can be observed quite easily which is further enabled and simplified by applying clusters of similar manifestations of the different parameters. For heatmap generation and clustering a web based tool called ClustVis was used [162]. This uses pheatmap R package (R package version 0.0.7) for heatmap and cluster generation [163].

Before data could be uploaded, they were normalized in GraphPad prism (lowest value per cytokine/chemokine or surface marker was set to 0 % and highest value to 100 %). The results were presented as percentages and were converted to a text file that could be uploaded to the web tool ClustVis.

Data were not further processed in the web tool, meaning no transformation of data nor a row centering were applied. For clustering distance of columns and rows the Euclidean model was chosen and the clustering method “complete” was applied for both, rows, and columns. The rows were ordered to display the tightest cluster first, in order to then orient and classify all further similarities according to this one.

As IL-12p70 concentrations were assessed by cytokine assays, this analyte was excluded in samples that were stimulated using recombinant IL-12. Data were exported as Encapsulated PostScript (EPS) file.

4. Results

4.1 Assay development – IMAP 1 and 2

For the analysis of relevant mediators of immune cells, two IMAPs with a total of 15 analytes were developed using the multiplex bead-based Luminex platform. IMAP 1 covers nine analytes (IL-4, IL-6, IL-8, IL-10, GM-CSF, IFN-γ, MCP-1, MIP-1β and TNF-α), while IMAP 2 covers another six markers (IL-1β, IL-1Ra, IL-12p70, VEGF, IL-13 and M-CSF). Several parameters were addressed during the assay development, as they are crucial for assay performance and guarantee validity and reproducibility of the measurements. Usually, as a first step during assay development, the most suitable capture and detection antibody pairs and recombinant proteins, used as standard proteins, had to be evaluated. However, for the development of the assays in this work, existing internal data as well as commercially available matching antibody pairs could be utilized. For this purpose, existing internal data could be used as well as commercially available matched paired antibodies. Appropriate antibody pairs in combination with their respective standard proteins were initially tested as single-plexes to confirm their overall performance (data not shown), after which they were used in the already cited IMAPs. Secondly, the buffer system and subsequent optimization were considered. Thirdly, cross-reactivity of compounds within an IMAP were evaluated and lastly, the most appropriate concentration of the individual detector antibodies applied in the multiplexed immunoassays was investigated.

The results of the assay development of IMAP 2 were compiled within the master`s thesis of Matthias Becker [164].

4.1.1 Buffer testing

The choice of a suitable buffer system is crucial in the development of a multiplex immunoassay, as it reduces both non-specific binding of assay components and sample matrix effects. In order to define a basic assay buffer system, three different buffers were tested for IMAP 1 and 2: a CBST (PBS-based buffer with 150 mM NaCl and 0.05 % Tween20), BRE and LCB, both supplemented with 0.05 % Tween20, as well. Standard curves were generated in each buffer and compared directly. The results were evaluated separately for each analyte using the standard curve profiles and the background signals, which were designated as blank values because these did not contain standard protein.

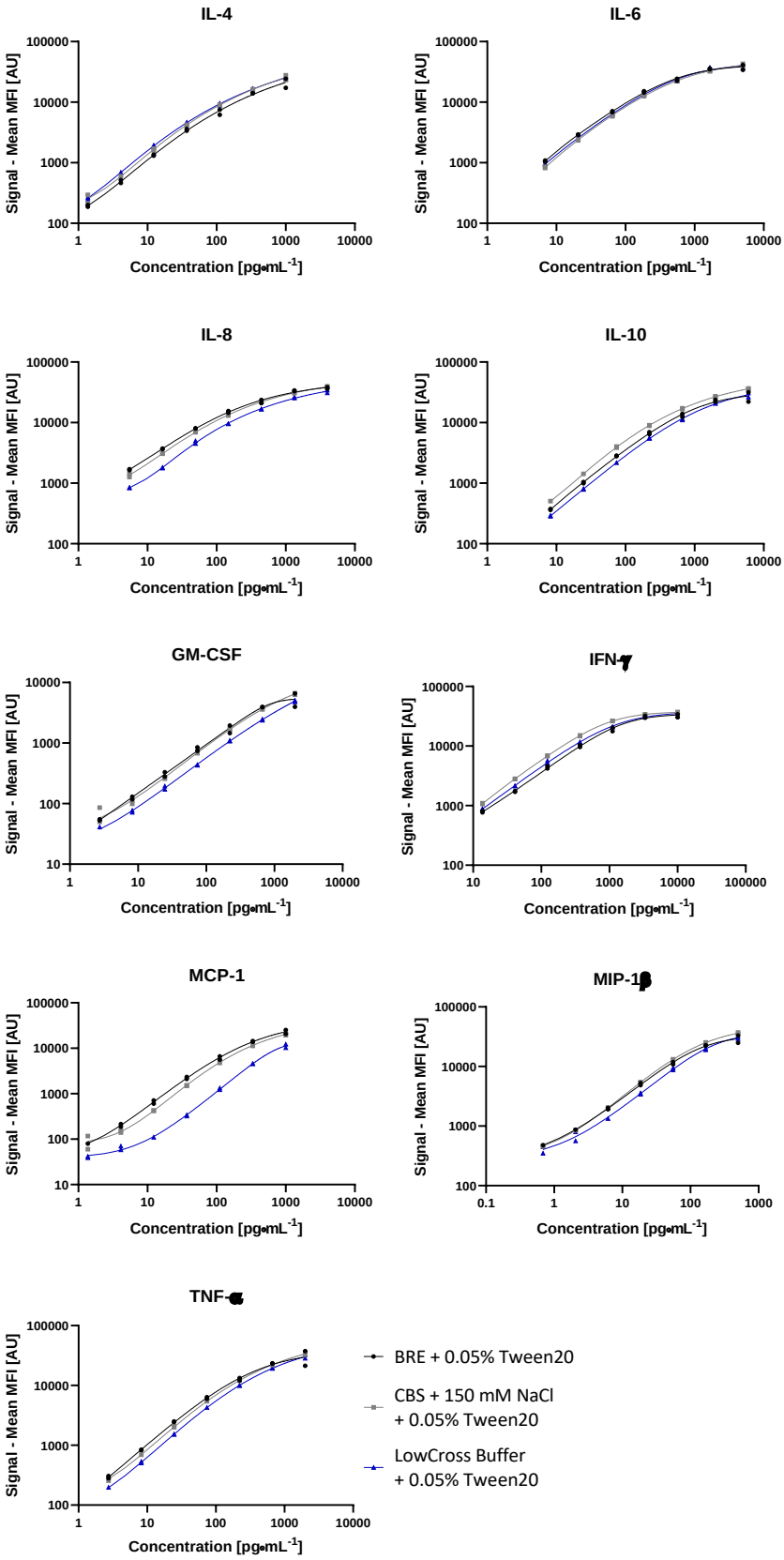

Figure 4: Results of testing suitable assay buffers for analytes of IMAP 1. *Standard curves produced in the respective buffers are directly compared and are presented as median fluorescent intensity (MFI) signal plotted against the nominal concentration in pg·mL^{-1} fitted with a 5-parametric logistic regression (1/Y^2 weighting). The analysis of each standard curve was performed in duplicates (n = 2), the respective individual values are presented. (BRE = Blocking reagent for ELISA; CBS = phosphate based buffer)*

The calibration curves generated in the three buffers for IMAP 1 (**Figure 4**) showed a sigmoidal shape with increasing concentrations for all analytes. With the exceptions of IL-8, IFN-γ and MIP-1β, the mean MFIs of the background signals were below 46 AU and therefore acceptable. For these three analytes, blank values ranged between 199 AU and 442 AU for all three basic buffers tested. There was no difference in standard curve between the three buffers for IL-6. For IL-8, GM-CSF, MCP-1, MIP-1β and TNF-α, the lowest signals for the standard curves were produced using LCB (blue line, **Figure 4**) while the remaining two buffers gave comparable signals (black = BRE and grey = CBST, **Figure 4**) at the different standard concentrations. MCP-1 in LCB showed the greatest difference to CBST and BRE. The two calibrators with the lowest concentrations had almost the same signals. For IL-4, the lowest signals of the standard curves were produced in BRE, although LCB and CBST yielded only slightly higher signals. CBST reached the highest signal for the calibrators of IL-10 and IFN-γ (grey line), followed by signals generated in BRE for IL-10. The lowest signals for the standard curve of IL-10 were in LCB. This was reversed for IFN-γ with BRE having the lowest signals. For GM-CSF, it was observed that the standard curve in BRE plateaued then bent (black). This effect was not present for either LCB or CBST. This plateau in BRE was also observed for IL-10, MIP-1β and TNF-α. There was substantial variation between replicates at the bottom of the standard curve for GM-CSF and MCP-1 in CBST (grey). This variation was also observed for the highest calibrator of IL-4, IL-6, IL-10, GM-CSF, MIP-1β and TNF-α in BRE.

Based on the more stable course of the standard curves, especially in the upper range, as well as the mainly low blank values, CBST was chosen as the basic buffer system for IMAP 1 and 2. For IMAP 2, the same buffers were tested to find the most suitable basic assay buffer for proper assay performance. The corresponding diagrams can be found in **Annex - Figure 3.** To investigate the high blank values detected for some analytes, the next step examined the cross-reactivity.

4.1.2 Cross-reactivity

Multiplex analysis is only possible if cross-reactivity between the different components involved can be excluded. Therefore, it had to be demonstrated that no cross-reactivity occurred among capture and detection antibodies, capture antibodies and analytes as well as analytes and detection antibodies. **Table 14A to C** shows the results of the respective experiments for IMAP 1.

To assess cross-reactivity between capture and detection antibodies, multiplexed beads coated with respective capture antibodies were incubated with single analyte-specific detection antibodies in the absence of standard proteins. The resulting MFI values were evaluated and signals below 120 AU were defined as acceptable. **Table 14A** depicts the results of these cross-reactivity experiments. While the vast majority of the MFI signals were below 120 AU, the combinations of detection antibodies for IFN-γ and MCP-1 with the capture antibody of IL-8 (440 AU & 181 AU), capture antibody coated beads for the analysis of IFN-γ and detection antibodies of IFN-γ and MCP-1 (349 AU & 146 AU) exceeded this limit. Values above 120 AU were also observed for the detection antibody of MCP-1 in combination with the capture antibody against TNF-α (157 AU) and for the capture antibody specific for MIP-1β with its paired detection antibody (131 AU) and with the detection antibodies of IFN-γ and MCP-1 (394 AU & 306 AU). Due to the comparatively high values in combination with the IFN-γ detection antibody, the latter was exchanged for the reduction of the non-specific interaction in the further course.

To examine cross-reactivity between analytes and capture antibodies, single standard proteins at the concentration of the highest calibrator were incubated with a mixture of coated beads and detection antibodies, respectively. The corresponding results are shown in **Table 14B**, as % recovery. According to Luminex Corp., recoveries above 1 % should be defined as being cross-reactive. All assessed recoveries were below 1 % with exception of those generated with the capture antibodies of IL-8 and MIP-1β, where slightly higher recoveries ranging between 1.10 % and 1.65 % were observed in combination with all analytes.

Lastly, to assess cross-reactivity between analytes and detection antibodies, coated beads and recombinant proteins, both provided as a mix, were incubated with single analyte-specific detection antibodies. The respective results are shown in **Table 14C,** again given as % recovery, with recoveries above 1 % defined as cross-reactive (see above). The detection antibody for IFN-γ gave increased recoveries of 1.31 % and 1.88 % in combination with recombinant IL-8 and MIP-1β. Higher recoveries between 1.05 % and 1.56 % were reached for detectors of IL-4, GM-CSF, MIP-1β and TNF-α in combination with recombinant INF-γ. All other recoveries were below 1 %.

To address the detected cross-reactivities, the detection antibody for the detection of IFN-γ was exchanged in the following steps and the assay buffer was optimized to reduce these unspecific interactions. Therefore, different blocker substances were investigated (4.1.3).

Although recoveries were greater than the recommended 1 % threshold, they could be considered acceptable for a multiplex research purpose assay.

Table 14: Results of cross-reactivity testing for IMAP 1. *(A) MFI signals of the cross-reactivity testing between the respective analyte specific capture and detection antibody. MFIs >120 AU were regarded as cross-reactivity. (B) Testing of cross-reactivity between the analyte and capture antibody. Recoveries shown as % are based on the signal generated with the analyte-specific combinations set to 100 %. Recoveries >1 % were rated as cross-reactivity. (C) Cross-reactivity testing between analyte and detection antibody. Calculation and evaluation correspond to that already described for (B). All values were assessed as duplicates (n = 2).*

A

Mean MFI [AU]		Multiplexed capture coated beads								
		IL-4	IL-6	IL-8	IL-10	GM-CSF	IFN-γ	MCP-1	MIP-1β	TNF-α
Detection antibody	IL-4	34	20	32	19	14	25	23	99	27
	IL-6	46	23	35	18	14	26	24	88	28
	IL-8	38	21	59	15	34	27	29	108	29
	IL-10	39	21	83	15	14	27	23	112	25
	GM-CSF	38	22	30	16	14	25	26	87	26
	IFN-γ	46	24	440	17	16	349	26	394	37
	MCP-1	113	86	181	90	63	146	101	306	157
	MIP-1β	68	43	97	27	25	48	57	131	45
	TNF-α	44	27	52	20	15	31	28	94	37

B

Recovery [%]		Multiplexed capture coated beads								
		IL-4	IL-6	IL-8	IL-10	GM-CSF	IFN-γ	MCP-1	MIP-1β	TNF-α
Recombinant protein	IL-4	100	0.086	1.16	0.092	0.626	0.691	0.297	1.33	0.221
	IL-6	0.274	100	1.15	0.098	0.671	0.613	0.297	1.26	0.212
	IL-8	0.322	0.207	100	0.093	0.682	0.630	0.308	1.28	0.220
	IL-10	0.314	0.086	1.65	100	0.717	0.642	0.293	1.28	0.200
	GM-CSF	0.294	0.080	1.17	0.151	100	0.665	0.293	1.31	0.212
	IFN-γ	0.308	0.092	1.16	0.101	0.984	100	0.314	1.27	0.385
	MCP-1	0.268	0.081	1.15	0.093	0.694	0.621	100	1.26	0.200
	MIP-1β	0.299	0.082	1.17	0.094	0.660	0.607	0.334	100	0.236
	TNF-α	0.309	0.077	1.10	0.087	0.688	0.623	0.279	1.30	100

C

Recovery [%]		Multiplexed capture coated beads								
		IL-4	IL-6	IL-8	IL-10	GM-CSF	IFN-γ	MCP-1	MIP-1β	TNF-α
Detection antibody	IL-4	100	0.060	0.116	0.075	0.326	1.06	0.224	0.441	0.284
	IL-6	0.222	100	0.090	0.056	0.291	0.592	0.199	0.387	0.348
	IL-8	0.267	0.060	100	0.066	0.740	0.940	0.253	0.497	0.218
	IL-10	0.236	0.052	0.241	100	0.314	0.518	0.203	0.523	0.178
	GM-CSF	0.260	0.060	0.092	0.069	100	1.05	0.222	0.438	0.207
	IFN-γ	0.337	0.089	1.31	0.116	0.676	100	0.336	1.88	0.576
	MCP-1	0.247	0.058	0.149	0.060	0.285	0.627	100	0.528	0.176
	MIP-1β	0.385	0.087	0.254	0.080	0.448	1.56	0.356	100	0.232
	TNF-α	0.366	0.075	0.144	0.079	0.396	1.09	0.244	0.427	100

For IMAP 2, cross-reactivity was evaluated using the same process with all results meeting their respective criteria (**Annex - Table 1A-C**).

4.1.3 IFN-γ detection antibody replacement and blocker testing

To further reduce non-specific binding and cross-reactivity, the IFN-γ detection antibody was replaced with a different antibody. This resulted in the reduction of the background signal of the IFN-γ detection and capture antibody interaction to 24 AU, and the recovery between the new IFN-γ detection antibody and the analytes from IMAP 1 was reduced to below 1 % (**Table 15**).

Table 15: Results of cross-reactivity analysis of the IFN-γ detection antibody after replacement. *(A) MFI signals of the cross-reactivity testing between the respective analyte specific capture and detection antibody. MFIs above 120 AU were regarded as cross-reactivity. (B) Cross-reactivity testing between analyte and detection antibody. Given recoveries in % are based on the signal generated with the analyte-specific combinations set to 100 %. Recoveries above 1 % were rated as cross-reactivity.*

A

Mean MFI [AU]	Multiplexed capture coated beads								
	IL-4	IL-6	IL-8	IL-10	GM-CSF	IFN-γ	MCP-1	MIP-1β	TNF-α
Detection antibody IFN-γ	19	22	33	16	14	24	25	86	25

B

Recovery [%]	Multiplexed capture coated beads								
	IL-4	IL-6	IL-8	IL-10	GM-CSF	IFN-γ	MCP-1	MIP-1β	TNF-α
Detection antibody IFN-γ	0.068	0.086	0.102	0.050	0.067	100	0.086	0.266	0.248

To reduce background levels in general and to minimize interaction between the MCP-1 detection antibody with capture antibodies of the other markers of IMAP 1, 5 $\mu g \cdot mL^{-1}$ CBII blocker as well as different concentrations of fetal bovine and horse serum were added to CBST for buffer optimization. For this purpose, the new detection antibody for IFN-γ was applied. Since data using only CBST were only available for the original IFN-γ detector, the corresponding signal is reported as "not analyzed" (N/A). The results of the buffer optimization experiment can be seen in **Table 16**. Evaluation is based on blank values as the main goal was to decrease background levels and increase sensitivity. Blank values were obtained by incubating detection antibodies and capture coated beads in the mixes as applied for multiplex analysis without calibrator protein.

The addition of the CBII blocker alone reduced the blank values of IL-8 (341 AU to 101 AU) and MIP-1β (276 AU to 98 AU), respectively. However, IL-4 background was increased from 35 AU

to 102 AU. The blank values generated by the addition of animal sera were far below the blank levels obtained in CBST and CBST in combination with CBII blocker and were comparable to each other. Ten additional background levels were checked and the CV was calculated to check for variation within a single experiment. While blank values produced in 5 % and 2.5 % FBS and horse serum, respectively, ranged from 3.19 % to 10.4 % for all analytes, the CVs achieved with 1.25 % of each serum ranged between 11.0 % and 31.7 %.

The final assay buffer composition of IMAP 1 was defined as CBST + 2.5 % FBS + 2.5 % horse serum + 5 µg·mL^{-1} CBII.

Table 16: Results of buffer optimization experiments of IMAP 1. *Comparison of blank values determined for the analytes of IMAP 1. MFI signals were measured in CBST buffer and CBST buffer supplemented with 5 µg·mL^{-1} CBII blocker. Additionally, fetal bovine serum (FBS) and horse serum were added in different concentrations. Mean values are presented, calculated from duplicate measurements (n = 2). For buffers containing animal sera 10 additional values were generated and respective CVs are listed in %.*

	Mean blank MFI [AU]								
CBST buffer + additives	**IL-4**	**IL-6**	**IL-8**	**IL-10**	**GM-CSF**	**IFN-γ**	**MCP-1**	**MIP-1β**	**TNF-α**
---	35	30	341	18	29	N/A	33	276	41
CBII	102	32	101	22	28	34	58	98	58
5 % FBS, 5 % horse serum, CBII	13	17	17	14	14	14	22	49	20
CV over 10 blank values [%]	7.65	3.19	8.35	5.58	7.34	5.83	5.64	6.10	7.88
2.5 % FBS, 2.5 % horse serum, CBII	14	17	18	12	12	14	25	54	20
CV over 10 blank values [%]	5.03	7.73	6.78	7.18	10.4	5.86	4.81	4.67	8.75
1.25 % FBS, 1.25 % horse serum, CBII	15	18	20	13	12	16	25	56	23
CV over 10 blank values [%]	31.7	13.8	28.2	21.4	22.8	17.2	11.0	19	17.1

The basic buffer of choice for IMAP 2 was the same as for IMAP 1 – CBST. To decrease background for IMAP 2 analytes, different concentrations of CBII blocker were added – 5, 10 and 50 µg·mL^{-1}. The most suitable blocker concentration was chosen based on the lowest MFI signals of the background and the CV values of these blanks. The respective data are attached in **Annex - Table 2**. The final buffer composition for the IMAP 2 was defined as CBST + 10 µg·mL^{-1} CBII blocker.

4.1.4 Optimization of detection antibody concentrations

An optimal concentration of the respective detection antibody in a multiplex immunoassay was a further parameter to be considered during assay development as this has a major influence on assay sensitivity. To minimize non-specific binding, the concentration of the detection antibody should be the lowest possible. For each analyte of IMAP 1 and 2, four different concentrations of detection antibodies were tested. For IMAP 1, 1 µg·mL^{-1},

0.5 µg·mL^{-1}, 0.25 µg·mL^{-1} and 0.1 µg·mL^{-1}, was used, while 0.25 µg·mL^{-1} was replaced with 0.2 µg·mL^{-1} for IMAP 2. Evaluation was performed, as already described for the basic buffer testing procedure, by comparison of the performance of the analyte-specific standard curves as well as background levels.

The results of testing different antibody concentrations are described for IL-10 and TNF-α as examples (**Figure 5**).

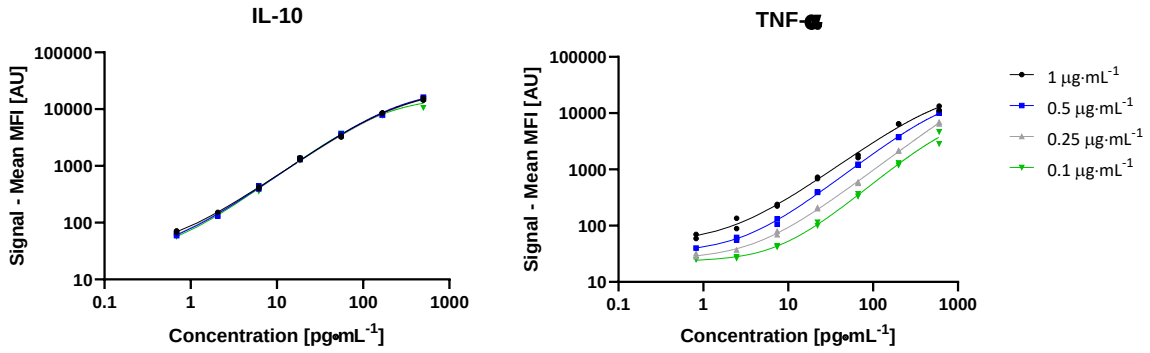

Figure 5: Standard curves generated by testing different detector antibody concentrations. *The direct comparison of the standard curves produced using divers detection antibody concentrations ranging between 0.1 and 1 µg·mL^{-1} is shown. The calibration curves are presented as MFI signal plotted against nominal concentration in pg·mL^{-1} with a 5-parametric logistic regression (1/Y^2 weighting). The analysis of each standard curve was performed in duplicates (n = 2), the respective individual values are plotted. Shown are standard curves for IL-10 and TNF-α as examples.*

For IL-10, no distinct differences were found between the four concentrations tested. Only for the highest calibrator, was there a marginal reduction in signal using detector antibody concentration 0.1 µg·mL^{-1} (green). Blank values generated at varying detector concentrations decreased from 33.3 AU at 1 µg·mL^{-1} to 23.5 AU at 0.1 µg·mL^{-1}. In contrast, clear differences were observed between the standard curves for TNF-α. While the highest signals were achieved at a detector concentration of 1 µg·mL^{-1} (black), the calibration curves generated with decreasing detector concentrations (blue, grey and green) shifted downwards, almost in parallel with 0.1 µg·mL^{-1} (green) having the lowest signals. This curve also showed almost no difference between the signals from the blank, the lowest calibrator and the second lowest calibrator, reducing the signal-to-noise (S/N) ratio. Although the blank MFI signal of the 1 µg·mL^{-1} detector concentration was around 50 AU it provided the highest S/N ratio of 1.28.

For all analytes of the two IMAPs, the most appropriate detector antibody concentration was determined based on the highest sensitivity evaluated by the S/N ratio and the signals and backgrounds obtained for the standard curves.

The final concentrations of the detection antibodies for the analytes of IMAP 1 and 2 are given in **Table 17A** and **B**.

Table 17: Optimal detection antibody concentrations determined for IMAP 1 (A) & 2 (B).

A	Analytes - IMAP 1								
	IL-4	IL-6	IL-8	IL-10	GM-CSF	IFN-γ	MCP-1	MIP-1β	TNF-α
Detection antibody conc. [µg·mL^{-1}]	1.00	0.250	0.100	0.100	0.250	0.250	0.250	0.250	1.00

B	Analytes - IMAP 2					
	IL-1β	IL-1Ra	IL-12p70	VEGF	IL-13	M-CSF
Detection antibody conc. [µg·mL^{-1}]	0.250	1.00	0.100	0.200	0.200	0.100

4.1.5 Standard concentrations

In the process of assay development, the nominal standard concentrations were adjusted, on the one hand, to be able to detect the analytes in the ranges in which they are present in the samples and, on the other hand, to ensure good performance. The final nominal standard concentrations of IMAPs 1 and 2 are shown in **Table 18A** and **B**.

Table 18: Nominal calibrator concentrations of IMAP 1 (A) & 2 (B). *(CAL = calibrator)*

A

	Nominal calibrator concentration [pg·mL^{-1}] - IMAP 1						
Analyte	CAL 1	CAL 2	CAL 3	CAL 4	CAL 5	CAL 6	CAL 7
IL-4	300	100	33.3	11.1	3.70	1.23	0.412
IL-6	81.0	27.0	9.00	3.00	1.00	0.333	0.111
IL-8	231	77.0	25.7	8.56	2.85	0.951	0.317
IL-10	265	88.3	29.4	9.81	3.27	1.09	0.364
GM-CSF	2,245	748	249	83.1	27.7	9.24	3.08
IFN-γ	400	133	44.4	14.8	4.94	1.65	0.549
MCP-1	901	300	100	33.4	11.1	3.71	1.24
MIP-1β	97.0	32.3	10.8	3.59	1.20	0.399	0.133
TNF-α	599	200	66.6	22.2	7.40	2.47	0.822

B

	Nominal calibrator concentration [pg·mL^{-1}] - IMAP 2						
Analyte	CAL 1	CAL 2	CAL 3	CAL 4	CAL 5	CAL 6	CAL 7
IL-1β	229	76.3	25.4	8.48	2.83	0.942	0.314
IL-1Ra	10,000	3,333	1,111	370	123	41.2	13.7
IL-12p70	702	234	78.0	26.0	8.67	2.89	0.963
VEGF	943	314	105	34.9	11.6	3.88	1.29
IL-13	296	98.7	32.9	11.0	3.65	1.22	0.406
M-CSF	176	58.7	19.6	6.52	2.17	0.724	0.241

4.1.6 Validation and quality control samples

Defined VS are necessary for the validation process, as well as QC samples for the subsequent sample measurements. In general, VS and QC samples either contain the native protein in assay matrix in a specific concentration or recombinant protein is spiked in to achieve the desired concentration. As the produced VS fulfilled the criteria for QC samples, they were used as such during later analysis. The nominal concentrations of these samples were determined over four independent runs. The respective nominal concentrations are shown in the following **Table 19A** and **B**. The samples were adjusted to cover the lower, middle and upper ranges of each analyte-specific standard curve. The untreated (unspiked) and partially pooled native sample (3.2.4.2) was chosen to lie within the calibrator range.

Table 19: Nominal concentrations of validation samples for the analytes of IMAP 1 (A) & 2 (B).

A

Validation samples - IMAP 1				
	Concentration incl. DF [pg·mL^{-1}]			
Analyte	**High**	**Mid**	**Low**	**Native sample**
IL-4	434	63.3	6.60	13.2
IL-6	95.4	14.9	1.69	281
IL-8	299	45.3	7.00	297
IL-10	216	41.6	5.72	12.4
GM-CSF	2,946	490	107	242
IFN-γ	461	67.3	7.01	135
MCP-1	1,139	237	39.4	83.6
MIP-1β	140	20.6	3.25	14.7
TNF-α	665	124	15.9	95.1

B

Validation samples - IMAP 2				
	Concentration incl. DF [pg·mL^{-1}]			
Analyte	**High**	**Mid**	**Low**	**Native sample**
IL-1β	328	68.2	6.09	69.9
IL-1Ra	9,283	728	90.8	526
IL-12p70	786	213	17.1	10.6
VEGF	1,640	263	46.0	154
IL-13	204	61.4	8.63	39.3
M-CSF	230	32.1	2.47	9.27

4.2 Validation of IMAP assays for the whole blood culture system

Following immunoassay development, IMAP 1 and 2 were first validated for the PBMC and THP-1 cell culture system and used for corresponding sample measurements. These data were

generated as part of the public funded project "System Immunology at Biological-Technical Interfaces", but are not part of this thesis and are therefore not presented. In addition, these assays were also validated for the measurement of supernatants from whole blood culture systems which is presented in this thesis.

The validation was carried out in a fit-for-purpose approach, oriented towards the guidelines of the EMA and the FDA. The following parameters were determined during the validation process of the Luminex cytokine immunoassays: calibrator performance, upper and lower limits of quantification, limit of detection, intra and inter assay precision, parallelism, dilution linearity and short-term as well as freeze-thaw stability.

4.2.1 Calibrator performance

For the validation of calibrator performance, the recovery rate and the CV were determined over the triplicate measurements of eight independent runs. The results are presented in **Table 20A** to **C** for the corresponding analytes of IMAP 1 and 2. The acceptance range for the recovery rate was from 80 % to 120 %, whereby the CV should lie below 20 %.

The recovery rates for the analytes of IMAP 1 (**Table 20**) ranged from 99.0 % to 104 % and the corresponding CVs lay between 4.68 % and 17.5 %. Only for calibrator 7 (CAL7) of the analyte MCP-1 did the CV reach 25.2 %.

Table 20: Results of the determination of calibrator performance for the analytes of IMAP 1. *(CAL = calibrator)*

Calibrator performance - IMAP 1								
Analyte		**CAL 1**	**CAL 2**	**CAL 3**	**CAL 4**	**CAL 5**	**CAL 6**	**CAL 7**
IL-4	nominal conc. [pg·mL^{-1}]	300	100	33.3	11.1	3.70	1.23	0.412
	assay conc. [pg·mL^{-1}]	303	101	33.6	11.2	3.85	1.23	0.418
	CV [%]	8.86	7.75	5.72	9.69	9.59	8.28	9.76
	recovery [%]	101	101	101	101	104	99.4	102
IL-6	nominal conc. [pg·mL^{-1}]	81.0	27.0	9.00	3.00	1.00	0.333	0.111
	assay conc. [pg·mL^{-1}]	81.7	27.0	9.03	3.07	1.01	0.335	0.113
	CV [%]	5.87	6.16	4.82	8.40	9.03	7.04	14.9
	recovery [%]	101	100	100	102	101	100	102
IL-8	nominal conc. [pg·mL^{-1}]	231	77.0	25.7	8.56	2.85	0.951	0.317
	assay conc. [pg·mL^{-1}]	233	78.0	25.5	8.64	2.95	0.952	0.322
	CV [%]	7.94	6.88	4.69	6.74	10.1	10.3	9.81
	recovery [%]	101	101	99.3	101	103	100	102
IL-10	nominal conc. [pg·mL^{-1}]	265	88.3	29.4	9.81	3.27	1.09	0.364
	assay conc. [pg·mL^{-1}]	268	88.4	29.7	9.95	3.33	1.10	0.368
	CV [%]	7.55	5.75	5.73	7.40	10.3	9.52	12.1
	recovery [%]	101	100	101	101	102	101	101
GM-CSF	nominal conc. [pg·mL^{-1}]	2,245	748	249	83.1	27.7	9.24	3.08
	assay conc. [pg·mL^{-1}]	2,281	749	252	84.4	28.4	9.28	3.14
	CV [%]	8.68	7.05	5.64	9.04	10.4	10.4	17.5
	recovery [%]	102	100	101	102	102	100	102
IFN-γ	nominal conc. [pg·mL^{-1}]	400	133	44.4	14.8	4.94	1.65	0.549
	assay conc. [pg·mL^{-1}]	405	135	44.5	15.1	5.15	1.64	0.557
	CV [%]	9.52	4.73	6.85	11.1	11.3	10.2	12.1
	recovery [%]	101	101	100	102	104	99.8	102
MCP-1	nominal conc. [pg·mL^{-1}]	901	300	100	33.4	11.1	3.71	1.24
	assay conc. [pg·mL^{-1}]	915	301	102	33.1	11.6	3.67	1.28
	CV [%]	9.40	6.36	4.68	8.14	9.74	7.35	25.2
	recovery [%]	102	100	102	99.3	104	99.0	104
MIP-1β	nominal conc. [pg·mL^{-1}]	97.0	32.3	10.8	3.59	1.20	0.399	0.133
	assay conc. [pg·mL^{-1}]	98.6	32.3	10.9	3.57	1.23	0.397	0.135
	CV [%]	9.52	4.59	4.35	5.77	8.12	7.36	11.9
	recovery [%]	102	100	101	99.4	103	99.6	101
TNF-α	nominal conc. [pg·mL^{-1}]	599	200	66.6	22.2	7.40	2.47	0.822
	assay conc. [pg·mL^{-1}]	605	201	66.5	22.5	7.60	2.46	0.833
	CV [%]	7.71	5.35	5.08	6.65	10.5	6.56	8.83
	recovery [%]	101	101	99.9	101	103	99.9	101

For the analytes of IMAP 2, recoveries ranged from 98.7 % to 106 %. With the exception of IL-13, for which the CV of calibrator 1 (CAL1) was 20.3 %, all other CVs ranged between 4.91 % and 17.9 %. The results are presented in **Table 21**.

Table 21: Results of the determination of calibrator performance for the analytes of IMAP 2.
(CAL = calibrator)

Calibrator performance - IMAP 2								
Analyte		**CAL 1**	**CAL 2**	**CAL 3**	**CAL 4**	**CAL 5**	**CAL 6**	**CAL 7**
IL-1β	nominal conc. [pg·mL^{-1}]	229	76.3	25.4	8.48	2.83	0.942	0.314
	assay conc. [pg·mL^{-1}]	235	76.9	25.6	8.67	2.94	0.940	0.321
	CV [%]	11.2	8.27	5.54	10.7	11.5	9.01	10.1
	recovery [%]	103	101	100	102	104	99.8	102
IL-1Ra	nominal conc. [pg·mL^{-1}]	10,000	3,333	1,111	370	123	41.2	13.7
	assay conc. [pg·mL^{-1}]	10,368	3,381	1,127	372	125	42.0	13.8
	CV [%]	16.3	11.6	4.91	6.39	8.64	9.44	9.92
	recovery [%]	104	101	101	101	102	102	101
IL-12p70	nominal conc. [pg·mL^{-1}]	702	234	78.0	26.0	8.67	2.89	0.963
	assay conc. [pg·mL^{-1}]	724	235	78.7	26.8	8.84	2.87	0.988
	CV [%]	11.4	9.49	6.80	11.3	10.4	8.29	12.0
	recovery [%]	103	100	101	103	102	99.4	103
VEGF	nominal conc. [pg·mL^{-1}]	943	314	105	34.9	11.6	3.88	1.29
	assay conc. [pg·mL^{-1}]	968	312	107	35.8	11.7	3.96	1.30
	CV [%]	5.87	10.9	6.90	9.31	9.97	11.7	11.7
	recovery [%]	103	99.4	102	103	100	102	101
IL-13	nominal conc. [pg·mL^{-1}]	296	98.7	32.9	11.0	3.65	1.22	0.406
	assay conc. [pg·mL^{-1}]	314	99.4	33.5	11.1	3.73	1.24	0.413
	CV [%]	20.3	11.0	6.49	8.93	9.82	11.1	17.9
	recovery [%]	106	101	102	101	102	102	102
M-CSF	nominal conc. [pg·mL^{-1}]	176	58.7	19.6	6.52	2.17	0.724	0.241
	assay conc. [pg·mL^{-1}]	182	58.9	19.8	6.64	2.23	0.715	0.249
	CV [%]	11.7	10.7	7.71	8.55	8.83	8.98	11.0
	recovery [%]	103	100	101	102	103	98.7	103

4.2.2 Quantification and detection limits

4.2.2.1 Lower and upper limits of quantification

For the determination of the LLOQ, the acceptance criteria were set to 75 to 125 % for the recovery (accuracy) while precision, represented by the CV, should be less than 25 %. The LLOQ is defined by the lowest concentration of serially diluted calibrator 4 that fulfills both criteria. The determination of the LLOQ is described here as an example for IL-6 in **Table 22**. The detailed results of all other analytes are shown in **Annex - Table 3** for IMAP 1 and **Annex - Table 4** for IMAP 2, respectively.

For IL-6, the lowest concentration for which the recovery and precision met the acceptance criteria was the 1:16 dilution of calibrator 4 at 0.188 pg·mL^{-1} (CV = 8.18 % and recovery = 98.4 %). Higher dilutions (dilution factors: 32, 64, 128) did not meet the acceptance criteria. The determined LLOQs of all analytes belonging to IMAP 1 and 2 are presented in **Table 23**. For the analytes IL-4, IL-8, IL-10, IFN-γ, TNF-α, IL-1β, IL-1Ra, IL-12p70, VEGF and

M-CSF the determined LLOQ was lower than the lowest calibrator 7. As these concentrations were therefore not defined by the analyte-specific standard curves, the lowest calibrator (CAL7) was defined as LLOQ for these analytes. For IL-6, GM-CSF, MCP-1, MIP-1β and IL-13 the LLOQ was determined to be higher than calibrator 7 but lower than calibrator 6 (indicated by asterisk). For the determination of concentrations of unknown samples values lower than the determined LLOQ were not regarded as valid and excluded from analysis.

The determination of the ULOQ was based on the generated results for calibrator 1 during the assessment of the calibrator performance, which is shown in **Table 20** (IMAP 1) and **Table 21** (IMAP 2). Acceptance criteria were set to a recovery from 75 % to 125 % and a CV lower 25 %. Based on this, the ULOQs of all analytes of IMAP 1 and 2 were determined (**Table 23**). No analyte showed a CV for the highest calibrator concentration above 25 % and recoveries ranged between 101 % and 106 %.

Table 22: Results of the determination of the lower limit of quantification (LLOQ) using the example of IL-6.*(CAL = calibrator; conc. = concentration)*

Lower limit of quantification									
		CAL 4 dilution							
Analyte		***1:2***	***1:4***	***1:8***	***1:16***	***1:32***	***1:64***	***1:128***	*CAL 4*
IL-6	nominal conc. [pg·mL^{-1}]	1.50	0.750	0.375	0.188	0.094	0.047	0.023	3.00
	assay conc. [pg·mL^{-1}]	1.32	0.720	0.389	0.184	0.092	0.031	0.040	
	CV [%]	8.19	6.98	13.4	8.18	***27.5***	***76.7***	***50.0***	
	recovery [%]	88.0	96.0	104	98.4	98.4	***67.0***	***171***	

Table 23: Quantification limits determined for the analytes of IMAP 1 (left) & 2 (right). *(LLOQ = Lower limit of quantification; ULOQ = Upper limit of quantification; * concentration above the lowest concentrated calibrator)*

Limits of quantification					
IMAP 1			**IMAP 2**		
	LLOQ	**ULOQ**		**LLOQ**	**ULOQ**
Analyte	**Concentration [pg·mL^{-1}]**		**Analyte**	**Concentration [pg·mL^{-1}]**	
IL-4	0.174	300	**IL-1β**	0.133	229
IL-6	*0.188	81.0	**IL-1Ra**	11.6	10,000
IL-8	0.267	231	**IL-12p70**	0.813	702
IL-10	0.307	265	**VEGF**	1.09	943
GM-CSF	*5.20	2,245	**IL-13**	*0.685	296
IFN-γ	0.463	400	**M-CSF**	0.204	176
MCP-1	*2.09	901			
MIP-1β	*0.225	97.0			
TNF-α	0.693	599			

4.2.2.2 Limit of detection

For the determination of the LOD, 20 replicates of the calibrator 8, which is defined as zero calibrator ("blank value") were assessed. The LOD was determined as the threefold standard deviation above the average signal of the 20 replicates of the blank value. Acceptance criteria were not needed as it is a calculated value. **Table 24A** and **B** presents the LODs calculated for the analytes of IMAP 1 and 2. All LOD values were lower than the lowest calibrator (CAL 7) which are presented in **Table 18A** (IMAP 1) and **B** (IMAP 2) of section 4.1.5. Besides determined LODs, **Table 24A** and **B** also contain information about the linear regression (R^2) and the parameters necessary for the definition of the LOD (e.g. slope, y-intercept), as well as the mean and standard deviation of the measured 20 replicates of the blank value.

Table 24: Limits of detection (LOD) determined for the analytes of the IMAP 1 (A) & 2 (B). *(SD = standard deviation; R^2 = coefficient of determination)*

A

Limit of detection - IMAP 1										
	Analytes	**IL-4**	**IL-6**	**IL-8**	**IL-10**	**GM-CSF**	**IFN-γ**	**MCP-1**	**MIP-1β**	**TNF-α**
Blank	Mean (MFI)	13.7	19.2	21.1	14.3	18.9	18.3	19.8	30.0	18.0
20 replicates	SD (MFI)	0.966	1.48	1.52	0.801	1.70	1.07	1.53	2.03	0.966
	slope	57.8	167	171	29.8	2.46	20.5	15.4	235	53.7
Linear regression	y-intercept	12.3	15.0	13.6	13.1	18.6	15.5	18.0	27.3	15.1
	R^2	0.995	0.981	0.978	0.995	0.974	0.964	0.968	0.990	0.997
LOD [pg·mL^{-1}]		**0.086**	**0.045**	**0.082**	**0.112**	**2.65**	**0.278**	**0.558**	**0.042**	**0.107**

B

Limit of detection - IMAP 2							
	Analytes	**IL-1β**	**IL-1Ra**	**IL-12p70**	**VEGF**	**IL-13**	**M-CSF**
Blank	Mean (MFI)	15.7	20.7	26.2	38.1	17.0	24.0
20 replicates	SD (MFI)	1.19	0.938	1.03	2.54	1.19	1.21
	slope	131	3.72	17.5	28.4	43.8	99.6
Linear regression	y-intercept	13.6	15.0	24.9	40.7	18.8	24.9
	R^2	0.997	0.995	0.997	1.000	1.000	0.999
LOD [pg·mL^{-1}]		**0.046**	**1.83**	**0.242**	**0.243**	**0.075**	**0.046**

4.2.3 Precision

The inter and intra assay precision was determined using the VS of the lower, middle and upper range as well as the sample containing native protein only. While the inter assay precision was determined over triplicates in eight independent runs, the intra assay precision was assessed by determining the CV of twelve replicates of the respective samples in a single run. Acceptance criteria were met with a precision, represented by CVs, below 20 %.

The results of IMAP 1 are shown in **Table 25** where CVs ranged from 3.81 to 16.5 % for the intra assay precision. For the inter assay precision, the CVs reached values between 6.22 % and 16.9 %.

Table 25: Results of intra and inter assay precision determination for the analytes of IMAP 1. *(VS = validation sample; NP = sample containing native protein only; CV = coefficient of variation; conc. = concentration)*

Precision - IMAP 1						
	Analyte		***VS - high***	***VS - mid***	***VS - low***	***NP***
Intra assay precision	**IL-4**	analyzed conc. [pg·mL^{-1}]	469	57.0	6.47	12.5
		CV [%]	16.5	7.88	7.42	9.88
	IL-6	analyzed conc. [pg·mL^{-1}]	97.1	13.9	1.48	312
		CV [%]	6.64	5.01	12.0	9.58
	IL-8	analyzed conc. [pg·mL^{-1}]	316	44.7	6.31	296
		CV [%]	11.8	5.64	9.98	3.81
	IL-10	analyzed conc. [pg·mL^{-1}]	218	40.2	6.08	9.98
		CV [%]	8.55	9.89	8.40	10.7
	GM-CSF	analyzed conc. [pg·mL^{-1}]	3,006	465	86.7	219
		CV [%]	10.6	6.57	8.36	12.5
	IFN-γ	analyzed conc. [pg·mL^{-1}]	522	63.0	6.70	151
		CV [%]	6.84	9.88	4.23	13.3
	MCP-1	analyzed conc. [pg·mL^{-1}]	1,155	219	29.9	66.7
		CV [%]	12.4	8.60	12.6	8.83
	MIP-1β	analyzed conc. [pg·mL^{-1}]	148	20.2	2.96	12.8
		CV [%]	9.71	6.33	6.86	6.63
	TNF-α	analyzed conc. [pg·mL^{-1}]	679	117	14.0	80.4
		CV [%]	9.97	8.02	5.43	8.83
Inter assay precision	**IL-4**	analyzed conc. [pg·mL^{-1}]	443	62.7	6.47	12.7
		CV [%]	11.6	6.22	11.9	14.8
	IL-6	analyzed conc. [pg·mL^{-1}]	95.3	15.0	1.62	297
		CV [%]	9.46	6.46	11.1	12.5
	IL-8	analyzed conc. [pg·mL^{-1}]	302	45.5	6.62	301
		CV [%]	9.05	6.36	12.7	7.77
	IL-10	analyzed conc. [pg·mL^{-1}]	218	42.9	5.99	12.5
		CV [%]	8.78	7.07	10.9	13.1
	GM-CSF	analyzed conc. [pg·mL^{-1}]	3,010	483	99.6	233
		CV [%]	14.3	6.67	15.5	12.7
	IFN-γ	analyzed conc. [pg·mL^{-1}]	473	66.2	6.94	134
		CV [%]	10.7	7.15	9.09	12.1
	MCP-1	analyzed conc. [pg·mL^{-1}]	1,088	222	35.7	77.9
		CV [%]	10.8	13.3	16.2	16.9
	MIP-1β	analyzed conc. [pg·mL^{-1}]	137	20.5	3.21	14.6
		CV [%]	10.3	11.5	12.7	12.4
	TNF-α	analyzed conc. [pg·mL^{-1}]	668	123	15.4	90.4
		CV [%]	12.6	7.70	10.9	12.1

For the analytes of IMAP 2, the intra and inter assay precision results are summarized in **Table 26**. While the determination of intra assay precision yielded CV values ranging from 4.16 %

and 12.8 %, results of the inter assay precision ranged between 6.73 % and 17.0 %. Only for VEGF the determined inter assay precision CVs were between 54.2 % to 63.2 %. Therefore, acceptance criteria for the inter assay precision were not fulfilled by VEGF.

Table 26: Results of intra and inter assay precision determination for the analytes of IMAP 2. *(VS = validation sample; NP = sample containing native protein only; CV = coefficient of variation; conc. = concentration)*

Precision - IMAP 2						
	Analyte		***VS - high***	***VS - mid***	***VS - low***	***NP***
Intra assay precision	**IL-1β**	analyzed conc. [pg·mL^{-1}]	352	66.7	5.11	75.1
		CV [%]	4.16	8.66	9.01	10.9
	IL-1Ra	analyzed conc. [pg·mL^{-1}]	9,637	669	75.9	490
		CV [%]	5.89	4.93	12.8	10.9
	IL-12p70	analyzed conc. [pg·mL^{-1}]	818	208	15.6	10.2
		CV [%]	5.11	6.49	6.22	7.83
	VEGF	analyzed conc. [pg·mL^{-1}]	2,719	421	69.9	63.1
		CV [%]	4.27	9.91	10.7	10.7
	IL-13	analyzed conc. [pg·mL^{-1}]	212	56.5	6.81	38.1
		CV [%]	6.76	6.88	9.74	12.0
	M-CSF	analyzed conc. [pg·mL^{-1}]	248	32.5	2.26	8.41
		CV [%]	5.18	7.52	7.38	10.3
Inter assay precision	**IL-1β**	analyzed conc. [pg·mL^{-1}]	328	67.8	5.97	69.8
		CV [%]	8.58	7.21	13.8	8.46
	IL-1Ra	analyzed conc. [pg·mL^{-1}]	9,035	723	89.3	506
		CV [%]	12.2	9.00	11.1	12.1
	IL-12p70	analyzed conc. [pg·mL^{-1}]	728	215	16.5	10.3
		CV [%]	16.6	6.73	11.5	11.3
	VEGF	analyzed conc. [pg·mL^{-1}]	1,778	286	51.5	162
		CV [%]	54.6	56.3	54.2	63.2
	IL-13	analyzed conc. [pg·mL^{-1}]	195	61.5	8.74	39.2
		CV [%]	12.3	11.8	14.1	10.6
	M-CSF	analyzed conc. [pg·mL^{-1}]	217	31.7	2.49	9.38
		CV [%]	17.0	7.86	12.1	14.5

4.2.4 Parallelism

Parallelism was determined by serial dilution of supernatants from whole blood-based stimulation assays. A total of three samples were used to assess parallelism and to determine appropriate dilution factors for sample analysis. The different serial dilutions (final dilution factors 4 to 131,072) were measured in triplicate. Mean values of the back-calculated concentrations of the different dilutions including the respective dilution factor were calculated. Based on these individual mean values, the reference concentration was calculated as the average of the mean values and then used to evaluate parallelism. The CV over all dilution levels of a particular sample should not exceed 20 %. The parallelism was

determined as recovery rate. This was calculated for each determined matrix concentration of the serial dilutions in relation to the reference value. Acceptance criteria were recovery values between 75 % and 125 %. Appropriate dilution factors for sample analysis for an analyte were defined when the CV of triplicates of a dilution step was below 20 % and recovery of the back-calculated concentration including the respective dilution factor was within 75 % and 125 %.

Table 27: Ranges of dilution factors determined during parallelism assessment of IMAP 1 & 2. *(N/A = not analyzed)*

		Parallelism - dilution factors ranges - IMAP 1 & 2		
	Analyte	***sample 1***	***sample 2***	***sample 3***
IMAP 1	**IL-4**	N/A	N/A	N/A
	IL-6	256 - 65,536	256 - 65,536	128 - 32,768
	IL-8	512 - 131,072	256 - 131,072	256 - 131,072
	IL-10	4 - 1,024	4 - 2,048	4 - 1,024
	GM-CSF	N/A	N/A	N/A
	IFN-γ	32 - 8,192	256 - 65,536	16 - 8,192
	MCP-1	16 - 2,048	8 - 512	8 - 2,048
	MIP-1β	1,024 - 131,072	2,048 - 131,072	1,024 - 131,072
	TNF-α	16 - 4,096	16 - 4,096	8 - 4,096
IMAP 2	**IL-1β**	32 - 8,192	32 - 8,192	16 - 8,192
	IL-1Ra	8 - 1,024	8 - 1,024	8 - 1,024
	IL-12p70	N/A	N/A	N/A
	VEGF	4 - 32	N/A	N/A
	IL-13	4 - 512	4 - 256	8 - 256
	M-CSF	N/A	N/A	8 - 32

Appropriate dilution factors for sample analysis for an analyte were defined when the CV of triplicates of a dilution step was below 20 % and recovery of the back-caclulated concentration including the respective dilution factor was within 75 % and 125 %.

Table 27 summarizes the dilution factors identified for IMAP 1 and 2 for which parallelism was confirmed. The detailed values of the determined and calculated concentrations and the respective recoveries are summarized in **Annex - Table 5** to **Annex - Table 10**. For all samples for IL-4, GM-CSF and IL-12p70, samples 2 and 3 for VEGF and samples 1 and 2 for M-CSF showed an increasing concentration with increasing dilution factors. Calculation of the reference value and consequently of the recovery rates were not feasible and parallelism could not be confirmed. For MCP-1, recoveries of 149 % and 163 % were reached for dilution factors 1,024 and 2,048 (**Annex - Table 6**) and the parallelism range was therefore defined from dilution factor 8 to 512 for sample 2. With respect to IL-1Ra, dilution factor 4 resulted in

recoveries of 55.8 %, 70.8 % and 51.5 % (**Annex - Table 8** to **Annex - Table 10**). For this analyte, an adjustment of the parallelism range was made to the dilution factors 8 to 1,024. An adjustment of the parallelism range to factor 8 was also carried out for the analytes IL-13 and M-CSF, which showed recoveries of 66.4 % (IL-13) and 64.4 % (M-CSF) at the 1:4 dilution for sample 3 and thus were outside the acceptance range. For all other analytes of the IMAPs the recoveries were between 75 % to 125 % and the dilution factor ranges were defined accordingly.

According to **Table 27** concentrations of the majority of the analytes can be determined either using dilution factor 8 or 512, apart from MIP-1β. Nevertheless, these dilution factors were defined for later concentration measurements for both IMAPs. For a detailed explanation refer to discussion section 5.2.3.

4.2.5 Dilution linearity

Dilution linearity was determined using a sample matrix containing defined concentrations of spiked recombinant proteins of the analytes of the respective IMAP. Recovery rates between 80 % and 120 % were accepted for the back-calculated concentrations within the reportable assay range, including the corresponding dilution factors. Recoveries were determined in relation to the respective reference values of the nominal spiked concentrations. Acceptance criteria for measured analyte concentrations close to the ULOQ or LLOQ were defined from 75 % to 125 %. Mean values were excluded from calculation if triplicate measurements of the different dilutions showed a CV higher 20 % or, in case of concentrations close to the LLOQ and ULOQ, higher than 25 %. **Table 28** presents the results of the determination of dilution linearity for IMAP 1, **Table 29** provides those of IMAP 2. Besides very few exceptions, the recoveries obtained were within the defined acceptance limits (80-120 %). Although the first measurable dilution of the sample within the standard curve for the analytes IFN-γ and IL-13 was 77 % and 124 %, respectively, these values were accepted as they were in range of the respective ULOQ. Same was accepted for the lowest measurable value of IL-1Ra reaching a recovery of 121 %.

Slight deviations were also observed for dilution factor 5,120 for IL-1β (recovery of 79.9 %), the first measurable value of IL-12p70 with 284 $pg \cdot mL^{-1}$ and a recovery of 121 % and the recovery of 125 % at dilution 3 (DL3) for VEGF. These recoveries were assessed less stringently

and considered acceptable within the context of a multiplexed immunoassay, since multiplexing imposes certain limitations on assay performance.

Table 28: Results of the determination of dilution linearity for IMAP 1. *Assay and matrix concentrations are given in pg·mL^{-1}. (<LLOQ or >ULOQ = concentration below/above the limit of quantification; n.q. = value cannot be quantified; conc. = concentration; DL = dilution; DF = dilution factor)*

Dilution linearity - IMAP 1												
	Reference		***DL 1***	***DL 2***	***DL 3***	***DL 4***	***DL 5***	***DL 6***	***DL 7***	***DL 8***	***DL 9***	***DL 10***	***DL 11***
Analyte	***[pg·mL^{-1}]***	*DF (1:x)*	*320*	*640*	*1280*	*2560*	*5120*	*10240*	*20480*	*40960*	*81920*	*163840*	*327680*
IL-4	*120,000*	assay conc. [pg·mL^{-1}]	> ULOQ	198	101	54.0	27.7	12.1	6.21	3.26	1.62	0.827	< LLOQ
		matrix conc. [pg·mL^{-1}]	n.q.	126,515	128,670	138,189	141,995	123,392	127,249	133,666	132,983	135,441	n.q.
		recovery [%]	n.q.	105	107	115	118	103	106	111	111	113	n.q.
IL-6	*30,000*	assay conc. [pg·mL^{-1}]	> ULOQ	45.9	24.0	12.9	6.70	2.89	1.50	0.797	0.423	0.210	< LLOQ
		matrix conc. [pg·mL^{-1}]	n.q.	29,363	30,660	33,058	34,304	29,628	30,652	32,631	34,679	34,406	n.q.
		recovery [%]	n.q.	97.9	102	110	114	98.8	102	109	116	115	n.q.
IL-8	*100,000*	assay conc. [pg·mL^{-1}]	> ULOQ	140	71.8	38.6	19.5	8.35	4.43	2.50	1.46	0.680	0.327
		matrix conc. [pg·mL^{-1}]	n.q.	89,316	91,964	98,850	100,045	85,538	90,726	102,400	119,603	111,411	107,042
		recovery [%]	n.q.	89.0	91.7	98.6	99.8	85.3	90.5	102	119	111	107
IL-10	*90,000*	assay conc. [pg·mL^{-1}]	> ULOQ	143	74.1	40.2	19.7	8.69	4.48	2.21	1.22	0.577	< LLOQ
		matrix conc. [pg·mL^{-1}]	n.q.	91,426	94,861	102,818	100,915	88,951	91,682	90,522	100,215	94,481	n.q.
		recovery [%]	n.q.	102	105	114	112	98.8	102	101	111	105	n.q.
GM-CSF	*1,000,000*	assay conc. [pg·mL^{-1}]	> ULOQ	1,281	688	384	207	95.4	52.8	27.6	14.7	6.89	< LLOQ
		matrix conc. [pg·mL^{-1}]	n.q.	820,090	880,401	981,871	1,058,185	976,862	1,081,617	1,131,861	1,202,586	1,128,858	n.q.
		recovery [%]	n.q.	82.0	88.0	98.2	106	97.7	108	113	120	113	n.q.
IFN-γ	*130,000*	assay conc. [pg·mL^{-1}]	313	166	89.6	49.6	26.1	11.5	6.08	3.29	1.68	0.750	< LLOQ
		matrix conc. [pg·mL^{-1}]	100,096	106,234	114,675	126,865	133,820	118,101	124,587	134,758	137,626	122,880	n.q.
		recovery [%]	77.0	81.7	88.2	97.6	103	90.8	95.8	104	106	94.5	n.q.
MCP-1	*450,000*	assay conc. [pg·mL^{-1}]	> ULOQ	619	318	183	103	45.3	22.7	10.5	5.75	2.95	< LLOQ
		matrix conc. [pg·mL^{-1}]	n.q.	395,934	406,417	469,239	529,647	464,247	463,872	430,353	471,313	483,874	n.q.
		recovery [%]	n.q.	88.0	90.3	104	118	103	103	95.6	105	108	n.q.
MIP-1β	*40,000*	assay conc. [pg·mL^{-1}]	> ULOQ	59.1	30.1	16.0	8.31	3.71	1.77	0.827	0.433	< LLOQ	
		matrix conc. [pg·mL^{-1}]	n.q.	37,841	38,524	40,892	42,564	37,956	36,318	33,860	35,499	n.q.	
		recovery [%]	n.q.	94.6	96.3	102	106	94.9	90.8	84.6	88.7	n.q.	
TNF-α	*240,000*	assay conc. [pg·mL^{-1}]	> ULOQ	326	165	92.2	48.2	21.0	11.0	5.78	3.04	1.61	< LLOQ
		matrix conc. [pg·mL^{-1}]	n.q.	208,358	210,927	235,904	246,596	215,347	224,529	236,612	248,764	263,236	n.q.
		recovery [%]	n.q.	86.8	87.9	98.3	103	89.7	93.6	98.6	104	110	n.q.

Table 29: Results of the determination of dilution linearity for IMAP 2. *(<LLOQ or >ULOQ = concentration below/above the limit of quantification; n.q. = value cannot be quantified; conc. = concentration; DL = dilution; DF = dilution factor)*

Dilution linearity - IMAP 2											
	Reference		***DL 1***	***DL 2***	***DL 3***	***DL 4***	***DL 5***	***DL 6***	***DL 7***	***DL 8***	***DL 9***	***DL 10***
Analyte	***[pg·mL^{-1}]***	*DF (1:x)*	*640*	*1280*	*2560*	*5120*	*10240*	*20480*	*40960*	*81920*	*163840*	*327680*
IL-1β	*120,000*	assay conc. [pg·mL^{-1}]	185	78.4	39.1	18.7	9.53	4.84	2.51	1.21	0.607	0.360
		matrix conc. [pg·mL^{-1}]	118,409	100,395	100,122	95,863	97,587	99,055	102,673	99,396	99,396	117,965
		recovery [%]	98.7	83.7	83.4	79.9	81.3	82.5	85.6	82.8	82.8	98.3
IL-1Ra	*4,500,000*	assay conc. [pg·mL^{-1}]	> ULOQ	3,846	1,697	916	465	216	105	54.1	27.4	16.6
		matrix conc. [pg·mL^{-1}]	n.q.	4,922,449	4,344,730	4,689,459	4,764,297	4,423,680	4,284,553	4,429,961	4,487,031	5,441,673
		recovery [%]	n.q.	109	96.5	104	106	98.3	95.2	98.4	99.7	121
IL-12p70	*300,000*	assay conc. [pg·mL^{-1}]	> ULOQ	284	116	56.3	27.3	14.5	7.75	3.96	1.91	< LLOQ
		matrix conc. [pg·mL^{-1}]	n.q.	363,486	296,789	288,307	279,825	297,028	317,440	324,676	313,481	n.q.
		recovery [%]	n.q.	121	98.9	96.1	93.3	99.0	106	108	104	n.q.
VEGF	*400,000*	assay conc. [pg·mL^{-1}]	740	349	195	74.9	40.2	18.7	11.1	5.73	2.83	< LLOQ
		matrix conc. [pg·mL^{-1}]	473,350	446,916	498,423	383,351	411,955	382,225	454,383	469,129	464,213	n.q.
		recovery [%]	118	112	125	95.8	103	95.5	114	117	116	n.q.
IL-13	*140,000*	assay conc. [pg·mL^{-1}]	270	101	46.5	23.0	11.0	5.97	3.04	1.58	0.793	< LLOQ
		matrix conc. [pg·mL^{-1}]	173,026	129,156	119,151	117,897	112,947	122,334	124,655	129,161	129,980	n.q.
		recovery [%]	124	92.3	85.1	84.2	80.7	87.4	89.0	92.3	92.8	n.q.
M-CSF	*80,000*	assay conc. [pg·mL^{-1}]	148	65.3	33.8	13.8	6.80	3.21	1.75	0.890	0.527	0.280
		matrix conc. [pg·mL^{-1}]	94,901	83,580	86,630	70,519	69,666	65,673	71,680	72,909	86,289	91,750
		recovery [%]	119	104	108	88.1	87.1	82.1	89.6	91.1	108	115

4.2.6 Analyte stability

The analyte stability was determined in dependence on the number of freeze-thaw cycles as well as on the storage temperature and time (short-term stability) during assay processing. The recovery rate of the determined concentration of the respective test sample (AS1-9) was calculated in relation to a freshly thawed reference sample (AS0), whereby 80 % to 120 % was considered acceptable. **Table 30A** and **B** shows the detailed results of the test and reference samples for the example IL-4. It should be noted that two reference samples had to be used to investigate short-term stability as the data were needed to be generated in two independent experiments due to lack of sample capacity on a single plate. The recoveries of the test samples AS4 and AS5 were determined with respect to reference 1 (AS0-1) while those of samples AS6 to AS9 were obtained in relation to reference 2 (AS0-2). This can be seen in **Table 30A** and **B**.

Table 30: Detailed results of freeze-thaw (A) and short-term (B) stability for IL-4. *For the determination of analyte stability only samples containing native protein were applied. (AS = analyte stability sample; AS0-1 = reference sample; RT = room temperature; conc. = concentration)*

A

Freeze-thaw stability					
		AS 1	***AS 2***	***AS 3***	***AS0-1***
Analyte	*freeze-thaw cycles*	*1*	*2*	*3*	*0*
IL-4	matrix conc. [pg·mL^{-1}]	11.6	12.6	10.8	*11.4*
	recovery [%]	102	110	94.4	

B

Short-term stability									
		AS 4	***AS 5***	***AS0-1***	***AS 6***	***AS 7***	***AS 8***	***AS 9***	***AS0-2***
	test temperature	*4 °C*	*4 °C*		*4 °C*	*RT*	*RT*	*RT*	
Analyte	*storage duration*	*2h*	*4h*		*24h*	*2h*	*4h*	*24h*	

Table 31 summarizes the freeze-thaw stability results for both IMAPs. While most of the recoveries determined ranged between 80 % and 120 %, two exceptions were observed for the analyte IFN-γ (IMAP 1, 121 %) and for the analyte IL-13 (IMAP 2, 126 %) in regard of AS2, i.e. after two freeze-thaw cycles. **Annex - Table 11** and **Annex - Table 12** show the detailed results of freeze-thaw stability determination of IMAP 1 and 2 in relation to the respective reference samples.

Table 31: Results of the determination of the freeze-thaw stability for IMAP 1 & 2. *For the determination of sample stability only samples containing native protein were applied. (AS = analyte stability sample)*

Freeze-thaw stability - recovery [%] - IMAP 1 & 2				
		AS 1	***AS 2***	***AS 3***
	freeze-thaw cycles	*1*	*2*	*3*
IMAP 1 analytes	**IL-4**	102	110	94.4
	IL-6	103	101	104
	IL-8	105	103	97.2
	IL-10	106	101	94.8
	GM-CSF	86.5	107	84.6
	IFN-γ	110	121	102
	MCP-1	91.1	87.5	96.3
	MIP-1β	88.3	112	91.7
	TNF-α	105	116	101
IMAP 2 analytes	**IL-1β**	88.3	100	80.7
	IL-1Ra	91.1	99.1	80.5
	IL-12p70	114	117	110
	VEGF	108	110	84.1
	IL-13	117	126	95.2
	M-CSF	103	116	99.4

In **Table 32,** the recovery rates of the short-term stability (AS4-AS9) after 2 h, 4 h and 24 h at 4 °C or RT are presented. Exceptions to recoveries not ranging in-between 80 % and 120 % were observed for IL-4 where 77.5 % were determined after 24 h at 4 °C (AS6). For AS9 in terms of IL-10 and MCP-1 stored at RT for 24 h, 74.2 % and 74.0 % were calculated, respectively. Final exceptions were seen for the analyte VEGF with AS6 and AS9 also resulting in recoveries below 80 % at 62.9 % and 58.2 %, respectively. The detailed results including the matrix concentrations and values of the reference samples of the short-term stability analysis can be found in **Annex - Table 13** (IMAP 1) and **Annex - Table 14** (IMAP 2), respectively.

Table 32: Results of the determination of the short-term stability for IMAP 1 & 2. *For the determination of sample stability only samples containing native protein were applied. (AS = analyte stability sample; RT = room temperature)*

Short-term stability - recovery [%] - IMAP 1 & 2							
		AS 4	***AS 5***	***AS 6***	***AS 7***	***AS 8***	***AS 9***
		test temperature					
		4 °C	*4 °C*	*4 °C*	*RT*	*RT*	*RT*
		storage duration at test temperature					
	Analyte	*2h*	*4h*	*24h*	*2h*	*4h*	*24h*
PANEL 1	**IL-4**	97.9	98.8	77.5	85.9	100	118
	IL-6	86.6	91.0	94.4	105	102	91.4
	IL-8	99.2	96.5	99.1	104	104	104
	IL-10	83.8	92.7	87.0	104	111	74.2
	GM-CSF	84.8	85.1	97.4	81.5	118	93.5
	IFN-γ	99.6	101	86.4	99.3	107	81.5
	MCP-1	93.0	81.0	81.3	103	96.6	74.0
	MIP-1β	102	86.8	91.7	101	100	89.7
	TNF-α	96.2	93.4	85.1	100	106	83.7
PANEL 2	**IL-1β**	87.0	86.9	84.4	93.1	102	84.6
	IL-1Ra	87.0	86.2	86.8	90.3	95.0	84.9
	IL-12p70	109	96.3	102	111	112	98.8
	VEGF	90.8	91.9	62.9	87.0	92.7	58.2
	IL-13	101	105	84.9	97.0	97.5	88.9
	M-CSF	98.7	95.5	92.2	107	103	97.8

4.3 Assay development – single molecule array based on SR-X platform

4.3.1 Assay buffer and detection antibody concentration optimization

For the four analytes IL-4, IL-12p70, IL-6 and TNF-α, assays were set up on the highly sensitive Simoa platform, as the sensitivity of the corresponding Luminex assays was not sufficient to analyze the analyte concentrations in sample matrix from whole blood cultures. In addition, the analytes IL-4 and IL-12p70 had previously shown poor results of parallelism during the validation process of IMAP 1 and 2. In total, three SR-X Simoa assays were developed to be able to measure these analytes in the samples of interest - a 2-plex for IL-6 and TNF-α and two single-plexes for the analysis of IL-4 and IL-12p70.

As already described for IMAP 1 and 2, SR-X assay development was also performed, with emphasis on the selection of a suitable basic assay buffer, buffer optimization and optimization of detection antibody concentration. The procedures and the acceptance and interpretation criteria were the same as those already described for the development of the Luminex assays. The corresponding results of the development parameters are summarized in **Table 33**. As a basic buffer, the Quanterix Homebrew Sample/Detector Diluent proved to

be the most suitable for each analyte. Only for IL-12p70 did the addition of 2 % horse serum and TruBlock at a 1:1000 dilution lead to a higher sensitivity (data not shown). The individual detection antibody concentrations were 0.250 µg·mL^{-1} for IL-4, 0.187 µg·mL^{-1} for IL-12p70 and for the 2-plex 0.075 µg·mL^{-1} (IL-6) and 0.100 µg·mL^{-1} (TNF-α) respectively. SBG concentration was for all assays defined as 150 pM.

Table 33: Assay composition details of the four analytes of developed Simoa SR-X assays. *Detection antibody concentrations, the basic buffer and the buffer additives declared as most suitable for the two single-plex assays IL-4 and IL-12p70 as well as for the 2-plex assay including IL-6 and TNF-α developed on the SR-X (Simoa) platform of the company Quanterix.*

	Simoa SR-X - analytes			
	IL-4	***IL-12p70***	***IL-6***	***TNF-α***
Detector antibody concentration [µg·mL^{-1}]	0.250	0.187	0.075	0.100
Basic buffer	QTX Homebrew Sample/Detector Diluent			
Buffer additives	---	2 % horse serum 1:1000 TruBlock	---	---

Additionally, cross-reactivity for IL-6 and TNF-α of the 2-plex was tested (**Annex - Table 15**). Although recovery between the analyte IL-6 and the capture and detection antibody of TNF-α was greater than 1 % threshold (1.22 and 1.61 %) this was considered acceptable for a research purpose assay.

4.3.2 Calibration curves and validation samples of Simoa assays

VS or QC samples (low, mid and high), respectively, were prepared to perform the assay validation procedure and to provide sufficient numbers of QC samples for the anticipated studies. The nominal concentrations of the calibration curves of the four analytes and those of the VS respectively QC samples are listed in **Table 34** and **Table 35**.

Table 34: Nominal calibrator concentrations determined for the Simoa SR-X assays.

	Nominal calibrator concentration [pg·mL^{-1}]						
Analyte	**CAL 1**	**CAL 2**	**CAL 3**	**CAL 4**	**CAL 5**	**CAL 6**	**CAL 7**
IL-4	30.0	7.50	1.88	0.469	0.117	0.029	0.007
IL-12p70	100	25.0	6.25	1.56	0.391	0.098	0.024
IL-6	30.0	8.57	2.45	0.700	0.200	0.057	0.016
TNF-α	90.0	25.7	7.35	2.10	0.600	0.171	0.049

Table 35: Nominal concentrations of validation samples generated for the Simoa SR-X assays.

	Validation sample concentration [pg·mL^{-1}]		
Analyte	**VS - high**	**VS - mid**	**VS - low**
IL-4	56.2	0.901	0.061
IL-12p70	92.5	4.30	0.410
IL-6	47.2	1.72	0.154
TNF-α	65.1	3.14	0.763

Figure 6 demonstrates the profiles of the four calibration curves of IL-4, IL-12p70, IL-6 and TNF-α and the location of the respective VS/QC samples using the SR-X instrument. The standard curves, fitted via a four-parametric logistic model with weighting 1/Y^2, exhibited a sigmoidal curve shape and the QC samples were in the upper, middle and lower range for each analyte.

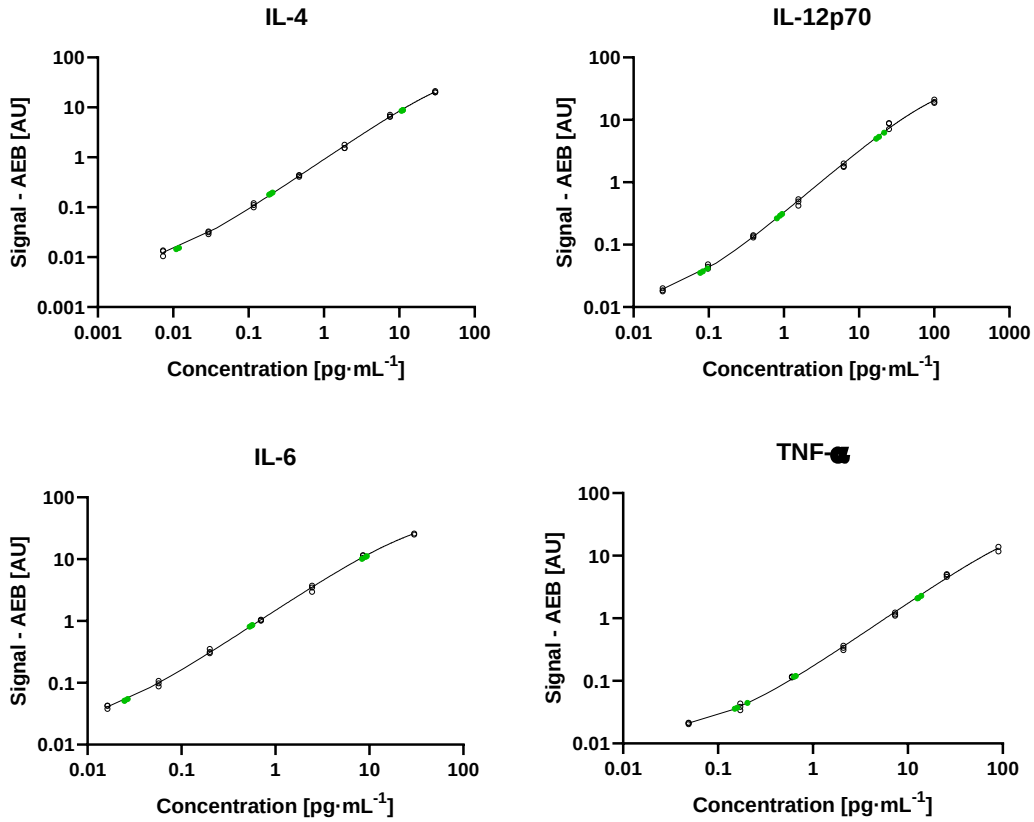

Figure 6: Standard curves and position of the validation samples of the developed Simoa SR-X assays. *The calibration curves are presented as average enzyme per bead (AEB) signal plotted against the nominal concentrations in pg·mL^{-1} with a 4-parametric logistic regression (1/Y^2 weighting). The analysis of each standard curve was performed in duplicates (n = 2), the respective individual values are plotted. VS are depicted in green and are also given in duplicates (n = 2), plotted as individual values.*

4.4 Validation of SR-X assays for the whole blood-based assay system

4.4.1 Calibrator performance

Calibrator performance of the three Simoa immunoassays was investigated over six independent runs. **Table 36** presents the expected nominal concentrations as well as the analyzed, back-calculated concentrations in pg·mL^{-1}. The associated CVs across the total of six plates and the resulting recoveries are shown. The acceptable range was defined from 80 % to 120 %, with a CV below 20 %.

The recoveries ranged between 93.9 % and 113 % (CAL3 and CAL2 of TNF-α) while the highest determined CV was 17.5 % for calibrator 7 of IL-12p70. Unlike the other analytes, the standard curve of IL-6 did not consist of 6 points rather than 7. Calibrator 2 was excluded after the validation evaluation resulted in a calibrator recovery for this point of 122 %. The validation was then re-evaluated under exclusion of this point.

Table 36: Results of the determination of calibrator performance for the Simoa SR-X assays. *(CAL = calibrator; CV = coefficient of variation; conc. = concentration)*

Calibrator performance - Simoa SR-X assays								
Analyte		**CAL 1**	**CAL 2**	**CAL 3**	**CAL 4**	**CAL 5**	**CAL 6**	**CAL 7**
IL-4	nominal conc. [pg·mL^{-1}]	30.0	7.50	1.88	0.469	0.117	0.029	0.007
	analyzed conc. [pg·mL^{-1}]	29.9	7.85	1.86	0.466	0.116	0.030	0.008
	CV [%]	7.13	6.05	5.24	3.42	5.80	5.47	17.2
	recovery [%]	99.6	105	99.0	99.5	98.9	101	106
IL-12p70	nominal conc. [pg·mL^{-1}]	100	25.0	6.25	1.56	0.391	0.098	0.024
	analyzed conc. [pg·mL^{-1}]	98.3	28.0	6.09	1.51	0.405	0.102	0.024
	CV [%]	11.3	11.5	7.00	8.20	4.09	9.32	17.5
	recovery [%]	98.3	112	97.4	96.5	104	105	98.5
IL-6	nominal conc. [pg·mL^{-1}]	30.0	excluded	2.45	0.700	0.200	0.057	0.016
	analyzed conc. [pg·mL^{-1}]	30.0		2.62	0.677	0.207	0.056	0.017
	CV [%]	5.70		12.0	9.07	10.8	10.5	10.4
	recovery [%]	100		107	96.8	104	97.7	105
TNF-α	nominal conc. [pg·mL^{-1}]	90.0	25.7	7.35	2.10	0.600	0.171	0.049
	analyzed conc. [pg·mL^{-1}]	89.3	29.0	6.90	2.06	0.630	0.171	0.054
	CV [%]	4.90	8.37	6.92	10.2	6.36	10.5	13.8
	recovery [%]	99.3	113	93.9	98.3	105	100.0	111

4.4.2 Quantification and detection limits

Quantification limits (ULOQ and LLOQ) as well as the LOD were determined for each analyte during assay validation of the three Simoa SR-X immunoassays. Detailed results of the experimental investigation of the LLOQ and the LOD are presented in **Annex - Table 16** and **Annex - Table 17**. The acceptance criteria were identical to those already described in section

4.2.2.1 for the IMAPs. The determination of the ULOQ was also based on the recoveries and CVs generated during the investigation of the calibrator performance. **Table 37** summarizes the limits of quantification and detection for IL-4, IL-12p70, IL-6 and TNF-α. For all four, the ULOQ was determined to be the highest calibrator. The values analyzed as LOD of theses markers lay below the respective lowest standard point (CAL7) as well as the LLOQ values evaluated for IL-6 and TNF-α, while the LLOQs of IL-4 and IL-12p70 matched with the respective calibrator 7.

Table 37: Quantification limits and limits of detection determined for the Simoa SR-X assays. *(LLOQ = Lower limit of quantification; ULOQ = Upper limit of quantification; LOD = limit of detection).*

Limits of quantification and detection - Simoa SR-X assays			
	LOD	LLOQ	ULOQ
Analyte	Concentration [pg·mL^{-1}]		
IL-4	0.002	0.007	30.0
IL-12p70	0.012	0.024	100
IL-6	0.003	0.005	30.0
TNF-α	0.006	0.016	90.0

4.4.3 Precision

For the SR-X assays, precision was determined using three VS, lying in the upper, middle, and lower parts of the analyte-specific standard curve. As these samples did not need to be spiked with recombinant protein, apart from VS H of the IL-12p70 assay, separate native samples were not necessary. While the inter assay precision was defined over the triplicates of six independent runs, the intra assay precision was assessed by the determination of the CV of twelve replicates of respective samples in a single run. Acceptance criterion was defined as a CV value below 20 %.

Table 38 presents the results of the investigation of intra and inter assay precision for the Simoa SR-X assays. All determined CV values were below 20 %, ranging between 2.96 % and 17.1 %.

Table 38: Results of intra and inter assay precision determination for the Simoa SR-X assays. *(VS = validation sample; CV = coefficient of variation; conc. = concentration)*

Precision - Simoa SR-X assays					
	Analyte		***VS - high***	***VS - mid***	***VS - low***
Intra assay precision	**IL-4**	analyzed conc. [pg·mL^{-1}]	55.8	0.797	0.061
		CV [%]	6.06	2.96	10.0
	IL-12p70	analyzed conc. [pg·mL^{-1}]	95.1	4.06	0.433
		CV [%]	9.15	7.94	17.5
	IL-6	analyzed conc. [pg·mL^{-1}]	47.9	1.59	0.153
		CV [%]	17.1	8.56	15.0
	TNF-α	analyzed conc. [pg·mL^{-1}]	63.4	2.92	0.849
		CV [%]	10.3	7.53	8.37
Inter assay precision	**IL-4**	analyzed conc. [pg·mL^{-1}]	57.6	0.897	0.060
		CV [%]	6.87	5.98	11.8
	IL-12p70	analyzed conc. [pg·mL^{-1}]	95.6	4.28	0.409
		CV [%]	8.54	5.45	11.2
	IL-6	analyzed conc. [pg·mL^{-1}]	49.9	1.85	0.161
		CV [%]	11.2	9.92	11.5
	TNF-α	analyzed conc. [pg·mL^{-1}]	68.5	3.29	0.800
		CV [%]	8.87	8.64	14.7

4.4.4 Parallelism

Three samples were used to determine parallelism. The resulting dilution factor ranges are listed in **Table 39**. Detailed evaluation containing dilutions factors, measured assay and calculated matrix concentrations as well as the recoveries calculated on base of the determined reference sample are presented in **Annex - Table 18** to **Annex - Table 20**.

Table 39: Ranges of dilution factors determined during parallelism assessment of Simoa SR-X assays.

Parallelism - Simoa SR-X assays - dilution factor ranges			
Analyte	**sample 1**	**sample 2**	**sample 3**
IL-4	5 - 10,240	5 - 10,240	10 - 160
IL-12p70	10 - 160	10 - 320	10 - 160
IL-6	10 - 640	5 - 40	320 - 10,240
TNF-α	10 - 160	10 - 160	320 - 10,240

For IL-4, dilution of sample 3 resulted in recoveries of 169 % for dilution factor 5, while all other observed recoveries were in the acceptable range from 75 % to 125 % for this analyte. For IL-12p70, all recoveries were acceptable except for dilution factor 5, where the recoveries were below the acceptance criteria for all three samples (55.4 %, 62.7 % and 74.6 %). Two samples (1 & 2) also revealed increased recoveries for the analyte TNF-α at dilution factor 5 (162 % and 165 %). For sample 1, the analyte IL-6 showed a recovery of 138 % at dilution

factor 5. All other recoveries were in the acceptance range. For the determination of analyte concentrations in whole blood supernatants the dilution factor was set to 5 for the analysis of IL-4. The other analytes, IL-6, TNF-α and IL-12p70, were defined to be analyzed using dilution factor 10.

4.4.5 Dilution linearity

Table 40 summarizes the results of dilution linearity determination of the assays developed on the SR-X platform for the analysis of IL-4, IL-12p70, IL-6 and TNF-α. Included are dilution factors, the respective assay and matrix concentrations as well as their recovery related to the reference value corresponding to the spike concentration of recombinant proteins. Recovery rates between 80 % and 120 % were accepted. Acceptance criteria for measured analyte concentrations close to the ULOQ or LLOQ were defined from 75 % to 125 %. Mean values are only taken from triplicate measurements of the different dilution if the CV was below 20 % or, in case of concentrations close to the LLOQ and ULOQ, below 25 %.
Acceptance criteria were obtained for each dilution and all analytes (81.3 % to 115 %).

Table 40: Results of the determination of dilution linearity for the Simoa SR-X assays. *(<LLOQ = concentration below the lower limit of quantification; n.q. = value cannot be quantified; conc. = concentration; DL = dilution; DF = dilution factor)*

Dilution linearity - Simoa SR-X assays													
Analyte	***Reference [pg·mL^{-1}]***		***DL 1***	***DL 2***	***DL 3***	***DL 4***	***DL 5***	***DL 6***	***DL 7***	***DL 8***	***DL 9***	***DL 10***	***DL 11***	***DL 12***
IL-4	*700*	DF (1:x)	*50*	*100*	*200*	*400*	*800*	*1600*	*3200*	*6400*	*12800*	*25600*	*51200*	*102400*
		assay conc. [pg·mL^{-1}]	15.3	7.32	3.47	1.72	0.819	0.397	0.200	0.098	0.047	0.025	0.011	< LLOQ
		matrix conc. [pg·mL^{-1}]	763	732	693	688	655	635	640	624	600	629	587	n.q.
		recovery [%]	109	105	99.0	98.3	93.6	90.7	91.4	89.2	85.7	89.9	83.8	n.q.
IL-12p70	*2,000*	DF (1:x)	*40*	*80*	*160*	*320*	*640*	*1280*	*2560*	*5120*	*10240*	*20480*	*40960*	*81920*
		assay conc. [pg·mL^{-1}]	45.2	22.5	11.3	5.58	2.77	1.71	0.739	0.387	0.192	0.109	0.053	0.028
		matrix conc. [pg·mL^{-1}]	1,807	1,801	1,814	1,784	1,771	2,183	1,891	1,983	1,966	2,229	2,154	2,307
		recovery [%]	90.4	90.1	90.7	89.2	88.5	109	94.6	99.2	98.3	111	108	115
IL-6	*1,600*	DF (1:x)	*50*	*100*	*200*	*400*	*800*	*1600*	*3200*	*6400*	*12800*	*25600*	*51200*	*102400*
		assay conc. [pg·mL^{-1}]	2.51	1.02	0.926	0.596	0.075	0.166	0.073	0.005	0.006	0.002	0.005	< LLOQ
		matrix conc. [pg·mL^{-1}]	1,571	1,715	1,673	1,302	1,890	1,678	1,542	1,563	1,611	1,528	1,405	n.q.
		recovery [%]	98.1	107	105	81.3	118	105	96.3	97.6	101	95.4	87.7	n.q.
TNF-α	*2,500*	DF (1:x)	*50*	*100*	*200*	*400*	*800*	*1600*	*3200*	*6400*	*12800*	*25600*	*51200*	*102400*
		assay conc. [pg·mL^{-1}]	50.4	25.2	12.5	5.19	3.29	1.59	0.791	0.404	0.227	0.098	< LLOQ	< LLOQ
		matrix conc. [pg·mL^{-1}]	2,518	2,519	2,491	2,076	2,631	2,541	2,532	2,585	2,911	2,521	n.q.	n.q.
		recovery [%]	101	101	99.5	82.9	105	101	101	103	116	101	n.q.	n.q.

4.5 Method comparison of Luminex and Simoa assays

4.5.1 Passing-Bablok regression

In order to be able to use and analyze the concentrations resulting from the SR-X technology analogously to those from the Luminex technology, the comparability of the two methods was investigated using IL-6 and TNF-α. Due to the lack of parallelism of the other two analytes, IL-4 and IL-12p70, with the Luminex assays, only values generated with the Simoa technology can be used.

60 samples were used for IL-6, 40 of which could also be used for TNF-α. While it would be optimum to have samples that cover the full range of the standard curve, the two methods did not have a comparable assay range, so this was only possible to a limited extent in overlapping concentration ranges.

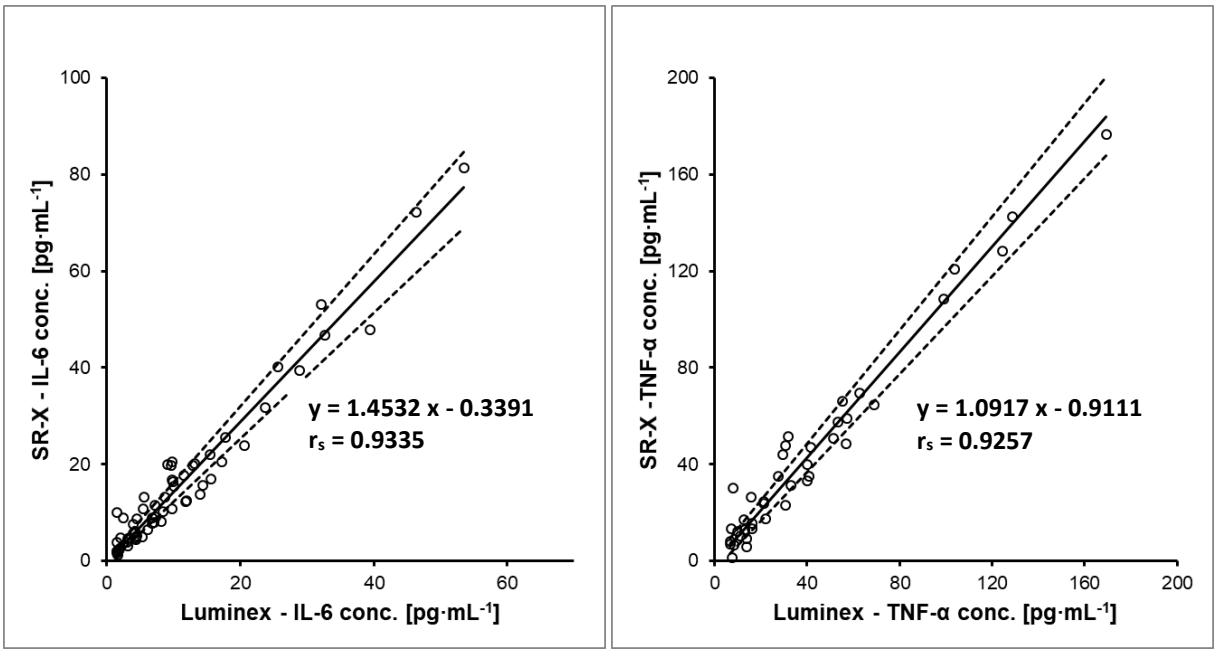

Figure 7: Plot of Passing-Bablok regression analysis. *Passing-Bablok regression was performed to compare the Luminex and the Simoa method for IL-6 (left) and TNF-α (right). Back-calculated concentrations (= conc.) (incl. dilution factor) determined by the Simoa method were plotted (y-axes) against those determined by Luminex assays (x-axes) in pg·mL^{-1}. Additionally, the linear Passing-Bablok regression lines (solid lines) as well as the regression equation are presented. The regression analysis was performed with 95 % confidence intervals (dashed lines). Further, the respective Spearman correlation coefficient r_s is given.*

The investigation of the bivariate relationship using Spearman correlation analysis revealed a rank correlation coefficient of 0.9335 for IL-6 and 0.9257 for TNF-α, respectively. The data collected with the two assays for both analytes correlated positively with each other. The correlation was significant at a level of 0.05.

The slope determined for IL-6 by Passing-Bablok regression analysis was 1.4532 (**Figure 7**) with a 95 % confidence interval (CI) from 1.3035 to 1.5750. The y-intercept for this analyte was -0.3391 and the corresponding 95 % CI ranged from -0.8293 to 0.4808. For TNF-α, a slope value of 1.0917 was obtained (**Figure 7**). The corresponding 95 % CI ranged from 1.0144 to 1.1741. For both methods the slope close to 1 also indicated a positive correlation of both methods. The value determined for the y-axis intercept was -0.9111 (95 % CI: -3.8975 to 1.5967). Looking at the 95 % CIs of the slope of both analytes, they did not contain the value 1, indicating that a proportional error was present. The 95 % CIs of the y-axis intercepts of both analytes included the value 0, which excludes a shift due to a random error [157]. The proportional difference was corrected mathematically by dividing the concentration values generated with the SR-X 2-plex for IL-6 and TNF-α by the respective value of the slope. The resulting slope after correction for IL-6 was 0.9893 (95 % CI: 0.8752 to 1.0788). For TNF-α, a slope of 0.9999 (95 % CI: 0.9290 to 1.0722) was obtained after correcting the proportional. Therefore, the factorial correction of the proportional differences improved the correlation. After mathematically adjusting the SR-X concentrations, both 95 % CIs included the value 1. The correction also influenced the y-intercept leading to a value of -0.1803 for IL-6 (95 % CI: -0.5623 to 0.3731) and of -0.8278 for TNF-α (95 % CI: -3.4529 to 1.4720). As both 95 % CIs of the respective y-intercept did enclose 0, prior as well as after correction of the proportional error, the existence of a systematic error could be excluded.

4.5.2 Bland-Altman method comparison

Correlation is an indicator of method agreement but should not alone be considered for the assessment of method comparability. Therefore, Blant-Altman analysis was performed in order to analyze differences of the two methods, again for IL-6 and TNF-α. In **Figure 8A-D** the average of back-calculated concentrations analyzed by Simoa and Luminex are plotted. While **Figure 8A** and **C** have plotted the absolute differences of the two methods on the y-axis, **Figure 8B** and **D** show the relative differences as percentage. An acceptance range for relative difference was internally defined from -35 % to 35 %. For Blant-Altman analysis, the values generated by Simoa SR-X and subsequently corrected according the Passing-Bablok regression were employed.

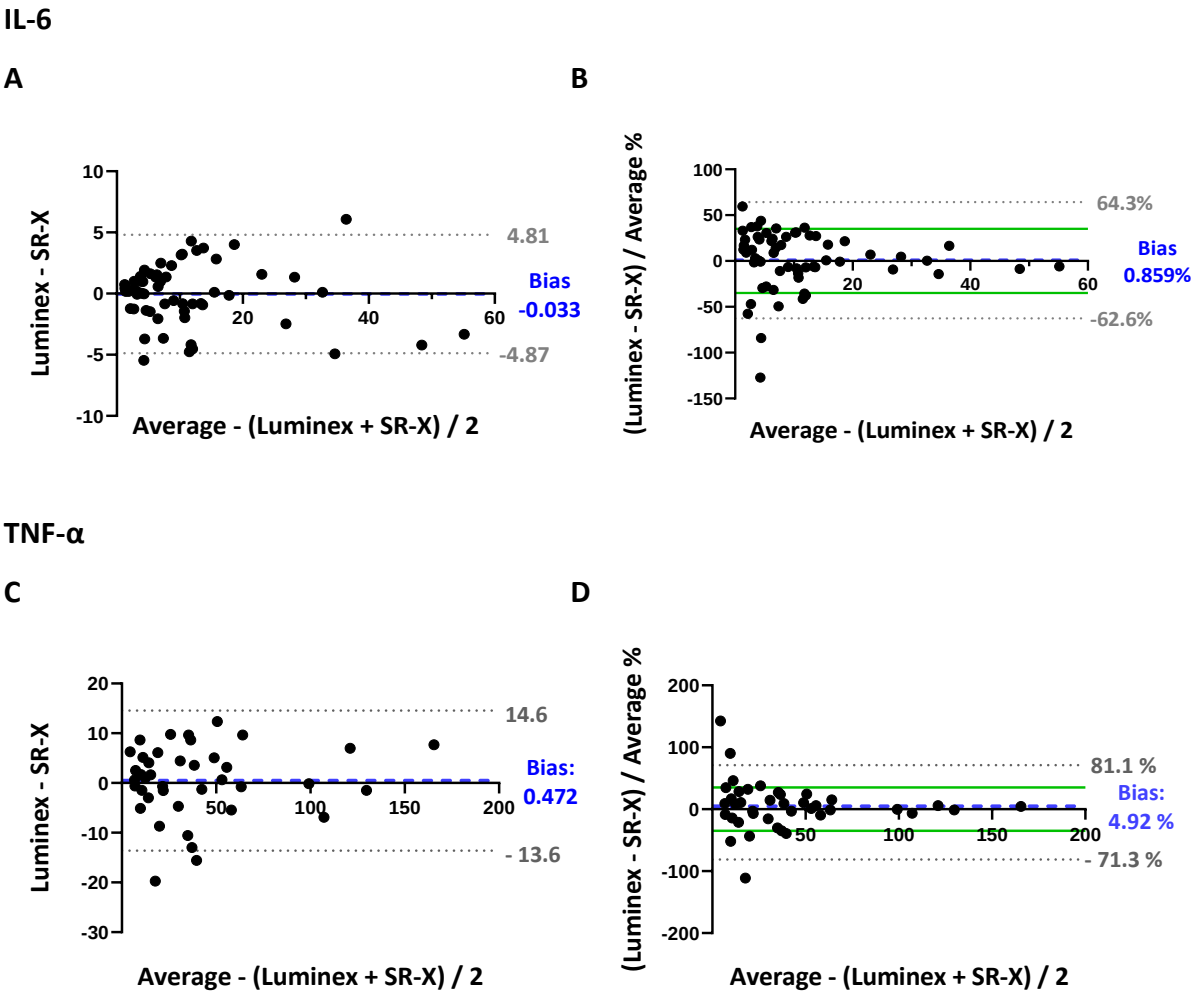

Figure 8: Blant Altman plots of differences generated for IL-6 and TNF-α. *Blant Altman analysis was performed to compare the methods Luminex and Simoa SR-X. In (A) and (C) differences (Luminex - SR-X) are given as absolute values as pg·mL^{-1} while (B) and (D) expresses the differences as percentages. The blue dashed line represents the bias. The 95 % confidence intervals are included as dotted lines in grey and the green lines represent the allowable range (-35 % - 35 %).*

To be able to calculate CIs for Blant-Altman analyses, the differences between the two methods were needed to be normally distributed. The Shapiro-Wilk test confirmed normal distribution of differences for TNF-α resulting in W = 0.9523 (p value = 0.0907), and for IL-6 in W = 0.9776 (p value = 0.3352). The bias of the Blant-Altman plot of IL-6 showed an absolute value of -0.033 (**Figure 8A**) and a relative value of 0.859 % (**Figure 8B**). For TNF-α, the bias was calculated to be 0.472 and 4.92 %, respectively (**Figure 8C** and **D**). This meant, the Simoa SR-X assay yielded higher values for IL-6 by 0.033 pg·mL^{-1} on average compared to the Luminex technology and IMAP 1 yielded higher concentrations for TNF-α by 0.472 pg·mL^{-1} compared to the Simoa assay. For TNF-α, the 95 % CI for absolute values was determined from -13.61 to 14.56 (**Figure 8C**) and from -71.29 % to 81.13 % (**Figure 8D**) for relative differences. For IL-6,

the 95 % CI of the absolute differences was determined from -4.87 to 4.81 (**Figure 8A**) and for the relative differences from -62.6 % to 64.3 % (**Figure 8B**). Meaning, in general, 4.87 pg·mL^{-1} above and 4.81 pg·mL^{-1} below the IL-6 concentration recorded with the Simoa technology were quantified with Luminex. For TNF-α, analogously, 13.6 pg·mL^{-1} more and 14.6 pg·mL^{-1} less, respectively, were analyzed by Luminex (see CIs of **Figure 8A** and **C**). For both analytes, 95 % of the differences were within the respective calculated confidence intervals while 20 % (TNF-α) and 23 % (IL-6) of the differences of individual samples analyzed with both methods in relation to the respective mean value lay outside the internally defined acceptance range of -35 % to 35 %. At lower average levels, the scattering of differences between the methods appears to be higher compared to higher averages of both methods for IL-6 and TNF-α, respectively (**Figure 8B** and **D**).

4.6 NK cell activation

Investigation of NK cell activity in whole blood assays was performed in four independent experiments. In the following section, the results of the experiments examining which effects the stimuli IL-12, IL-18, IL-2, R848 and K562 and their specific combinations have on NK cell activation and effector function are compared (see **Table 13** in 3.3.2). Flow cytometry datasets were therefore supplemented with data from corresponding cytokine readouts using the developed and validated Luminex and SR-X assays. The cell number of K562 cells used for whole blood culture experiments was 1.25 x 10^5 cells, as determined through a pilot titration experiment (data not shown). In order to be able to examine the expression of the surface markers CD69, CD25 and CD107a on NK cells, it was first necessary to identify NK cells. This was done by gating lymphocytes in accordance to their expression of surface markers CD3 and CD56. NK cells were then identified as CD3-CD56+ lymphocytes (see also gating strategy **Annex - Figure 2**).

4.6.1 CD69 and CD25 expression on NK cells

NK cell activation can be investigated by checking the expression of surface markers by flow cytometric analysis. Following, expression levels of CD96 and CD25 on the surface of NK cells are shown (**Figure 9**).

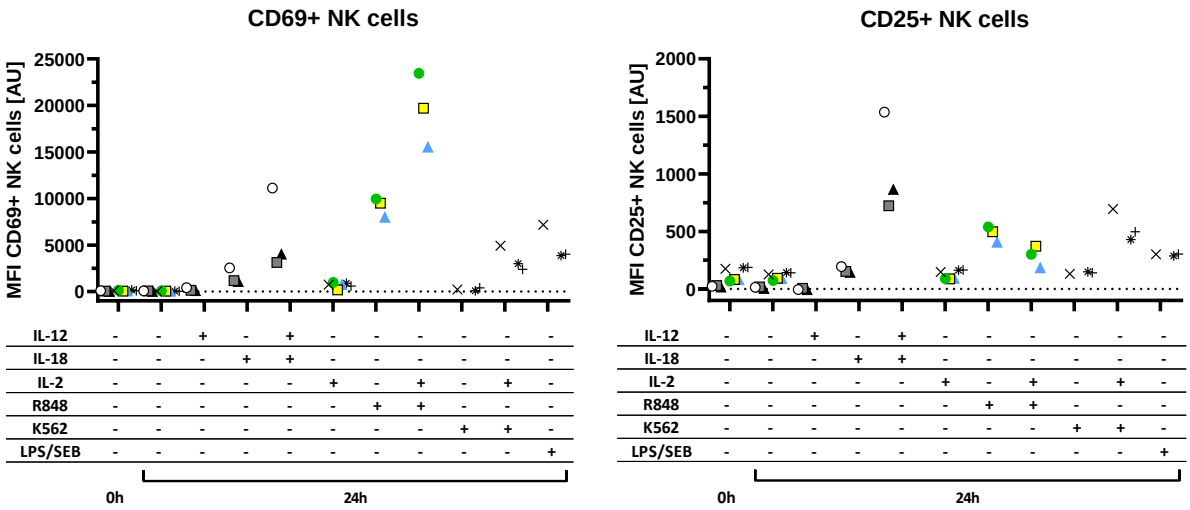

Figure 9: Expression of surface molecules CD69 and CD25 on NK cells. *Whole blood assays were cultured over 24 h after blood donation and the addition of stimuli with exception of the unstimulated control at t = 0 h. Flow cytometric analyses, carried out directly after culture, were performed in singles (n = 1). The results are displayed as MFI and are based on viable NK cells gated as $CD3^{-}CD56^{+}$. Whole blood assays were stimulated using IL-12 and IL-18, respectively R848 and IL-2, either alone or in combination. K562 were added in a cell number of 1.25 x 10^{5} cells, without or in combination with IL-2. The combination of lipopolysaccharide (LPS) and staphylococcal enterotoxin B (SEB) was used as further stimulus. Data from three individual experimental culture approaches were compared (1^{st}: donor A-C, 2^{nd}: donor D-F and 3^{rd}: donor G-I).*

For CD69, the highest intensities were found after stimulating the cells of whole blood with the combination of R848 + IL-2 ranging approximately between 15,000 and 23,500 AU. Increased signals in comparison to unstimulated controls (0 h and 24 h) were also observed using R848 alone, but the signals were approximately half of the highest achieved levels. Slightly increased signals in relation to the controls were observed for IL-18, the combination IL-12 + IL-18, K562 together with IL-2 and for LPS/SEB. However, the signals measured for donor A after stimulation with IL-12 + IL-18 were on average approximately three times higher than those obtained for donor B and C. The same phenomenon could be observed for donor G after K562 + IL-2 and LPS/SEB stimulation, although differences were smaller. Other stimuli gave signals comparable to the unstimulated controls.

CD25 signal intensities were in general lower compared to CD69 signal intensities. Highest signals were detected for the combination of IL-12 and IL-18 where, again, donor A gave higher signals compared to donors B and C. The signals of donor G based on K562 + IL-2 stimulation were only marginally lower than those just described for donor B and C after IL-12 + IL-18 stimulation. Slightly lower signals could be observed for donor H and I when K562 in combination of IL-2 was used. These were comparable to the signals reached after the

stimulation using R848 alone respectively in combination with IL-2. Signals after LPS/SEB stimulation were comparable as well. Remaining stimuli gave results that were not distinguishable from signals derived from the unstimulated control whole blood assays.

4.6.2 CD107a expression on NK cells

CD107a (also referred to as LAMP-1, Lysosomal-associated membrane protein 1) is another surface marker involved in the process of degranulation. **Figure 10** shows the relative amount of NK cells that were analyzed as CD107a positive after stimulation with either IL-12, IL-18, IL-2, R848, K562 cells and LPS/SEB or corresponding combinations. Also, signals measured for unstimulated controls after 0 h and 24 h are included.

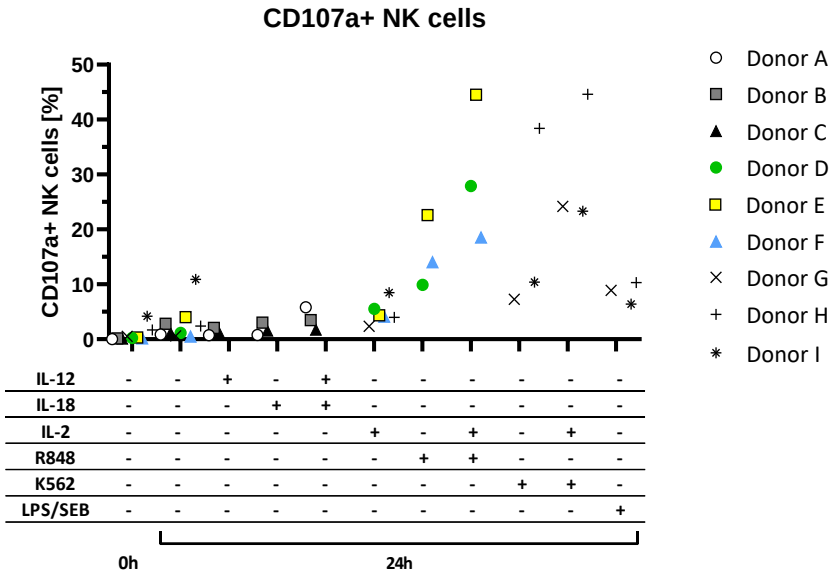

Figure 10: Percentage of CD107a positive NK cells*. Whole blood assays were cultured over 24 h after blood donation and the application of stimuli with exception of the unstimulated control at t = 0 h. Flow cytometric analyses carried out directly after culture were performed in singles (n = 1). The results are displayed as percentage of CD107a$^+$ NK cells of parent viable NK cells gated as CD3$^-$CD56$^+$ cells. Whole blood assays were stimulated using IL-12 and IL-18, respectively R848 and IL-2, either alone or in combination. K562 were added in a cell number of 1.25 x 10^5 cells, without or in combination with IL-2. The combination of lipopolysaccharide (LPS) and staphylococcal enterotoxin B (SEB) was used as further stimulus. Data from three individual experimental culture approaches are compared (1st: donor A-C, 2nd: donor D-F and 3rd: donor G-I).*

Stimulation with IL-12, IL-18, and their combination as well as with IL-2 and LPS/SEB resulted in comparable or only slightly increased amounts of CD107a positive NK cells in relation to unstimulated controls. In contrast, the amount of NK cells carrying CD107a on their surface increased after stimulation with TLR agonist R848. Even higher amounts were observed when stimulated with R848 in combination with IL-2, although differences in-between donors D to F

did exist. While the lowest relative amount was observed for donor F with 18.5 %, donor E reached 44.5 %. Slightly increased amounts of CD107a positive NK cells could be seen when K562 cells were used as a stimulus in the whole blood-based assay for donors G and I, while signals of donor H were approximately four times higher. Even more NK cells carrying CD107a on their surface were found for all three donors G to I, when K562 cells were combined with IL-2, peaking for donor H in 44.6 %. These results were comparable to values achieved for the combination of R848 + IL-2.

4.6.3 TNF-α and IFN-γ cytokine readout

Following, the results of cytokine readouts of the markers TNF-α and IFN-γ are described as shown in **Figure 11**. For the measurements of TNF-α and IFN-γ shown below, the developed and validated Luminex and Simoa assays were used.

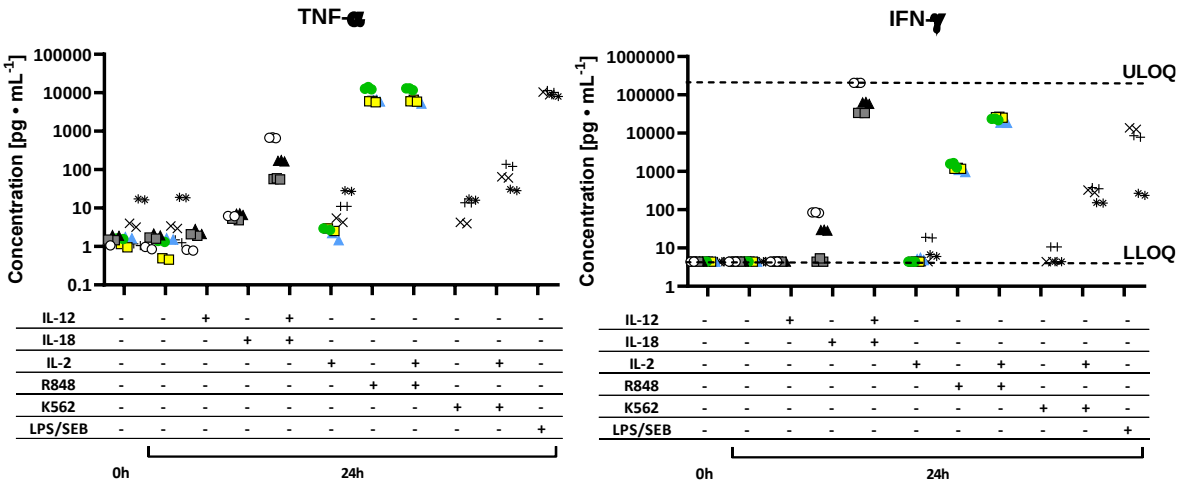

Figure 11: TNF-α and IFN-γ levels in whole blood culture supernatants. *Whole blood assays were cultured over 24 h after blood donation and the addition of stimuli with exception of the unstimulated control at t = 0 h. Measurements were performed in duplicates (n = 2; TNF-α values determined by SR-X measurements) and triplicates (n = 3, Luminex measurements). Concentrations are given in pg·mL^{-1}. Whole blood cultures were stimulated using IL-12 and IL-18, respectively IL-2 and R848, either alone or in combination. K562 were added in a cell number of 1.25 x 10^5 cells, without or in combination with IL-2. The combination of lipopolysaccharide (LPS) and staphylococcal enterotoxin B (SEB) was used as further stimulus. Data from three individual experimental culture approaches are compared (1st: donor A-C, 2nd: donor D-F and 3rd: donor G-I). Upper and lower limit of quantification (LLOQ and ULOQ) are displayed as dashed lines. The presentation of the quantification limits for TNF-α was not meaningful because data generated with the Luminex assay as well as with the Simoa assay were used. The measured signals were within the respective quantification limits.*

For TNF-α, as well as for IFN-γ, comparable concentration levels to the unstimulated control at t = 0 h and after 24 h were observed after 24 h-stimulation with IL-12, IL-2 and the co-

culture with K562 cells. However, TNF-α concentrations obtained for donor I were higher for the unstimulated controls after 0 h and 24 h. While IL-18 stimulation led to concentration levels of TNF-α comparable to the unstimulated cultures, the IFN-γ concentrations varied between donors (A: 84.1 ± 1.69 pg·mL^{-1}; B: 4.72 ± 0.557 pg·mL^{-1} and C: 29.3 ± 0.763 pg·mL^{-1}). The combinations of K562 + IL-2 and IL-12 + IL-18 resulted in increased TNF-α levels and even higher concentrations were achieved by stimulation with R848, the combination of R848 + IL-2 and after stimulation with LPS/SEB.

Increased IFN-γ concentrations of about 150 to 370 pg·mL^{-1} after K562 + IL-2 stimulation were shown. These ranges were comparable with IFN-γ concentrations after LPS/SEB stimulation of donor I. For donors G and H, the combination of LPS/SEB led to higher IFN-γ concentrations between approximately 7,500 and 14,000 pg·mL^{-1}. These concentrations were thus 30 to 56 times higher than the concentration determined for donor I. IFN-γ levels after stimulation with R848 + IL-2 could be compared to those achieved for Donor G after LPS/SEB stimulation, while R848 alone reached concentrations lying approximately between 950 and 1,250 pg·mL^{-1}. Highest concentrations could be observed after stimulation with IL-12 + IL-18. While donors B and C showed concentrations of about 33,500 pg·mL^{-1} and 62,000 pg·mL^{-1}, the ULOQ of the assay is reached (204,800 pg·mL^{-1}) when analyzing donor A. Corresponding IFN-γ concentrations were expected above this value.

4.6.4 Granzyme B levels

To further investigate degranulation effector events, granzyme B levels in whole blood culture supernatants were analyzed. Concentrations in unstimulated controls after 0 h and 24 h were too low to be determined in regard of donors A to E. Only for donor C, a concentration of 2.05 pg·mL^{-1} could be measured after 24 h. For donors F to I, the results were highly different between donors, although values after 0 h and 24 h were comparable within one donor. The measured granzyme B concentrations are presented in **Figure 12**.

For donors A and C, an increase of granzyme B concentrations was obtained when IL-12 was used for stimulation in combination with IL-18 compared to the achieved signals when these stimuli were used alone. However, this was the only sample that gave a quantifiable concentration of donor B. Using IL-2, increased concentrations in relation to unstimulated controls were found for donors F to I. The granzyme B concentration gained for donor D was comparable to the results of donors F to I, while donor E resulted in lower levels. Compared

to IL-2 stimulation, R848 showed increased granzyme B levels. The highest granzyme B concentrations of all experiments were observed after combining stimuli IL-2 and R848 with 14,453 to 30,668 pg·mL^{-1}. These were followed by levels achieved by LPS/SEB stimulation (603 to 13,595 pg·mL^{-1}). While the measured granzyme B concentration after K562 stimulation was comparable to the levels after IL-2 stimulation, K562 combined with IL-2 resulted in higher concentrations between 461 to 1,462 pg·mL^{-1}.

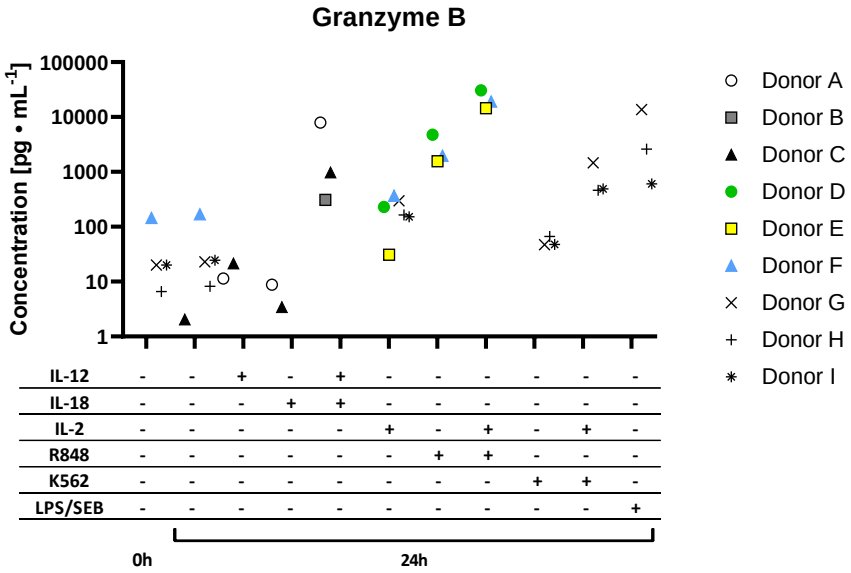

Figure 12: Granzyme B levels in whole blood culture supernatants. *Whole blood assays were cultured over 24 h after blood donation and the addition of stimuli with exception of the unstimulated control at t = 0 h. Measurements were performed in singles (n = 1) using granzyme B ELISA. Concentrations are given in pg·mL^{-1}. Whole blood assays were stimulated using IL-12 and IL-18, respectively R848 and IL-2, either alone or in combination. K562 were added in a cell number of 1.25 x 10^5 cells, without or in combination with IL-2. The combination of lipopolysaccharide (LPS) and staphylococcal enterotoxin B (SEB) was used as further stimulus. For some samples, concentrations were not detectable. These are not represented in the graph. Data from three individual experimental culture approaches were compared (1st: donor A-C, 2nd: donor D-F and 3rd: donor G-I). Quantification limits are not available.*

4.6.5 Activation of other immune cell populations present in whole blood

To compare how different stimuli impacted NK cells and to understand the effects on other immune cells of the whole blood culture system, a heatmap was generated using the web tool ClustVis [162] (**Figure 13**). All results included came from cytokine readouts using Luminex and Simoa readouts and flow cytometric analysis for donors A to I. Results recorded in the course of the three sub-experiments were correlated with each other and compared by grouping similar patterns into clusters. The color scaling from blue (0 %, lowest value) via yellow (50 %) to red (100 %, highest value) indicates the level of the signals obtained via the activation

markers used for the individual cell populations or the level of the cytokine concentrations measured, which were normalized per row. GM-CSF, VEGF and M-CSF were not included due to the previously described validation results outside the acceptable validation criteria. When IL-12 was used as a stimulus, the measurement results gained for IL-12 were removed from the comparison and included in the heatmap as “N/A” (not analyzed, shown in white). The “Control” refers to the unstimulated whole blood culture at time point t = 0 h, while “unstimulated” refers to the whole blood assay cultured over 24 h without any stimulus.

There was almost no difference between the control, the unstimulated sample and the samples stimulated with IL-12 or IL-18 alone for donors A (white), B (grey) and C (black). For monocytes only, low signals of CD62L were observed after 24 h when stimulated with IL-18. In comparison to the corresponding control and unstimulated samples the combination of IL-12 and IL-18 resulted in slightly increased signals for CD69 on CD4+ and CD8+ T cells, monocytes, PMNs (polymorphonuclear neutrophils), Tregs and NK cells. In addition, increased levels of the surface marker CD25 could be observed for NK cells as well as for CD8+ T cells. Most cytokine levels were not influenced by the stimuli IL-12, IL-18 and their combination apart from IL-1Ra and IFN-γ. After stimulation using IL-12 and IL-18 in combination, low levels of CD62L on monocytes and PMNs were shown as well. Further, few relative amounts of CD107a positive NK cells were detected.

Regarding donors D (green), E (yellow) and F (light blue), results determined for controls and unstimulated samples after 0 h and 24 h, respectively, were comparable. The same cluster included samples stimulated with IL-2. While increasing signals could be seen after 24 h of culturing without a stimulus (unstimulated) for the activation marker CD86 on monocytes, even higher signals were detected after IL-2 stimulation. A further difference between the control and the unstimulated sample compared to the IL-2 stimulation were lower levels of CD62L after IL-2 treatment on the surface of monocytes. These were comparable to those received after stimulation with R848 and the combination of R848 and IL-2. Similar levels could be observed for CD62L on PMNs but not, when IL-2 alone was used. All other signals of surface markers and cytokine concentrations were substantially elevated after R848 + IL-2 stimulation compared to controls after 0 h and 24 h as well as to the treatment with IL-2 alone. The only exceptions were IL-4, IL-8 and CD69 on monocytes. All other markers and cytokine concentrations were either similarly increased after stimulation with R848 or R848 and IL-2 in combination or the effects were slightly enhanced by the combination of stimuli in

comparison to R848 alone. This could be seen for the expression of the surface markers CD107a and CD69 on NK cells, for IFN-γ as well as for CD69 on CD4+ and CD8+ T cells or on Tregs. However, these differences were very marginal.

For donors G (dark blue), H (orange) and I (red) the controls, unstimulated samples as well as the treatments with IL-2 or K562 alone were grouped in one cluster due to similar signal and concentration patterns. The only exception was the stimulation with K562 cells on donor H that was clustered together with the three K562 + IL-2 treated samples based on high levels of CD69 expression on monocytes that is more comparable to these samples. Stimulation with the combination of K562 + IL-2 or IL-2 and K562 alone resulted in almost no signaling from CD62L on monocytes and PMNs. The combination of K562 + IL-2 resulted in high CD107a expression on NK cells, also observed for donor H, when K562 cells were employed without IL-2. Increased signals were obtained for CD25 on NK cells. Further, slightly increased levels of IL-8, of CD69 on NK cells, $CD4^+$ T cells and Tregs, of CD25 on monocytes as well as of MCP-1 and IL-1Ra were observed compared to controls after 0 h and 24 h when cells were treated with K562 and IL-2 simultaneously.

The treatment by LPS/SEB led to increased levels of all cytokines apart from IFN-γ, but also increased the expression of CD69 on CD4+ T cells and Tregs, as well as CD69 and CD25 expression on NK cells. Further, the expression of CD69, CD86 and CD25 surface markers on B cells were higher compared to the controls, as well as the expression of CD69 on PMNs and the expression of CD25 on monocytes. For CD8+ T cells, higher levels of CD107a+ cells were detected for donors G and H compared to controls. Again, CD62L signals on monocytes and PMNs were close to 0 % by treating cells with LPS/SEB.

It could be observed that the application of the single stimulants and stimulant combinations used for the respective three different donors of each sub-experiment were mostly grouped in the same cluster. The use of individual stimuli usually led to surface marker expression levels and cytokine levels that were clustered together with those of the two controls (control and unstimulated) of the respective sub-experiment. Differences between the controls at 0 h and 24 h of the individual sub-experiments were recognizable. With regard to signals of CD62L, CD25 on CD4+ and CD8+ T cells as well as of CD86 on monocytes, variances between sub-experiment 1 (donors A, B, C) and the remaining sub-experiments 2 (donors D, E, F) and 4 (donors G, H, I) could be observed. The overall comparison of all results showed that the expression of most surface markers of tested immune cell populations of whole blood as well

as cytokine concentrations were affected most by the combination of R848 and IL-2 or R848 alone, followed by LPS/SEB treatment. While, in comparison, LPS/SEB led to intermediate expression levels of surface markers on regarded immune cells, high levels were observed after the treatment with R848 or R848 in combination with IL-2. However, the highest IFN-γ concentrations and expression levels of CD25 on NK cells over all experiments and donors were achieved by using IL-12 and IL-18 in combination. Highest TNF-α levels were detected after stimulation with LPS/SEB, R848 and R848 in combination with IL-2, respectively. The highest expression levels of CD107a on NK cells by comparing all experiments and donors could be seen after K562 + IL-2 stimulation. This stimulation also led to the comparatively highest expression of CD69 on monocytes. For donor I, increased IL-4 concentrations were observed while this marker was, apart from LPS/SEB stimulation, almost undetectable. Further, differences in CD86 expression on monocytes after IL-2 stimulation between different experiments for donors D to F and G to I were obtained. Here, differences in the expression of CD62L between the controls and unstimulated samples after 24 h of cultivation between the different sub-experiments did exist as well.

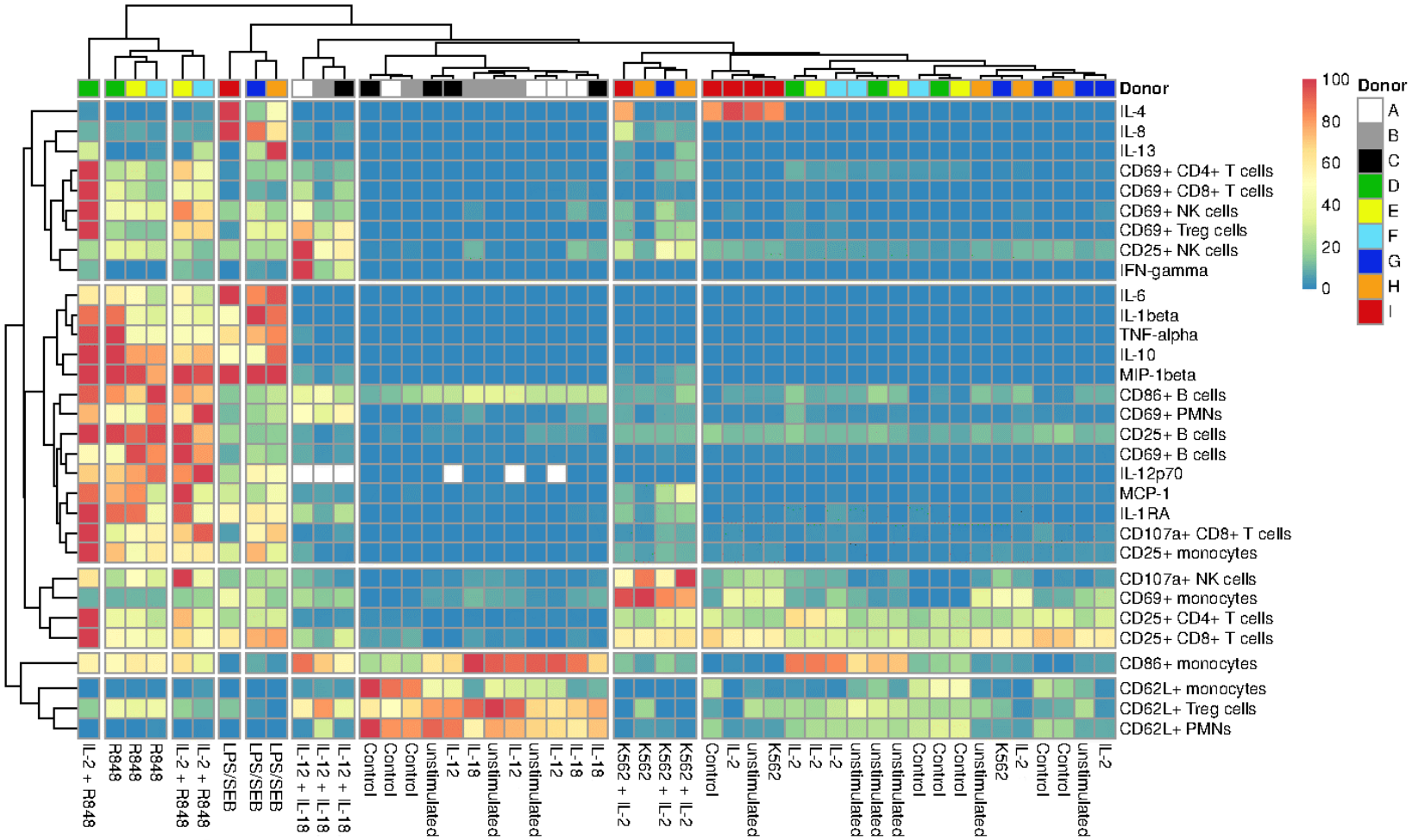

Figure 13: Heatmap of surface marker expression and cytokine levels. *Surface markers on different immune cell populations and cytokine levels present in whole blood after stimulation with IL-12, IL-18, IL-2, R848, K562 cells and respective combinations were investigated. Three independent whole blood culture-based experiments comprising nine donors (A-I) were compared. Annotations on top show clustering of the samples. Negative controls were applied referred to as "Control" (= unstimulated sample at t = 0 h) and "unstimulated" (= unstimulated sample at t = 24 h). Data were normalized in rows, with the highest value corresponding to 100 % (red) and the lowest value to 0 % (blue). The stimuli and corresponding combinations as well as controls are given on the x-axis while the y-axis shows the cytokines and chemokines analyzed using the developed and validated assays as well as the surface markers determined on specific immune cell populations of the peripheral blood.*

5. Discussion

Within the project "Systems Immunology at Biological-Technical Interfaces", two multiplex immunoassays were developed utilizing bead-based Luminex technology. These “inflammatory multiplex analyte panels” (IMAPs) 1 and 2 were used to investigate and characterize the effects of implant materials and their surface properties on the immune response in three different cell culture systems of ascending complexity. Both IMAPs were validated to enable robust and accurate cytokine quantification in supernatants from three cell culture systems – THP-1, PBMC and the whole blood cultures (TruCulture).

The THP-1 cell culture system represents the culture system with the lowest matrix complexity, which was studied in this project. These are human monocytes initially isolated from a patient suffering on acute monocytic leukemia [165]. THP-1 cells are often used to study the function and structure of monocytes in immunological research [166]. PBMCs are the cell culture system of the next degree of complexity. PBMCs consist of isolated lymphocytes, monocytes, and macrophages, which are purified from peripheral blood and are used, for instance, to investigate cytokine release upon immune cell stimulation to address various immunological questions [113]. The most complex cell culture system in the series is the whole blood culture system, which includes all immune cells of the peripheral blood as well as erythrocytes, platelets and all soluble factors present, providing a more complete picture of an immunological reaction.

Analytes measured with the IMAP 1 and 2 assay kits were selected based on their involvement within an immune response to biomaterials [167, 168]. After a biomaterial is implanted into the body, blood proteins are first adsorbed to the surface of the biomaterial and the coagulation cascade, complement and platelets are activated and lead to priming and activation of PMNs, monocytes and macrophages [167, 169, 170]. PMNs play the main role during acute inflammatory events while monocytes and macrophages are the driving force during chronic inflammation processes [167]. "Classically activated" (M1) macrophages maintain the state of inflammation [167, 168] while "alternatively activated" (M2a, M2b and M2c) macrophages, act in a regulatory manner on the immunological response and are involved in the repair of damaged tissue and the healing of wounds [167, 168]. The analytes of IMAP 1 and 2 were selected based on these events in order to be able to distinguish and assess the different processes in the cell cultures.

For the quantification of four analytes, which were present at very low concentrations,

additional highly sensitive assays based on single-molecule arrays were developed using the ultrasensitive Simoa SR-X platform. These assays were also validated for the whole blood system. The assay development procedures for the Luminex and Simoa assay as well as the elaborate assay validation efforts represented main parts of this work.

In this thesis, the developed and validated Luminex IMAPs as well as Simoa immunoassays were used to investigate the activation of NK cells by NK cell-specific stimulants in whole blood culture systems in combination with flow cytometric analysis. In addition, it was investigated whether other immune cell populations are activated by the NK cell-specific stimulants and, if so, which ones. These experiments were performed in close cooperation with HOT Screen GmbH. In the following section, the results of the development of the Luminex IMAPs as well as the Simoa assays are discussed, and the validation results are assessed. Subsequently, the results of NK cell activation based on the respective cytokine readouts and flow cytometry analysis are discussed within the context of their scientific objectives.

Immunoassays are indispensable nowadays for research and clinics and are used not only in clinical diagnostics or biopharmaceutical analysis and research, but also in the course of environmental monitoring or food analysis. Since the 1960s and the first implementation of an immunoassay, a major development process has taken place, leading to the appearance of numerous bioanalytical platforms and immuno-analytical systems. ELISAs are still considered the gold standard due to their high specificity, accuracy and sensitivity, ease of use and are used for the detection of a multitude of analytes. Building on this, it became possible to create automated processes using robotics, improve technologies in terms of sensitivity and create cost-efficient tools to perform high-throughput procedures [171]. A key step towards cost efficiency and high-throughput applications was the possibility to simultaneously detect and quantify several analytes in one reaction vessel, referred to as multiplexing. Compared to conventional ELISA applications, the sample volume required for the measurement can be drastically reduced and only one analytical run is required at a time instead of several, largely independent of the number of analytes. Luminex provides one platform offering this possibility of multiplexing [11, 15]. Despite this great advantage, this technology is sometimes not sensitive enough to detect biomarkers that are only present at very low concentrations (low $pg \cdot mL^{-1}$ range or below). In this case, the Simoa technology developed by Quanterix can be used, which is able to quantify low analyte concentrations even in the sub-$pg \cdot mL^{-1}$ range [16-18, 20]. This application can also be used for multiplexing approaches [19, 22].

5.1 Assay development and assay optimization

The quality and performance of immunoassays is strongly dependent on various factors that need to be considered and optimized during the developmental phase. Only then, the best possible precision and sensitivity can be achieved, which is a pre-requisite for valid and reproducible results. Therefore, suitable buffer systems were investigated, and their compositions were adapted and optimized to the needs of the respective assay components and target sample matrices. In addition, the concentrations of the detection antibodies were adjusted and optimized for the specific analysis.

The first step in immunoassay development is usually the identification of suitable capture and detector antibody pairs as well as standard proteins for the detection and quantification of the desired analytes. For this purpose, it was possible to refer to and to combine already existing in-house data from various different projects. Therefore, the search for antibody pairs was not part of this work. Commercially available monoclonal, but also polyclonal antibodies and recombinant proteins were used and applied for the immunoassays.

A crucial factor to be considered at the very beginning of immunoassay development is to find a suitable buffer system that enables a good assay performance and at the same time a low background signal and suitability for the selected matrix. This is especially important when a multiplex assay will be developed. As a basic buffer system, solutions based on, for example, Tris, phosphate but also on HEPES or MES can be employed. Since each single and multiplex immunoassay requires specially adapted buffer formulations, it is advisable to reconsider this point with each individual assay development in a very early stage. Simple buffer solutions or more complex buffer media, some of which are commercially available, can be used for this purpose [172].

For the three buffer systems tested for IMAP 1 and 2, no exceptional differences could be found with regard to the course of the standard curves. However, the LCB was the most unsuitable within this comparison as the lowest signals of the respective standard curves for more than 50 % of the analytes of IMAP 1 were achieved. Further, in the case of MCP-1 within IMAP 1, the signals of the two lowest calibrator concentrations could barely be distinguished from each other, leading to a strong reduction of sensitivity. The reason for choosing CBST was the higher stability of the signals in the upper part of the standard curve. Within the area of a plateau, which was observed for some analytes when using BRE, a back-calculation of unknown analyte concentrations in samples using the standard concentration cannot be made

unequivocally. Even small deviations of comparable signals will then become noticeable in strong deviations of the back-calculated concentrations and negatively influence reproducibility and validity of results. Under certain circumstances, the corresponding standard curve would need to be capped at the top and the width of the quantification range would be narrowed. Thus, CBST was set as the base buffer system, as it provided acceptable background signals for most analytes in comparison. The only exceptions were IL-8, MCP-1 and MIP-1β. Furthermore, the highest signals of the standard curves could be obtained on average with this buffer. This is the basis for the goal of ensuring quantification over a broad assay range.

Although the buffer CBST represented an adequate buffer system, non-specific binding still occurred, leading to the high background signals of some analytes. These had to be investigated and could be reduced by checking cross-reactivity and by the performance of assay optimization.

As for the SR-X assays, the Homebrew Sample/Detector Diluent of the company Quanterix already provided satisfactory results after the first run, further assay buffers were not tested. Only background levels for IL-12p70 were relatively high demanding for buffer optimization as well which had to be addressed.

Cross-reactivity between assay components is a kind of non-specific binding described as a signal based on the binding of antibodies to substances other than the target analyte [173]. The chosen three-step sandwich immunoassay format reduced cross-reactivity between assay components by immobilizing and concentrating the analyte of interest by binding the epitope to a capture antibody before a labeled detection antibody is added in a next step [174]. Further, the implementation of in-between washing steps as performed for the developed assays reduced cross-reactivity by eliminating unbound components. Nevertheless, in a multiplex assay setup, additional combinatorial interactions between the assay reagents like detection and capture antibodies as well as the respective analytes or recombinant proteins are present [174, 175]. This reinforces the presence of cross-reactivity, potentially affecting assay performance by influencing the limits of detection and quantification. Cross-reactivity testing is strongly recommended because the quality and reproducibility of multiplex immunoassays depends on the specificity of the applied antibodies, in particular the capture antibodies, that should reliably bind their target molecule [175].

The detected cross-reactivities between capture and detection antibodies of some analytes of

IMAP 1 could be reduced by the replacement of the IFN-γ detection antibody leading to significantly lower background signals. Further, assay buffer optimization led to a reduction of the slight non-specific binding of the detection antibody against MCP-1 to other capture antibodies, but as well to more stable and lower background values were achieved, especially with respect to IL-8, MCP-1 and MIP-1β. For this purpose, the CBST buffer, already supplemented with NaCl to reduce non-specific binding (empirical value), was additionally provided with a blocking reagent against heterophilic antibodies. According to the manufacturer this is a suitable blocking reagent for sandwich immunoassays utilizing monoclonal and polyclonal antibodies [176], an effect that was also observed here. False positive signals can be reduced as these reagents block the bridging of heterophilic and so called human anti-mouse antibodies (HAMA). These antibodies, which can be available in human samples, may cross-link the reagent antibodies, leading to a detectable antibody complex without a captured analyte. Then its detection suggests a positive signal for the actual analyte and leads to false high results [173, 177, 178]. In addition to these specific blocking reagents, animal sera are also a popular and often used agent to minimize non-specific binding. By adding fetal bovine serum and horse serum to the assay buffer, the blank values, especially of IL-8 and MIP-1β, could be significantly reduced. The concentration of the animal sera was chosen to be 2.5 % as it had the lowest variation of blank signals. The addition of animal serum also reduced the background levels for the Simoa assay to detect IL-12p70 and led to an increase in sensitivity, possibly by binding of unspecific antibodies or proteins to proteins present in the animal sera. The background level of MCP-1 was for this experiment already reduced to acceptable levels without the addition of buffer supplements. According to experience, this could be attributed to the longer storage of freshly coated beads over one or two weeks before application in assay runs which leads to increased blocking of newly generated beads and thus less unspecific binding possibilities.

Further minor cross-reactivities detected between detection antibodies and recombinant proteins, for assays of both methods (Luminex and Simoa) were acceptable. The respective calculated recovery rates were only marginally higher than the defined acceptance limit of 1 %. These minor deviations were accepted because the assays developed in this thesis are fit-for-purpose approaches that are used in the context of research applications. Furthermore, these are multiplex immunoassays, which by nature have a much higher probability of cross-reactivity between the various assay components of the different analytes. In this regard and

as sensitivity was not affected by these minor cross-reactivities, these deviations were accepted.

For IMAP 2, no cross-reactivity was detected between the respective assay components tested. Nevertheless, the optimized concentration of the blocking reagent of heterophilic antibodies fulfilled its intended task to lower blank values and at the same time reduced the deviation between the replicates (CV) leading to a lower LOD and therefore contributing to a better sensitivity.

During assay development, the concentration of detection antibodies was also optimized. As shown by the example of the detection antibody titration for IL-10 and TNF-α, the change in concentration can indeed have a major impact on the overall assay performance (TNF-α) or may leave it completely unaffected (IL-10). Therefore, it is strongly recommended to determine the optimal concentration experimentally for each analyte of a multiplex but also for each individual immunoassay. At best, this can not only lead to a reduction of costs, as less detection antibody has to be used, but also to an increase in sensitivity due to a resulting optimized standard curve or reduced background. In the course of these immunoassay developments, the appropriate detection antibody concentration could be determined for each and every assay and target analyte of interest and optimized multiplexed and sinlgeplexed immunoassays based on the requirements for the analysis could be provided.

5.2 Immunoassay validation

Assay validation was performed to verify the accuracy of the immunoassays developed, as well as to demonstrate that they are suitable for their intended use. The validation was performed in a fit-for-purpose approach [28] considering the guidelines of the US Food and Drug Administration (FDA) [24] and the European Medicines Agency (EMA) [23]. The following parameters were determined during the validation process: calibration curve model, limit of detection as well as upper and lower limit of quantification, inter and intra assay precision, parallelism, dilution linearity and analyte short-term and freeze-thaw stability. Since stability is not an assay-specific parameter, but is dependent on the analytes themselves in a given matrix, this validation parameter was only investigated in the course of the validation of the two IMAPs and adopted for the Simoa SR-X assays.

5.2.1 Model of the calibration curves, detection and quantification limits

The validation of the calibration curve model was an applicability test analyzed by precision and recovery. Without exception, the suitability was demonstrated for the standard curves of the assays developed on the Simoa SR-X platform. Since the standard curves showed very good reproducibility and stability over all validation runs, a valid back-calculation of unknown analyte concentrations was ensured using the standard curves. Although the second standard curve point did not meet the precision and recovery rate across the six validation runs of the analyte IL-6, the guidelines are being followed [23, 24]. The suitability of the calibration curve models could also be demonstrated for the majority of the analytes of the two IMAPs. The reason for the poor precision of calibrator 7 in case of MCP-1 is the potentially insufficient sensitivity of the antibody pair in the concentration range around 1.24 $pg \cdot mL^{-1}$. Thus, no reliable quantification is possible in this concentration range, which in turn was reflected in the low precision. Because of this, this point was not included in the quantification range. However, it is still listed as an anchor point and included in the respective curve fitting for improving the overall curve fitting. In general, anchor points can improve curve fitting especially in the curve ends by stabilizing the fit. These calibrators used as anchor point are either above or below the quantification range. Therefore, they do not have to fulfil the respective acceptance criteria [23, 24, 29]. For MCP-1, the calibrator was reduced to six standard points. Hence, also this standard curve still meets all the requirements of the guidelines [23, 24]. Theoretically, the same procedure could have been carried out for calibrator 1 of the analyte IL-13, an analyte included in IMAP 2. However, in the course of determining the upper limit of quantification, a precision of up to 25 % was accepted. This point fulfils this acceptance criterion and remained part of the standard curve model. The defined fitting models with the selected weighting best reflected the standard curves of both methods and thus contributed to a valid back-calculation when determining unknown concentrations. These fitting models must be maintained in any analysis and a very good reason would be needed for changing them.

The assay range is defined by determining the limits in which a particular analyte is detectable (LOD) and quantifiable (LLOQ and ULOQ). These limits were determined in the course of the respective assay validation for each analyte.

Since the LOD for each analyte of the Luminex and Simoa SR-X assays was determined below the respective calibrator of the lowest concentration, the entire range spanned by the

calibration curve could be used for the detection of the analytes. However, this is only the limit at which a signal generated by the binding and detection of target analyte molecules clearly distinguishes itself from the background [27, 28]. This does not yet indicate whether the signal can be reliably converted back into a concentration on the basis of the standard curve. For this purpose, quantification limits were defined [23-25, 28].

For the two IMAPs as well as for the Simoa SR-X assays, the highest calibrator concentration could be defined as ULOQ, since the acceptance criteria for CV and recovery were met. Thus, in this concentration range, the target analyte quantification in a test sample could be guaranteed and was considered valid.

With regard to the determination of the LLOQ, for all four SR-X analytes, IL-6, TNF-α, IL-4 and IL-12p70, the lowest calibrator concentration (CAL7) could be defined as the lowest concentration at which the respective analyte could be reliably back-calculated. The same was true for 10 analytes of IMAP 1 and 2. Only for the analytes IL-6, GM-CSF, MCP-1, MIP-1β and IL-13 the concentration of the determined LLOQ was between the seventh and sixth calibration point (CAL7 and CAL6). Thus, in the concentration range of the calibrator with the lowest concentration (CAL7), no reliable quantification of mentioned analytes could be guaranteed. For MCP-1, this result was consistent with the validation results of the calibration curve model, with CAL7 set as the anchor point. Although there was no valid back-calculation in the range of the lowest standard concentration of these five markers, they are, with the exception of MCP-1, further used as standard points. However, only concentrations equal to or greater than the concentration defined as LLOQ were considered valid and were used for analysis.

The aim of developing the analytes IL-6, TNF-α, IL-4 and IL-12p70 on the Simoa SR-X platform was to detect the respective analytes below the quantification limits of the IMAPs. This should be achieved through higher sensitivities than the corresponding Luminex assays. By comparing the LLOQs of the analytes of the different methods, it was found that for IL-4 the sensitivity was increased by a factor of 25. For IL-12p70, sensitivity was increased by a factor of 34, and for IL-6 and TNF-α, sensitivity was increased 38-fold and 43-fold, respectively. This increased sensitivity is based on the single molecule array technique. As with conventional ELISA, signal amplification takes place, but in contrast to ELISA in an extremely small reaction volume of 50 fL. Thus, even with very few sandwich complexes bound to the beads, i.e. at very low analyte concentrations, there is a high accumulation of the fluorescent product and thus a

detectable signal [18].

5.2.2 Inter and intra assay precision

Another important validation parameter for confirming assay quality and performance is precision, which is defined as the degree of concordance between independent test results [25]. Intra assay precision, to assess deviations during a single run, and inter assay precision, to assess reproducibility between independent runs, were investigated [23-25].

The intra and inter assay precision was confirmed for all analytes of the Simoa SR-X assays as well as for IMAP 1, as all CVs were in the acceptable range. Likewise, the acceptance criteria were met for the analytes in IMAP 2. Drastically high CVs were only obtained for VEGF in the course of determining inter assay precision. Due to this high variance between different analytical runs, reproducibility and validity could not be confirmed for this analyte. For this reason, measured VEGF concentrations were not considered and not used for the evaluation of scientific questions. This poor precision for VEGF could have different reasons. Possibly, non-optimal buffer conditions or the binding characteristics of the antibodies used could have had a negative effect on the determination of this parameter. However, this remains speculation. Since the VEGF assay was an integral part of the corresponding multiplex assay, it was not possible to remove it from the multiplex assay. A change in the composition of the assay reagents would have resulted in such a large change that the validation could no longer be considered valid and would therefore have had to be at least partially repeated. To nevertheless analyze VEGF, a single-plex could be developed or a commercial assay could be used.

5.2.3 Parallelism and dilution linearity

The aim of parallelism experiments is to show whether the binding properties of the capture and detector antibodies to the endogenous protein correspond to those of the recombinant protein used as a standard [179]. For this reason, only endogenous material is used for the investigation of this validation parameter, whereby it is necessary that the endogenous concentration is relatively high [23, 25]. Dilution effects on the quantification of endogenous analytes in the sample matrix are investigated. At the same time, statements can be made about the selectivity, the occurrence of matrix effects can be evaluated and the required minimum dilution of the samples can be determined [180]. A non-existing parallelism means

that the re-calculation of the diluted sample results in wrong concentration values. Thus, a comparison of two different dilutions of a sample is not possible. This was true for three analytes of the two IMAPs, namely IL-4, GM-CSF and IL-12p70 and further for two of the three samples analyzed for parallelism for the analytes VEGF and M-CSF. Although, parallelism could be demonstrated on the third remaining sample, it cannot be ruled out for future measurements that the binding to the recombinant protein is different from that to the endogenously occurring analytes. Therefore, the result of parallelism was assessed as "not determinable" for VEGF and M-CSF.

For the analytes IL-1Ra and IL-13, recoveries outside the acceptance range of the lowest dilution factor of 4 suggest interference from matrix effects as higher dilutions achieved acceptable recoveries. Matrix effects are a consistent deviation in the determination of the analyte concentration between two different matrices [181] – in this case between a sample that is less diluted and one that is more diluted in assay buffer. In addition to the target analytes to be detected, the sample matrix contains other endogenous components that can, for example, bind non-specifically to beads and/or interact with the detection system and thus lead to false positive results. In addition, these could be molecules which, due to their immunological background, interact specifically with assay components and also lead to false positive signals or suppress signals, such as the heterophilic antibodies already mentioned [182].

In particular for MCP-1, the dilutions 1:1,024 and 1:2,048 should not be considered. Although two other samples yielded acceptable recoveries for these dilutions, the deviations from the acceptable range were too large to be tolerated. Comparability of concentrations obtained in this dilution range is not guaranteed. In order to cover all analytes of IMAP 1 and 2, it was necessary to perform sample measurements in two different dilutions. These were set to the final dilution factors 8 and 512. With one of these two dilution factors, most concentrations for all analytes were measurable and fulfilled the acceptance criteria of parallelism, apart from MIP-1β. It must be mentioned here that the samples used were not representative for all analytes, as lower concentrations would have been necessary for some analytes, such as MIP-1β. Since native samples are necessary to determine the parallelism, samples were generated via LPS/SEB stimulation in order to get all analytes in a detectable range, including e.g. IL-4 and IL-12p70, which are predominantly present in low concentrations. This required a high stimulation, which then led to other analytes (like e.g. MIP-1β, IL-8 or MCP-1) being

very highly concentrated. Thus, parallelism data in the low range could not be obtained for these analytes. However, later sample measurements using dilution factors 8 and 512 showed that the concentrations obtained at both dilution factors were well comparable and acceptable (data not shown). Thus, parallelism can be assumed for all analytes at these two dilution factors.

Looking at the results of the determination of parallelism of the Simoa SR-X assays, interferences due to matrix effects were also assumed at the lowest dilution factors 5 for the analytes IL-6, TNF-α and IL-12p70. In order to detect these analytes, samples will be measured with the final dilution factor 10 in the future. Although relatively high deviations are plotted for IL-4 in one sample for the dilution factor 5, the samples for this analyte are measured with the dilution factor 5. This is because the other two samples generated acceptable recoveries for this dilution. In addition, further samples were measured with dilution factors 5 and 100 (data not shown), which showed a very good comparability of the back-calculated concentrations. Thus, the deviation at dilution factor 5 of the sample was considered as an outlier in the course of the parallelism determination.

The determination of the dilution linearity shows whether the concentration of the analyte to be determined, which is above the ULOQ, can be quantified with sufficient accuracy after dilution into the quantifiable range. It is tested whether the relation of the signal to the concentration of the analyte in the biological sample is linear after dilution. Here, the influence of the matrix components becomes negligible due to the high dilution [23, 25]. In contrast to parallelism, dilution linearity uses recombinant protein spiked into the sample matrix. For the Simoa SR-X assays, a linear relationship of signal to concentration was demonstrated without exception and all recoveries were obtained within the acceptance range. For IMAP 1 and 2, dilution linearity could also be shown for all analytes. For a few dilutions of individual analytes, the very small deviations from the defined acceptance criteria could be accepted under the aspect that these are exploratory assays. In addition, multiplexing often requires compromises to be made as it often affects assay performance. The simultaneous detection of multiple analytes within a multiplexed assay involves the interaction of assay components. However, this can be accepted to a certain extent.

5.2.4 Analyte stability

To exclude that storage conditions or steps during sample preparation have an influence on

the concentration determination of the target analyte, the stability of the analyte in the sample matrix is investigated under certain conditions [23-25, 27, 28]. It is possible that samples have to be subjected to multiple measurements (repeat measurements, use in different assays, etc.). Consequently, this entails several freezing and thawing cycles. Freezing can cause several stress factors capable of denaturing proteins. These include, for example, ice formation, solute concentration due to crystallization of water and eutectic crystallizations of buffer solutions leading to pH changes [183]. Further, proteins are known to lose their structure and function at room temperature over time. Denaturation takes place by unfolding of proteins as they are losing their tertiary and secondary structures [184]. Protein denaturation can in turn influence the detection or quantification. The structural change of the target analyte could alter the binding behavior of the assay antibodies or lead to them no longer being able to recognize and bind their specific target. This would result in an incorrect quantification.

As the deviations from the acceptance range observed for INF-γ (IMAP 1) and IL-13 (IMAP 2) after two freeze-thaw cycles were within a tolerable range and due to the fact that three freeze-thaw cycles do not seem to have any influence, freeze-thaw stability was considered to be given after three freeze-thaw cycles. Therefore, samples can be frozen and thawed up to three times without affecting the respective quantification in a way that obtained data can no longer be compared.

Short-term stability was given for all analytes of the two IMAPs. Only the storage of the sample matrix for 24 h at room temperature or 4 °C affected the analyte stability of IL-4, IL-10, MCP-1 and VEGF and influenced the quantification. Thus, it was shown that storage of samples for 24 h neither at room temperature nor in a refrigerator is recommended for these analytes. Instead, the samples should preferably be stored at -80 °C.

5.3 Comparability of methods

The two analytes IL-6 and TNF-α were developed and successfully validated as part of the IMAP 1 but also as a 2-plex on the Simoa SR-X platform. In order to complement Luminex datasets of the two markers with data from the Simoa assay, in case the sensitivity of the Luminex assay is not sufficient, the comparability of the two methods must be given.

The two methods applied for testing comparability were the Passing-Bablok regression and Blant-Altman plots. Both methods are recommended for the comparison of two analytical

methods. The Passing-Bablok regression determines a linear regression line and can detect proportional and systematic errors, while the Blant-Altman method describes the agreement of two analytical methods by analyzing the differences of the two analytical methods.
The results of Passing-Bablok regression, but also the rank correlation coefficient according to Spearman, showed that there was a good correlation within the overlapping dynamic ranges of IL-6 and TNF-α of both methods and that results based on both methods can be compared. However, it should be mentioned that most samples had concentrations in the lower range of the comparison range. Optimally, more concentrations in the higher range would have been desirable, but these could unfortunately not be obtained. A correlation analysis provides a quantification of the extent to which two variables are related to each other. However, a high correlation does not necessarily mean good comparability, as the concentration values of the two methods examined may still differ. Passing-Bablok regression allows the proportional and constant error between the methods to be determined and thus makes it possible to correct the errors [157] and adjust the two methods to each other by, for example, factorial adjustment. This was performed for the Simoa assays of IL-6 and TNF-α to correct for the detected proportional error for both analytes. Afterwards concentration values of the Luminex and the Simoa method could be used equally. In order to examine the level of agreement between the results produced by the two methods, Blant-Altman analysis of differences can be carried out [161]. This was applied in the course of this thesis using the data generated on the Luminex platform together with the corrected concentration values of the Simoa method. Since the bias, which represents the average of the differences, was very close to zero for IL-6 and TNF-α, it could be concluded that the two methods are well comparable. The absolute differences between the methods for both analytes were considered minimal. In addition, the relative differences could be assessed as marginal for higher concentrations, while it could certainly be assessed as significant for low concentrations. It was striking that for both analytes lower relative differences between the methods tended to be detected at higher concentrations. In addition, a certain amount of more than 20 % of the differences in relation to the respective mean value lay outside the internally defined acceptance range. Since neither of the two methods can be defined as a reference method, none of the two methods could be defined as the more correct one, which would have required the use of standardized reference material, which was not available. Looking at the standard curve ranges in which the affected concentrations were determined,

it was noticeable that the back-calculation took place within the linear range of the calibrator of the Simoa SR-X assays. In the Luminex assay, however, these concentration ranges were recorded in the lower third of the two standard curves. It could be speculated that the results of the SR-X method could be slightly more reliable because the back-calculation of the concentrations here tends to be better than in the already outlying range, where the back-calculation of these concentrations is done in the Luminex method. However, both methods for IL-6 and TNF-α quantification, have been successfully validated and the back-calculation was shown to be reliable, also in the lower area of the Luminex standard curves. Since the same standard protein was used for both assays, the differences could be due to different binding properties of the different detection and capture antibodies used. However, since the majority of the differences were within the defined acceptance range, the respective bias were close to zero and also the results of the Passing-Bablok regression analysis indicated a very good comparability. Therefore, the two applied methods were classified as comparable for the intended use. Nevertheless, it could be interesting to examine the accuracy of the two methods by using so-called reference standards which are offered by the WHO [185]. Reference standards are very well characterized and mostly recombinant proteins, which are used to achieve a biological standardization, also of immunoassays [186]. These defined recombinant proteins could be spiked into sample matrix at the appropriate, known concentrations to investigate the accuracy of the methods in the areas in question. The calculation of the recovery rate related to the target value (= spike concentration) would reflect the accuracy of the two methods [23-25].

5.4 Analysis of NK cell stimulation

After assay validation was considered successful, at least for the majority of analytes, and both methods were shown to be comparable, the immunoassays could be used to study NK cell stimulation in whole blood cultures. Datasets were supplemented by flow cytometric analyses of immunological relevant cell surface receptors using a multi-parametric panel.

NK cells are a subgroup of lymphocytes and are one of the first to respond to viral invasion and cellular degeneration. As part of the innate immune system, they mediate the anti-viral and anti-tumor immune response and are therefore of great interest for clinical application [114]. For experimental studies, it is necessary to be able to specifically activate NK cells. Several suitable stimulants have already been reported, which were tested in the whole blood

culture system in the course of this work. The specificity of these stimulants for NK cells and whether other immune cell populations of the peripheral blood are activated at the same time were investigated. In addition, K562 cells were used as an NK cell-specific cellular target to find out whether this, next to the stimulant combinations IL-12 + IL-18 and R848 + IL-2, could be used as a standard NK cell stimulant in the whole blood culture system.

The surface markers CD69 and CD25 are cell activity markers that appear on the NK cell surface after activation [187-189]. Therefore, the detection of their expression by flow cytometry was used to determine whether NK cell activation occurred in whole blood assays. It was found that NK cells could be activated mainly by the combination of the stimuli IL-12 + IL-18, or K562 + IL-2 and R848 + IL-2, but also by R848 alone. The use of the remaining stimulants alone led, if at all, only to a very low expression of the surface markers and thus to a very low activation of the NK cells, which is supported by the results of Leong et al. [190]. Here, the use of IL-12, IL-15 and IL-18 alone did not result in any significant expression of CD25 in purified NK cells and thus no significant NK cell activation, as well. Further they report, the combination of these cytokines, however, increased CD25 expression 16-fold [190]. This synergistic effect has been demonstrated by several groups [144, 147, 191, 192].

An increased expression of CD69 on NK cells was achieved by R848 that was even further enhanced by the application of R848 in combination with IL-2. The combination of the stimulants IL-12 + IL-18, on the other hand, rather supported the expression of CD25. In both cases, NK cell stimulation was assumed. Following the results of Clausen et al. [189], it could be carefully presumed that the stimulation by R848 promotes an increased cytotoxic activity for the NK cells, which was additionally reinforced by the addition of IL-2. In this study, CD69, which is known as a marker for activated NK cells in general but also for the activation of other immune cell types [193], was more precisely identified as a suitable marker for NK cell cytotoxic activity. Furthermore, CD25 was declared to be a potential indicator for the proliferative potential of NK cells [189]. Thus, it could be speculated cautiously that the stimulation of NK cells by using IL-12 and IL-18 in combination is more likely to be stimulated in the direction of proliferation. However, other cytokines, such as IL-2, IL-15 and IL-21, are associated with NK cell proliferation in the literature [114, 194]. In contrast, IL-12 in combination with IL-18 is rather reported in connection with an increased production and release of IFN-γ from NK cells [114, 195], although a synergy between IL-12 and IL-18 has been reported for the proliferation and activation of NK cells in mice [196, 197]. In order to

investigate the situation in more detail, further experiments could be conducted to investigate the proliferation rate. However, CD107a expression, a degranulation marker, on NK cells, showed markedly higher signals of CD107a positive NK cells after stimulation with R848 with and without IL-2 than after stimulation with IL-12 + IL-18, supporting the hypothesis that increased expression of CD69 on NK cells could indicate increased cytotoxicity.

Consistent with the results of this thesis, increased CD69 expression levels were also detected in highly purified NK cells after stimulation with R848 in another report [144]. However, it was supposed here that despite high purification, accessory cells were present that could influence NK cell activation through the release of IL-12. Therefore, they added an IL-12 neutralizing antibody during stimulation with R848. The result was that R848 was no longer able to induce the expression of CD69. This showed that stimulation via R848 was dependent on the contribution of accessory cells [144]. Looking at the heatmap (**Figure 13**), the results of this work showed an activation of wide immune cell populations after stimulation with R848, alone and in combination with IL-2, as evidenced by the increased expression of activity markers and a high release of various cytokines, including IL-12p70. Consequently, it is reasonable to assume that accessory cells may also have been involved in the stimulation of NK cells and on corresponding CD69 expression when using R848 as stimulus. In addition to NK cells, CD4+ and CD8+ T cells, regulatory T cells, B cells, PMNs and monocytes were activated, which was reflected in the increased expression of CD69, CD25 and CD86 on the surface of the respective cell population. As far as the surface marker CD62L, also called L-selectin, is effected, it should be noted that cell activation leads to the detachment of CD62L [198]. Surface protein expression of CD62L is constitutive and occurs on the membrane of most circulating leukocytes. After activation by a large number of cell activators, CD62L is shed from the membrane [198-200]. Thus, the low expression levels of CD62L were assessed as activation and observed for monocytes and PMNs after stimulation with R848 ± IL-2.

NK cell activation was achieved by using K562 cells with IL-2, whereas K562 without the addition of IL-2 increased the expression of CD69 and CD25 on NK cells only very slightly. This was in agreement with the results of Dons`koi et al. [201], where only a part of the peripheral blood NK cells expressed CD69 on their surface after activation by K562 cells [201]. The fact that K562 cells in combination with IL-2 had a stronger influence on the activation of NK cells could be explained on the basis that the pro-inflammatory cytokines IL-2, IL-15 and IL-21 can alter the expression pattern of NK cell surface receptors. IL-2, together with IL-15, is associated

with the induction of the expression of KIRs on KIR-negative cell populations and can lead to the expression of the activating NK cell receptors C-type lectin-like receptor NKG2D and the natural cytotoxic receptor NKp44 [202]. Thus, it is plausible that K562 cells in combination with IL-2 may have induced NK cell activation, which was stronger compared to K562 without additives. Presumably, the repertoire of the KIRs was modified by IL-2 in such a way that the effector functions of NK cells were enhanced.

The results of Hart et al., which demonstrated the influence of other cells on NK cell activation, as mentioned above in the context of R848 [144], illustrate the difficulty of interpreting results in the whole blood culture system. Due to the high complexity, it is highly possible that other cells contributed indirectly to NK cell activation. They also illustrate the difficulty of comparing the results with literature that report studies based on simple and less complex culture systems, such as purified NK cells or NK cell lines.

The involvement of further cells in NK cell activation was also shown when the stimulants LPS/SEB were used. Both agents are not specific NK cell activators. Whereas LPS causes the activation of monocytes, macrophages, neutrophils and immature dendritic cells by binding TLR4 [203-205], SEB does activate monocytes and macrophages by interacting with HLA-DR, a part of MHC class II molecules. Further, T cells are activated by the interaction of SEB with specific elements of the T cell receptor (TCR), more precisely, with the variable domain of its β-chain [206, 207]. This activation was confirmed by the comparatively moderate increase in the expression of the activity markers CD69 and CD25 on CD4+ and CD8+ T cells, Tregs, monocytes, but also PMNs. In addition, the measured levels of various cytokines, including IL-4, IL-8, IL-13, IL-6, IL-1β, TNF-α, IL-10 and MIP-1β, were increased. Further cytokine concentrations were slightly increased, as for example IL-12p70, MCP-1 and IL-1Ra. It is known that activation of immune cells by LPS and SEB results in the release of many cytokines, including TNF-α, IL-1β and IL-6 [208], but also IL-2, IL-4, IFN-γ [209], IL-8, IL-10, IL-12, IL-15, TGF-β [210] and MIP-1β [211]. Thus, the results of the analyses in the course of this work corresponded to previously published observations. The increased IL-13 concentrations in the supernatant after LPS/SEB activation were supposed to originate from activated CD4+ T cells, as they were shown to release this cytokine [97]. Although LPS/SEB does not act directly on NK cells, an activation of NK cells, albeit relatively weak, was observed by the expression of CD25 and CD69. Presumably, NK cell-activating cytokines, such as IL-2, IL-12, IL-15, IL-18 and IL-21 [122, 212], were released by the activation of monocytes and T cells which then led to

NK cell activation. Detection of these cytokines in the whole blood culture supernatants, as was done for IL-12p70, would be recommended to confirm this hypothesis.

CD107a is utilized as an indicator for the degranulation of cytotoxic lymphocytes [213-217]. NK cells exert their cytotoxic function by releasing the contents of lytic granules into the immunological synapse between the NK cell and the target cell. In addition to granzymes, perforin, granulysin and cathepsins, the contents of these lytic granules also include CD107a/LAMP-1, CD107b/LAMP-2 and CD63/LAMP-3 [213, 218-221]. After release of this content, CD107a appears on the NK cell surface. Although the role of CD107a is not yet fully understood, it has already been shown to be involved in the transport of granzyme B to target cells and also in the transport of perforin to the lytic granules [217]. Thus, it significantly influences the cytotoxicity of NK cells and is correlated with the release of granzyme B. It is also thought to protect the NK cells themselves from the contents of the lytic granules after they have been released, thereby preventing NK cell suicide associated with degranulation [213].

The results of this work showed a correlation between CD107a expression on NK cells and granzyme B levels in whole blood culture supernatants except for the stimulant combinations IL-12 + IL-18 and LPS/SEB. For both combinations, increased granzyme B levels were detected but the expression levels of CD107a on NK cells were very low. It should be noted that granzyme B is not exclusively secreted by NK cells but also by activated cytotoxic CD8+ T cells [128, 222]. Since CD8+ T cells also showed markedly increased CD107a expression after stimulation with LPS/SEB, but also after stimulation with R848 alone or in combination with IL-2, it is assumed that these contributed to the increased granzyme B concentrations in the whole blood culture supernatant. However, it is questionable how the increased granzyme B levels occurred after IL-12 + IL-18 stimulation. Since the expression levels of CD107a were very low on both, NK cells and CD8+ T cells, degranulation process seemed to have been initiated only to a lesser extent by these cells. In the literature, it is described that CD4+ T cells also express granzyme B [223-227]. Moreover, the combination of IL-12 and IL-18 is not only considered a potent stimulus for NK cell activation, but is also known to activate Th1 cells, which respond by producing IFN-γ [228]. When examining the outcome of stimulation of whole blood with IL-12 + IL-18, it could be concluded that CD4+ T cells were activated by the increased expression of the surface marker CD69. It could also be suggested that activated Th1 cells, among other cells, contributed to the increased concentration of IFN-γ in the

supernatant. The increased TNF-α concentration, together with the levels produced in NK cells, could also be associated with activated Th1 cells. Another indication of Th1 cell activation would be an increased release of IL-2 [229]. The analysis of IL-2 levels in the supernatant could shed light on the question whether Th1 cells were involved. However, this cytokine was not part of employed IMAP 1 or 2.

It should be noted that CD8+ T cells are the most prominent provider of granzyme B during immunological reactions [223]. Whether the increased levels of granzyme B thus result exclusively from CD4+ T cells remains a matter of speculation for the moment. Hypothetically, very few extremely active NK cells or CD8+ T cells could also be the origin of the measured granzyme B. To investigate this question, however, intracellular granzyme B staining in the respective purified cell populations in question would be necessary, which would have to be examined by flow cytometric analysis.

Another hypothesis to explain the discrepancy between the low expression of CD107a on the NK cell surface and the measured granzyme B levels after IL-12 + IL-18 stimulation is based on the recycling of CD107a. During the degranulation process, the lysosomal protein CD107a is exocytosed, with expression reaching its highest level one hour after addition of the stimulant [213, 216]. Thereafter, CD107a accumulates in a large and spatially stable cluster. Adjacent to these accumulations, lysosomal compartments reach the plasma membrane and originally exocytosed CD107a is taken up into an intracellular compartment via endocytosis [230]. It is possible that this process was somehow accelerated by stimulation with IL-12 and IL-18 or the peaking of CD107a expression took place to an earlier time point before the actual analysis. Thus, the surface marker would be almost completely recycled at the time of CD107a analysis while granzyme B was still measurable in the supernatant after secretion. This would suggest that flow cytometric analysis at earlier time points might have been preferable. To be able to make precise statements in this regard, the CD107a analysis could also be carried out using a protein transport inhibitor (e.g. monensin or brefeldin A). This way, the expression of surface markers at a certain point in time would be fixed and a comparison of the CD107a expression at a defined point in time would be possible. However, this was not desired at that time, as it would have distorted the culture conditions. R848 and K562 in combination with and without IL-2 showed a correlation between the expression of CD107a and the granzyme B concentration in the supernatant, as already mentioned. Involvement of CD8+ T cells cannot be ruled out when R848 is used as a stimulant, as these cells also express CD107a. However,

the stimulation by K562 with IL-2 towards degranulation seemed to be NK cell specific and the granzyme B concentration appeared to be largely originated from NK cells. Latter could even be markedly higher if one considers the fact that, compared to all other stimuli used, target cells were present in this case. This means that the majority of the granzyme B produced by the NK cells reached the interior of the target cell via degranulation on a direct path across the immune synapse, after which it induces apoptosis. This amount of granzyme B was therefore no longer available for determination via ELISA. It could therefore be assumed that the granzyme B concentrations in the presence of K562 would have to be estimated much higher in order to compare them realistically to these caused by other stimulants.

The evaluation of cytokine concentrations, in particular IFN-γ and TNF-α, allows only vague statements about NK cell activity. Both cytokines are produced and secreted in high concentrations by activated NK cells [65, 78, 80, 84, 85], but other immune cell populations also release these cytokines [67, 81-83]. The levels of TNF-α and IFN-γ let assume a high activation of NK cells and an increase in the production of other cytokines on the one hand, and, on the other hand, an activation of the degranulation process by R848. These effects were enhanced when IL-2 was used in combination leading to the hypothesis that the enhancement of the effects of R848 was due to priming of NK cells by IL-2 which was already mentioned in previous reports [212, 231]. This has been shown for primary NK cells that responded to R848 by pre-activation with IL-2, although they cannot usually be activated directly by R848 [144]. However, R848 also led to the activation of the other immune cell populations like CD4+ and CD8+ T cells, regulatory T cells, B cells, PMNs and monocytes. Their involvement in the IFN-γ and TNF-α concentration in the supernatant could not be excluded. The same applied to the cytokine concentrations measured after stimulation with LPS/SEB. In both cases, intracellular cytokine staining with subsequent flow cytometric analysis could provide information. The increased IFN-γ and TNF-α concentrations achieved by stimulation with IL-12 in combination with IL-18 could be interpreted to mean that these stimuli activate the NK cells more in the direction of cytokine production and release than in that of the degranulation process. This contrasts with K562 cells, which produced lower cytokine levels and led to increased expression of CD107a and granzyme B levels. By binding to their specific receptors, IL-12R and IL-18R on T cells, B cells, NK cells, and T cells, IL-12 and IL-18 are reported to activate respective cells leading to increased release of primarily IFN-γ, TNF-α, but also GM-CSF and IL-2 [96, 232-234]. When IL-12 and IL-18 were used as single stimuli, these

activities were not observed. But in combination the results were in line with reports in literature emphasizing again the synergistic effect [234].

Although R848, used alone and in combination with IL-2, caused a broad activation of the immune system, which was in magnitude more or less comparable to that of LPS/SEB, stimulation with R848 with and without IL-2 was more NK cell specific. This could be seen in the higher expression of the surface markers CD69 and CD107a on NK cells. The comparatively high concentrations of TNF-α and IFN-γ after LPS/SEB and R848 ± IL-2 stimulation, but also the activation of further immune cells and the strong release of further cytokines showed the broad and rapid activation of the entire immune system. This activation of the full range of immune cells present in whole blood underlines the importance of the R848 binding receptors - namely TLR7 and TLR8. They are among the most important pattern-recognition receptors (PRRs) of the immunological system that recognize pathogen-associated molecular patterns (PAMPs), to be more precise, single-stranded RNA of viral genomes [235, 236]. Since viruses account for the majority of human infections, it is only plausible that TLR7 and TLR8 were evolutionarily designed to activate the immune system as quickly as possible, thereby affecting a wide variety of immune cells.

An apparently more specific activation of the NK cells is achieved by the combination of IL-12 + IL-18, although some other immune cell types were slightly activated as well. However, although expression of CD25 and CD69 let assume NK cell activation, the expression of the surface marker CD107a was very low. Therefore, it was concluded that the degranulation process was less stimulated by these cytokines than NK cell cytokine production of mainly TNF-α and IFN-γ. A moderate co-activation of further immune cells was observed compared to the other stimulants and combinations used. However, the presumption of the involvement of activated Th1 cells remains.

Arguably, the most NK cell-specific of the stimulants tested appeared to be K562 cells, especially in combination with IL-2. NK cell activation, recognizable by the expression levels of the surface markers CD69, CD25 and CD107a was achieved, with only little activation of further immune cell populations like PMNs, CD4+ T cells and Tregs. Only monocytes were slightly more activated (CD62L and CD69 expression). In addition, the increased granzyme B levels in the supernatant indicated NK cell activation, especially after no CD107a was seen on CD8+ T cells after K562 ± IL-2 stimulation. NK cell activation appears to be triggered by K562 in the direction of the degranulation process rather than promoting cytokine production in

NK cells. This was underlined by the comparatively moderate concentrations of IFN-γ and TNF-α, and the high concentration of granzyme B in the supernatant. Due to the highest NK cell specificity, K562 cells would be a very suitable stimulus for the application in whole blood culture experiments. However, the standard use of whole blood cultures requires the storage of the tubes at -20 °C until they are used. The freezing process would damage and destroy the cells without the addition of cell-stabilizing agents. Thus, the use of K562 in whole blood assays would only be possible if a suitable fixation reagent could be found that would protect the cells from damage and would not later affect the culture and the experimental setup. Attempts to fix and then freeze the K562 cells were performed and also analyzed via flow cytometry and cytokine readout, but unfortunately were not successful (data not shown). The differences between the donors that were observed relatively frequently were due to naturally occurring variation in the immune response that has already been shown for whole blood cultures [237]. This diversity is seen as an advantage by evolution. New virus variants in the human population thus always encounter individuals who naturally exhibit increased resistance, which then ultimately prevail.

It should be mentioned that the data collected only represent a small insight into the feasibility of activating NK cells by means of the stimulants used. To be able to make precise statements, further analyses are necessary. It would be useful to repeat the experiments with an increased number of donors to be able to provide statistically significant statements. In addition, intracellular granzyme B and cytokine staining with subsequent flow cytometric analysis would be desirable. This would allow the determination of which cell populations are involved, for example, in the release of IFN-γ and TNF-α or granzyme B, and more detailed statements could be made regarding the NK cell specificity of the respective stimulants.

6. Conclusions

For this thesis, two multiplex immunoassays were developed for the analysis of supernatants from whole blood cultures based on the Luminex platform. IMAP 1 consists of nine analytes (IL-4, IL-6, IL-8, IL-10, GM-CSF, IFN-γ, MCP-1, MIP-1β and TNF-α) and IMAP 2 of six analytes (IL-1β, IL-1Ra, IL-12p70, VEGF, IL-13 und M-CSF). In addition, highly sensitive Simoa immunoassays for the analytes IL-4 and IL 12p70 (single-plexes) and for IL-6 and TNF-α (2-plexes) were developed to complement the multiplex assays developed with significantly higher sensitivities than on the Luminex platform. All assays were developed within the project "System Immunology at Biological-Technical Interfaces" and were designed to investigate immune responses to different implant materials and their surface properties, specifically the precise quantification of the listed analytes in supernatants from THP-1, PBMC and whole blood cultures.

In subsequent stages of the project and after the developmental phase, the immunoassays were validated in a fit-for-purpose approach. Besides the assay development, this thesis covers the validation process of the Luminex and SR-X Simoa assays for the whole blood culture system in course of the project. Validation was performed considering the relevant regulatory guidelines of the FDA and EMA [23, 24]. The applicability of the assay ranges and acceptable assay sensitivities were confirmed during validation for all analytes and immunoassays and were in conformance with the respective guidelines. However, concentration values generated for samples of interest were excluded from further analyses for the analytes VEGF, GM-CSF and M-CSF based on validation results while IL-4 and IL-12p70 were only used resulting from the Simoa assays. All other validation parameters demonstrated the applicability, reproducibility and validity of the respective assays for their use in quantifying analyte concentrations in supernatants of the whole blood culture system.

By Passing-Bablok regression analysis and Blant-Altman plots, concentration values of IL-6 and TNF-α from both, Luminex and Simoa measurements, could be used equally after the latter had been adjusted by an analyte-specific factor.

Following development and establishment, the successfully validated immunoassays were used to analyze NK cell activation in the immunological complexity of whole blood cultures.

For this, it was investigated whether the stimulants IL-12, IL-18, IL-2, R848 and K562 cells, known to be NK cell specific activators, and respective combinations of these also specifically activate NK cells in the presence of all immune cells of the peripheral blood and whether and

to which extent these other immune cells are activated as well. In addition, K562 cells were used as an NK cell-specific cellular target to find out whether these, in addition to the other stimulants, can be used as a stimulant by default in the whole blood culture system. It was found that the stimulant combinations IL-12 + IL-18, R848 + IL-2 and K562 + IL-2 were able to induce the strongest activation of NK cells. A synergistic effect had already been shown by other groups and confirmed these results. R848, alone or in combination with IL-2, was observed to be a potent activator of the degranulation process of NK cells and, at the same time, on their cytokine production. As a TLR agonist, R848 with and without IL-2, further led to a broad activation of other immune cell populations of the peripheral blood. An involvement of these in NK cell activation or also in cytokine release cannot be ruled out here and further investigations, such as intracellular cytokine staining, should be carried out. This way, an involvement of CD8+ T cells in the observed effects (granzyme B concentrations) could be demonstrated or excluded.

However, the combination of IL-12 and IL-18 activated NK cells more in the direction of cytokine production as an effector function than in the direction of the degranulation process. To confirm this, further analyses would be needed regarding the expression of the surface marker CD107a on NK cells. Further, the involvement of Th1 cells in cytokine production, especially of IFN-γ, should be investigated by intracellular cytokine staining as IL-12 in combination with IL-18 are also known to be a potent combination of stimuli to these cells.

The most NK cell-specific stimulant combination in the series was K562 cells in combination with IL-2. They activated the degranulation process to a large extent and simultaneously led to the release of INF-γ and TNF-α. Other cytokines were detected in comparatively low concentrations and the activation of other cell populations was marginal. However, they are unsuitable for standard application as NK cell stimulants in whole blood cultures at the present time, as a suitable fixation system must first be found.

All results of NK cell stimulation analysis should be substantiated by investigations of further donors, reproduction of the results and, as mentioned, additional cytokine measurements in the supernatant but also intracellularly.

In summary, the results give a very good first insight into NK cell stimulation of whole blood culture systems based on cytokine readout and flow cytometry analysis results. All tested combinations of stimuli successfully activated NK cells and K562 as a cellular target was shown to, in relation to the other stimuli used, most specifically activate NK cells.

References

1. Yalow R.S., Berson S.A., *Assay of Plasma Insulin in Human Subjects by Immunological Methods*. Nature. 1959; **184 (Suppl 21)**: 1648-9.
2. Berson S.A., et al., *Insulin-I131 Metabolism in Human Subjects: Demonstration of Insulin Binding Globulin in the Circulation of Insulin Treated Subjects*. J Clin Invest. 1956; **35**(2): 170-90.
3. Wu A.H., *A Selected History and Future of Immunoassay Development and Applications in Clinical Chemistry*. Clin Chim Acta. 2006; **369**(2): 119-24.
4. Wild D., Chapter 1.2 - *Immunoassay for Beginners*. In: The Immunoassay Handbook (Fourth Edition). Wild D., editor. 4 ed. Oxford: Elevisier; 2013. p. 7-10.
5. Hage D.S., *Immunoassays*. Anal Chem. 1999; **71**(12): 294r-304r.
6. Köhler G., Milstein C., *Continuous Cultures of Fused Cells Secreting Antibody of Predefined Specificity*. Nature. 1975; **256**(5517): 495-7.
7. Lipman N.S., et al., *Monoclonal Versus Polyclonal Antibodies: Distinguishing Characteristics, Applications, and Information Resources*. Ilar j. 2005; **46**(3): 258-68.
8. Wide L., Porath J., *Radioimmunoassay of Proteins with the Use of Sephadex-Coupled Antibodies*. Biochimica et Biophysica Acta (BBA) - General Subjects. 1966; **130**(1): 257-60.
9. Catt K., Tregear G.W., *Solid-Phase Radioimmunoassay in Antibody-Coated Tubes*. Science. 1967; **158**(3808): 1570-2.
10. Graham H., Chandler D.J., Dunbar S.A., *The Genesis and Evolution of Bead-Based Multiplexing*. Methods. 2019; **158**: 2-11.
11. Kellar K.L., Iannone M.A., *Multiplexed Microsphere-Based Flow Cytometric Assays*. Exp Hematol. 2002; **30**(11): 1227-37.
12. Fischer S.K., et al., *Emerging Technologies to Increase Ligand Binding Assay Sensitivity*. Aaps j. 2015; **17**(1): 93-101.
13. Gu D., et al., *Purification of R-Phycoerythrin from Gracilaria Lemaneiformis by Centrifugal Precipitation Chromatography*. J Chromatogr B Analyt Technol Biomed Life Sci. 2018; **1087-1088**: 138-41.
14. Isailovic D., et al., *Formation of Fluorescent Proteins by the Attachment of Phycoerythrobilin to R-Phycoerythrin Alpha and Beta Apo-Subunits*. Anal Biochem. 2006; **358**(1): 38-50.
15. Vignali D.A., *Multiplexed Particle-Based Flow Cytometric Assays*. J Immunol Methods. 2000; **243**(1-2): 243-55.
16. Rissin D.M., et al., *Simultaneous Detection of Single Molecules and Singulated Ensembles of Molecules Enables Immunoassays with Broad Dynamic Range*. Anal Chem. 2011; **83**(6): 2279-85.
17. Chang L., et al., *Single Molecule Enzyme-Linked Immunosorbent Assays: Theoretical Considerations*. J Immunol Methods. 2012; **378**(1-2): 102-15.
18. Rissin D.M., et al., *Single-Molecule Enzyme-Linked Immunosorbent Assay Detects Serum Proteins at Subfemtomolar Concentrations*. Nat Biotechnol. 2010; **28**(6): 595-9.
19. Rivnak A.J., et al., *A Fully-Automated, Six-Plex Single Molecule Immunoassay for Measuring Cytokines in Blood*. J Immunol Methods. 2015; **424**: 20-7.
20. Wilson D.H., et al., *The Simoa Hd-1 Analyzer: A Novel Fully Automated Digital Immunoassay Analyzer with Single-Molecule Sensitivity and Multiplexing*. J Lab Autom. 2016; **21**(4): 533-47.

21. Kan C.W., et al., *Isolation and Detection of Single Molecules on Paramagnetic Beads Using Sequential Fluid Flows in Microfabricated Polymer Array Assemblies*. Lab Chip. 2012; **12**(5): 977-85.

22. Rissin D.M., et al., *Multiplexed Single Molecule Immunoassays*. Lab Chip. 2013; **13**(15): 2902-11.

23. EMA. *Guideline on Bioanalytical Method Validation*. European Medicines Agency; Comittee for Medicinal Products for Human Use (CHMP). 2013.

24. FDA. *Bioanalytical Method Validation: Guidance for Industry*. U.S. Department of Health and Human Services, Food and Drug Administration, Center for Drug Evaluation and Research, Center for Veterinary Medicine. 2018.

25. Andreasson U., et al., *A Practical Guide to Immunoassay Method Validation*. Front Neurol. 2015; **6**(179).

26. ISO/IEC 17025, *General Requirements for the Competence of Testing and Calibration Laboratories*, 2017, (ISO) I.O.f.S.

27. Findlay J.W., et al., *Validation of Immunoassays for Bioanalysis: A Pharmaceutical Industry Perspective*. J Pharm Biomed Anal. 2000; **21**(6): 1249-73.

28. Lee J.W., et al., *Fit-for-Purpose Method Development and Validation for Successful Biomarker Measurement*. Pharm Res. 2006; **23**(2): 312-28.

29. Azadeh M., et al., *Calibration Curves in Quantitative Ligand Binding Assays: Recommendations and Best Practices for Preparation, Design, and Editing of Calibration Curves*. The AAPS Journal. 2017; **20**(1): 22.

30. Belanger L., Sylvestre C., Dufour D., *Enzyme-Linked Immunoassay for Alpha-Fetoprotein by Competitive and Sandwich Procedures*. Clin Chim Acta. 1973; **48**(1): 15-8.

31. Murphy K., Weaver C. *Janeway Immunologie*. 9th ed: Springer Spektrum; 2018.

32. Zhang J.M., An J., *Cytokines, Inflammation, and Pain*. Int Anesthesiol Clin. 2007; **45**(2): 27-37.

33. Cavaillon J.M., *Pro- Versus Anti-Inflammatory Cytokines: Myth or Reality*. Cell Mol Biol (Noisy-le-grand). 2001; **47**(4): 695-702.

34. Palomino D.C., Marti L.C., *Chemokines and Immunity*. Einstein (Sao Paulo). 2015; **13**(3): 469-73.

35. Raz E., Mahabaleshwar H., *Chemokine Signaling in Embryonic Cell Migration: A Fisheye View*. Development. 2009; **136**(8): 1223-9.

36. Vivier E., et al., *Functions of Natural Killer Cells*. Nature Immunology. 2008; **9**(5): 503-10.

37. Loux T.J., Lotze M.T., Zeh H.J., Chapter 14 - *Nk Cells as Recipients of Cytokine Signals*. In: Natural Killer Cells. Lotze M.T., Thomson A.W., editors. San Diego: Academic Press; 2010. p. 189-201.

38. Garlanda C., Jaillon S., Chapter Cytokines and their receptors - *The Interleukin-1 Family*. In: Encyclopedia of Immunobiology. Ratcliffe M.J.H., editor. Oxford: Academic Press; 2016. p. 438-46.

39. Dinarello C.A., *Biologic Basis for Interleukin-1 in Disease*. Blood. 1996; **87**(6): 2095-147.

40. Lopez-Castejon G., Brough D., *Understanding the Mechanism of Il-1β Secretion*. Cytokine Growth Factor Rev. 2011; **22**(4): 189-95.

41. Sims J.E., Smith D.E., *The Il-1 Family: Regulators of Immunity*. Nature Reviews Immunology. 2010; **10**(2): 89-102.

42. Masters S.L., et al., *Horror Autoinflammaticus: The Molecular Pathophysiology of Autoinflammatory Disease (*)*. Annu Rev Immunol. 2009; **27**: 621-68.

43. Hirano T., et al., *Complementary DNA for a Novel Human Interleukin (Bsf-2) That Induces B Lymphocytes to Produce Immunoglobulin*. Nature. 1986; **324**(6092): 73-6.

44. Hunter C.A., Jones S.A., *Il-6 as a Keystone Cytokine in Health and Disease*. Nature Immunology. 2015; **16**(5): 448-57.

45. Li B., Jones L.L., Geiger T.L., *Il-6 Promotes T Cell Proliferation and Expansion under Inflammatory Conditions in Association with Low-Level Rorγt Expression*. J Immunol. 2018; **201**(10): 2934-46.

46. Lehrskov L.L., Christensen R.H., *The Role of Interleukin-6 in Glucose Homeostasis and Lipid Metabolism*. Semin Immunopathol. 2019; **41**(4): 491-9.

47. Rothaug M., Becker-Pauly C., Rose-John S., *The Role of Interleukin-6 Signaling in Nervous Tissue*. Biochim Biophys Acta. 2016; **1863**(6 Pt A): 1218-27.

48. Choy E., Rose-John S., *Interleukin-6 as a Multifunctional Regulator: Inflammation, Immune Response, and Fibrosis*. Journal of Scleroderma and Related Disorders. 2017; **2**(2_suppl): S1-S5.

49. Akira S., Taga T., Kishimoto T., *Interleukin-6 in Biology and Medicine*. Adv Immunol. 1993; **54**: 1-78.

50. Brennan K., Zheng J., Chapter - *Interleukin 8*. In: Xpharm: The Comprehensive Pharmacology Reference. Enna S.J., Bylund D.B., editors. New York: Elsevier; 2007. p. 1-4.

51. Huber A.R., et al., *Regulation of Transendothelial Neutrophil Migration by Endogenous Interleukin-8*. Science. 1991; **254**(5028): 99-102.

52. Deshmane S.L., et al., *Monocyte Chemoattractant Protein-1 (Mcp-1): An Overview*. J Interferon Cytokine Res. 2009; **29**(6): 313-26.

53. Griffith J.W., Sokol C.L., Luster A.D., *Chemokines and Chemokine Receptors: Positioning Cells for Host Defense and Immunity*. Annu Rev Immunol. 2014; **32**: 659-702.

54. Yoshimura T., et al., *Purification and Amino Acid Analysis of Two Human Monocyte Chemoattractants Produced by Phytohemagglutinin-Stimulated Human Blood Mononuclear Leukocytes*. J Immunol. 1989; **142**(6): 1956-62.

55. Yoshimura T., et al., *Human Monocyte Chemoattractant Protein-1 (Mcp-1). Full-Length Cdna Cloning, Expression in Mitogen-Stimulated Blood Mononuclear Leukocytes, and Sequence Similarity to Mouse Competence Gene Je*. FEBS Lett. 1989; **244**(2): 487-93.

56. Ziegler S.F., et al., *Induction of Macrophage Inflammatory Protein-1 Beta Gene Expression in Human Monocytes by Lipopolysaccharide and Il-7*. J Immunol. 1991; **147**(7): 2234-9.

57. Kim J.J., et al., *Intracellular Adhesion Molecule-1 Modulates Beta-Chemokines and Directly Costimulates T Cells in Vivo*. J Clin Invest. 1999; **103**(6): 869-77.

58. Krzysiek R., et al., *Antigen Receptor Engagement Selectively Induces Macrophage Inflammatory Protein-1 Alpha (Mip-1 Alpha) and Mip-1 Beta Chemokine Production in Human B Cells*. J Immunol. 1999; **162**(8): 4455-63.

59. Oliva A., et al., *Natural Killer Cells from Human Immunodeficiency Virus (Hiv)-Infected Individuals Are an Important Source of Cc-Chemokines and Suppress Hiv-1 Entry and Replication in Vitro*. J Clin Invest. 1998; **102**(1): 223-31.

60. Sallusto F., et al., *Distinct Patterns and Kinetics of Chemokine Production Regulate Dendritic Cell Function*. Eur J Immunol. 1999; **29**(5): 1617-25.

61. Lapinet J.A., et al., *Gene Expression and Production of Tumor Necrosis Factor Alpha, Interleukin-1beta (Il-1beta), Il-8, Macrophage Inflammatory Protein 1alpha (Mip-1alpha), Mip-1beta, and Gamma Interferon-Inducible Protein 10 by Human Neutrophils Stimulated with Group B Meningococcal Outer Membrane Vesicles*. Infect Immun. 2000; **68**(12): 6917-23.

62. Menten P., Wuyts A., Van Damme J., *Macrophage Inflammatory Protein-1*. Cytokine Growth Factor Rev. 2002; **13**(6): 455-81.

63. Maurer M., von Stebut E., *Macrophage Inflammatory Protein-1*. Int J Biochem Cell Biol. 2004; **36**(10): 1882-6.

64. Carswell E.A., et al., *An Endotoxin-Induced Serum Factor That Causes Necrosis of Tumors*. Proc Natl Acad Sci U S A. 1975; **72**(9): 3666-70.

65. Bradley J.R., *Tnf-Mediated Inflammatory Disease*. J Pathol. 2008; **214**(2): 149-60.

66. Mehta A.K., Gracias D.T., Croft M., *Tnf Activity and T Cells*. Cytokine. 2018; **101**: 14-8.

67. Parameswaran N., Patial S., *Tumor Necrosis Factor-A Signaling in Macrophages*. Critical reviews in eukaryotic gene expression. 2010; **20**(2): 87-103.

68. Brennan F.M., Maini R.N., Feldmann M., *Tnf Alpha--a Pivotal Role in Rheumatoid Arthritis?* Br J Rheumatol. 1992; **31**(5): 293-8.

69. Plevy S.E., et al., *A Role for Tnf-Alpha and Mucosal T Helper-1 Cytokines in the Pathogenesis of Crohn's Disease*. J Immunol. 1997; **159**(12): 6276-82.

70. Navikas V., Link H., *Review: Cytokines and the Pathogenesis of Multiple Sclerosis*. J Neurosci Res. 1996; **45**(4): 322-33.

71. Kassiotis G., Kollias G., *Uncoupling the Proinflammatory from the Immunosuppressive Properties of Tumor Necrosis Factor (Tnf) at the P55 Tnf Receptor Level: Implications for Pathogenesis and Therapy of Autoimmune Demyelination*. The Journal of experimental medicine. 2001; **193**(4): 427-34.

72. Kurimoto I., Streilein J.W., *Tumor Necrosis Factor-Alpha Impairs Contact Hypersensitivity Induction after Ultraviolet B Radiation Via Tnf-Receptor 2 (P75)*. Exp Dermatol. 1999; **8**(6): 495-500.

73. Ferguson T.A., Herndon J.M., Dube P., *The Immune Response and the Eye: A Role for Tnf Alpha in Anterior Chamber-Associated Immune Deviation*. Invest Ophthalmol Vis Sci. 1994; **35**(5): 2643-51.

74. Masli S., Turpie B., *Anti-Inflammatory Effects of Tumour Necrosis Factor (Tnf)-Alpha Are Mediated Via Tnf-R2 (P75) in Tolerogenic Transforming Growth Factor-Beta-Treated Antigen-Presenting Cells*. Immunology. 2009; **127**(1): 62-72.

75. Hodge-Dufour J., et al., *Inhibition of Interferon Gamma Induced Interleukin 12 Production: A Potential Mechanism for the Anti-Inflammatory Activities of Tumor Necrosis Factor*. Proceedings of the National Academy of Sciences of the United States of America. 1998; **95**(23): 13806-11.

76. Black R.A., et al., *A Metalloproteinase Disintegrin That Releases Tumour-Necrosis Factor-Alpha from Cells*. Nature. 1997; **385**(6618): 729-33.

77. Cabal-Hierro L., Lazo P.S., *Signal Transduction by Tumor Necrosis Factor Receptors*. Cell Signal. 2012; **24**(6): 1297-305.

78. Almishri W., et al., *Tnfα Augments Cytokine-Induced Nk Cell Ifnγ Production through Tnfr2*. J Innate Immun. 2016; **8**(6): 617-29.

79. Wheelock E.F., *Interferon-Like Virus-Inhibitor Induced in Human Leukocytes by Phytohemagglutinin*. Science. 1965; **149**(3681): 310-1.

80. Burke J.D., Young H.A., *Ifn-Γ: A Cytokine at the Right Time, Is in the Right Place*. Semin Immunol. 2019; **43**: 101280.

81. Matsushita H., et al., *Cytotoxic T Lymphocytes Block Tumor Growth Both by Lytic Activity and Ifnγ-Dependent Cell-Cycle Arrest*. Cancer Immunol Res. 2015; **3**(1): 26-36.

82. Gao Y., et al., *Gamma Delta T Cells Provide an Early Source of Interferon Gamma in Tumor Immunity*. J Exp Med. 2003; **198**(3): 433-42.

83. Kasahara T., et al., *Interleukin 2-Mediated Immune Interferon (Ifn-Gamma) Production by Human T Cells and T Cell Subsets*. J Immunol. 1983; **130**(4): 1784-9.

84. Cooper M.A., et al., *Human Natural Killer Cells: A Unique Innate Immunoregulatory Role for the Cd56(Bright) Subset*. Blood. 2001; **97**(10): 3146-51.

85. Yu J., et al., *Pro- and Antiinflammatory Cytokine Signaling: Reciprocal Antagonism Regulates Interferon-Gamma Production by Human Natural Killer Cells*. Immunity. 2006; **24**(5): 575-90.

86. Schroder K., et al., *Interferon-Gamma: An Overview of Signals, Mechanisms and Functions*. J Leukoc Biol. 2004; **75**(2): 163-89.

87. Boehm U., et al., *Cellular Responses to Interferon-Gamma*. Annu Rev Immunol. 1997; **15**: 749-95.

88. Perussia B., et al., *Immune Interferon and Leukocyte-Conditioned Medium Induce Normal and Leukemic Myeloid Cells to Differentiate Along the Monocytic Pathway*. J Exp Med. 1983; **158**(6): 2058-80.

89. Young H.A., Hardy K.J., *Role of Interferon-Gamma in Immune Cell Regulation*. J Leukoc Biol. 1995; **58**(4): 373-81.

90. Finkelman F.D., et al., *Ifn-Gamma Regulates the Isotypes of Ig Secreted During in Vivo Humoral Immune Responses*. J Immunol. 1988; **140**(4): 1022-7.

91. Carnaud C., et al., *Cutting Edge: Cross-Talk between Cells of the Innate Immune System: Nkt Cells Rapidly Activate Nk Cells*. J Immunol. 1999; **163**(9): 4647-50.

92. Stern A.S., et al., *Purification to Homogeneity and Partial Characterization of Cytotoxic Lymphocyte Maturation Factor from Human B-Lymphoblastoid Cells*. Proc Natl Acad Sci U S A. 1990; **87**(17): 6808-12.

93. Vignali D.A., Kuchroo V.K., *Il-12 Family Cytokines: Immunological Playmakers*. Nat Immunol. 2012; **13**(8): 722-8.

94. Ma X., Trinchieri G., *Regulation of Interleukin-12 Production in Antigen-Presenting Cells*. Adv Immunol. 2001; **79**: 55-92.

95. O'Shea J.J., Paul W.E., *Regulation of T(H)1 Differentiation--Controlling the Controllers*. Nat Immunol. 2002; **3**(6): 506-8.

96. Trinchieri G., *Interleukin-12 and the Regulation of Innate Resistance and Adaptive Immunity*. Nat Rev Immunol. 2003; **3**(2): 133-46.

97. Junttila I.S., *Tuning the Cytokine Responses: An Update on Interleukin (Il)-4 and Il-13 Receptor Complexes*. Front Immunol. 2018; **9**: 888.

98. Minty A., et al., *Lnterleukin-13 Is a New Human Lymphokine Regulating Inflammatory and Immune Responses*. Nature. 1993; **362**(6417): 248-50.

99. Gadani S.P., et al., *Il-4 in the Brain: A Cytokine to Remember*. J Immunol. 2012; **189**(9): 4213-9.

100. Gordon S., *Alternative Activation of Macrophages*. Nat Rev Immunol. 2003; **3**(1): 23-35.

101. Chomarat P., et al., *Interferon Gamma Inhibits Interleukin 10 Production by Monocytes*. J Exp Med. 1993; **177**(2): 523-7.

102. Seki S., et al., *Role of Liver Nk Cells and Peritoneal Macrophages in Gamma Interferon and Interleukin-10 Production in Experimental Bacterial Peritonitis in Mice*. Infect Immun. 1998; **66**(11): 5286-94.

103. Verma R., et al., *A Network Map of Interleukin-10 Signaling Pathway*. J Cell Commun Signal. 2016; **10**(1): 61-7.

104. Blanco P., et al., *Dendritic Cells and Cytokines in Human Inflammatory and Autoimmune Diseases*. Cytokine Growth Factor Rev. 2008; **19**(1): 41-52.

105. Couper K.N., Blount D.G., Riley E.M., *Il-10: The Master Regulator of Immunity to Infection*. The Journal of Immunology. 2008; **180**(9): 5771-7.

106. Arend W.P., et al., *Interleukin-1 Receptor Antagonist: Role in Biology*. Annu Rev Immunol. 1998; **16**: 27-55.

107. Palmer G., et al., *Type I Il-1 Receptor Mediates Il-1 and Intracellular Il-1 Receptor Antagonist Effects in Skin Inflammation*. J Invest Dermatol. 2007; **127**(8): 1938-46.

108. Hamilton J.A., *Gm-Csf in Inflammation*. J Exp Med. 2020; **217**(1).

109. Hamilton J.A., *Colony-Stimulating Factors in Inflammation and Autoimmunity*. Nat Rev Immunol. 2008; **8**(7): 533-44.

110. Burgess A.W., Metcalf D., *The Nature and Action of Granulocyte-Macrophage Colony Stimulating Factors*. Blood. 1980; **56**(6): 947-58.

111. Hamilton J.A., *Rheumatoid Arthritis: Opposing Actions of Haemopoietic Growth Factors and Slow-Acting Anti-Rheumatic Drugs*. Lancet. 1993; **342**(8870): 536-9.

112. HOT Screen GmbH. *Truculture* [web page]. HOT Screen GmbH. Available from: www.hot-screen.de/services/truculture, Date cited: 14.04.2022.

113. Schmolz M., Eisinger D. *Truculture®: A Simple Whole Blood Collection and Culture System for Quantifying Physiological Interactions of the Human Immune System in the Clinic*.

114. Abel A.M., et al., *Natural Killer Cells: Development, Maturation, and Clinical Utilization*. Front Immunol. 2018; **9**: 1869.

115. Rosenau W., Moon H.D., *Lysis of Homologous Cells by Sensitized Lymphocytes in Tissue Culture*. J Natl Cancer Inst. 1961; **27**: 471-83.

116. Smith H.J., *Antigenicity of Carcinogen-Induced and Spontaneous Tumours in Inbred Mice*. Br J Cancer. 1966; **20**(4): 831-7.

117. Oldham R.K., *Natural Killer Cells: Artifact to Reality: An Odyssey in Biology*. Cancer Metastasis Rev. 1983; **2**(4): 323-36.

118. Kiessling R., Klein E., Wigzell H., *"Natural" Killer Cells in the Mouse. I. Cytotoxic Cells with Specificity for Mouse Moloney Leukemia Cells. Specificity and Distribution According to Genotype*. Eur J Immunol. 1975; **5**(2): 112-7.

119. Kiessling R., et al., *"Natural" Killer Cells in the Mouse. Ii. Cytotoxic Cells with Specificity for Mouse Moloney Leukemia Cells. Characteristics of the Killer Cell*. Eur J Immunol. 1975; **5**(2): 117-21.

120. Carrega P., Ferlazzo G., *Natural Killer Cell Distribution and Trafficking in Human Tissues*. Front Immunol. 2012; **3**: 347.

121. Langers I., et al., *Natural Killer Cells: Role in Local Tumor Growth and Metastasis*. Biologics. 2012; **6**: 73-82.

122. Paul S., Lal G., *The Molecular Mechanism of Natural Killer Cells Function and Its Importance in Cancer Immunotherapy*. Front Immunol. 2017; **8**(1124).

123. Lanier L.L., *Up on the Tightrope: Natural Killer Cell Activation and Inhibition*. Nat Immunol. 2008; **9**(5): 495-502.

124. Tremblay-McLean A., et al., *Expression of Ligands for Activating Natural Killer Cell Receptors on Cell Lines Commonly Used to Assess Natural Killer Cell Function*. BMC Immunol. 2019; **20**(1): 8.

125. Vivier E., et al., *Targeting Natural Killer Cells and Natural Killer T Cells in Cancer*. Nat Rev Immunol. 2012; **12**(4): 239-52.

126. Vivier E., et al., *Innate or Adaptive Immunity? The Example of Natural Killer Cells*. Science (New York, N.Y.). 2011; **331**(6013): 44-9.

127. Lanier L.L., *Nk Cell Recognition*. Annu Rev Immunol. 2005; **23**: 225-74.

128. Prager I., Watzl C., *Mechanisms of Natural Killer Cell-Mediated Cellular Cytotoxicity*. J Leukoc Biol. 2019; **105**(6): 1319-29.

129. Pardo J., et al., *Granzymes Are Essential for Natural Killer Cell-Mediated and Perf-Facilitated Tumor Control*. Eur J Immunol. 2002; **32**(10): 2881-7.

130. Topham N.J., Hewitt E.W., *Natural Killer Cell Cytotoxicity: How Do They Pull the Trigger?* Immunology. 2009; **128**(1): 7-15.

131. Smyth M.J., et al., *Activation of Nk Cell Cytotoxicity*. Mol Immunol. 2005; **42**(4): 501-10.

132. Guicciardi M.E., Gores G.J., *Life and Death by Death Receptors*. Faseb j. 2009; **23**(6): 1625-37.

133. Ashkenazi A., Dixit V.M., *Death Receptors: Signaling and Modulation*. Science. 1998; **281**(5381): 1305-8.

134. van den Bosch G., et al., *Granulocyte-Macrophage Colony-Stimulating Factor (Gm-Csf) Counteracts the Inhibiting Effect of Monocytes on Natural Killer (Nk) Cells*. Clin Exp Immunol. 1995; **101**(3): 515-20.

135. Walzer T., et al., *Natural-Killer Cells and Dendritic Cells: "L'union Fait La Force"*. Blood. 2005; **106**(7): 2252-8.

136. Kaplan D.H., et al., *Demonstration of an Interferon Gamma-Dependent Tumor Surveillance System in Immunocompetent Mice*. Proc Natl Acad Sci U S A. 1998; **95**(13): 7556-61.

137. Marçais A., et al., *Regulation of Mouse Nk Cell Development and Function by Cytokines*. Front Immunol. 2013; **4**: 450.

138. Grimm E.A., et al., *Lymphokine-Activated Killer Cell Phenomenon. Iii. Evidence That Il-2 Is Sufficient for Direct Activation of Peripheral Blood Lymphocytes into Lymphokine-Activated Killer Cells*. J Exp Med. 1983; **158**(4): 1356-61.

139. Strausser J.L., Rosenberg S.A., *In Vitro Growth of Cytotoxic Human Lymphocytes. I. Growth of Cells Sensitized in Vitro to Alloantigens*. J Immunol. 1978; **121**(4): 1491-5.

140. Bamford R.N., et al., *The Interleukin (Il) 2 Receptor Beta Chain Is Shared by Il-2 and a Cytokine, Provisionally Designated Il-T, That Stimulates T-Cell Proliferation and the Induction of Lymphokine-Activated Killer Cells*. Proc Natl Acad Sci U S A. 1994; **91**(11): 4940-4.

141. Gasteiger G., et al., *Il-2-Dependent Tuning of Nk Cell Sensitivity for Target Cells Is Controlled by Regulatory T Cells*. J Exp Med. 2013; **210**(6): 1167-78.

142. Skak K., Frederiksen K.S., Lundsgaard D., *Interleukin-21 Activates Human Natural Killer Cells and Modulates Their Surface Receptor Expression*. Immunology. 2008; **123**(4): 575-83.

143. Wu Z., et al., *Interleukin-2 from Adaptive T Cells Enhances Natural Killer Cell Activity against Human Cytomegalovirus-Infected Macrophages*. J Virol. 2015; **89**(12): 6435-41.

144. Hart O.M., et al., *Tlr7/8-Mediated Activation of Human Nk Cells Results in Accessory Cell-Dependent Ifn-Gamma Production*. J Immunol. 2005; **175**(3): 1636-42.

145. Akira S., Sato S., *Toll-Like Receptors and Their Signaling Mechanisms*. Scand J Infect Dis. 2003; **35**(9): 555-62.

146. Vasilakos J.P., Tomai M.A., *The Use of Toll-Like Receptor 7/8 Agonists as Vaccine Adjuvants*. Expert Rev Vaccines. 2013; **12**(7): 809-19.

147. Lusty E., et al., *Il-18/Il-15/Il-12 Synergy Induces Elevated and Prolonged Ifn-Γ Production by Ex Vivo Expanded Nk Cells Which Is Not Due to Enhanced Stat4 Activation*. Mol Immunol. 2017; **88**: 138-47.

148. Klein E., et al., *Properties of the K562 Cell Line, Derived from a Patient with Chronic Myeloid Leukemia*. Int J Cancer. 1976; **18**(4): 421-31.

149. Nishimura M., et al., *Protection against Natural Killer Cells by Interferon-Gamma Treatment of K562 Cells Cannot Be Explained by Augmented Major Histocompatibility Complex Class I Expression*. Immunology. 1994; **83**(1): 75-80.

150. Singh N., et al., *Inflammation and Cancer*. Ann Afr Med. 2019; **18**(3): 121-6.

151. Li Z., et al., *Chronic Inflammation Links Cancer and Parkinson's Disease*. Front Aging Neurosci. 2016; **8**: 126.

152. Aggarwal B.B., *Nuclear Factor-Kappab: The Enemy Within*. Cancer Cell. 2004; **6**(3): 203-8.

153. Grabarek Z., Gergely J., *Zero-Length Crosslinking Procedure with the Use of Active Esters*. Anal Biochem. 1990; **185**(1): 131-5.

154. Shapiro S.S., Wilk M.B., *An Analysis of Variance Test for Normality (Complete Samples)*. Biometrika. 1965; **52**(3/4): 591-611.

155. Schober P., Boer C., Schwarte L.A., *Correlation Coefficients: Appropriate Use and Interpretation*. Anesth Analg. 2018; **126**(5): 1763-8.

156. Caruso J.C., Cliff N., *Empirical Size, Coverage, and Power of Confidence Intervals for Spearman's Rho*. Educ Psychol Meas. 1997; **57**(4): 637-54.

157. Bilić-Zulle L., *Comparison of Methods: Passing and Bablok Regression*. Biochem Med (Zagreb). 2011; **21**(1): 49-52.

158. Passing H., Bablok W., *A New Biometrical Procedure for Testing the Equality of Measurements from Two Different Analytical Methods. Application of Linear Regression Procedures for Method Comparison Studies in Clinical Chemistry, Part I*. J Clin Chem Clin Biochem. 1983; **21**(11): 709-20.

159. Keller T. ACOMED statistik. *Passing Bablok Regression with Cusum Test* [Excel tool]. ACOMED statistik. Available from: www.acomed-statistik-tools.de, Date cited: 06-14-2022.

160. Bland J.M., Altman D.G., *Measuring Agreement in Method Comparison Studies*. Stat Methods Med Res. 1999; **8**(2): 135-60.

161. Giavarina D., *Understanding Bland Altman Analysis*. Biochem Med (Zagreb). 2015; **25**(2): 141-51.

162. Metsalu T., Vilo J. *Clustvis: A Web Tool for Visualizing Clustering of Multivariate Data (Beta)* [R package based webtool]. Available from: biit.cs.ut.ee/clustvis, Date cited: 06-14-2022.

163. Metsalu T., Vilo J., *Clustvis: A Web Tool for Visualizing Clustering of Multivariate Data Using Principal Component Analysis and Heatmap*. Nucleic Acids Res. 2015; **43**(W1): W566-70.

164. Becker M. *Validation and Application of a Multiplex Immunoassay for the Systematic Characterisation of the Immune Response Towards Implant Material* [Masters Thesis]: Eberhard Karls Universität Tübingen; 2018.

165. Tsuchiya S., et al., *Establishment and Characterization of a Human Acute Monocytic Leukemia Cell Line (Thp-1)*. Int J Cancer. 1980; **26**(2): 171-6.

166. Bosshart H., Heinzelmann M., *Thp-1 Cells as a Model for Human Monocytes*. Annals of translational medicine. 2016; **4**(21): 438.

167. Franz S., et al., *Immune Responses to Implants - a Review of the Implications for the Design of Immunomodulatory Biomaterials*. Biomaterials. 2011; **32**(28): 6692-709.

168. Arango Duque G., Descoteaux A., *Macrophage Cytokines: Involvement in Immunity and Infectious Diseases*. Frontiers in Immunology. 2014; **5**.

169. Gorbet M.B., Sefton M.V., *Biomaterial-Associated Thrombosis: Roles of Coagulation Factors, Complement, Platelets and Leukocytes*. Biomaterials. 2004; **25**(26): 5681-703.

170. Wilson C.J., et al., *Mediation of Biomaterial-Cell Interactions by Adsorbed Proteins: A Review*. Tissue Eng. 2005; **11**(1-2): 1-18.

171. Vashist S.K., Luong J.H.T., Chapter 1 - *Immunoassays: An Overview*. In: Handbook of Immunoassay Technologies. Vashist S.K., Luong J.H.T., editors.: Academic Press; 2018. p. 1-18.

172. He J., Chapter 5.1 - *Practical Guide to Elisa Development*. In: The Immunoassy Handbook (Fourth Edition). Wild D., editor. 4 ed. Oxord: Elevisier; 2013. p. 381-93.

173. Davis C., Chapter 1.3 - *Immunoassay Performance Measures*. In: The Immunoassay Handbook (Fourth Edition). Wild D., editor. 4 ed. Oxford: Elevisier; 2013. p. 11-26.

174. Juncker D., et al., *Cross-Reactivity in Antibody Microarrays and Multiplexed Sandwich Assays: Shedding Light on the Dark Side of Multiplexing*. Curr Opin Chem Biol. 2014; **18**: 29-37.

175. Tighe P.J., et al., *Elisa in the Multiplex Era: Potentials and Pitfalls*. Proteomics. Clinical applications. 2015; **9**(3-4): 406-22.

176. Merck. Millipore. *Chemiblock Ii Heterophile Blocking Agent - Data Sheet* [PDF]. Millipore. Available from: www.merckmillipore.com/Web-DE-Site/de_DE/-/EUR/ShowDocument-File?ProductSKU=MM_NF-CBII-K&DocumentId=/deepweb/assets/sigmaaldrich/product/documents/253/578/cbii-k.pdf&DocumentUID=357953619&DocumentType=DS&Language=EN&Country=NF&Origin=PDP, Date cited: 04-21-2022.

177. Liddell E., Chapter 3.1 - *Antibodies*. In: The Immunoassay Handbook (Fourth Edition). Wild D., editor. 4 ed. Oxford: Elevisier; 2013. p. 245-65.

178. Kaplan I.V., Levinson S.S., *When Is a Heterophile Antibody Not a Heterophile Antibody? When It Is an Antibody against a Specific Immunogen*. Clin Chem. 1999; **45**(5): 616-8.

179. Mehta D., Purushothama S., Stevenson L., *Parallelism: The Foundation of Biomarker Assay Development and Validation*. Bioanalysis. 2018; **10**(12): 897-9.

180. Tu J., Bennett P., *Parallelism Experiments to Evaluate Matrix Effects, Selectivity and Sensitivity in Ligand-Binding Assay Method Development: Pros and Cons*. Bioanalysis. 2017; **9**(14): 1107-22.

181. Wild D., Sheehan C., Chapter 3.5 - *Standardization and Calibration*. In: The Immunoassay Handbook (Fourth Edition). Wild D., editor. 4 ed. Oxford: Elevisier; 2013. p. 315-22.

182. Rissin D.M., Wilson D.H., Duffy D.C., Chapter 2.13 - *Measurement of Single Protein Molecules Using Digital Elisa*. In: The Immunoassay Handbook (Fourth Edition). Wild D., editor. Oxford: Elivisier; 2013. p. 223-42.

183. Cao E., et al., *Effect of Freezing and Thawing Rates on Denaturation of Proteins in Aqueous Solutions*. Biotechnology and Bioengineering. 2003; **82**(6): 684-90.

184. Chen Y.-C., et al., *Thermal Stability, Storage and Release of Proteins with Tailored Fit in Silica*. Scientific Reports. 2017; **7**(1): 46568.

185. WHO. World Health Organization. *Who International Biological Reference Preparations, Held and Distributed by the Who International Laboratories for Biological Standards, Cytokines / Growth Factors* [PDF file]. World Health Organization. Available from: cdn.who.int/media/docs/default-source/biologicals/blood-products/catalogue/cytokines-and-growth-factors.pdf?sfvrsn=eee26f77_2, Date cited: 04-14-2022.

186. Jeffcoate S.L., *Role of Reference Materials in Immunoassay Standardization*. Scand J Clin Lab Invest Suppl. 1991; **205**: 131-3.

187. Rudnicka K., Matusiak A., Chmiela M., *Cd25 (Il-2r) Expression Correlates with the Target Cell Induced Cytotoxic Activity and Cytokine Secretion in Human Natural Killer Cells*. Acta Biochim Pol. 2015; **62**(4): 885-94.

188. Borrego F., et al., *Cd69 Is a Stimulatory Receptor for Natural Killer Cell and Its Cytotoxic Effect Is Blocked by Cd94 Inhibitory Receptor*. Immunology. 1999; **97**(1): 159-65.

189. Clausen J., et al., *Functional Significance of the Activation-Associated Receptors Cd25 and Cd69 on Human Nk-Cells and Nk-Like T-Cells*. Immunobiology. 2003; **207**(2): 85-93.

190. Leong J.W., et al., *Preactivation with Il-12, Il-15, and Il-18 Induces Cd25 and a Functional High-Affinity Il-2 Receptor on Human Cytokine-Induced Memory-Like Natural Killer Cells*. Biol Blood Marrow Transplant. 2014; **20**(4): 463-73.

191. Yoshimoto T., et al., *Interleukin 18 Together with Interleukin 12 Inhibits Ige Production by Induction of Interferon-Γ Production from Activated B Cells*. Proceedings of the National Academy of Sciences. 1997; **94**(8): 3948-53.

192. Munder M., et al., *Murine Macrophages Secrete Interferon Γ Upon Combined Stimulation with Interleukin (Il)-12 and Il-18: A Novel Pathway of Autocrine Macrophage Activation*. Journal of Experimental Medicine. 1998; **187**(12): 2103-8.

193. Sancho D., Gómez M., Sánchez-Madrid F., *Cd69 Is an Immunoregulatory Molecule Induced Following Activation*. Trends Immunol. 2005; **26**(3): 136-40.

194. Wagner J., et al., *A Two-Phase Expansion Protocol Combining Interleukin (Il)-15 and Il-21 Improves Natural Killer Cell Proliferation and Cytotoxicity against Rhabdomyosarcoma*. Frontiers in Immunology. 2017; **8**.

195. Poznanski S.M., et al., *Combined Stimulation with Interleukin-18 and Interleukin-12 Potently Induces Interleukin-8 Production by Natural Killer Cells*. J Innate Immun. 2017; **9**(5): 511-25.

196. Lauwerys B.R., et al., *Cytokine Production and Killer Activity of Nk/T-Nk Cells Derived with Il-2, Il-15, or the Combination of Il-12 and Il-18*. J Immunol. 2000; **165**(4): 1847-53.

197. Lauwerys B.R., Renauld J.C., Houssiau F.A., *Synergistic Proliferation and Activation of Natural Killer Cells by Interleukin 12 and Interleukin 18*. Cytokine. 1999; **11**(11): 822-30.

198. Ivetic A., Hoskins Green H.L., Hart S.J., *L-Selectin: A Major Regulator of Leukocyte Adhesion, Migration and Signaling*. Frontiers in Immunology. 2019; **10**(1068).

199. Smalley D.M., Ley K., *L-Selectin: Mechanisms and Physiological Significance of Ectodomain Cleavage*. J Cell Mol Med. 2005; **9**(2): 255-66.

200. Fan H., Derynck R., *Ectodomain Shedding of Tgf-Alpha and Other Transmembrane Proteins Is Induced by Receptor Tyrosine Kinase Activation and Map Kinase Signaling Cascades*. Embo j. 1999; **18**(24): 6962-72.

201. Dons'koi B.V., Chernyshov V.P., Osypchuk D.V., *Measurement of Nk Activity in Whole Blood by the Cd69 up-Regulation after Co-Incubation with K562, Comparison with Nk Cytotoxicity Assays and Cd107a Degranulation Assay*. Journal of Immunological Methods. 2011; **372**(1): 187-95.

202. de Rham C., et al., *The Proinflammatory Cytokines Il-2, Il-15 and Il-21 Modulate the Repertoire of Mature Human Natural Killer Cell Receptors*. Arthritis Research & Therapy. 2007; **9**(6): R125.

203. Hailman E., et al., *Stimulation of Macrophages and Neutrophils by Complexes of Lipopolysaccharide and Soluble Cd14*. The Journal of Immunology. 1996; **156**(11): 4384.

204. Lu Y.C., Yeh W.C., Ohashi P.S., *Lps/Tlr4 Signal Transduction Pathway*. Cytokine. 2008; **42**(2): 145-51.

205. Vaure C., Liu Y., *A Comparative Review of Toll-Like Receptor 4 Expression and Functionality in Different Animal Species*. Frontiers in Immunology. 2014; **5**.

206. Krakauer T., *Staphylococcal Superantigens: Pyrogenic Toxins Induce Toxic Shock*. Toxins. 2019; **11**(3): 178.

207. Kunkl M., et al., *Binding of Staphylococcal Enterotoxin B (Seb) to B7 Receptors Triggers Tcr- and Cd28-Mediated Inflammatory Signals in the Absence of Mhc Class Ii Molecules*. Frontiers in Immunology. 2021; **12**.

208. Ngkelo A., et al., *Lps Induced Inflammatory Responses in Human Peripheral Blood Mononuclear Cells Is Mediated through Nox4 and Giα Dependent Pi-3kinase Signalling*. Journal of Inflammation. 2012; **9**(1).

209. Sperber K., et al., *Cytokine Secretion Induced by Superantigens in Peripheral Blood Mononuclear Cells, Lamina Propria Lymphocytes, and Intraepithelial Lymphocytes*. Clinical and diagnostic laboratory immunology. 1995; **2**(4): 473-7.

210. Rossol M., et al., *Lps-Induced Cytokine Production in Human Monocytes and Macrophages*. Crit Rev Immunol. 2011; **31**(5): 379-446.

211. Sherry B., et al., *Induction of the Chemokine Beta Peptides, Mip-1 Alpha and Mip-1 Beta, by Lipopolysaccharide Is Differentially Regulated by Immunomodulatory Cytokines Gamma-Ifn, Il-10, Il-4, and Tgf-Beta*. Mol Med. 1998; **4**(10): 648-57.

212. Wu Y., Tian Z., Wei H., *Developmental and Functional Control of Natural Killer Cells by Cytokines*. Frontiers in Immunology. 2017; **8**.

213. Cohnen A., et al., *Surface Cd107a/Lamp-1 Protects Natural Killer Cells from Degranulation-Associated Damage*. Blood. 2013; **122**(8): 1411-8.

214. Alter G., Malenfant J.M., Altfeld M., *Cd107a as a Functional Marker for the Identification of Natural Killer Cell Activity*. J Immunol Methods. 2004; **294**(1-2): 15-22.

215. Betts M.R., et al., *Sensitive and Viable Identification of Antigen-Specific Cd8+ T Cells by a Flow Cytometric Assay for Degranulation*. J Immunol Methods. 2003; **281**(1-2): 65-78.

216. Bryceson Y.T., et al., *Cytolytic Granule Polarization and Degranulation Controlled by Different Receptors in Resting Nk Cells*. J Exp Med. 2005; **202**(7): 1001-12.

217. Krzewski K., et al., *Lamp1/Cd107a Is Required for Efficient Perforin Delivery to Lytic Granules and Nk-Cell Cytotoxicity*. Blood. 2013; **121**(23): 4672-83.

218. de Saint Basile G., Ménasché G., Fischer A., *Molecular Mechanisms of Biogenesis and Exocytosis of Cytotoxic Granules*. Nat Rev Immunol. 2010; **10**(8): 568-79.

219. Peters P.J., et al., *Cytotoxic T Lymphocyte Granules Are Secretory Lysosomes, Containing Both Perforin and Granzymes*. J Exp Med. 1991; **173**(5): 1099-109.

220. Bryceson Y.T., et al., *Functional Analysis of Human Nk Cells by Flow Cytometry*. Methods Mol Biol. 2010; **612**: 335-52.

221. Page L.J., et al., *L Is for Lytic Granules: Lysosomes That Kill*. Biochim Biophys Acta. 1998; **1401**(2): 146-56.

222. Ewen C.L., Kane K.P., Bleackley R.C., *A Quarter Century of Granzymes*. Cell Death Differ. 2012; **19**(1): 28-35.

223. Lin L., et al., *Granzyme B Secretion by Human Memory Cd4 T Cells Is Less Strictly Regulated Compared to Memory Cd8 T Cells*. BMC Immunology. 2014; **15**(1): 36.

224. Tamang D.L., et al., *Induction of Granzyme B and T Cell Cytotoxic Capacity by Il-2 or Il-15 without Antigens: Multiclonal Responses That Are Extremely Lytic If Triggered and Short-Lived after Cytokine Withdrawal*. Cytokine. 2006; **36**(3-4): 148-59.

225. Meyer T., et al., *Poly(I:C) Costimulation Induces a Stronger Antiviral Chemokine and Granzyme B Release in Human Cd4 T Cells Than Cd28 Costimulation*. J Leukoc Biol. 2012; **92**(4): 765-74.

226. Brown D.M., *Cytolytic Cd4 Cells: Direct Mediators in Infectious Disease and Malignancy*. Cell Immunol. 2010; **262**(2): 89-95.

227. Quezada S.A., et al., *Tumor-Reactive Cd4(+) T Cells Develop Cytotoxic Activity and Eradicate Large Established Melanoma after Transfer into Lymphopenic Hosts*. J Exp Med. 2010; **207**(3): 637-50.

228. Nakanishi K., *Unique Action of Interleukin-18 on T Cells and Other Immune Cells*. Frontiers in Immunology. 2018; **9**.

229. Raphael I., et al., *T Cell Subsets and Their Signature Cytokines in Autoimmune and Inflammatory Diseases*. Cytokine. 2015; **74**(1): 5-17.

230. Liu D., et al., *Integrin-Dependent Organization and Bidirectional Vesicular Traffic at Cytotoxic Immune Synapses*. Immunity. 2009; **31**(1): 99-109.

231. Wang K.S., Frank D.A., Ritz J., *Interleukin-2 Enhances the Response of Natural Killer Cells to Interleukin-12 through up-Regulation of the Interleukin-12 Receptor and Stat4*. Blood. 2000; **95**(10): 3183-90.

232. Tugues S., et al., *New Insights into Il-12-Mediated Tumor Suppression*. Cell Death & Differentiation. 2015; **22**(2): 237-46.

233. Henry C.J., et al., *Il-12 Produced by Dendritic Cells Augments Cd8+ T Cell Activation through the Production of the Chemokines Ccl1 and Ccl17*. Journal of immunology (Baltimore, Md. : 1950). 2008; **181**(12): 8576-84.

234. Nakamura S., et al., *Expression and Responsiveness of Human Interleukin-18 Receptor (Il-18r) on Hematopoietic Cell Lines*. Leukemia. 2000; **14**(6): 1052-9.

235. Carty M., Bowie A.G., *Recent Insights into the Role of Toll-Like Receptors in Viral Infection*. Clinical and experimental immunology. 2010; **161**(3): 397-406.

236. Marcken M.d., et al., *Tlr7 and Tlr8 Activate Distinct Pathways in Monocytes During Rna Virus Infection*. Science Signaling. 2019; **12**(605): eaaw1347.

237. Duffy D., et al., *Functional Analysis Via Standardized Whole-Blood Stimulation Systems Defines the Boundaries of a Healthy Immune Response to Complex Stimuli*. Immunity. 2014; **40**(3): 436-50.

ANNEX

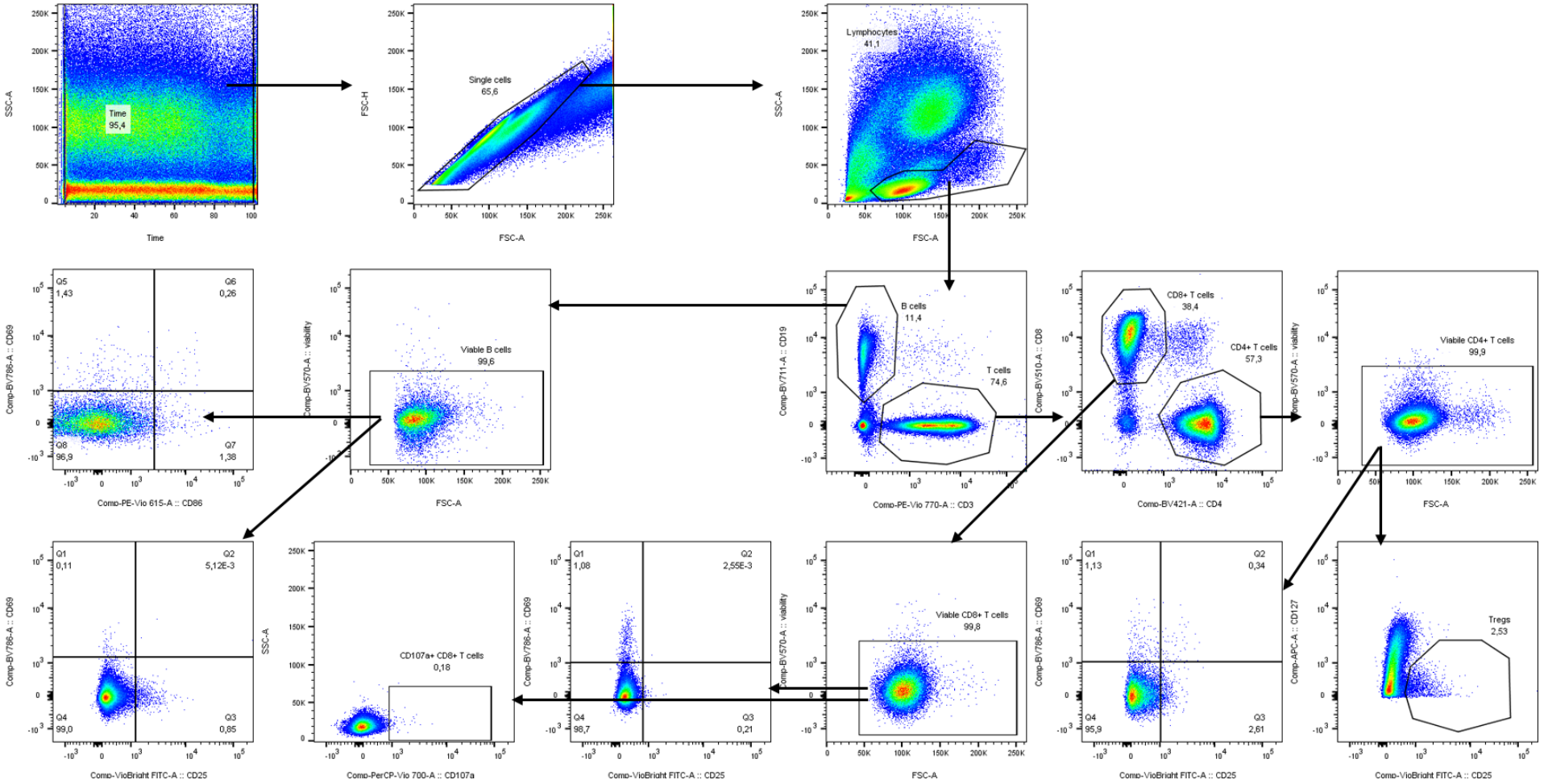

ANNEX - Figure 1: Gating strategy for flow cytometric analysis using FlowJo software – part 1: gating procedure of T and B cell populations.

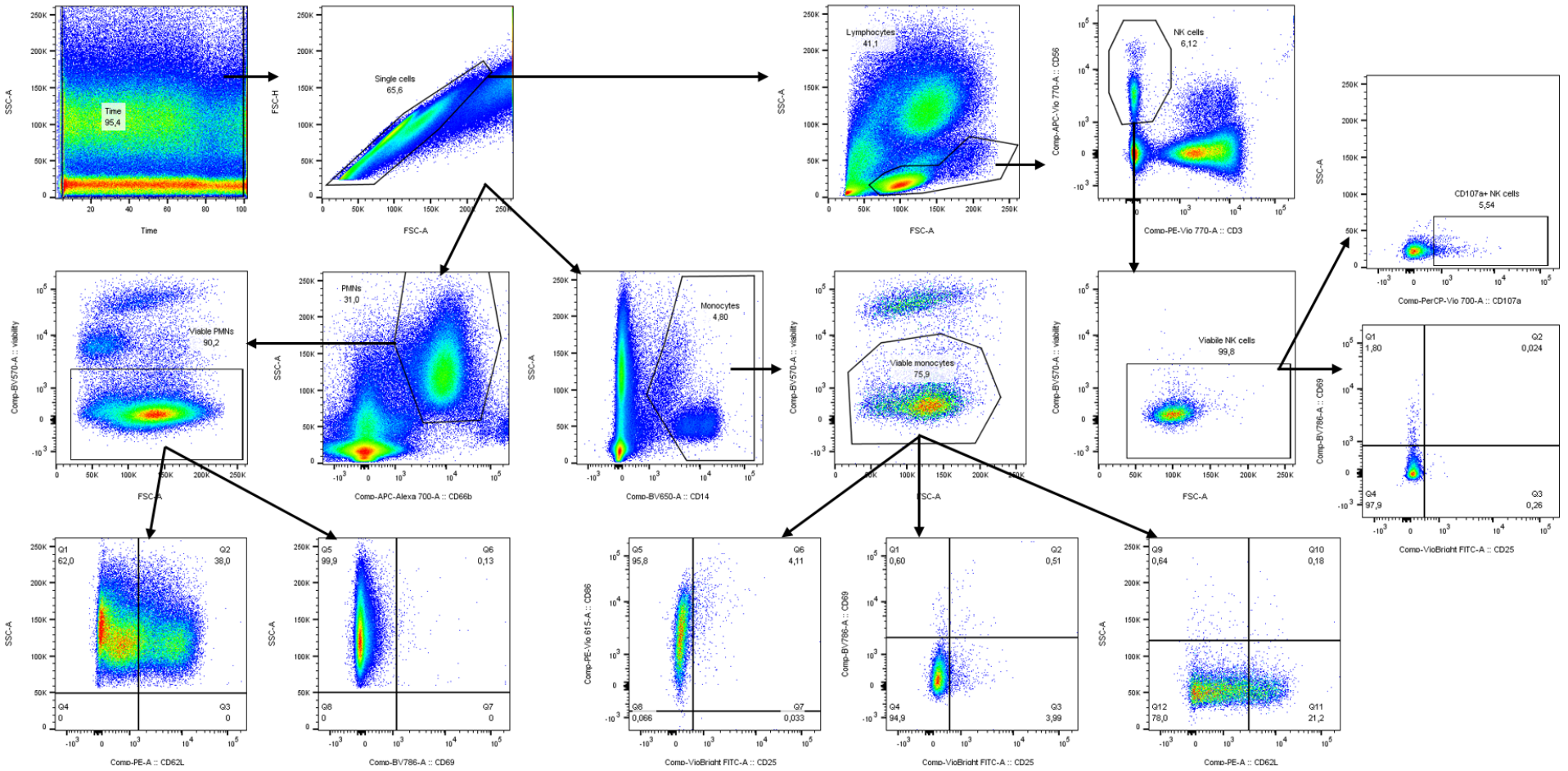

ANNEX - Figure 2: Gating strategy for flow cytometric analysis using FlowJo software – part 2: gating procedure of NK cells, PMNs and monocytes.

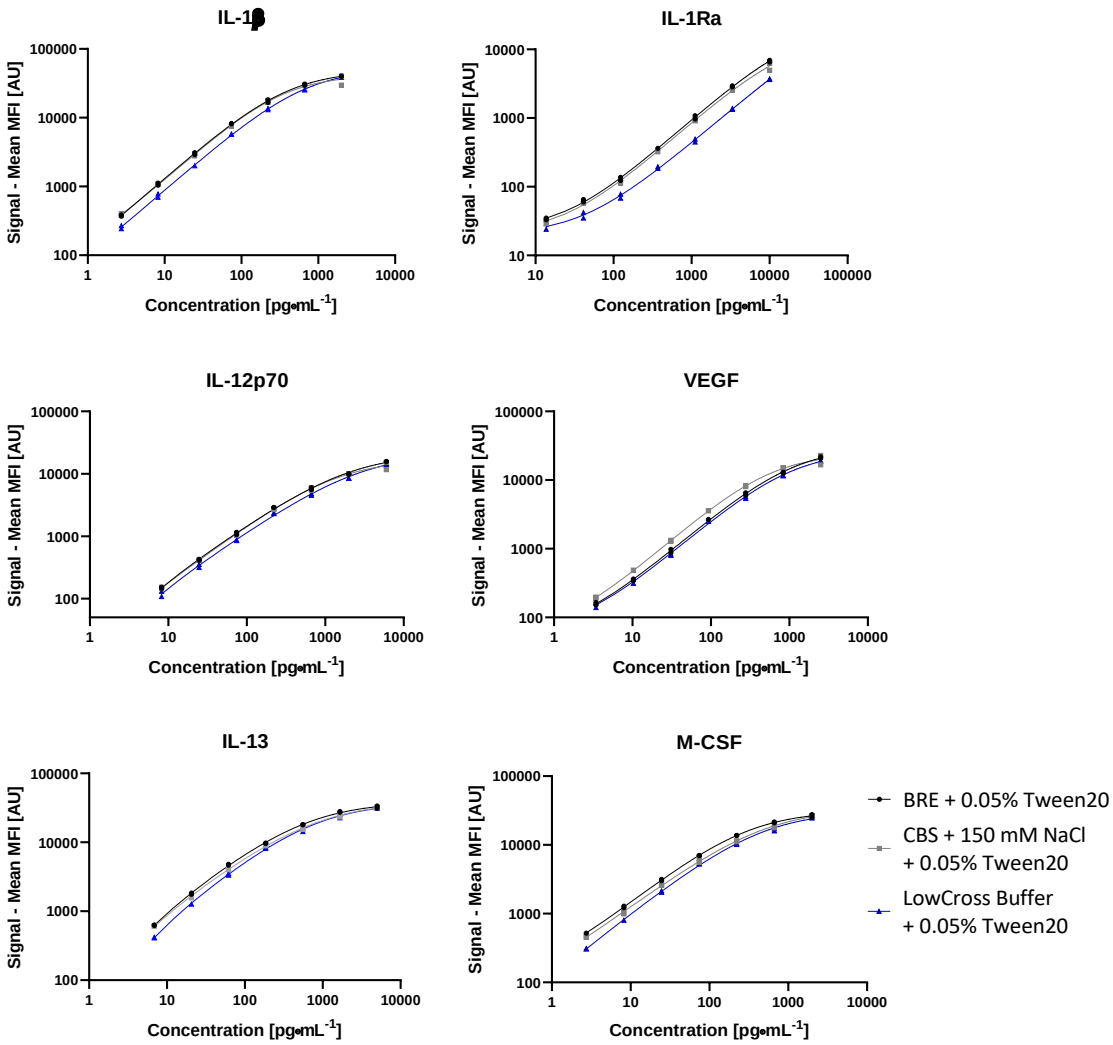

ANNEX - Figure 3: Results of testing suitable basic assay buffers for IMAP 2. *The direct comparison of the standard curves produced in the respective buffers is shown for each analyte of IMAP 1. The calibration curves are presented as median fluorescent intensity (MFI) signal plotted against the nominal concentration in pg·mL^{-1} fitted with a 5-parametric logistic regression (1/Y^2 weighting). The analysis of each standard curve was performed in duplicates (n = 2), the respective individual values are presented. (BRE = Blocking reagent for ELISA; CBS = phosphate based buffer). The buffer tests for IMAP 2 were carried out by Matthias Becker.*

ANNEX - Table 1: Results of cross-reactivity testing for IMAP 2. *(A) MFI signals of the cross-reactivity testing between the respective analyte specific capture and detection antibody. MFIs above 120 AU were regarded as cross-reactivity. (B) Testing of cross-reactivity between the analyte and capture antibody. Given recoveries in % are based on the signal generated with the analyte-specific combinations set to 100 %. Recoveries above 1 % were rated as cross-reactivity. (C) Cross-reactivity testing between analyte and detection antibody. Calculation and evaluation correspond to that already described for (B). All values were assessed as duplicates (n = 2). Matthias Becker carried out the measurements for the cross-reactivity testing of IMAP 2.*

A

Mean MFI [AU]		Multiplexed capture coated beads					
		IL-1β	IL-1Ra	IL-12p70	VEGF	IL-13	M-CSF
Detection antibody	IL-1β	34	16	18	37	9	19
	IL-1Ra	27	14	13	40	9	18
	IL-12p70	28	15	11	34	8	21
	VEGF	28	14	16	36	8	24
	IL-13	38	17	27	41	12	25
	M-CSF	94	35	68	66	42	39

B

Recovery [%]		Multiplexed capture coated beads					
		IL-1β	IL-1Ra	IL-12p70	VEGF	IL-13	M-CSF
Recombinant protein	IL-1β	100	0.370	0.253	0.305	0.129	0.168
	IL-1Ra	0.166	100	0.214	0.291	0.109	0.123
	IL-12p70	0.174	0.287	100	0.339	0.119	0.145
	VEGF	0.159	0.290	0.147	100	0.123	0.131
	IL-13	0.193	0.321	0.239	0.305	100	0.238
	M-CSF	0.165	0.278	0.176	0.241	0.097	100

C

Recovery [%]		Multiplexed capture coated beads					
		IL-1β	IL-1Ra	IL-12p70	VEGF	IL-13	M-CSF
Detection antibody	IL-1β	100	0.175	0.155	0.142	0.079	0.068
	IL-1Ra	0.122	100	0.164	0.198	0.075	0.062
	IL-12p70	0.104	0.494	100	0.464	0.283	0.198
	VEGF	0.106	0.187	0.187	100	0.073	0.081
	IL-13	0.114	0.175	0.155	0.173	100	0.072
	M-CSF	0.091	0.164	0.127	0.142	0.055	100

ANNEX - Table 2: Results of buffer optimization for IMAP 2 using different concentrations of CBII blocker. *MFI signals of the blank values were determined in CBST and varying concentrations of CBII blocker. Means were calculated from duplicate measurements (n = 2) and CVs (coefficients of variation) were determined as relative standard deviations related to the mean. Matthias Becker carried out the buffer optimization for IMAP 2.*

	Analytes - IMAP 2											
	IL-1β		IL-1Ra		IL-12p70		VEGF		IL-13		M-CSF	
CBII conc. [µg·mL^{-1}]	Mean MFI [AU]	CV [%]	Mean MFI [AU]	CV [%]	Mean MFI [AU]	CV [%]	Mean MFI [AU]	CV [%]	Mean MFI [AU]	CV [%]	Mean MFI [AU]	CV [%]
5	21	12.5	18	8.1	16	30.9	44	17.7	13	42.9	29	5.6
10	18	7.7	16	7.0	13	14.0	39	9.1	9	10.9	28	6.9
50	19	30.1	17	10.6	17	79.8	41	31.1	12	83.2	24	10.8

ANNEX - Table 3: Results of the determination of the lower limit of quantification (LLOQ) for the analytes of IMAP 1.*The nominal concentrations of the respective analytes defined as LLOQ are shown in bold. The values in bold, italics and highlighted in grey are the determined CVs and recoveries that did not meet the acceptance criteria.*

Lower limit of quantification - IMAP 1									
		CAL 4 dilution							
Analyte		***1:2***	***1:4***	***1:8***	***1:16***	***1:32***	***1:64***	***1:128***	*CAL 4*
IL-4	nominal conc. [pg·mL^{-1}]	5.56	2.78	1.39	0.694	0.347	**0.174**	0.087	11.1
	assay conc. [pg·mL^{-1}]	4.59	2.69	1.39	0.694	0.356	0.190	0.127	
	CV [%]	16.1	7.46	8.04	8.55	15.5	11.0	23.2	
	recovery [%]	82.6	97.0	99.8	100	102	109	***146***	
IL-6	nominal conc. [pg·mL^{-1}]	1.50	0.750	0.375	**0.188**	0.094	0.047	0.023	3.00
	assay conc. [pg·mL^{-1}]	1.32	0.720	0.389	0.184	0.092	0.031	0.040	
	CV [%]	8.19	6.98	13.4	8.18	***27.5***	***76.7***	***50.0***	
	recovery [%]	88.0	96.0	104	98.4	98.4	***67.0***	***171***	
IL-8	nominal conc. [pg·mL^{-1}]	4.28	2.14	1.07	0.535	**0.267**	0.134	0.067	8.56
	assay conc. [pg·mL^{-1}]	3.56	2.10	1.09	0.561	0.269	0.131	0.072	
	CV [%]	11.1	6.42	8.24	9.28	10.8	***47.0***	***85.3***	
	recovery [%]	83.1	98.2	102	105	101	98.3	107	
IL-10	nominal conc. [pg·mL^{-1}]	4.91	2.45	1.23	0.613	**0.307**	0.153	0.077	9.81
	assay conc. [pg·mL^{-1}]	4.22	2.43	1.22	0.628	0.361	0.164	0.103	
	CV [%]	9.53	7.63	9.44	9.48	17.0	***25.5***	***36.8***	
	recovery [%]	86.0	99.0	99.7	102	118	107	***134***	
GM-CSF	nominal conc. [pg·mL^{-1}]	41.6	20.8	10.4	**5.20**	2.60	1.30	0.650	83.1
	assay conc. [pg·mL^{-1}]	36.2	21.6	10.8	5.77	3.18	1.75	0.658	
	CV [%]	10.2	11.6	16.3	19.3	***40.0***	***64.4***	***85.7***	
	recovery [%]	87.0	104	104	111	122	***135***	101	
IFN-γ	nominal conc. [pg·mL^{-1}]	7.41	3.70	1.85	0.926	**0.463**	0.231	0.116	14.8
	assay conc. [pg·mL^{-1}]	6.36	3.72	1.97	0.990	0.493	0.277	0.158	
	CV [%]	10.9	9.42	12.5	11.0	11.7	***42.5***	***54.1***	
	recovery [%]	85.8	100	107	107	107	120	***137***	
MCP-1	nominal conc. [pg·mL^{-1}]	16.7	8.34	4.17	2.09	1.04	0.521	0.261	33.4
	assay conc. [pg·mL^{-1}]	12.6	7.13	3.81	1.93	0.922	0.680	0.377	
	CV [%]	7.15	10.4	6.00	10.1	***37.4***	11.8	21.5	
	recovery [%]	75.4	85.4	91.4	92.3	88.4	***130***	***144***	
MIP-1β	nominal conc. [pg·mL^{-1}]	1.80	0.898	0.449	**0.225**	0.112	0.056	0.028	3.59
	assay conc. [pg·mL^{-1}]	1.52	0.788	0.404	0.218	0.087	0.053	0.028	
	CV [%]	9.46	5.23	7.73	10.5	***26.4***	***45.4***	***52.0***	
	recovery [%]	84.9	87.7	90.1	97.0	77.2	95.0	101	
TNF-α	nominal conc. [pg·mL^{-1}]	11.1	5.55	2.77	1.39	**0.693**	0.347	0.173	22.2
	assay conc. [pg·mL^{-1}]	9.52	5.49	2.72	1.44	0.747	0.308	0.215	
	CV [%]	8.92	7.28	6.90	12.8	10.7	***42.1***	***28.0***	
	recovery [%]	85.8	98.9	98.0	104	108	88.8	124	

ANNEX - Table 4: Results of the determination of the lower limit of quantification (LLOQ) for the respective analytes of IMAP 2.*The nominal concentrations of the respective analytes defined as LLOQ are shown in bold. The values in bold, italics and highlighted in grey are the determined CVs and recoveries that did not meet the acceptance criteria.*

Lower limit of quantification - IMAP 2									
		CAL 4 dilution							
Analyte		***1:2***	***1:4***	***1:8***	***1:16***	***1:32***	***1:64***	***1:128***	*CAL 4*
IL-1β	nominal conc. [pg·mL^{-1}]	4.24	2.12	1.06	0.530	0.265	**0.133**	0.044	8.48
	assay conc. [pg·mL^{-1}]	4.15	2.25	1.16	0.654	0.300	0.138	0.039	
	CV [%]	9.79	8.22	10.9	11.3	8.98	14.4	***60.8***	
	recovery [%]	97.8	106	110	123	113	104	***58.5***	
IL-1Ra	nominal conc. [pg·mL^{-1}]	185	92.6	46.3	23.1	**11.6**	5.79	1.93	370
	assay conc. [pg·mL^{-1}]	179	92.1	47.9	24.9	10.8	4.66	2.30	
	CV [%]	3.50	6.47	9.54	8.90	16.2	***37.1***	***26.6***	
	recovery [%]	96.7	99.4	103	108	93.1	80.6	79.3	
IL-12p70	nominal conc. [pg·mL^{-1}]	13.0	6.50	3.25	1.63	**0.813**	0.406	0.135	26.0
	assay conc. [pg·mL^{-1}]	12.9	7.02	3.51	1.87	0.901	0.438	0.347	
	CV [%]	9.12	9.43	11.6	10.8	18.4	***46.3***	***58.0***	
	recovery [%]	98.9	108	108	115	111	108	***171***	
VEGF	nominal conc. [pg·mL^{-1}]	17.5	8.73	4.37	2.18	**1.09**	0.546	0.182	34.9
	assay conc. [pg·mL^{-1}]	16.9	9.20	4.92	2.67	1.28	0.542	0.140	
	CV [%]	12.8	11.1	10.7	13.7	17.4	***35.5***	***98.6***	
	recovery [%]	96.8	105	113	122	118	99.4	***51.3***	
IL-13	nominal conc. [pg·mL^{-1}]	5.48	2.74	1.37	**0.685**	0.343	0.171	0.057	11.0
	assay conc. [pg·mL^{-1}]	5.17	2.74	1.42	0.724	0.322	0.163	0.085	
	CV [%]	7.52	7.06	8.60	14.8	***27.0***	***38.5***	***63.5***	
	recovery [%]	94.3	99.9	103	106	94.1	94.9	99.2	
M-CSF	nominal conc. [pg·mL^{-1}]	3.26	1.63	0.815	0.407	**0.204**	0.102	0.034	6.52
	assay conc. [pg·mL^{-1}]	3.21	1.68	0.859	0.450	0.210	0.106	0.044	
	CV [%]	7.41	5.98	7.80	7.45	9.52	***38.2***	***42.2***	
	recovery [%]	98.5	103	105	110	103	104	85.9	

ANNEX - Table 5: Results of parallelism (PL) determination for IMAP 1 using sample 1. *Assay and matrix concentrations are given in pg·mL^{-1}. (<LLOQ = concentration below the lower limit of quantification; n.q. = value cannot be quantified; conc. = concentration; DF = dilution factor; CVs (grey) = relative differences between matrix concentrations [pg·mL^{-1}] used to calculate the reference)*

Parallelism - IMAP 1 - sample 1										
Analyte	***Reference [pg·mL^{-1}]*** *(CV)*		***PL 1***	***PL 2***	***PL 3***	***PL 4***	***PL 5***	***PL 6***	***PL 7***	***PL 8***	***PL 9***
IL-4	*cannot be genereated*	DF (1:x)	*4.00*	*8.00*	*16.0*	*32.0*	*64.0*	*128*	*256*	*512*	*1,024*
		assay conc.	106	65.8	36.6	23.8	13.4	7.45	4.02	1.95	1.15
		matrix conc.	423	527	585	763	857	953	1,029	998	1,181
		recovery [%]					n.q.				
IL-6	*21260* *(4.71 %)*	DF (1:x)	*256*	*512*	*1,024*	*2,048*	*4,096*	*8,192*	*16,384*	*32,768*	*65,536*
		assay conc.	80.6	38.6	21.7	10.3	5.61	2.62	1.26	0.673	0.313
		matrix conc.	20,646	19,758	22,200	21,094	22,965	21,436	20,644	22,064	20,535
		recovery [%]	97.1	92.9	104	99.2	108	101	97.1	104	96.6
IL-8	*68342* *(6.40 %)*	DF (1:x)	*512*	*1,024*	*2,048*	*4,096*	*8,192*	*16,384*	*32,768*	*65,536*	*131,072*
		assay conc.	114	65.0	32.5	17.1	8.54	4.42	2.21	1.08	0.517
		matrix conc.	58,325	66,519	66,553	70,219	69,960	72,472	72,308	70,997	67,721
		recovery [%]	85.3	97.3	97.4	103	102	106	106	104	99.1
IL-10	*710* *(10.7 %)*	DF (1:x)	*4.00*	*8.00*	*16.0*	*32.0*	*64.0*	*128*	*256*	*512*	*1,024*
		assay conc.	151	87.3	45.3	23.8	12.6	6.33	2.83	1.21	0.630
		matrix conc.	603	698	724	762	807	810	724	620	645
		recovery [%]	84.9	98.3	102	107	114	114	102	87.2	90.8
GM-CSF	*cannot be genereated*	DF (1:x)	*4.00*	*8.00*	*16.0*	*32.0*	*64.0*	*128*	*256*	< LLOQ	
		assay conc.	98.3	63.5	45.5	28.7	17.8	10.3	6.55	n.q.	
		matrix conc.	393	508	728	920	1,140	1,313	1,678	n.q.	
		recovery [%]				n.q.					
IFN-γ	*9302* *(4.38 %)*	DF (1:x)	*32.0*	*64.0*	*128*	*256*	*512*	*1,024*	*2,048*	*4,096*	*8,192*
		assay conc.	302	141	69.3	36.0	16.6	9.35	4.55	2.29	1.19
		matrix conc.	9,674	9,015	8,870	9,223	8,513	9,578	9,312	9,366	9,748
		recovery [%]	104	96.9	95.4	99.1	91.5	103	100	101	105
MCP-1	*7299* *(10.3 %)*	DF (1:x)	*16.0*	*32.0*	*64.0*	*128*	*256*	*512*	*1,024*	*2,048*	< LLOQ
		assay conc.	479	247	130	60.7	28.5	13.4	6.26	3.02	n.q.
		matrix conc.	7,657	7,916	8,299	7,764	7,299	6,854	6,410	6,192	n.q.
		recovery [%]	105	108	114	106	100	93.9	87.8	84.8	n.q.
MIP-1β	*67381* *(4.98 %)*	DF (1:x)	*1,024*	*2,048*	*4,096*	*8,192*	*16,384*	*32,768*	*65,536*	*131,072*	
		assay conc.	68.2	33.8	17.7	8.14	3.96	2.07	0.940	0.507	
		matrix conc.	69,816	69,120	72,677	66,656	64,826	67,939	61,604	66,410	
		recovery [%]	104	103	108	98.9	96.2	101	91.4	98.6	
TNF-α	*7950* *(11.7 %)*	DF (1:x)	*16.0*	*32.0*	*64.0*	*128*	*256*	*512*	*1,024*	*2,048*	*4,096*
		assay conc.	429	239	128	61.8	30.2	12.7	7.61	3.96	2.26
		matrix conc.	6,867	7,659	8,175	7,916	7,721	6,484	7,793	8,117	9,243
		recovery [%]	86.4	96.3	103	99.6	97.1	81.6	98.0	102	116

ANNEX - Table 6: Results of parallelism (PL) determination for IMAP 1 using sample 2. *Assay and matrix concentrations are given in pg·mL^{-1}. (<LLOQ = concentration below the lower limit of quantification; n.q. = value cannot be quantified; conc. = concentration; DF = dilution factor; CVs (grey) = relative differences between matrix concentrations [pg·mL^{-1}] used to calculate the reference)*

Parallelism - IMAP 1 - sample 2											
Analyte	***Reference [pg·mL^{-1}]*** *(CV)*		***PL 1***	***PL 2***	***PL 3***	***PL 4***	***PL 5***	***PL 6***	***PL 7***	***PL 8***	***PL 9***	***PL 10***
IL-4	*cannot be genereated*	DF (1:x)	*4.00*	*8.00*	*16.0*	*32.0*	*64.0*	*128*	*256*	*512*	*1,024*	*2,048*
		assay conc.	36.9	23.1	14.5	9.17	6.53	3.92	2.07	1.42	0.840	0.537
		matrix conc.	148	185	231	293	418	502	531	727	860	1,099
		recovery [%]					n.q.					
IL-6	*13675* *(7.98 %)*	DF (1:x)	*256*	*512*	*1,024*	*2,048*	*4,096*	*8,192*	*16,384*	*32,768*	*65,536*	< LLOQ
		assay conc.	46.6	24.0	12.8	6.94	3.54	1.62	0.923	0.427	0.223	n.q.
		matrix conc.	11,934	12,307	13,114	14,220	14,513	13,244	15,128	13,981	14,636	n.q.
		recovery [%]	87.3	90.0	95.9	104	106	96.8	111	102	107	n.q.
IL-8	*43101* *(11.5 %)*	DF (1:x)	*256*	*512*	*1,024*	*2,048*	*4,096*	*8,192*	*16,384*	*32,768*	*65,536*	*131,072*
		assay conc.	130	71.9	38.7	21.2	11.5	5.47	2.91	1.37	0.743	0.340
		matrix conc.	33,364	36,811	39,673	43,329	47,063	44,810	47,677	45,001	48,715	44,564
		recovery [%]	77.4	85.4	92.0	101	109	104	111	104	113	103
IL-10	*989* *(9.42 %)*	DF (1:x)	*4.00*	*8.00*	*16.0*	*32.0*	*64.0*	*128*	*256*	*512*	*1,024*	*2,048*
		assay conc.	279	125	59.7	31.9	16.3	7.34	3.19	1.71	1.02	0.527
		matrix conc.	1,117	1,000	955	1,021	1,043	940	817	874	1,048	1,079
		recovery [%]	113	101	96.6	103	105	95.0	82.6	88.3	106	109
GM-CSF	*cannot be genereated*	DF (1:x)	*4.00*	*8.00*	*16.0*	*32.0*	*64.0*	*128*	< LLoQ			
		assay conc.	63.0	45.7	25.0	20.2	14.2	8.25	n.q.			
		matrix conc.	252	366	400	647	906	1,056	n.q.			
		recovery [%]				n.q.						
IFN-γ	*57787* *(10.4 %)*	DF (1:x)	*256*	*512*	*1,024*	*2,048*	*4,096*	*8,192*	*16,384*	*32,768*	*65,536*	< LLOQ
		assay conc.	176	98.0	59.1	29.6	15.2	7.22	3.79	1.81	0.930	n.q.
		matrix conc.	45,065	50,152	60,483	60,559	62,409	59,119	62,150	59,201	60,948	n.q.
		recovery [%]	78.0	86.8	105	105	108	102	108	102	105	n.q.
MCP-1	*4377* *(8.38 %)*	DF (1:x)	*8.00*	*16.0*	*32.0*	*64.0*	*128*	*256*	*512*	*1,024*	*2,048*	< LLOQ
		assay conc.	550	245	134	71.0	34.3	15.9	9.87	6.37	3.48	n.q.
		matrix conc.	4,397	3,921	4,282	4,541	4,387	4,061	5,052	6,526	7,127	n.q.
		recovery [%]	100	89.6	97.8	104	100	92.8	115	149	163	n.q.
MIP-1β	*134687* *(3.26 %)*	DF (1:x)	*2,048*	*4,096*	*8,192*	*16,384*	*32,768*	*65,536*	*131,072*			
		assay conc.	63.5	33.5	16.2	8.39	4.33	1.98	1.02			
		matrix conc.	130,028	137,271	132,874	137,516	141,885	129,980	133,257			
		recovery [%]	96.5	102	98.7	102	105	96.5	98.9			
TNF-α	*5850* *(11.4 %)*	DF (1:x)	*16.0*	*32.0*	*64.0*	*128*	*256*	*512*	*1,024*	*2,048*	*4,096*	< LLOQ
		assay conc.	326	182	98.7	44.9	19.5	10.0	5.80	3.20	1.70	n.q.
		matrix conc.	5,213	5,811	6,316	5,745	5,001	5,127	5,943	6,547	6,950	n.q.
		recovery [%]	89.1	99.3	108	98.2	85.5	87.6	102	112	119	n.q.

ANNEX - Table 7: Results of parallelism (PL) determination for IMAP 1 using sample 3. *Assay and matrix concentrations are given in pg·mL^{-1}. (<LLOQ = concentration below the lower limit of quantification; n.q. = value cannot be quantified; conc. = concentration; DF = dilution factor; CVs (grey) = relative differences between matrix concentrations [pg·mL^{-1}] used to calculate the reference)*

Parallelism - IMAP 1 - sample 3											
Analyte	***Reference [pg·mL^{-1}]*** *(CV)*		***PL 1***	***PL 2***	***PL 3***	***PL 4***	***PL 5***	***PL 6***	***PL 7***	***PL 8***	***PL 9***	***PL 10***
IL-4	*cannot be genereated*	DF (1:x)	*4.00*	*8.00*	*16.0*	*32.0*	*64.0*	*128*	*256*	*512*	*1,024*	< LLoQ
		assay conc.	43.5	32.0	17.0	11.2	6.70	4.07	2.45	1.26	0.743	n.q.
		matrix conc.	174	256	273	357	429	521	627	645	761	n.q.
		recovery [%]					n.q.					
IL-6	*8285* *(5.09 %)*	DF (1:x)	*128*	*256*	*512*	*1,024*	*2,048*	*4,096*	*8,192*	*16,384*	*32,768*	< LLoQ
		assay conc.	70.6	32.9	16.2	7.76	3.79	1.94	1.07	0.487	0.257	n.q.
		matrix conc.	9,032	8,423	8,306	7,943	7,755	7,960	8,765	7,974	8,410	n.q.
		recovery [%]	109	102	100	95.9	93.6	96.1	106	96.2	102	n.q.
IL-8	*52590* *(5.59 %)*	DF (1:x)	*256*	*512*	*1,024*	*2,048*	*4,096*	*8,192*	*16,384*	*32,768*	*65,536*	*131,072*
		assay conc.	223	101	48.9	24.7	12.7	6.83	3.35	1.62	0.810	0.360
		matrix conc.	57,091	51,833	50,060	50,633	52,115	55,979	54,941	52,975	53,084	47,186
		recovery [%]	109	98.6	95.2	96.3	99.1	106	104	101	101	89.7
IL-10	*731* *(5.34 %)*	DF (1:x)	*4.00*	*8.00*	*16.0*	*32.0*	*64.0*	*128*	*256*	*512*	*1,024*	< LLoQ
		assay conc.	181	92.1	42.4	22.1	11.3	6.15	2.98	1.52	0.667	n.q.
		matrix conc.	723	737	678	707	725	787	764	777	683	n.q.
		recovery [%]	98.9	101	92.7	96.7	99.1	108	104	106	93.4	n.q.
GM-CSF	*cannot be genereated*	DF (1:x)	*4.00*	*8.00*	*16.0*	*32.0*	*64.0*	*128*	< LLoQ			
		assay conc.	74.2	49.3	30.7	20.8	11.6	7.74	n.q.			
		matrix conc.	297	394	491	664	744	991	n.q.			
		recovery [%]				n.q.						
IFN-γ	*4951* *(11.6 %)*	DF (1:x)	*16.0*	*32.0*	*64.0*	*128*	*256*	*512*	*1,024*	*2,048*	*4,096*	*8,192*
		assay conc.	276	137	67.5	37.2	19.4	9.71	4.49	2.66	1.41	0.720
		matrix conc.	4,418	4,375	4,317	4,757	4,973	4,972	4,594	5,448	5,762	5,898
		recovery [%]	89.2	88.4	87.2	96.1	100	100	92.8	110	116	119
MCP-1	*3797* *(11.5 %)*	DF (1:x)	*8.00*	*16.0*	*32.0*	*64.0*	*128*	*256*	*512*	*1,024*	*2,048*	< LLoQ
		assay conc.	444	205	106	56.6	28.7	14.4	8.80	3.93	2.17	n.q.
		matrix conc.	3,553	3,281	3,387	3,621	3,668	3,685	4,506	4,028	4,444	n.q.
		recovery [%]	93.6	86.4	89.2	95.4	96.6	97.0	119	106	117	n.q.
MIP-1β	*48186* *(6.07 %)*	DF (1:x)	*1,024*	*2,048*	*4,096*	*8,192*	*16,384*	*32,768*	*65,536*	*131,072*		
		assay conc.	49.3	22.9	12.3	6.08	2.91	1.38	0.787	0.330		
		matrix conc.	50,490	46,886	50,545	49,807	47,732	45,220	51,555	43,254		
		recovery [%]	105	97.3	105	103	99.1	93.8	107	89.8		
TNF-α	*3331* *(6.48 %)*	DF (1:x)	*8.00*	*16.0*	*32.0*	*64.0*	*128*	*256*	*512*	*1,024*	*2,048*	*4,096*
		assay conc.	395	194	103	50.2	27.4	13.0	6.71	3.17	1.56	0.937
		matrix conc.	3,164	3,103	3,282	3,213	3,508	3,327	3,434	3,249	3,195	3,837
		recovery [%]	95.0	93.1	98.5	96.4	105	99.9	103	97.5	95.9	115

ANNEX - Table 8: Results of parallelism (PL) determination for IMAP 2 using sample 1. *Assay and matrix concentrations are given in pg·mL^{-1}. (<LLOQ = concentration below the lower limit of quantification; n.q. = value cannot be quantified; conc. = concentration; DF = dilution factor; CVs (grey) = relative differences between matrix concentrations [pg·mL^{-1}] used to calculate the reference)*

Parallelism - IMAP 2 - sample 1												
Analyte	***Reference [pg·mL^{-1}]*** *(CV)*		***PL 1***	***PL 2***	***PL 3***	***PL 4***	***PL 5***	***PL 6***	***PL 7***	***PL 8***	***PL 9***	***PL 10***
IL-1β	*5513* *(8.88 %)*	DF (1:x)	*32.0*	*64.0*	*128*	*256*	*512*	*1,024*	*2,048*	*4,096*	*8,192*	
		assay conc.	196	89.1	43.8	20.5	11.0	4.68	2.45	1.45	0.660	
		matrix conc.	6,279	5,705	5,600	5,235	5,632	4,792	5,011	5,953	5,407	
		recovery [%]	114	103	101	94.7	102	86.7	90.7	108	97.8	
IL-1Ra	*26259* *(13.7 %)*	DF (1:x)	*4.00*	*8.00*	*16.0*	*32.0*	*64.0*	*128*	*256*	*512*	*1,024*	< LLOQ
		assay conc.	3,661	2,658	1,416	762	394	215	113	63.3	27.1	n.q.
		matrix conc.	14,644	21,265	22,651	24,379	25,245	27,488	28,940	32,393	27,709	n.q.
		recovery [%]	55.8	81.0	86.3	92.8	96.1	105	110	123	106	n.q.
IL-12p70	*cannot be generated*	DF (1:x)	*4.00*	*8.00*	*16.0*	< LLOQ						
		assay conc.	2.41	2.08	1.26	n.q.						
		matrix conc.	9.63	16.6	20.2	n.q.						
		recovery [%]		n.q.								
VEGF	*63.2* *(11.4 %)*	DF (1:x)	*4.00*	*8.00*	*16.0*	*32.0*	< LLOQ					
		assay conc.	13.3	8.62	3.96	2.11	n.q.					
		matrix conc.	53.0	68.9	63.3	67.6	n.q.					
		recovery [%]	83.8	109	100	107	n.q.					
IL-13	*713* *(6.76 %)*	DF (1:x)	*4.00*	*8.00*	*16.0*	*32.0*	*64.0*	*128*	*256*	*512*	< LLOQ	
		assay conc.	171	99.0	48.0	23.2	10.9	5.23	2.61	1.32	n.q.	
		matrix conc.	685	792	767	744	700	669	669	678	n.q.	
		recovery [%]	96.0	111	108	104	98.2	93.8	93.8	95.0	n.q.	
M-CSF	*cannot be generated*	DF (1:x)	*4.00*	*8.00*	*16.0*	*32.0*	*64.0*	< LLOQ				
		assay conc.	2.17	1.37	0.740	0.440	0.280	n.q.				
		matrix conc.	8.69	11.0	11.8	14.1	17.9	n.q.				
		recovery [%]			n.q.							

ANNEX - Table 9: Results of parallelism (PL) determination for IMAP 2 using sample 2. *Assay and matrix concentrations are given in pg·mL^{-1}. (<LLOQ = concentration below the lower limit of quantification; n.q. = value cannot be quantified; conc. = concentration; DF = dilution factor; CVs (grey) = relative differences between matrix concentrations [pg·mL^{-1}] used to calculate the reference)*

Parallelism - IMAP 2 - sample 2											
Analyte	***Reference [pg·mL^{-1}]*** *(CV)*		***PL 1***	***PL 2***	***PL 3***	***PL 4***	***PL 5***	***PL 6***	***PL 7***	***PL 8***	***PL 9***	***PL 10***
IL-1β	*5439* *(9.59 %)*	DF (1:x)	*32.0*	*64.0*	*128*	*256*	*512*	*1,024*	*2,048*	*4,096*	*8,192*	
		assay conc.	197	94.5	43.2	19.6	9.92	4.97	2.30	1.32	0.707	
		matrix conc.	6,293	6,046	5,528	5,023	5,079	5,086	4,717	5,393	5,789	
		recovery [%]	116	111	102	92.3	93.4	93.5	86.7	99.1	106	
IL-1Ra	*24283* *(9.54 %)*	DF (1:x)	*4.00*	*8.00*	*16.0*	*32.0*	*64.0*	*128*	*256*	*512*	*1,024*	< LLOQ
		assay conc.	4,440	2,720	1,468	802	377	186	98.8	53.3	28.7	n.q.
		matrix conc.	17,762	21,757	23,487	25,648	24,124	23,785	25,284	27,290	29,406	n.q.
		recovery [%]	70.8	86.7	93.6	102	96.1	94.8	101	109	117	n.q.
IL-12p70	*cannot be genereated*	DF (1:x)	*4.00*	*8.00*	*16.0*	< LLOQ						
		assay conc.	2.31	1.58	1.07	n.q.						
		matrix conc.	9.25	12.6	17.2	n.q.						
		recovery [%]		n.q.								
VEGF	*cannot be genereated*	DF (1:x)	*4.00*	*8.00*	*16.0*	*32.0*	< LLOQ					
		assay conc.	10.1	6.68	3.66	2.27	n.q.					
		matrix conc.	40.3	53.5	58.6	72.5	n.q.					
		recovery [%]			n.q.							
IL-13	*201* *(7.47 %)*	DF (1:x)	*4.00*	*8.00*	*16.0*	*32.0*	*64.0*	*128*	*256*	< LLOQ		
		assay conc.	45.6	24.7	13.1	6.50	3.07	1.48	0.890	n.q.		
		matrix conc.	182	198	209	208	197	189	228	n.q.		
		recovery [%]	90.4	98.1	104	103	97.6	93.8	113	n.q.		
M-CSF	*cannot be genereated*	DF (1:x)	*4.00*	*8.00*	*16.0*	*32.0*	*64.0*	< LLOQ				
		assay conc.	1.54	1.20	0.810	0.500	0.280	n.q.				
		matrix conc.	6.15	9.57	13.0	16.0	17.9	n.q.				
		recovery [%]			n.q.							

ANNEX - Table 10: Results of parallelism (PL) determination for IMAP 2 using sample 3. *Assay and matrix concentrations are given in pg·mL^{-1}. (< LLOQ = concentration below the lower limit of quantification; n.q. = value cannot be quantified; conc. = concentration; DF = dilution factor; CVs (grey) = relative differences between matrix concentrations [pg·mL^{-1}] used to calculate the reference)*

Parallelism - IMAP 2 - sample 3												
Analyte	***Reference [pg·mL^{-1}]*** *(CV)*		***PL 1***	***PL 2***	***PL 3***	***PL 4***	***PL 5***	***PL 6***	***PL 7***	***PL 8***	***PL 9***	***PL 10***
IL-1β	*2460* *(12.8 %)*	DF (1:x)	*16.0*	*32.0*	*64.0*	*128*	*256*	*512*	*1,024*	*2,048*	*4,096*	*8,192*
		assay conc.	173	84.1	41.0	17.2	8.45	4.41	2.05	1.09	0.617	0.370
		matrix conc.	2,771	2,692	2,623	2,207	2,163	2,256	2,096	2,232	2,526	3,031
		recovery [%]	113	109	107	89.7	87.9	91.7	85.2	90.8	103	123
IL-1Ra	*18637* *(13.1 %)*	DF (1:x)	*4.00*	*8.00*	*16.0*	*32.0*	*64.0*	*128*	*256*	*512*	*1,024*	< LLOQ
		assay conc.	2,400	1,801	1,038	527	293	159	80.1	39.3	20.9	n.q.
		matrix conc.	9,600	14,411	16,607	16,879	18,778	20,415	20,508	20,125	21,374	n.q.
		recovery [%]	51.5	77.3	89.1	90.6	101	110	110	108	115	n.q.
IL-12p70	*cannot be genereated*	DF (1:x)	*4.00*	*8.00*	< LLOQ							
		assay conc.	1.98	1.43	n.q.							
		matrix conc.	7.92	11.4	n.q.							
		recovery [%]		n.q.								
VEGF	*cannot be genereated*	DF (1:x)	*4.00*	*8.00*	*16.0*	*32.0*	*64.0*	< LLOQ				
		assay conc.	12.5	8.48	4.90	2.63	1.42	n.q.				
		matrix conc.	50.1	67.8	78.3	84.2	90.7	n.q.				
		recovery [%]			n.q.							
IL-13	*284* *(4.52 %)*	DF (1:x)	*4.00*	*8.00*	*16.0*	*32.0*	*64.0*	*128*	*256*	< LLOQ		
		assay conc.	49.6	35.8	18.1	9.24	4.95	2.26	1.23	n.q.		
		matrix conc.	198	287	289	296	317	289	315	n.q.		
		recovery [%]	66.4	95.9	96.9	99.0	106	96.8	105	n.q.		
M-CSF	*6.85* *(7.95 %)*	DF (1:x)	*4.00*	*8.00*	*16.0*	*32.0*	< LLOQ					
		assay conc.	1.10	0.803	0.417	0.233	n.q.					
		matrix conc.	4.41	6.43	6.67	7.47	n.q.					
		recovery [%]	64.4	93.8	97.3	109	n.q.					

ANNEX - Table 11: Detailed listing of the results of freeze-thaw stability determination of IMAP 1. *(AS = analyte stability sample; Ref. = reference sample; conc. = concentration)*

Freeze-thaw stability - IMAP 1					
		AS 1	***AS 2***	***AS 3***	***Ref.***
Analyte	*freeze-thaw cycles*	*1*	*2*	*3*	*0*
IL-4	matrix conc. [pg·mL^{-1}]	11.6	12.6	10.8	*11.4*
	recovery [%]	102	110	94.4	
IL-6	matrix conc. [pg·mL^{-1}]	346	338	348	*335*
	recovery [%]	103	101	104	
IL-8	matrix conc. [pg·mL^{-1}]	331	324	306	*315*
	recovery [%]	105	103	97.2	
IL-10	matrix conc. [pg·mL^{-1}]	13.8	13.0	12.3	*13.0*
	recovery [%]	106	101	94.8	
GM-CSF	matrix conc. [pg·mL^{-1}]	198	245	193	*228*
	recovery [%]	86.5	107	84.6	
IFN-γ	matrix conc. [pg·mL^{-1}]	151	166	140	*137*
	recovery [%]	110	121	102	
MCP-1	matrix conc. [pg·mL^{-1}]	72.4	69.5	76.5	*79.4*
	recovery [%]	91.1	87.5	96.3	
MIP-1β	matrix conc. [pg·mL^{-1}]	14.9	19.0	15.5	*16.9*
	recovery [%]	88.3	112	91.7	
TNF-α	matrix conc. [pg·mL^{-1}]	92.5	102	89.8	*88.5*
	recovery [%]	105	116	101	

ANNEX - Table 12: Detailed listing of the results of freeze-thaw stability determination of IMAP 2. *(AS = analyte stability sample; Ref. = reference sample; conc. = concentration)*

Freeze-thaw stability - IMAP 2					
		AS 1	***AS 2***	***AS 3***	***Ref.***
Analyte	*freeze-thaw cycles*	*1*	*2*	*3*	*0*
IL-1β	matrix conc. [pg·mL^{-1}]	70.3	79.7	64.2	*79.6*
	recovery [%]	88.3	100	80.7	
IL-1Ra	matrix conc. [pg·mL^{-1}]	532	579	470	*584*
	recovery [%]	91.1	99.1	80.5	
IL-12p70	matrix conc. [pg·mL^{-1}]	12.3	12.7	11.9	*10.8*
	recovery [%]	114	117	110	
VEGF	matrix conc. [pg·mL^{-1}]	239	245	187	*222*
	recovery [%]	108	110	84.1	
IL-13	matrix conc. [pg·mL^{-1}]	48.9	52.7	39.7	*41.7*
	recovery [%]	117	126	95.2	
M-CSF	matrix conc. [pg·mL^{-1}]	11.7	13.1	11.3	*11.3*
	recovery [%]	103	116	99.4	

ANNEX - Table 13: Detailed listing of the results of short-term stability determination of IMAP 1. *(AS = analyte stability sample; Ref. = reference sample; RT = room temperature, conc. = concentration)*

Short-term stability - IMAP 1									
		AS 4	***AS 5***	***Ref.***	***AS 6***	***AS 7***	***AS 8***	***AS 9***	***Ref.***
		test temperature							
		4 °C	*4 °C*		*4 °C*	*RT*	*RT*	*RT*	
		storage duration at test temperature							
Analyte		*2h*	*4h*		*24h*	*2h*	*4h*	*24h*	
IL-4	matrix conc. [pg·mL^{-1}]	11.2	11.3	*11.4*	8.21	9.11	10.6	12.5	*10.6*
	recovery [%]	97.9	98.8		77.5	85.9	100	118	
IL-6	matrix conc. [pg·mL^{-1}]	290	305	*335*	297	329	321	288	*315*
	recovery [%]	86.6	91.0		94.4	105	102	91.4	
IL-8	matrix conc. [pg·mL^{-1}]	312	304	*315*	303	319	319	319	*306*
	recovery [%]	99.2	96.5		99.1	104	104	104	
IL-10	matrix conc. [pg·mL^{-1}]	10.9	12.0	*13.0*	10.2	12.2	13.0	8.71	*13.4*
	recovery [%]	83.8	92.7		87.0	104	111	74.2	
GM-CSF	matrix conc. [pg·mL^{-1}]	194	194	*228*	203	170	245	195	*208*
	recovery [%]	84.8	85.1		97.4	81.5	118	93.5	
IFN-γ	matrix conc. [pg·mL^{-1}]	136	138	*137*	115	132	142	108	*133*
	recovery [%]	99.6	101		86.4	99.3	107	81.5	
MCP-1	matrix conc. [pg·mL^{-1}]	73.8	64.3	*79.4*	59.0	74.5	70.1	53.6	*72.5*
	recovery [%]	93.0	81.0		81.3	103	96.6	74.0	
MIP-1β	matrix conc. [pg·mL^{-1}]	17.3	14.7	*16.9*	15.6	17.1	17.0	15.2	*17.0*
	recovery [%]	102	86.8		91.7	101	100	89.7	
TNF-α	matrix conc. [pg·mL^{-1}]	85.1	82.7	*88.5*	92.8	109	116	91.2	*109*
	recovery [%]	96.2	93.4		85.1	100	106	83.7	

ANNEX - Table 14: Detailed listing of the results of short-term stability determination of IMAP 2. *(AS = analyte stability sample; Ref. = reference sample; RT = room temperature, conc. = concentration)*

Short-term stability - IMAP 2								
		AS 4	***AS 5***	***Ref.***	***AS 6***	***AS 7***	***AS 8***	***AS 9***	***Ref.***
		test temperature							
		4 °C	*4 °C*		*4 °C*	*RT*	*RT*	*RT*	
		storage duration at test temperature							
Analyte		*2h*	*4h*		*24h*	*2h*	*4h*	*24h*	
IL-1β	matrix conc. [pg·mL^{-1}]	69.3	69.2	*79.6*	62.6	69.1	75.7	62.7	*74.1*
	recovery [%]	87.0	86.9		84.4	93.1	102	84.6	
IL-1Ra	matrix conc. [pg·mL^{-1}]	508	504	*584*	517	538	567	506	*596*
	recovery [%]	87.0	86.2		86.8	90.3	95.0	84.9	
IL-12p70	matrix conc. [pg·mL^{-1}]	11.9	10.4	*10.8*	11.6	12.6	12.7	11.2	*11.3*
	recovery [%]	109	96.3		102	111	112	98.8	
VEGF	matrix conc. [pg·mL^{-1}]	202	204	*222*	234	324	346	217	*373*
	recovery [%]	90.8	91.9		62.9	87.0	92.7	58.2	
IL-13	matrix conc. [pg·mL^{-1}]	42.1	43.7	*41.7*	37.1	42.3	42.6	38.8	*43.7*
	recovery [%]	101	105		84.9	97.0	97.5	88.9	
M-CSF	matrix conc. [pg·mL^{-1}]	11.2	10.8	*11.3*	7.68	8.91	8.61	8.15	*8.33*
	recovery [%]	98.7	95.5		92.2	107	103	97.8	

A

Mean AEB [AU]		multiplexed capture coated beads	
		IL-6	**TNF-α**
detection antibody	**IL-6**	0.005	0.003
	TNF-α	0.012	0.014

B

Recovery [%]		multiplexed capture coated beads	
		IL-6	**TNF-α**
recombinant protein	**IL-6**	100	1.22
	TNF-α	0.392	100

C

Recovery [%]		multiplexed capture coated beads	
		IL-6	**TNF-α**
detection antibody	**IL-6**	100	1.61
	TNF-α	0.525	100

ANNEX - Table 15: Results of cross - reactivity testing for Simoa SR-X assays. *(A) AEB signals of the cross-reactivity testing between the respective analyte- specific capture and detection antibody. AEBs above 2 AU were regarded as cross-reactivity.*
(B) Testing of cross-reactivity between the analyte and capture antibody. Given recoveries in % are based on the signal generated with the analyte-specific combinations set to 100 %. (C) Cross-reactivity testing between analyte and detection antibody. Calculation and evaluation correspond to that already described for (B). All values were assessed as duplicates (n = 2).

ANNEX - Table 16: Results of the determination of the lower limit of quantification (LLOQ) for the analytes of the developed Simoa SR-X assays.*The nominal concentrations of the respective analytes defined as LLOQ are shown in bold. The values in bold, italics and highlighted in grey are the determined CVs and recoveries that did not meet the acceptance criteria.*

Lower limit of quantification - Simoa SR-X assays										
		CAL 4 dilution								
Analyte		***1:2***	***1:4***	***1:8***	***1:16***	***1:32***	***1:64***	***1:128***	***1:256***	*CAL 4*
IL-4	nominal conc. [pg·mL^{-1}]	0.234	0.117	0.059	0.029	0.015	**0.007**	0.004	0.002	*0.469*
	analyzed conc. [pg·mL^{-1}]	0.223	0.120	0.062	0.030	0.015	0.007	0.003	0.002	
	CV [%]	3.60	4.33	14.6	6.32	11.7	23.7	***36.5***	***42.6***	
	recovery [%]	95.2	103	106	104	99.5	96.9	88.0	109	
IL-12p70	nominal conc. [pg·mL^{-1}]	0.781	0.391	0.195	0.098	0.049	**0.024**	0.012	0.006	*1.56*
	analyzed conc. [pg·mL^{-1}]	0.755	0.389	0.199	0.104	0.049	0.027	0.007	0.006	
	CV [%]	4.87	6.55	8.67	9.42	12.7	16.2	***74.1***	***47.8***	
	recovery [%]	96.7	99.5	102	107	99.8	112	***55.2***	92.9	
IL-6	nominal conc. [pg·mL^{-1}]	0.350	0.175	0.087	0.044	0.022	0.011	**0.005**	0.003	*0.700*
	analyzed conc. [pg·mL^{-1}]	0.346	0.191	0.096	0.048	0.024	0.012	0.007	0.004	
	CV [%]	6.65	10.1	8.75	10.3	11.5	24.9	19.2	***29.0***	
	recovery [%]	98.8	109	109	110	111	106	122	***130***	
TNF-α	nominal conc. [pg·mL^{-1}]	1.05	0.525	0.262	0.131	0.066	0.033	**0.016**	0.008	*2.10*
	analyzed conc. [pg·mL^{-1}]	1.06	0.545	0.276	0.133	0.068	0.030	0.019	0.006	
	CV [%]	6.40	9.90	6.66	16.9	13.6	14.1	20.4	***58.1***	
	recovery [%]	101	104	105	101	103	92.7	115	78.4	

ANNEX - Table 17: Limits of detection determined for the analytes of the Simoa SR-X assays.*(CAL = calibrator; SD = standard deviation; R^2 = coefficient of determination)*

Limit of detection - Simoa SR-X assays					
		Analyte			
		IL-4	***IL-12p70***	***IL-6***	***TNF-α***
CAL 8 20 replicates	Mean (MFI)	0.005	0.012	0.010	0.012
	SD (MFI)	0.001	0.001	0.001	0.001
Linear regression	slope	0.914	0.328	1.09	0.479
	y-intercept	0.005	0.012	0.010	0.012
	R^2	0.999	0.999	0.999	0.999
LOD [pg·mL^{-1}]		**0.002**	**0.012**	**0.003**	**0.006**

ANNEX - Table 18: Results of parallelism (PL) determination for the Simoa SR-X assays using sample 1. *(<LLOQ = concentration below the lower limit of quantification; n.q. = value cannot be quantified; conc. = concentration; DF = dilution factor; CVs (grey) = relative differences between matrix concentrations [pg·mL^{-1}] used to calculate the reference)*

Parallelism - Simoa SR-X assays - sample 1													
Analyte	***Reference [pg·mL^{-1}]*** *(CV)*		***PL 1***	***PL 2***	***PL 3***	***PL 4***	***PL 5***	***PL 6***	***PL 7***	***PL 8***	***PL 9***	***PL 10***	***PL 11***	***PL 12***
IL-4	*111* *(4.27 %)*	DF (1:x)	*5.00*	*10.0*	*20.0*	*40.0*	*80.0*	*160*	*320*	*640*	*1,280*	*2,560*	*5,120*	*10,240*
		assay conc. [pg·mL^{-1}]	22.1	11.3	5.93	2.77	1.46	0.722	0.329	0.168	0.085	0.043	0.021	0.010
		matrix conc. [pg·mL^{-1}]	110	113	119	111	117	116	105	108	109	110	106	104
		recovery [%]	99.8	103	107	100	106	104	95.2	97.4	98.1	99.1	96.0	93.9
IL-12p70	*4.9* *(3.98 %)*	DF (1:x)	*5.00*	*10.0*	*20.0*	*40.0*	*80.0*	*160*	< LLOQ					
		assay conc. [pg·mL^{-1}]	0.731	0.473	0.236	0.125	0.065	0.030	n.q.					
		matrix conc. [pg·mL^{-1}]	3.65	4.73	4.71	5.01	5.17	4.87	n.q.					
		recovery [%]	74.6	96.5	96.2	102	106	99.3	n.q.					
IL-6	*16.4* *(15.1 %)*	DF (1:x)	*5.00*	*10.0*	*20.0*	*40.0*	*80.0*	*160*	*320*	*640*	< LLOQ			
		assay conc. [pg·mL^{-1}]	4.53	1.96	0.937	0.327	0.202	0.106	0.052	0.022	n.q.			
		matrix conc. [pg·mL^{-1}]	22.7	19.6	18.7	13.1	16.2	16.9	16.6	14.1	n.q.			
		recovery [%]	138	120	114	76.1	98.8	103	102	86.1	n.q.			
TNF-α	*14.4* *(11.4 %)*	DF (1:x)	*5.00*	*10.0*	*20.0*	*40.0*	*80.0*	*160*	< LLOQ					
		assay conc. [pg·mL^{-1}]	4.66	1.70	0.713	0.360	0.173	0.078	n.q.					
		matrix conc. [pg·mL^{-1}]	23.3	17.0	14.3	14.4	13.8	12.5	n.q.					
		recovery [%]	162	118	99.2	100	96.0	86.7	n.q.					

ANNEX - Table 19: Results of parallelism (PL) determination for the Simoa SR-X assays using sample 2. *(<LLOQ = concentration below the lower limit of quantification; n.q. = value cannot be quantified; conc. = concentration; DF = dilution factor; CVs (grey) = relative differences between matrix concentrations [pg·mL^{-1}] used to calculate the reference)*

Parallelism - Simoa SR-X assays - sample 2													
Analyte	***Reference [pg·mL^{-1}]*** *(CV)*		***PL 1***	***PL 2***	***PL 3***	***PL 4***	***PL 5***	***PL 6***	***PL 7***	***PL 8***	***PL 9***	***PL 10***	***PL 11***	***PL 12***
IL-4	*203* *(6.96 %)*	DF (1:x)	*5.00*	*10.0*	*20.0*	*40.0*	*80.0*	*160*	*320*	*640*	*1,280*	*2,560*	*5,120*	*10,240*
		assay conc. [pg·mL^{-1}]	35.2	21.1	10.8	5.39	2.79	1.33	0.573	0.300	0.154	0.081	0.040	0.020
		matrix conc. [pg·mL^{-1}]	176	211	217	216	223	213	184	192	197	206	202	203
		recovery [%]	86.6	104	107	106	110	105	90.3	94.4	96.7	101	99.5	100.0
IL-12p70	*14.1* *(9.65 %)*	DF (1:x)	*5.00*	*10.0*	*20.0*	*40.0*	*80.0*	*160*	*320*	< LLOQ				
		assay conc. [pg·mL^{-1}]	1.77	1.25	0.648	0.362	0.175	0.102	0.045	n.q.				
		matrix conc. [pg·mL^{-1}]	8.86	12.5	13.0	14.5	14.0	16.4	14.5	n.q.				
		recovery [%]	62.7	88.4	91.7	102	99.3	116	102	n.q.				
IL-6	*0.642* *(12.8 %)*	DF (1:x)	*5.00*	*10.0*	*20.0*	*40.0*	< LLOQ							
		assay conc. [pg·mL^{-1}]	0.124	0.074	0.027	0.017	n.q.							
		matrix conc. [pg·mL^{-1}]	0.618	0.741	0.544	0.665	n.q.							
		recovery [%]	96.3	115	84.8	104	n.q.							
TNF-α	*13.3* *(14.0 %)*	DF (1:x)	*5.00*	*10.0*	*20.0*	*40.0*	*80.0*	*160*	< LLOQ					
		assay conc. [pg·mL^{-1}]	4.39	1.53	0.702	0.268	0.150	0.090	n.q.					
		matrix conc. [pg·mL^{-1}]	22.0	15.3	14.0	10.7	12.0	14.4	n.q.					
		recovery [%]	165	115	106	80.8	90.4	108	n.q.					

ANNEX - Table 20: Results of parallelism (PL) determination for the Simoa SR-X assays using sample 3. *(<LLOQ = concentration below the lower limit of quantification; n.q. = value cannot be quantified; conc. = concentration; DF = dilution factor; CVs (grey) = relative differences between matrix concentrations [pg·mL^{-1}] used to calculate the reference)*

Parallelism - Simoa SR-X assays - sample 3									
Analyte	***Reference [pg·mL^{-1}]*** *(CV)*		***PL 1***	***PL 2***	***PL 3***	***PL 4***	***PL 5***	***PL 6***	***PL 7***
IL-4	*4.61* *(17.1 %)*	DF (1:x)	*5.00*	*10.0*	*20.0*	*40.0*	*80.0*	*160*	< LLOQ
		assay conc. [pg·mL^{-1}]	1.56	0.577	0.249	0.112	0.049	0.024	n.q.
		matrix conc. [pg·mL^{-1}]	7.79	5.77	4.97	4.49	3.93	3.88	n.q.
		recovery [%]	169	125	108	97.5	85.3	84.1	n.q.
IL-12p70	*7.76* *(10.2 %)*	DF (1:x)	*5.00*	*10.0*	*20.0*	*40.0*	*80.0*	*160*	< LLOQ
		assay conc. [pg·mL^{-1}]	0.859	0.647	0.381	0.213	0.100	0.051	n.q.
		matrix conc. [pg·mL^{-1}]	4.30	6.47	7.62	8.52	8.03	8.17	n.q.
		recovery [%]	55.4	83.4	98.2	110	103	105	n.q.
IL-6	*8997* *(11.5 %)*	DF (1:x)	*320*	*640*	*1,280*	*2,560*	*5,120*	*10,240*	
		assay conc. [pg·mL^{-1}]	30.8	16.3	6.95	3.48	1.48	0.813	
		matrix conc. [pg·mL^{-1}]	9,849	10,435	8,893	8,920	7,562	8,323	
		recovery [%]	109	116	98.8	99.1	84.0	92.5	
TNF-α	*4148* *(6.86 %)*	DF (1:x)	*320*	*640*	*1,280*	*2,560*	*5,120*	*10,240*	
		assay conc. [pg·mL^{-1}]	13.9	7.09	3.06	1.51	0.771	0.408	
		matrix conc. [pg·mL^{-1}]	4,440	4,535	3,918	3,872	3,947	4,175	
		recovery [%]	107	109	94.6	93.5	95.3	101	

List of Publications

Stefanie Lerche, Milan Zimmermann, Isabel Wurster, Benjamin Roeben, Franca Laura Fries, Christian Deuschle, Katharina Waniek, Ingolf Lachmann, Thomas Gasser, Meike Jakobi, Thomas O. Joos, Nicole Schneiderhan-Marra, and Kathrin Brockmann. “CSF and Serum Levels of Inflammatory Markers in PD: Sparse Correlation, Sex Differences and Association With Neurodegenerative Biomarkers.” Front. Neurol. (2022).
http://doi.org/10.3389/fneur.2022.834580

Nora Feuerer, Julia Marzi, Eva M. Brauchle, Daniel A. Carvajal Berrio, Florian Billing, Martin Weiss, Meike Jakobi, Nicole Schneiderhan-Marra, Christopher Shipp, and Katja Schenke-Layland. “Lipidome profiling with Raman microspectroscopy identifies macrophage response to surface topographies of implant materials.” PNAS (2021).
http://doi.org/10.1073/pnas.2113694118

Bjoern Traenkle, Philipp D. Kaiser, Stefania Pezzana, Jennifer Richardson, Marius Gramlich, Teresa R. Wagner, Dominik Seyfried, Melissa Weldle, Stefanie Holz, Yana Parfyonova, Stefan Nueske, Armin M. Scholz, Anne Zeck, Meike Jakobi, Nicole Schneiderhan-Marra, Martin Schaller, Andreas Maurer, Cécile Gouttefangeas, Manfred Kneilling, Bernd J. Pichler, Dominik Sonanini, and Ulrich Rothbauer. “Single-Domain Antibodies for Targeting, Detection, and In Vivo Imaging of Human CD4+ Cells.” Front. Immunol. (2021).
http://doi.org/10.3389/fimmu.2021.799910

Florian Billing, Bernadette Walter, Simon Fink, Elsa Arefaine, Luisa Pickarski, Sandra Maier, Robin Kretz, Meike Jakobi, Nora Feuerer, Nicole Schneiderhan-Marra, Claus Burkhardt, Markus Templin, Anne Zeck, Rumen Krastev, Hanna Hartmann, and Christopher Shipp. “Altered Proinflammatory Responses to Polyelectrolyte Multilayer Coatings Are Associated with Differences in Protein Adsorption and Wettability.” ACS Appl. Mater. Interfaces (2021).
http://doi.org/10.1021/acsami.1c16175

Florian Billing, Meike Jakobi, Dagmar Martin, Karin Gerlach, Elsa Arefaine, Martin Weiss, Nicole Schneiderhan-Marra, Hanna Hartmann, and Christopher Shipp. “The immune response to the SLActive titanium dental implant surface in vitro is predominantly driven by innate immune cells.” J Immunol Regen Med (2021).
http://doi.org/10.1016/j.regen.2021.100047

Michael Ghosh, Hanna Hartmann, Meike Jakobi, Léo März, Leon Bichmann, Lena K. Freudenmann, Lena Mühlenbruch, Sören Segan, Hans-Georg Rammensee, Nicole Schneiderhan-Marra, Christopher Shipp, Stefan Stevanović, and Thomas O. Joos. “The Impact of Biomaterial Cell Contact on the Immunopeptidome.” Front. Bioeng. Biotechnol. (2020).
http://doi.org/10.3389/fbioe.2020.571294

Vasiliki Panagiotakopoulou, Dina Ivanyuk, Silvia De Cicco, Wadood Haq, Aleksandra Arsić, Cong Yu, Daria Messelodi, Marvin Oldrati, David C. Schöndorf, Maria-Jose Perez, Ruggiero Pio Cassatella, Meike Jakobi, Nicole Schneiderhan-Marra, Thomas Gasser, Ivana Nikić-Spiegel, and Michela Deleidi. "Interferon-γ signaling synergizes with LRRK2 in neurons and microglia derived from human induced pluripotent stem cells." Nat Commun. (2020). htts://doi.org/10.1038/s41467-020-18755-4

Sören Segan*, Meike Jakobi*, Paree Khokhani, Sascha Klimosch, Florian Billing, Markus Schneider, Dagmar Martin, Ute Metzger, Antje Biesemeier, Xin Xiong, Ashutosh Mukherjee, Heiko Steuer, Bettina-Maria Keller, Thomas Joos, Manfred Schmolz, Ulrich Rothbauer, Hanna Hartmann, Claus Burkhardt, Günter Lorenz, Nicole Schneiderhan-Marra, and Christopher Shipp. "Systematic Investigation of Polyurethane Biomaterial Surface Roughness on Human Immune Responses in vitro." Biomed Res Int (2020). http://doi.org/10.1155/2020/3481549

Hans-Georg Rammensee, Karl-Heinz Wiesmüller, P. Anoop Chandran, Henning Zelba, Elisa Rusch, Cécile Gouttefangeas, Daniel J. Kowalewski, Moreno Di Marco, Sebastian P. Haen, Juliane S. Walz, Yamel Cardona Gloria, Johanna Bödder, Jill-Marie Schertel, Antje Tunger, Luise Müller, Maximilian Kießler, Rebekka Wehner, Marc Schmitz, Meike Jakobi, Nicole Schneiderhan-Marra, Reinhild Klein, Karoline Laske, Kerstin Artzner, Linus Backert, Heiko Schuster, Johannes Schwenck, Alexander N. R. Weber, Bernd J. Pichler, Manfred Kneilling, Christian la Fougère, Stephan Forchhammer, Gisela Metzler, Jürgen Bauer, Benjamin Weide, Wilfried Schippert, Stefan Stevanović and Markus W. Löffler. "A new synthetic toll-like receptor 1/2 ligand is an efficient adjuvant for peptide vaccination in a human volunteer." J Immunother Cancer (2019). http://doi.org/10.1186/s40425-019-0796-5

*shared first authors